
Effect and consequence analysis of expanding PIN-technology in various types of heavy machinery

by

Øyvind Karlsen

Thesis submitted in fulfilment of
the requirements for the degree of
PHILOSOPHIAE DOCTOR
(PhD)



Department of Mechanical and Structural Engineering and Materials Science
Faculty of Science and Technology
2022

University of Stavanger
NO-4036 Stavanger
NORWAY
www.uis.no

©2022 Øyvind Karlsen

ISBN:978-82-8439-148-9

ISSN:1890-1387

PhD: Thesis UiS No. 684

Preface

This research with the corresponding thesis was carried within the regulations of an Industrial PhD program, at the University of Stavanger (www.uis.no). The research was funded by the Research Council of Norway (www.forskningsradet.no) through project 283821, and Bondura Technology AS (www.bondura.no). The project was initiated in February 2018 and submitted in December 2022.

Prof. Hirpa G. Lemu from the University of Stavanger, Department of Mechanical and Structural Engineering and Materials Science, Faculty of Science and Technology, supervised the project throughout its duration.

The research work and corresponding tests were carried out at the University of Stavanger, and at the premises of the company Urdal Services AS in cooperation with Coba Måleteknikk AS.

The required PhD courses have been completed at the University of Stavanger, during the project phase.

- TN900 Theory of Science and Ethics
- TN910 Innovation in Research Projects
- MSK900 Advanced Mechanical Design and Simulation
- OFF915 PhD Project Course in Mechanical Engineering and Materials Science
- MSK550 Computer aided Engineering

Acknowledgements

First and foremost, I would like to express my love and gratitude to my family, my dearest beloved Lorena, and my sweet children Aurora Viviana, Anthony, and Florencia. It would not have been possible to complete this wonderful project without their constant understanding and patience. ¡Los amo!

I wouldn't have been who I am and where I am today without the love and care I received from my father and deceased mother, who guided me through my childhood and youth.

My deepest gratitude and highest respects to my mentor and supervisor, Prof. Hirpa G. Lemu, for his believe in me and the project, his patience, calm and guidance through this long period. He gave me the inspiration to continue even when the horizon looked so dark and far away.

I am forever grateful to Mr. Soheil Salahshour and Mr. Muhammad Maaz Akhtar for accepting the challenge to write a paper each, together with me and with Prof. Lemu.

I want to express my gratitude to the engineers at Bondura, Mr. Imad Berkani and Mr. Enok Nærland, all the involved employees at the University of Stavanger, and the PhD students at my student office, for their constant support and inspiration.

I also want to express my thanks to Mr. Carl Odvar Hoel at COBA, and Mr. Henrik Tveit at SKF, for their valuable help and support before, during, and after the external tests.

Abstract

Expanding pin systems can be applied in any joint, moveable, or fixed, in any type of machine, crane, or equipment, in almost any type of industry, globally. There are a variety of different versions of expanding pins depending on the type and severity of challenges the joints are exposed to during operation, or assembly and disassembly. There are expanding pins with one sleeve only, typically for non-moveable joints connecting structure to structure. Other pins have two sleeves for wedge locking the pin assembly to the machine supports, or even four sleeves so the pin can be locked to a bearing as well.

The main advantages with these types of pin solutions are reduced wear, reduced risk of pin breakage, loosening, and crack damages on the pin and machine supports, reduced loss of operational or production time, reduced loss of work hours in mounting and disassembling of machines, cranes, and other equipment. In addition, improved functionality of bearings, improved huge flange shear capacities, and the possibility to use the expanding pin system in combination with 3D printed repair inserts to reduce downtime due to repairs of damaged pin supports. This coincides with societal, and authority requirements regarding reduction of losses due to inefficient or incorrect machines, material, procedures, and mindset.

The expanding PIN-technology (also referred to as Bondura Technology) is a relatively new invention whose mechanics, failure characteristics and associated effects and consequences when used in various heavy machinery are not well documented. Thus, this thesis is intended to fill the knowledge gap through literature studies, surveys, experimental tests, calculations, and numerical analysis approaches. The experimental tests focused on, (a) studying the effects of expanding pin applied in spherical bearings, (b) investigating how to reduce the downtime when repair of support bores is required using the expanding

pin as a tool in combination with 3D printed repair inserts, (c) improving huge flange shear capacity, (d) understanding how self-loosening of preloaded bolts can be avoided, and (e) identifying the interactions and stress behaviour between pin and support.

In this thesis, results from nine published studies about the effects and consequences regarding use of expanding pins in heavy machinery are presented. The studies are mainly based on, (i) a questionnaire-based survey among 58 stakeholders related to expanding pins, based in 10 countries and 3 continents, (ii) traditional expanding pin systems, and (iii) some newly developed pin solutions, in addition to (iv) two literature studies.

The study results indicate that stakeholders such as OEMs, Engineering companies (or departments), End-users, and those working with service, repair, and maintenance, highly value expanding pin solutions, compared to standard cylindrical pins. The studied pin solution is regarded as safer, faster to install and retrieve, less risk of wear damage, and it is also seen as an important economical factor. In addition, the expanding pin solution can improve bearing function and flange shear capacities, and the anti-loosening bolt can prevent bolt-nut loosening due to vibrations.

List of appended papers

- Paper I [1]** **KARLSEN, Ø.**; LEMU, H. G. Questionnaire-based survey of experiences with the use of expanding PIN systems in mechanical joints. *Results in Engineering*, 2021, vol. 9, p. 100212. <https://doi.org/10.1016/j.rineng.2021.100212>
- Paper II [2]** **KARLSEN, Ø.**; LEMU, H. G.; BERKANI, I. An investigation of the effects and consequences combining expanding dual pin with radial spherical plain bearings. *Applied Mechanics*, 2022, vol. 3, no 2, p. 573-589. <https://doi.org/10.3390/applmech3020034>
- Paper III [3]** **KARLSEN, Ø.**; LEMU, H. G.; BERKANI, I. A Novel Technique for Temporarily Repair and Improvement of Damaged Pin Joint Support Bores. *Applied Mechanics*, 2022, vol. 3, no 4, p. 1206-1222. <https://doi.org/10.3390/applmech3040069>
- Paper IV [4]** **KARLSEN, Ø.**; LEMU, H. G. Safety related study of Expanding Pin Systems Application in Lifting and Drilling Equipment within Construction, Offshore, and Marine sectors. In: *IOP Conference Series: Materials Science and Engineering*. IOP Publishing, 2021. p. 012026. [doi:10.1088/1757-899X/1201/1/012026](https://doi.org/10.1088/1757-899X/1201/1/012026)
- Paper V [5]** AKHTAR, M. M.; **KARLSEN, Ø.**; LEMU, H. G. Study of Bondura® Expanding PIN System-Combined Axial and Radial Locking System. *Strojniski Vestnik/Journal of Mechanical Engineering*, 2021, vol. 67, no 12. p. 625-634. <https://doi.org/10.5545/sv-jme.2021.7306>
- Paper VI [6]** SALAHSHOUR, S.; **KARLSEN, Ø.**; LEMU, H. G. Experimental and Numerical Studies of Stress Distribution in an Expanding Pin Joint System. *Applied Mechanics*, 2021, vol. 3, no 1, p. 46-63. <https://doi.org/10.3390/applmech3010003>

-
- Paper VII [7] **KARLSEN, Ø.**; LEMU, H. G. Comparative Study on Loosening of Anti-loosening Bolt and Standard Bolt System. *Engineering Failure Analysis*, 2022, vol. 140, 106590
<https://doi.org/10.1016/j.engfailanal.2022.106590>
- Paper VIII [8] **KARLSEN, Ø.**; LEMU, H. G. Fretting Fatigue and Wear of Mechanical Joints: Literature Study. In: *IOP Conference Series: Materials Science and Engineering*. IOP Publishing, 2019. p. 012015. [doi:10.1088/1757-899X/700/1/012015](https://doi.org/10.1088/1757-899X/700/1/012015)
- Paper IX [9] **KARLSEN, Ø.**; LEMU, H. G. On Modelling Techniques for Mechanical Joints: Literature Study. In: *International Workshop of Advanced Manufacturing and Automation*. Springer, Singapore, 2019. p. 116-125.
https://doi.org/10.1007/978-981-15-2341-0_15

Declaration of Authorship

All nine papers in this thesis have co-authors. The author of this PhD thesis was the first author for all the papers, except [Paper V](#) and [VI](#).

Conference papers: [IV](#), [VIII](#), [IX](#)

Conferences: COTech & OGTech (2021 Stavanger), COTech (2019 Stavanger), and IWAMA (2019 Plymouth), respectively.

Journal papers: [I](#), [II](#), [III](#), [V](#), [VI](#), [VII](#)

Journals: Results in Engineering, Applied Mechanics, Strojnicki Vestnik/Journal of Mechanical Engineering, and Engineering Failure Analysis.

First authors: Ø. Karlsen ([I](#), [II](#), [III](#), [IV](#), [VII](#), [VIII](#), [IX](#)), M.M. Akhtar ([V](#)), and S. Salahshour ([VI](#)).

Second authors: Ø. Karlsen ([V](#), [VI](#)), and H.G. Lemu ([I](#), [II](#), [III](#), [IV](#), [VII](#), [VIII](#), [IX](#)).

Third authors: H.G. Lemu ([V](#), [VI](#)), and I. Berkani ([II](#), [III](#)).

- **Paper I:** This paper was based on a questionnaire survey regarding experiences with the use of expanding pin systems in mechanical joints, with 58 responders from 10 countries. The design of the questions and questionnaire survey was done by the first author, as were the implementation and execution of the survey. The first author (Karlsen) decided to perform a survey among stakeholders relate to expanding pins, and both authors

discussed the results and the format for the final paper, where the second author (Lemu) had an important role. Both authors went through the final manuscript separately and together before submission.

- **Paper II:** Based on feed-back from the industry, the first author (Karlsen) decided to write this article, which investigates the use of expanding pins in combination with a radial spherical plain bearing from the company SKF. The article is based on experimental tests on UiS, and at a third-party premises. The first author defined the objectives, and all test requirements and test procedures, in addition to writing the paper. The third author (Berkani) did a valuable job in making 2D and 3D drawings of the test pins, jigs, and set-ups, and in addition, together with the second author (Lemu) he gave valuable assessment and participating in discussions, testing, paper writing, and the preparations for submission.
- **Paper III:** Information from various industries indicates that repair of worn and damaged support bores in pivot joints is a time consuming and costly process. The first author (Karlsen) came up with the idea of testing out and writing a paper on a repair method using 3D printed inserts in combination with use of expanding pin systems, to temporarily compensate for the damages until the main repair can be done. As for **Paper II**, the first author defined the objectives, and all test requirements and test procedures, preparing the worn supports and additional 3D scanning, in addition to writing the paper. The third author (Berkani) did a valuable job in making 2D and 3D drawings of the test pins, 3D inserts, jigs, and set-ups, and in addition, together with the second author (Lemu) he gave valuable assessment and participating in discussions, testing, paper writing, and the preparations for submission.

-
- **Paper IV:** The first author (Karlsen) prepared and submitted a second paper based mainly, but not only, on the information obtained from the survey from [Paper I](#). The manuscript was written by the first author, guided by the second author (Lemu), and both authors participated in important discussions and changes of views, and both went through the final manuscript separately and together before submission.
 - **Paper V:** The fifth paper was based on the Master Thesis of the first author Mr. Muhammad Maaz Akhtar, which was again based on an invention by the second author (Karlsen), where the company Bondura Technology has got a patent of the invention. The second author presented the idea of the objectives, scope of work, and technical solution for the scientific paper, and first the author (Akhtar) wrote the paper. First and second author together with third author (Lemu), had continuously meeting and discussions during the production and writing of the paper, and all authors went through the final manuscript separately and together before submission.
 - **Paper VI:** This paper was based on the Master Thesis of the first author, Mr. Soheil Salahshour, which was based on a pin product from the company Bondura Technology. As for [Paper V](#), the second author (Karlsen) presented the idea, the objectives, and the technical solution for the scientific paper, and first the author wrote the paper, with continuously follow-up, meetings, and discussions with the first and third author (Lemu). All the authors went through the final manuscript separately and together before submission.
 - **Paper VII:** The seventh paper was based on an invention made by the first author (Karlsen) (with pending national and

international patents) and feed-back from the industry, especially the Offshore Wind Industry. The article is based on experimental tests on UiS premises, and some FEA from a third party. The first author, in cooperation with the engineers at Bondura, defined the objectives, and all test requirements and test procedures (based on input from DnV), in addition to writing the paper. The second author (Lemu) gave valuable assessments and participated in valuable discussions and preparations for submission of the paper.

- **Paper VIII** and **XI**: Both these papers were based on the Industrial PhD course *OFF915 PhD Project Course in Mechanical Engineering and Materials Science*, taught by second author Professor Hirpa G. Lemu. The two papers are both literature studies, about *Fretting fatigue and wear of mechanical joints* and *Modelling techniques for mechanical joints*, respectively. Both authors contributed to the main ideas, and the first author (Karlsen) performed the literature study and paper writing, with valuable and important discussions, guidance, and advice from the second author, on both content and execution. Both authors went through the final manuscript separately and together before submission. Both the course OFF915 and the two related papers were highly valuable for the first author, as an introduction to scientific writing after more than 25 years away from university studies and scientific writing.

Table of Contents

Preface	iii
Acknowledgements	iv
Abstract	v
List of appended papers.....	vii
Declaration of Authorship.....	ix
List of abbreviations.....	xvi
Part I: Thesis summary.....	xviii
1 Introduction	1
1.1 Background – motivation and objectives	1
1.1.1 Pin function and typical positions	2
1.1.2 Traditional cylindrical pin types.....	8
1.1.3 Expanding pin types	10
1.1.4 Research objectives.....	14
1.2 Research questions.....	15
1.3 Thesis organization	17
1.4 Paper relevance and ranking	19
1.5 Limitations and sources of possible inaccuracies.....	20
2 Literature and theoretical background.....	25
2.1 Contact pressure in interference fit	26
2.2 Hoop, and radial stresses.....	30
2.3 Hertzian contact area and stress	31
2.4 Bolts, nuts, and threads	33
2.5 Strain gauges, strains, and stresses.....	40
3 Research Methodology and Materials.....	45
3.1 General.....	45
3.2 Questionnaire-based survey	45

3.3	Experimental tests	49
3.3.1	An investigation of the effects and consequences of combining Expanding Dual Pin with radial spherical plain bearings	50
3.3.2	A novel technique for temporarily repair and improvement of damaged pin joint support bores	57
3.3.3	Study of Bondura® Expanding PIN System – Combined Axial and Radial Locking System	61
3.3.4	Experimental and Numerical Studies of Stress Distribution in an Expanding Pin Joint System	65
3.3.5	Comparative study on loosening of anti-loosening bolt and standard bolt system	67
3.4	Analytical approaches and numerical analysis	77
3.4.1	An Investigation of the Effects and Consequences of Combining Expanding Dual Pin with Radial Spherical Plain Bearings	78
3.4.2	A novel technique for temporarily repair and improvement of damaged pin joint support bores	79
3.4.3	Study of Bondura® Expanding PIN System – Combined Axial and Radial Locking System	82
3.4.4	Experimental and Numerical Studies of Stress Distribution in an Expanding Pin Joint System	84
3.4.5	Comparative study on loosening of anti-loosening bolt and standard bolt system	87
4	Results and Discussions	91
4.1	General	91
4.2	Thematic area-based discussion of results	91
4.2.1	Results of questionnaire-based survey (Papers I and IV)	92
4.2.2	Results of studies of traditional expanding pin solutions (Papers II, III, and VI)	111
4.2.3	Results of studies of newly developed pin solutions (Papers V, and VII)	135
4.3	Summary of appended papers	147
4.3.1	Paper I: Questionnaire-based survey of experiences with the use of expanding PIN systems in mechanical joints	147
4.3.2	Paper II: An Investigation of the Effects and Consequences of Combining Expanding Dual Pin with Radial Spherical Plain Bearings	150
4.3.3	Paper III: A novel technique for temporarily repair and improvement of damaged pin joint support bores	153

4.3.4	Paper IV: Safety related study of Expanding Pin systems application in lifting and drilling equipment within Construction, Offshore, and Marine sectors	155
4.3.5	Paper V: Study of Bondura® Expanding PIN System – combined axial and radial locking system	158
4.3.6	Paper VI: Experimental and Numerical Studies of Stress Distribution in an Expanding Pin Joint System	162
4.3.7	Paper VII: Comparative study on loosening of anti-loosening bolt and standard bolt system	165
4.3.8	Paper VIII: Fretting fatigue and wear of mechanical joints: Literature study	169
4.3.9	Paper IX: On modelling Techniques for Mechanical Joints: Literature Study	172
5	Conclusions and Future Outlook.....	177
6	Scientific and Practical Contribution	182
	Part II: Appended Papers.....	191
	Appendix A	202
	Appendix B	211

List of abbreviations

2D	2 dimensions
3D	3 dimensions
ABS	American Bureau of Shipping
AISI	American Iron and Steel Institute
ASTM	The American Society for Testing and Material
CAD	Computer-aided design
CMM	Coordinate Measuring Machine
CN	Cyanoacrylate
CS	Company size
DAQ	Data Acquisition system
DIN	German Institute for Standardisation
DnV/DNV	Det Norske Veritas
EN	European norm
EPS	Expanding Pin System
FE	Finite Element
FEA	Finite Element Analysis
HDG	Hot Dipped Galvanized
HV	Hochfeste Boltzen mit Vorspannung (high resistance bolts for pretension)
ID	Inner diameter
IFL	Interference fit level
ISO	International Organization for Standardization
LVDT	Linear variable differential transformer
NTP	National Pipe Taper
OD	Outer diameter
OEM	Original Equipment Manufacturer
POM	Polyoxymethylene
PTFE	Polytetrafluoroethylene
RQ	Research question
RSPB	Radial Spherical Plain Bearing
SEM	Scanning electron microscope
TUV	Technischer Überwachungsverein
UTS	Unified Thread Standard

VDI	Verein Deutscher Ingenieure
-----	-----------------------------

Part I: Thesis summary

1 Introduction

1.1 Background – motivation and objectives

Building construction can be seen as techniques involved in the assembly and erection of structures [10]. Early humans used simple methods, primarily for construction of shelters and protection from the effects of climate, predators, and other humans, for short time use. Over time, the needs changed, and more refined structures and forms appeared, especially within the agriculture societies. People started to stay longer periods at the same place, and their needs for different and improved quality imposed a development of their constructions, to comply with their growing needs.

From the *Neolithic period* (9000 – 5000 BC), also known as “New Stone Age”, with Stonehenge as a well-known and iconic megalith, and through the *Copper and Bronze Age* (5000 – 3.100 BC), and further up to today the humans have developed many different techniques and tools with the aim to realize the most incredible constructions, or statues. Well known examples can be the pyramids in the ancient Egypt, Mexico, Peru, Sudan and many other places, the Great Wall of China, Machu Picchu in Peru, the many roman aqueducts in Europe, the Moais at the Easter Island (Rapa Nui) of Chile etc. In addition, the more modern constructions such as extremely high buildings, long bridges of different kinds and huge Oil&Gas platforms like Troll A in the North Sea, huge tunnel systems, and offshore floating wind turbine systems require high levels of engineering, material knowledge and quality, project planning, construction knowledge, specialized tools, and machines.

In many of today’s industries humans are dependent on some kind of heavy machinery to realize the tasks they are not able to realize them self, or not willing or allowed to realize. The traditional construction industry uses a high number and a wide range of different cranes to move loads and materials from one spot to another, the mining industry uses

Introduction

trucks, shovels, dozers, drill rigs, front loaders, and many other types of machines. The Oil&Gas industry uses a wide range of cranes and drilling equipment, and the maritime industry have cranes, hydraulic hatches, A-frames, etc.

Most of this equipment often has some common denominators, such as pins or bolts in the joints. Pins designed to take shear loads, in this thesis also called shear pins, are installed in almost any type of heavy equipment and machinery in a wide range of industries, world-wide. There are needs for power transmissions and connecting techniques in most mechanical joints, moveable or fixed, to transfer power or forces from one mechanical part to another, such as for cranes, drilling equipment, giant wheels, mining vehicles, displacement compensation systems, space vehicle launch systems, etc.

The company Bondura has developed and delivered a wide range of *expanding pin systems* for both pivot or rotary joints and fixed joints in many different industries, during the last 35 years. The first patent was approved or granted in 1989, whereas the pin products got a DnV Type Approval Certificate in 1991. The first expanding pin systems were installed for testing in a drilling machinery at Smedvig Offshore's semi-submersible rig West Alpha. In 1993, the Bondura® expanding pin system was successfully tested, approved, and classified as *Proven Technology* by the Det Norske Veritas (DNV) and Statoil (now Equinor). Bondura delivers pins "all over" the world, both through direct customer contact and through partner agreements in defined geographical areas, to clients as OEM's, Engineering / project companies, Service & Maintenance related companies, and direct to end users, to mention some.

1.1.1 Pin function and typical positions

Pinned joints, either pivot joints or fixed, interference or clearance fitted, standard cylindrical type or expanding pins, can be found in a variety of

Introduction

industries, equipment, and machines, all over the world, within subsea, onshore, offshore, air and space. A pinned joint makes it possible to connect two or more parts in a safe and beneficial way, and to transfer power, loads and forces from one part to the next or turn one directional movement into rotational movement. As requirements for transmitted power is increasing, the mechanical joints and connections are exposed to increasing loads and stresses at the contact areas, which must be dealt with.

A pin is normally taking radially directed shear forces only, and maybe a small portion of bending moments, but normally not axial loads as for standard bolt-nut systems. Pins in general are widely used in a wide range of machinery, tools, cranes, vehicles etc. to make them capable of performing certain movements, in relation with their function. The pin in a joint is a vital part to make the crane, [Figure 1.1](#), able to move a load in three directions, lifting it up vertically and moving it along the two horizontal directions, and (3) finally placing it at the planned location.

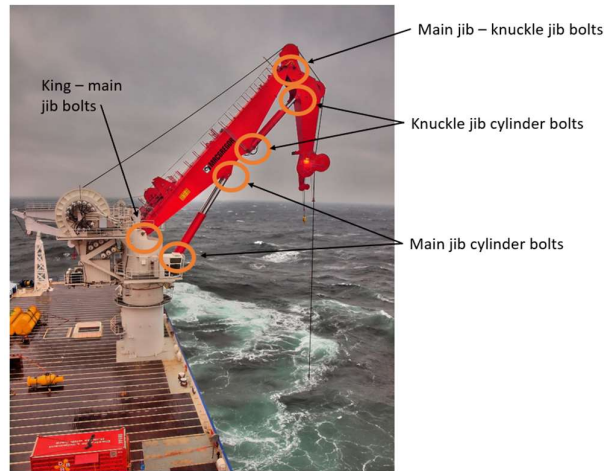


[Figure 1.1](#). Pin positions – marine crane (with approval from the MacGregor Company)



Figure 1.2. Pin positions – heave compensation system

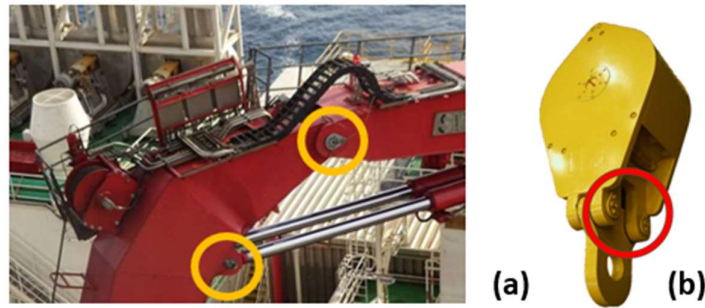


Figure 1.3. Pin positions – (a) pipe handling crane, and (b) travelling block

The pin is typically placed in joints that connect (i) a structural part of the crane to another structural part, (ii) a hydraulic cylinder to a structural part, and (iii) at the centre of turning sheaves for cables etc. [Figure 1.2](#) illustrates pin positions for a heave compensation system, where relative movements between two locations are reduced, or eliminated, as also mentioned in [Paper IV](#), and [Figure 1.3](#) shows pin positions in (a) a pipe handling crane, and (b) a travelling block for lifting purposes, respectively.

In many cases, especially at boats and ships, the A-frame is an efficient tool for lifting and handling purposes, as shown in [Figure 1.4](#). The frame normally has a fixed shape but can turn around the pinned joints that

Introduction

unite the frame leg with the foot structure. In addition, it has several hydraulic cylinders that supplies the necessary force to make the frame turn around the pinned joints, and a rotating sheave for wire.

More specialized equipment, such as wave energy converters (Figure 1.5), where wave energy is converted into electrical energy, also depend heavily on well-functioning pins and joints.



Figure 1.4. Pin position on a A-frame

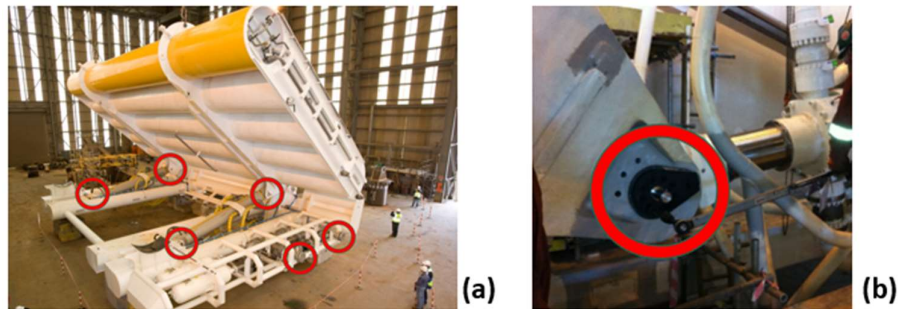


Figure 1.5. Wave energy converter – (a) pin positions, and (b) hydraulic cylinder pin

Introduction



Figure 1.6. Earth moving vehicle (with approval from Doosan Infracore Norway)



Figure 1.7. Dumper truck – Norway

Vehicles specialized within mining and earth moving (Figures 1.6 and 1.7), such as excavators, backhoe loaders, bulldozers, and dump trucks are often heavily exposed to vibrations, high loads, shock loads, and heavy wear and fatigue. The pins in such heavy machinery might be exposed not only to the physical loads, but also to wear due to fine sand and dust grains, vibrations and corrosion when exposed to salt and other chemical substances and minerals.

Even equipment used in amusement parks is heavily dependent on well-working pin joints. A Giant Wheel, as illustrated at Figure 1.8, often



Figure 1.8. Giant Wheel – Rotterdam

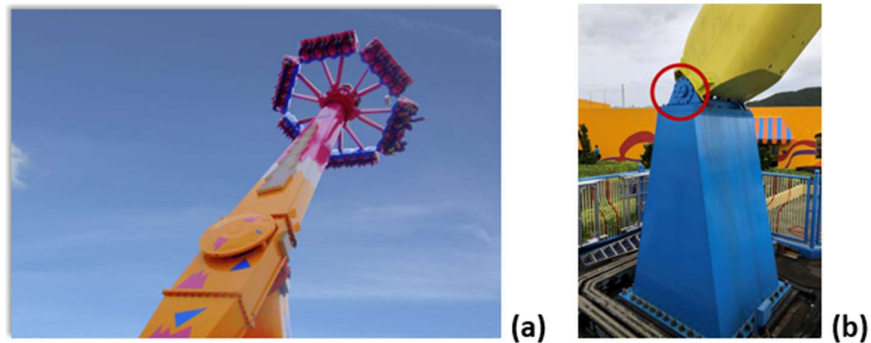


Figure 1.9. Fun Park equipment – (a) seats, and (b) foot-leg pinned joint

contains a high number of pins to keep the outer wheel secure and stable during its rotation. Figure 1.9 shows a fun-park machine where high shock loads and heavily oscillating reaction forces are transferred down to the base or foot connection.

1.1.2 Traditional cylindrical pin types

In this thesis, the expression “*shear pin*” is meant for a pin in a joint which is exposed to, and designed to resist radial shear loads, and not a safety pin which will cut at a certain shear load to protect its equipment. The expression “*dowel pin*” is also often used for the traditional cylindrical pin. There are several types of pin connections in use, often depending on the OEMs’, end-users’, or mechanical design requirements, based on conditions or requirements for installation, operation and retrieval of pins, other limitations, or life-cycle cost calculations. Such pin connections can typically be divided into two main types of fits, (a) clearance fit, and (b) interference fit pins. Depending on the pin and corresponding support bore diameters, and tolerances, a third type of fit, often referred to as transition fit could be of either type (a) or (b).

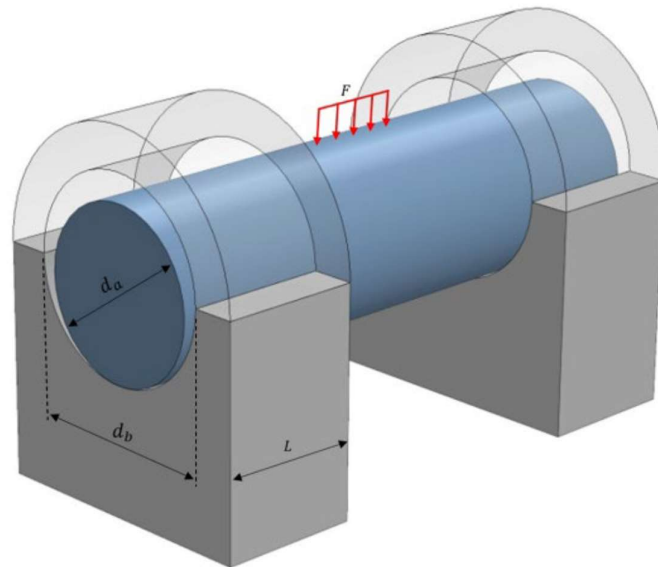


Figure 1.10. An illustration of a cylindrical pin in support

Introduction

The *clearance fit pin*, as shown in [Figure 1.10](#), is the most common pin type in most heavy machinery. This is due to its relatively low production costs, low expected installation and retrieval costs, historically long presence in mechanical equipment, and lack of knowledge of alternative solutions, among designers and decision makers. The clearance fit pin has a diameter slightly smaller than the bore diameter where to be installed, maybe down to a few hundredth of a millimetre in difference. Such a pin can move within the bore when it is exposed to vibrations, oscillating external forces, impacts, etc., and wear and ovality might occur, over time. Other factors that might affect the joint negatively can be the frequency and maximum values of vibrations, humidity and corrosion, small size dust and sand grains at surfaces in contact, material hardness and strength of surfaces in contact, and not to forget the human factors such as incorrect lubrication, incorrect dimensions or tolerances, incorrect installation, etc.

When wear occurs at the bore surface, its shape changes and the bore diameter could increase. Hence, the total contact area between the pin and the bore is reduced, and the contact stresses increase due to the reduced contact area, and further mechanical wear, ovality, fretting wear and corrosion can lead to major damages. It is common for the OEMs to apply low-cost clearance pin solutions in their designs, to reduce the overall machine and equipment costs to become more price competitive and thereafter sell their own pins as original spare parts to maintain the equipment guarantee towards their clients.

There are several types of *interference fit pin* solutions, where the pin surfaces and the support bore surfaces are meant to be in contact normally with a pre-defined or required contact or interference pressure – p_f –, as mentioned in [Paper VIII](#). The pin diameter must be slightly bigger than the bore diameter, prior to mating, to get an interference fit after mating. The required interference fit can traditionally be achieved by either (i) shrink fitting by cooling down the pin and/or heating up the bore inner surface before installing the pin, and thereafter interference fit

is ensured when both parts are at the same temperatures or (ii) press fitting by axially pressing the pin into the bore using a high-pressure tool. In both cases, a contact pressure is created between the surfaces in contact. In the latter case, there will be high friction forces between the two surfaces in contact due to the relative sliding under pressure, which could affect or damage the surfaces.

The created contact pressure during interference fit depends on the diameter difference between pin and bore, the elasticity modulus and Poisson's ratio of the involved materials, and the dimensions of the shaft and the hub. In the case of shrink fit, high-energy activities with high/low temperatures are required while high hydraulic pressure is needed for press fit. Disassembling or retrieving a pin that has been installed as interference fit might be demanding because it is considerably more complicated to reverse the process.

1.1.3 Expanding pin types

In addition to the above-described fits, a third type of interference fit can be achieved by the expanding pin solution, as shown in [Figure 1.11](#). The expanding sleeves of this solution can be seen partly in [Figure 1.12](#), as a combination of a clearance pin (at installation and retrieval), and a type of interference fit pin (during operation). The expanding pin locks to the support and prevents any relative movements between the pin and support, hence it prevents any wear and ovality to occur.

There are a variety of different technical solutions of expanding pin systems, but they typically have the following in common:

- A load bearing pin with at least one conically shaped end.
- At least one cylindrical sleeve with corresponding conical inner surface to fit each coned pin end. The sleeves have 4 axial cuts to ease the mechanical radial expansion, either partly or completely cut-through.

Introduction

- One endplate at each coned pin end to transfer axial force from the screws into the sleeve, which subsequently expands radially.
- Tightening screws to be torqued and consequently push the endplate axially.
- Some solutions have tightening nuts instead of screws and plate.
- Some solutions have double set of expanding sleeves at one or both ends.
- Some solutions have a centre hole with an axle to pull one sleeve (blind, or hidden end) into wedged position.
- Some solutions have a combination of radial expanding capability, and axially preloading of the pin.

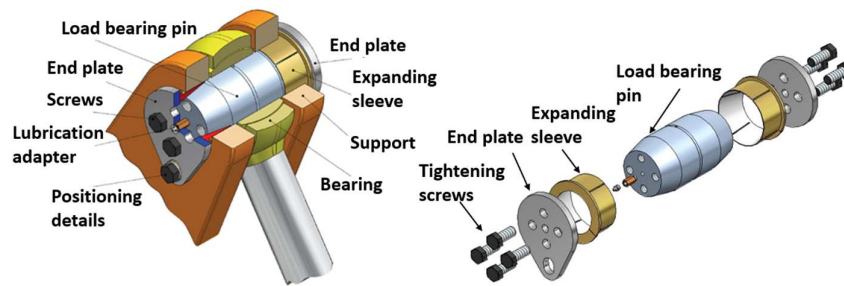


Figure 1.11. An illustration of an expanding pin, (a) in support, and (b) as exploded view

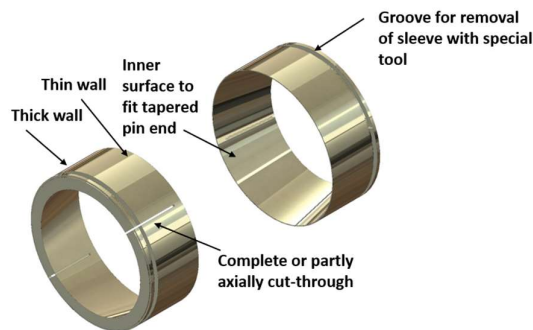
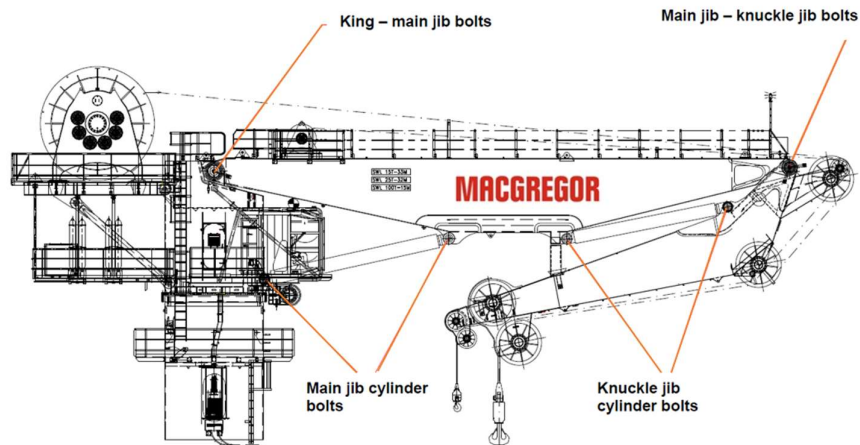


Figure 1.12. An illustration of an axially cut conical sleeve

Introduction

The expanding pin is installed as a clearance fit pin with a defined installation tolerance to ease both the installation and the retrieval process. When installed, the tightening screws are torqued to a predefined level and each sleeve is pushed axially and expands radially and hence wedge locks the pin assembly to the support. [Figure 1.13](#) illustrates typical positions for expanding pin systems in MacGregor knuckle boom marine cranes.

The expanding pin system has a different load-failure process compared to the more common cylindrical pinned joint system, as can be seen in [Figure 1.14](#). The load-failure process for expanding pinned joints, compared to those with cylindrical pins, indicates reduced risks for personnel and equipment, less production downtime, and reduced costs, as described by various stakeholders, such as OEMs, Engineering companies, Service and Maintenance companies, and End-users, as presented in [Paper I](#) and [Paper IV](#).



[Figure 1.13](#). An illustration of typical expanding pin positions at a knuckle boom crane (with approval from the MacGregor Company)

Introduction

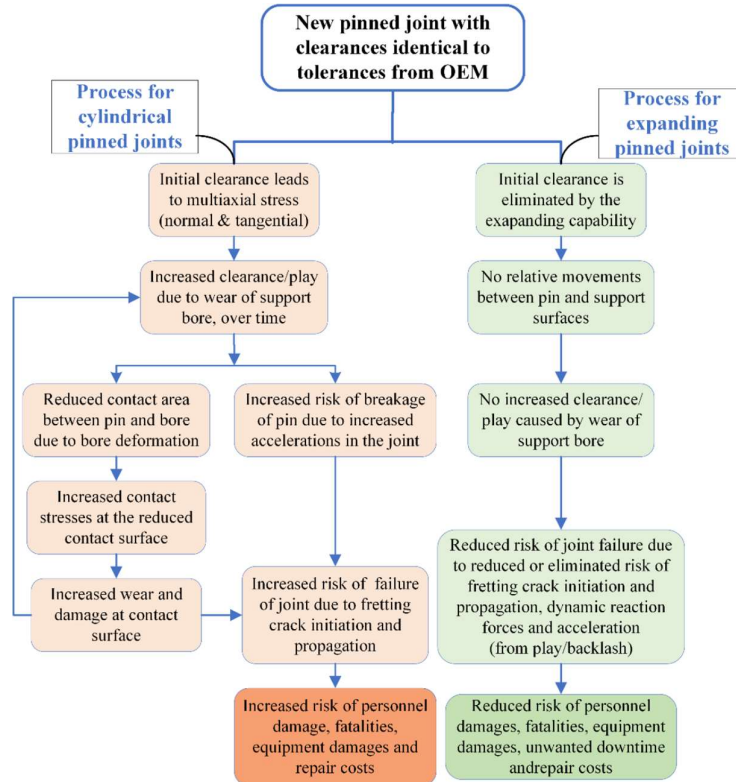


Figure 1.14. Load - failure processes for cylindrical pinned joints and expanding pinned joints (arrows indicate the outcome)

The expanding pin systems are all *customized*, where two pins seldomly are identically, unless they are meant for the same type of machine, and maybe the same joint. Typical variables that must be accounted for in an expanding pin system are:

- Physical dimensions such as length, diameter at the supports and mid-part, and support thicknesses, in addition to tolerances.
- Availability for installation and retrieval of pins.
- Requirements for lubrications.
- Material properties such as yield and ultimate strength, elongation, Charpy-V values, and surface hardness.

- Corrosion resistance level, which can be achieved by use of different stainless-steel materials.
- Vibrations, shock-loads, temperature changes and much more

In addition, different industries and clients could require that the pin systems must comply with different *third-party certification bodies* like DNV, ABS, TUV and others, various industry standards, material certificate requirements, and internal company specifications. The third-party certification could typically be a Type Approval Certificate or Product Design Assessment which is valid for a defined range of typical pin solutions, for a defined number of years. Pin designs that are more specialized might need a specific certification, often called Unit Certification (a one-time certification), with follow-up and approval of the specific production process, material certificate etc.

1.1.4 Research objectives

The general objective of this PhD project is to study the effects and consequences of the use of expanding pins in heavy equipment and machinery, as indicated by the thesis title and the research questions listed in Chapter 1.2. The expression “**effect and consequence analysis**” in the thesis title is meant to include and be understood as:

- 1) An analysis of the *experiences and perceptions* of the most important type of stakeholders, around the use of expanding pin systems compared to the use of standard cylindrical pins, in heavy machinery. Important stakeholders would typically be companies as the original machine and equipment manufacturers (OEMs), those responsible for engineering and project management, companies working with maintenance and repairs of the heavy equipment, and those operating the equipment and machines, often called End-users.
- 2) An analysis of *operational and mechanical behaviour consequences* of certain expanding pins and preloaded bolt

Introduction

systems, such as material stress, self-loosening capabilities, and effects on corresponding equipment such as bearings.

To achieve the general objective, the following specific objectives, were defined:

- (i) Perform questionnaire-based studies ([Papers I and IV](#)) of stakeholders' perceptions of expanding pin solutions compared to standard cylindrical pins, when it comes to safety, installation, and retrieval easiness, operability and economic impacts.
- (ii) Investigate the use of expanding pin solutions in spherical plain bearings ([Paper II](#)), by measure experimentally the bearing radial deformations and resistance to rotate as function of increased pin tightening and external load.
- (iii) Investigate experimentally the use and effects of some relatively new pin inventions ([Papers V and VII](#)) with axial-radial locking capabilities, and a pretensioned anti-loosening bolt concept.
- (iv) Study stress distribution in, and mechanical functionality of, a mechanical joint with expanding pin installed, ([Papers III and VI](#)) through experimental and numerical techniques.
- (v) Perform literature studies ([Papers VIII and IX](#)) around fretting wear and fatigue in mechanical joints, and some known modelling techniques, to acquire more knowledge within those areas.

1.2 Research questions

Bolted and pinned joints in most heavy mechanical machinery, like cranes, excavators, drilling equipment, dumpers etc. are normally using traditional cylindrical clearance fit pin solutions in one form or another. Such cylindrical pins have in general a very simple design and are relatively low-cost solutions, but they are generally unable to prevent damages at the contacting surfaces between pin and supports, during exposed operations. A cylindrical pin needs installation clearance against the bore, and that clearance is partly the reason why the pin can move

Introduction

relative to the bore during service and operation. If the machine joint is exposed to heavy and repeating or oscillating loads over time, vibrations, and additionally exposed to corrosive moisture and fine abrasive dust, the relative movements between the pin and the bore can easily result in surface damages, with following wear, shape deformations and increased play in the joint. The increased play results in decreased contact surfaces over time, hence increased contact pressure and increased accelerations in the mechanical system, and then increased reaction forces in the pin, which again results in even more wear and additional increased play, see [Figure 1.14](#).

The expanding pin solution will efficiently eliminate the installation tolerance between the pin and the bore after installation, thus eliminating the damaging issues with wear and increased unwanted play. In addition, it is possible to eliminate the installation tolerance between pin and bearing, typically for moveable joints, and between pin and bushing (or between two structures) for fixed joints. The current thesis aims to answer the following research questions (RQ):

- RQ1:** From an operational point of view: What are the differences between expanding pin solutions and the clearance fit pin solutions, when it comes to; *installation, operation, and retrieval* of pins, in addition to *economic impacts*?
- RQ2:** In what way could the expanding pin solutions influence heavy machinery's and personnel's *health and safety*, compared to use of standard cylindrical pins?
- RQ3:** What could be the *impacts* on the pin-bore joint and its contact surfaces when using expanding pin solutions, instead of the more common clearance fit cylindrical pins?
- RQ4:** In what way can *self-loosening* of preloaded bolts and failure of corresponding flanged joints be prevented?

1.3 Thesis organization

This thesis is organized and presented in two main parts: Part I – Thesis summary and Part II – Appended papers.

Part I: The first main part comprises of 6 sections: Introduction, Literature and Theoretical Background, Research Methodology and Materials, Results and Discussions, Conclusions and Future Outlook, and finally Scientific and Practical Contribution.

- (i) First section is an *introduction* where the background is given, with motivation and objectives for the investigation and thesis, including a short description is given of function and positions for both standard cylindrical pins and expanding pin types. The research questions are defined, the thesis organization is shown together with the paper's relevance. Finally, possible limitations of the research work are listed.
- (ii) Some *literature and theoretical background* on analytical methods applied are added in the second section.
- (iii) Third section describes the *research methodology and materials* used in this research project, in relation to questionnaire-based surveys, experimental tests, and analytical and numerical approaches.
- (iv) The *results and discussions* based on the work can be found in the fourth section, together with summary of the appended and published papers.
- (v) Fifth section presents the *conclusions* of the study, and indicates possible areas for future investigations, or outlooks.
- (vi) The final section presents the *scientific and practical contribution* from this PhD study.

Part II: The second part of the thesis contains the full versions of the published papers, [Paper I – IX](#).

The relationship between the research questions and the research papers are indicated in [Figure 1.15](#). The literature studies presented in [Paper VIII](#) and [Paper IX](#) helped the PhD candidate to gain more knowledge about numerical methods such as FE, fretting wear, corrosion, and fatigue, in general. In addition, these two papers also gave valuable knowledge and experience in writing scientific papers, and the corresponding publication process.

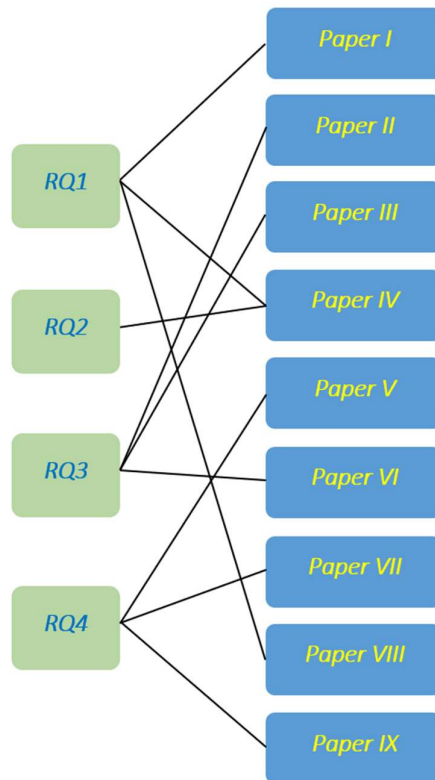


[Figure 1.15](#). Interrelation between research questions and published research papers

1.4 Paper relevance and ranking

All papers included in this thesis are relevant for the investigation and for the writing of the thesis, but the papers where the author of this thesis is the first author are valued more than where he is the second author. In addition, there have been used different methods to achieve the results, and some of the papers coincide better with the PhD thesis main objectives, than others, as indicated in [Table 1.1](#) and [1.2](#). The highest point (3) represents the most valued papers.

It can be seen from [Table 1.2](#) that the papers with most importance and highest relevance are [Paper I](#), [Paper II](#) , and [Paper III](#), where the PhD

[Table 1.1.](#) Basis for ranking of the papers in the thesis

Method		Points		
		3	2	1
i)	Author	First	Second	Third
ii)	Main method	Survey & experimental	Analytical & numerical	Literature study
iii)	Coincidence	High	Medium high	Medium
iv)	Publication	Journal	Conference	Other

[Table 1.2.](#) Ranking of the papers in the thesis

Papers	i)	ii)	iii)	iv)	Total:	Ranking:
I	3	3	3	3	12	1
II	3	3	3	3	12	
III	3	3	3	3	12	
IV	3	3	3	2	11	2
V	2	3	3	3	11	
VI	2	3	3	3	11	
VII	3	3	2	3	11	
VIII	3	1	2	2	8	3
IX	3	1	1	2	7	4

candidate was the main author, the method applied was interviews and experiments, which give better and more complete answers on the research questions, and in addition the coincidence with the Thesis title is high, and the papers were published in journals.

1.5 Limitations and sources of possible inaccuracies

There is limited information, literature and studies about wedges applied on expanding pin solutions, and this PhD study focuses primarily on such wedges integrated in a pin for mechanical joints in heavy machinery. There might exist others, and different, expanding pin solutions but this study mainly focuses on the known solutions based on the product range of the funding company for this thesis, Bondura Technology, and some companies working with similar products. The study is based mainly on questionnaire-based surveys and experimental tests with corresponding analysis, in addition to some literature studies, and less numerical analysis as FEA, and analytical analysis.

The following points could have a negative effect on the accuracy of the achieved results:

Questionnaire-based surveys:

- It could be a challenge to reach the correct person or persons to answer a questionnaire-based survey.
- Although the number of respondents was 58 it is believed it could have been higher, and then maybe given more accurate results.
- The potential respondents were defined from the company Bondura's client and contact list, in addition to a web search on companies assumed to have, or work with, equipment and machines where expanding pins could be an option. This could be defined as a possible *sampling error* [11], where the solution would be to increase the sample size.

Introduction

- Even small changes of questioning wording or order can potentially affect the answers, according to Martin [12] and Roopa and Rani [13]. The total number of respondents was 58, where 34 received and responded in English, and 24 in Norwegian, where a few were answered by phone or directly in e-mail.

Experimental tests:

- In the work reported in four of the papers (Paper II, III, V, and VI) a hand torque wrench was applied to reach the required torque, which can show incorrect values. The torque wrench applied for the tests in Paper V and VI was not re-calibrated in time, but for the Papers II and III, new torque wrenches were applied.
- For the results published in Papers II, III, and VII, hydraulic jacks or test machines with corresponding load measuring cells were applied. Incorrect calibration of the equipment can lead to errors in the measurements.
- It is an advantage to perform multiple identical experimental tests to reduce variations of the results. In Table 2 [5], each pin size (Ø50 mm and Ø80 mm) was torqued from 0 to 140 Nm, but only once.
- The use of strain gauge measurements also includes a risk of signal errors due to problems with glue, foil, wire welding, incorrect strain gauge, uncertainty in relation with the gauge factor, incorrect compensation for temperature changes during strain measurements, and others. In Paper V one of the strain gauges gave clearly incorrect values and was therefore not considered in further evaluations.
- In Paper III only static configurations were applied when investigating the effectiveness of the repair insert, by measuring strains. A full-scale test at a machine in normal operation could have given more exact results.

Introduction

- It is always uncertainty related to the choice of K-factor value for the torque – preload relationship formula for a threaded bolt-nut systems, as described in Chapter 2.4.
- The incorrect or missing use of lubrication can affect the measured results.
- In [Paper VI](#) a test boss was applied to resemble a support for an expanding pin system. The test boss had a non-varying thickness, (inner and outer diameter) 360° over its surface, but a support at a machinery will have at least varying outer diameter, which probably would result in differences in stresses.

Analytical and numerical approaches:

- The measured radial expansion (by CMM) of the inner ring of a spherical plain bearing by tightening an expanding pin solution was applied as input to calculate the *ring inner pressure* and the *ring tangential (hoop) stress*, see [Paper II](#). The measured radial expansion values were put into formulas for open-ended thick-walled tube, with zero temperature effects and zero outer pressure. The thick-walled tube theory is based on constant outer diameter over the tube length or bearing inner ring in this case. The outer diameter of the ring is not constant over its length, but the variation is small if a small section of the ring is analysed.
- Limitations of computer capacity can lead to the use of increased mesh sizes in FEA, and consequently reduced accuracy of the results. A FE analysis was performed in [Paper VI](#) where some of the results for the pin were not in good agreement with the corresponding theoretical results, and reason was suggested to be related to mesh size.

Literature studies:

- As for a questionnaire-based survey, a literature study must comply with certain requirements to have a value for the author.

Introduction

Batinic et al. [11] wrote about *coverage errors* for surveys, which is a mismatch between the target population and the sampling frame. For a literature study this could be a similar mismatch between the type of articles the researcher is looking for, and the type of articles which are available where he is searching for them. The coverage errors can be reduced by increasing the sampling frame, or search area, where to look for the type of articles in question.

- Another problem related to literature studies could be the number of studies cited from previous literature. By citing a high number of relevant earlier studies, the accuracy and correctness of the literature study increases.
- There is not much literature available on expanding sleeve/pin solutions for use in heavy machinery, nor comparisons with cylindrical pins. There is some literature on expanding sleeves (without axial cuts), about their function and fatigue life, especially within medicine and healthcare.
- [Paper IX](#) is a literature study about modelling techniques for mechanical joints, which might have coverage errors as described above, or too few citations, due to being the first paper in the PhD project, and the author's inexperience with writing scientific papers.

Introduction

2 Literature and theoretical background

There is not much literature available about expanding pin solutions used as alternatives to cylindrical clearance or interference fit shear pins in heavy machinery, although tapered pins with interference fit is widely used in different ways in the fields of aerospace, maritime and nuclear engineering, and in various machinery, with Berkani et al. [14] being one exception. The two first submitted and published articles [8,9] included in this thesis were written as literature studies, with focus on getting more knowledge about modelling techniques, fretting fatigue and wear in general, and specifically in mechanical pinned joints. The short versions of the two articles can be found in Chapter 4.3.

Although there is not much literature available on the expanding pin solutions used as shear pins for heavy machinery, there are examples of conical sleeves in pivot joints, and coned sleeves used in various applications. Andrzejuk et al. [15] analysed a conical sleeve, without any axial cuts or slits, on a pivot joint with axial force (as described by Salahshour et al. in Paper VI), where they evaluated energy dissipation of a friction pair on surfaces in contact, both experimentally and theoretically. In addition, they included structural friction, elastic, and frictional effects by considering Lamé's problem or theorem for thick-walled cylinders. The results from the study of Andrzejuk et al. [15] were compared with the work reported in Paper VI, where the FEA results for the sleeve, including contact pressure and radial stress, were close to the corresponding values calculated using the formulas for reference [15]. Ning et al. [16] studied the interference fit of a coned sleeve and the influence of various design factors on the contact pressure, such as cone sleeve length, cone friction coefficient, interference level and cone sleeve diameter. The coned sleeve in that study had no axial cuts, and the roller/sleeve fit tolerance was defined by calculating the allowable design minimum and maximum interference, which were based on minimum transmitted torque and material yield strength, respectively.

Tapered interference fits can eliminate the need for keyways, which can negatively affect the strength and efficiency of the joint. Zhao and Shang [17] developed a model and a numerical analysis to investigate the influence of the tapered part of a shaft on the interference fit between the shaft and the hub. Their results show that the taper plays an important role in relation to the interference fit. They performed numerical analysis and presented results for the influence of the taper on the radial and tangential stress, for both the propeller hub and shaft.

The basic formulas used or made references to in Papers I – IX are given and/or developed in Chapter 2.1 to 2.5 and are meant to give the readers some general information and basic knowledge.

2.1 Contact pressure in interference fit

The classical contact pressure, $-p-$, in an interference fit connection, presented in Paper VIII, under assumption of axis symmetry, infinitely long with hollowed shaft and hub of different materials, and plane stress as described by Childs [18] can be expressed in Equation (1) as:

$$p = \frac{\delta}{(2 \times b) \times \left[\frac{1}{E_o} \left(\frac{c^2 + b^2}{c^2 - b^2} + \nu_o \right) + \frac{1}{E_i} \left(\frac{b^2 + a^2}{b^2 - a^2} - \nu_i \right) \right]} \quad (1)$$

Where δ is the diametrical difference between bore and shaft, E_o and E_i are the elastic modulus for the bore and shaft respectively and ν_o and ν_i are the corresponding Poisson's ratios. The radii $-a-$, $-b-$, and $-c-$ are shown in Figure 2.1. If the two parts are made of same or similar materials, then $E_o = E_i = E$ and $\nu_o = \nu_i = \nu$, and the contact pressure can be expressed as indicated in Equation (2):

$$p = \frac{E \times \delta \times (c^2 - b^2) \times (b^2 - a^2)}{2 \times b \times 2 \times b^2 \times (c^2 - a^2)}, \quad (2)$$

where $-p-$ represents the interference pressure, $-o-$ and $-i-$ are subscripts for outer and inner components, $-E-$ the Young's modulus, $-\nu-$ Poisson's ratio, $-\delta-$ interference fit level, $-a-$ shaft inner radius, $-b-$ shaft outer and hub inner radius, and $-c-$ hub outer radius.

This formula for the interference or mating pressure, $-p-$, would not fully describe the mating pressure between an expanding pin solution, as illustrated in [Figure 1.11](#) with axially cut sleeves as in [Figure 1.12](#), and its supports, but it could give an indication of the relationship between interference pressure and Interference Fit Level (IFL). The sleeve has four axially cuts to ease the expansion, which means there are axial slots giving no or reduced contact between the sleeve (as a part of the pin assembly) and the hub. In addition, the sleeve (representing the shaft) is often a little shorter than the support (hub) thickness, of two reasons: (i) to prevent the sleeve to slide into the centre part area of the joint where it might be a bushing or bearing, and (ii) to ease the installation by having a "resting shoulder" that keeps the pin perfectly horizontal after installation, but before torquing. The load bearing pin in an expanding pin assembly could have a centre hole with its radius represented by $-a-$ in [Equations \(1\)](#) and [\(2\)](#), depending on the type and function of pin, but

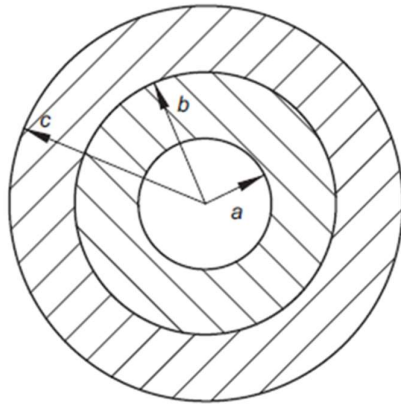


[Figure 2.1](#). An illustration of a cross-section of an interference fit

in general, it would be small, or not exist, which gives $a = 0$. The thickness of the support ($c - b$) in a pinned joint could also be varying, as for a pad eye shaped support. Although the pin and support materials often are different as described in Paper I, there is no significant difference in their elasticity modules and Poisson's ratios. By setting $a = 0$ into Equation (2), it can be expressed as described by Pedersen [19], and mentioned in Paper VIII, as Equation (3):

$$p_f = \frac{E \times \delta \times (c^2 - b^2) \times b^2}{2 \times (2 \times b) \times b^2 \times c^2} = \frac{E \times \delta_d}{2 \times D_f} \times \left(1 - \left(\frac{D_f}{D_h}\right)^2\right) \quad (3)$$

where $p_f = p$ (interference pressure), $\delta_d = \delta$ (interference fit level), $D_f = 2b$ (pin outer and support inner diameter), and $D_h = 2c$ (support outer diameter).

Several studies have indicated that the size of the interference fit level affects the risk of fatigue and fretting fatigue [20-22], and by choosing a desired interference fit level, the required interference pressure can be calculated, as indicated in Equations (1) - (3). In addition, the change of diameters and the tensile / compressive stresses of the outer / inner components can be found, and the maximum torque T which can be transmitted [18] is expressed in Equation (4):

$$T = 2fp\pi b^2 L = (p \times (2 \times b \times \pi \times L)) \times b \times f, \quad (4)$$

where $-T-$ is the maximum transmitted torque, $-f-$ is coefficient of friction, and $-L-$ length of interference fit.

The torque T can be used as an indication of how much an installed expanding pin assembly resist at each expended end before it starts rotating in the supports in a case where the bearing fails, locks to the pin and introduce the torque. The calculated interference pressure can also be used as input to calculate how much the pin assembly resists before starting to slide axially in the supports, if such loads are present.

Since Equation (3) might be inaccurate when calculating the interference pressure, or contact pressure, for an expanding pin solution, due to variations in support thickness and missing information about the interference fit level, the contact pressure can be calculated from a geometrical view, illustrated in Figure 2.2. The total axial tightening force - F_a - is equal to the total sum of tightening forces - F_i - from each tightening screw, or bolt, and the sum of both the axial and radial reaction forces depend also on the tapered angle - α - and the friction coefficients - μ_{fr} - on the surfaces in contact. The tightening force - F_a - results in the two normal forces - N_1 - and - N_2 -, where the subscripts 1 and 2 represent the contact surface pin-sleeve and sleeve-support, respectively.

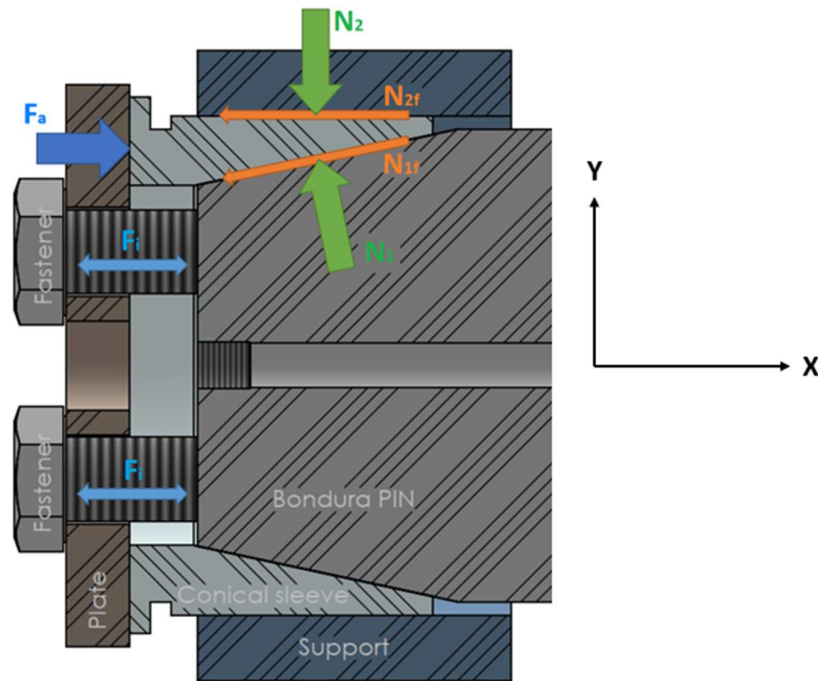


Figure 2.2. Forces in an expanding pin due to tightening

Reaction force N_1 can be decomposed into N_{1x} and N_{1y} , and N_{1f} into N_{1fx} and N_{1fy} . By summarizing all the forces in X-direction, and then Y-direction, the following relationships between the imposed tightening force – F – and the two normal forces – N_1 – and – N_2 – becomes clear, as given in Equation (5) and Equation (6):

$$N_1 = \frac{F_a}{2 \times \mu_{fr} \times \cos(\alpha) + (1 - (\mu_{fr})^2) \times \sin(\alpha)} \quad (5)$$

$$N_2 = N_1 \times [\cos(\alpha) - \mu_{fr} \times \sin(\alpha)] \quad (6)$$

The contact pressure, or stress, – p – between the sleeve and the support can easily be calculated, see Equation (7), when the normal force – N_2 – is calculated as indicated in Equation (6).

$$p = \frac{N_2}{A} = \frac{N_2}{D_f \times \pi \times L} \quad (7)$$

The calculated contact pressure – p – from Equation (7), can be applied in the Equations (1) and (3) to get an approximate *interference fit level* for an expanding pin solution, with the inaccuracies indicated earlier.

2.2 Hoop, and radial stresses

In an interference fit connection, whether it is a press-fit or a shrink-fit type of connection, the expansion of the hub results in both contact pressure at the surfaces in contact, radial and tangential / hoop stresses through the hub wall, as discussed in Paper VI. Equation (8) and Equation (9) are general for an open cylinder with both internal and external pressure as described by Collins, Busby and Staab [23], where (+) stress is tension, and (-) is compression.

$$\sigma_r = \frac{p_i \times a^2 - p_o \times b^2 + \frac{(a^2 \times b^2)}{r^2} \times (p_o - p_i)}{b^2 - a^2} \quad (8)$$

$$\sigma_t = \frac{p_i \times a^2 - p_o \times b^2 - \frac{(a^2 \times b^2)}{r^2} \times (p_o - p_i)}{b^2 - a^2} \quad (9)$$

where $-\sigma_r-$ represents radial stress at the hub, $-\sigma_t-$ tangential stress, $-p_o-$ outer pressure, $-p_i-$ inner pressure, $-a-$ hub inner diameter, $-b-$ hub outer diameter, and $-r-$ radius where stresses are calculated. In a situation with positive inner pressure, but zero outer pressure on the hub ($p_o = 0$), the formulas give:

$$\sigma_r = \frac{a^2 \times p_i}{b^2 - a^2} \times \left(1 - \frac{b^2}{r^2}\right) \quad (10)$$

$$\sigma_t = \frac{a^2 \times p_i}{b^2 - a^2} \times \left(1 + \frac{b^2}{r^2}\right) \quad (11)$$

$$\sigma_r + \sigma_t = \frac{2 \times a^2 \times p_i}{b^2 - a^2} = \text{constant} \quad (12)$$

From [Equation \(10\)](#) and [Equation \(11\)](#) it can be seen that both stresses will be lowest (absolute values) at the outer surface, $r = b$, with the radial stress equal to zero. Maximum radial stress (negative) and tangential hoop stress (positive) are found at the hub inner surface, $r = a$. [Equation \(12\)](#) states that the sum of the radial and tangential stress over the hub thickness is constant. A cylinder with closed ends, and internal pressure would have axial stresses in addition, but this was not included in the analysis and tests in [Paper VI](#).

2.3 Hertzian contact area and stress

The localized stress that develops when two curved surfaces come in contact and deform slightly, from an external imposed load is called

Hertzian contact stress, as briefly presented in Paper I, where contact stresses between pin and support, or cylinder inside cylinder, were compared for three different cases, (i) a new cylindrical pin, (ii) a used cylindrical pin, and (iii) an expanding pin solution. The contact footprint for two cylinders, no.1 on the top of no.2, as illustrated in Figure 2.3, is a rectangular area, with length $-L-$ and width $-2b-$ [23]. A situation with cylinder no.1 lying inside cylinder no. 2 is illustrated in Figure 2.4.

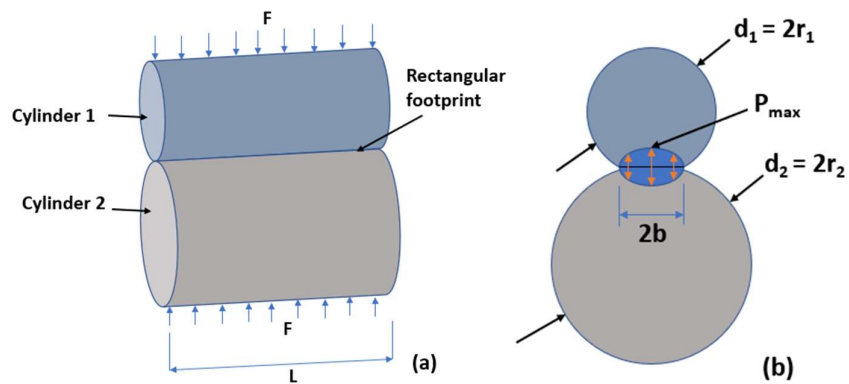


Figure 2.3. Two cylinders in contact, (a) side-view, and (b) cross-sectional view

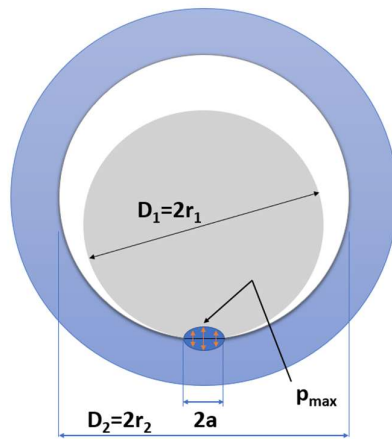


Figure 2.4. Cylinders-inside-cylinder contact

The equations for the half contact width – a –, the maximum contact stress – p_{max} –, and average contact stress – p_{av} – (Figure 2.4) are shown in Equation (13), Equation (14), and Equation (15), respectively, and applied in the attached Paper I. In a situation with a cylinder on top of another cylinder, as in Figure 2.3, the inverse of the bigger radius – $1/r_2$ – is added in Equation (13) instead of subtracted, and half the width is named – b – instead of – a –.

$$a = \sqrt{\frac{2 \times F \times \left(\frac{1 - \nu_1^2}{E_1} + \frac{1 - \nu_2^2}{E_2} \right)}{\pi \times L \times \frac{1}{2} \times \left(\frac{1}{r_1} - \frac{1}{r_2} \right)}} \quad (13)$$

$$p_{max} = \frac{2 \times F}{\pi \times a \times L} \quad (14)$$

$$p_{av} = \frac{F}{A_{contact}} = \frac{F}{2 \times a \times L} \quad (15)$$

2.4 Bolts, nuts, and threads

Bolts are widely used to connect two, or more parts, and for the expanding pin systems described in this thesis, the bolts are often called *tightening screws*, as long as their function is to push the sleeves axially. This is done to avoid confusion with the load bearing pin which often is called a bolt. Paper V describes the relationship between torque and resulting preload in a bolt. In addition, preloaded bolts were applied in the experimental tests described in Paper VII. A bolt system will normally consist of the bolt head and shank with threads as one part, and minimum one threaded nut as the second part. The shank can have a non-threaded and a threaded part, where the threads are described by the distance between each, the *pitch*, their *major* and *minor* diameters, or top-to-top and bottom-to-bottom thread diameters, respectively. In

addition, there are different shapes of the tread tops and bottoms (rounded, flat or acute angle), and different *lead angles*. The threads can be *coarse* which is common where repeated insertions and removals is expected, and *fine* threads are more resistant to self-loosening because of their smaller *helix angle*. The sum of the lead and helix angles is 90 degrees.

In a bolted connection, as for bolted flanges with standard bolt/nut system, it is vital to achieve the required preload in each bolt, to avoid or prevent bolt loosening, which is common in a system exposed to vibrations especially. There exist different methods how to control the preload, but not all are practically or economically possible. The most accurate methods require access to both bolt ends to measure the exact elongation, and then the axial bolt load can be calculated. A more practical, but less accurate method would be to control the applied torque on the nut, or bolt head.

The equations describing the relationship between the applied torque – T_i – and the resulting preload – F_i – for *squared threads* can be developed as indicated by the [Equations \(16\) to \(26\)](#) below, and [Figure 2.5](#), where the load is being lifted, which represents a nut or bolt tightening situation. For non-square threads the torque-preload relationship is described with the [Equations \(27\) to \(33\)](#) by Norton [24].

By summing up all the forces, in [Figure 2.5](#), in x and y directions the force – F – can be expressed as a function of the load – P –, the thread friction coefficient – μ_t –, and the lead angle – λ –. The friction force – f – is dependent of the contact force – N –, where $f = \mu_t N$.

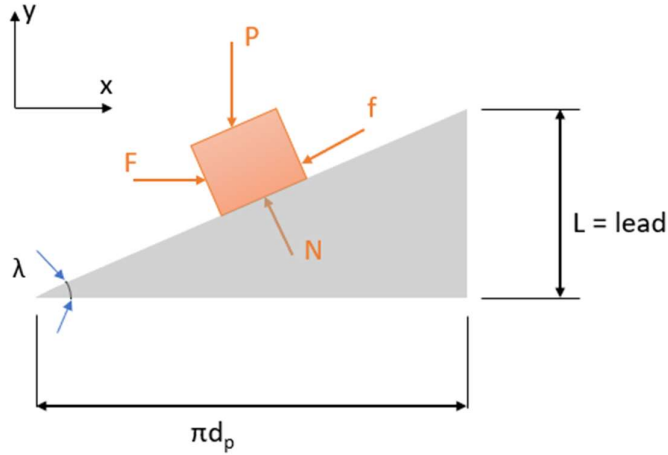


Figure 2.5. Lifting load – nut or bolt tightening on square threads

$$\begin{aligned} \sum F_x = 0 &= F - f \cos \lambda - N \sin \lambda \\ &= F - \mu_t N \cos \lambda - N \sin \lambda \end{aligned} \quad (16)$$

$$F = N(\mu_t \cos \lambda + \sin \lambda) \quad (17)$$

$$\begin{aligned} \sum f_y = 0 &= N \cos \lambda - f \sin \lambda - P \\ &= N \cos \lambda - \mu_t N \sin \lambda - P \end{aligned} \quad (18)$$

$$N = \frac{P}{(\cos \lambda - \mu_t \sin \lambda)} \quad (19)$$

By combining Equations (17) and (19) the expression becomes:

$$F = P \times \frac{(\mu_t \cos \lambda + \sin \lambda)}{(\cos \lambda - \mu_t \sin \lambda)} \quad (20)$$

The force – F – from [Equations \(20\)](#) and [\(21\)](#) is the required force to lift the load, and – d_p – is the pitch diameter. The required *thread tightening torque* – T_{tt} – becomes:

$$T_{tt} = F \frac{d_p}{2} = P \frac{d_p}{2} \times \frac{(\mu_t \cos \lambda + \sin \lambda)}{(\cos \lambda - \mu_t \sin \lambda)} \quad (21)$$

The torque can be rewritten into [Equation \(23\)](#) if taking geometrical relationship in [Equation \(22\)](#) into consideration.

$$\tan \lambda = \frac{L}{\pi d_p} \quad (22)$$

$$T_{tt} = P \frac{d_p}{2} \times \frac{(\mu_t \pi d_p + L)}{(\pi d_p - \mu_t L)} \quad (23)$$

The torque – T_{tt} – represents the required thread tightening torque, and d_b is the mean bearing, or bolt head, contact diameter, but in addition ([Equation \(24\)](#)) the required *bearing tightening torque* – T_{tb} – must be defined.

$$T_{tb} = \mu_b P \frac{d_b}{2} \quad (24)$$

The required total tightening torque – T_T – to lift the load – P – is the sum of the thread and bearing torques, – T_{tt} – and T_{tb} –, and can be expressed as [Equation \(25\)](#).

$$T_T = T_{tt} + T_{tb} = \frac{P d_p}{2} \times \frac{(\mu_t \pi d_p + L)}{(\pi d_p - \mu_t L)} + \mu_b P \frac{d_b}{2} \quad (25)$$

A formula for lowering the load, which represents the nut or bolt loosening, can be developed the same way, but then the force – F – and the friction force – f – switch sides in [Figure 2.5](#), and the formula for the required total loosening torque ([Equation \(26\)](#)) – T_L – becomes the sum

of the thread loosening torque – T_{lt} – and bearing loosening torque – T_{lb} –:

$$T_L = T_{lt} + T_{lb} = \frac{Pd_p}{2} \times \frac{(\mu_t \pi d_p - L)}{(\pi d_p + \mu_t L)} + \mu_b P \frac{d_b}{2} \quad (26)$$

From [Equations \(25\)](#) and [\(26\)](#) it can be concluded that it requires less force to lower the load, T_L , than to lift it, T_T , which means lower torque to loosen a bolt or nut, than to tightening it. The – L – is subtracted instead of added in the numerator for the loosening formula, and the – $\mu_t L$ – is added instead of subtracted in the denominator, and both these differences reduce the loosening torque – T_L – compared to the tightening torque – T_T –.

The above formulas for tightening and loosening torques are based on square screw threads. In a situation where the threads are non-square but have a thread angle – α –, the formulas for the tightening and loosening torques become slightly different. [Figure 2.6](#) illustrates the shape of such a thread indicating the radial angle.

The shape of the thread changes the direction of the normal force from N when the angle $\alpha = 0$ to $N \cos \alpha$ when $\alpha > 0$, in [Equations \(16\)](#) and [\(18\)](#).

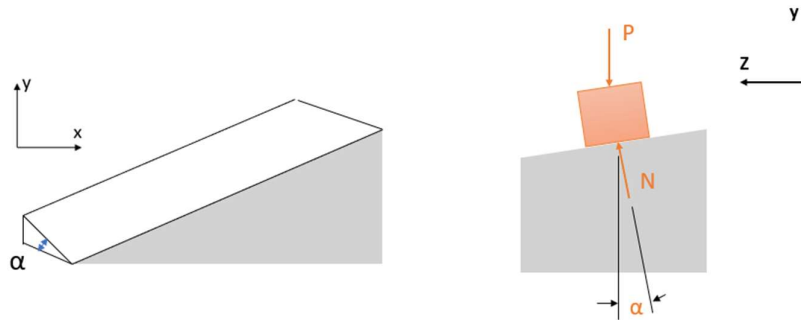


[Figure 2.6](#). Thread shape with radial angle

F and f are not affected by the angle α . Equation (16) can be re-written into Equation (27).

$$\sum F_x = 0 = F - f \cos \lambda - (N \cos \alpha) \sin \lambda \quad (27)$$

The total *tightening* and *loosening* torque, $-T_{T\alpha}$ and $-T_{L\alpha}$, for a bolt/nut with tread angle $\alpha > 0$ can then be expressed by Equations (28) and (29):

$$T_{T\alpha} = \frac{P d_p}{2} \times \frac{(\mu_t \pi d_p + L \cos \alpha)}{(\pi d_p \cos \alpha - \mu_t L)} + \mu_b P \frac{d_b}{2} \quad (28)$$

$$T_{L\alpha} = \frac{P d_p}{2} \times \frac{(\mu_t \pi d_p - L \cos \alpha)}{(\pi d_p \cos \alpha + \mu_t L)} + \mu_b P \frac{d_b}{2} \quad (29)$$

The torque required to reach a certain preload is described in Equation (28), but the relationship can be generalized and simplified by substitute Equation (22) into Equation (28), as described in Equation (30), (31), and (32).

$$T_{T\alpha} = \frac{P d_p}{2} \times \frac{(\mu_t \pi d_p + (\tan \lambda \pi d_p) \cos \alpha)}{(\pi d_p \cos \alpha - \mu_t (\tan \lambda \pi d_p))} + \mu_b P \frac{d_b}{2} \quad (30)$$

This can be generalized and simplified to:

$$\begin{aligned} T_i &= F_i \frac{d}{2} \times \frac{(\mu_t + \tan \lambda \cos \alpha)}{(\cos \alpha - \mu_t \tan \lambda)} + F_i \frac{(1 + 1.5)d}{4} \mu_b \\ &= k F_i d, \end{aligned} \quad (31)$$

where $-d_p-$ is the pitch diameter, which is set equal to bolt diameter $-d-$, and $-d_b-$ is bearing diameter which is set equal to the average of the bolt diameter and standard head size of $1.5d$, and

$$k_i \cong 0.5 \frac{(\mu_t + \tan\lambda \cos\alpha)}{(\cos\alpha - \mu_t \tan\lambda)} + 0.625\mu_b \quad (32)$$

– k_i – is called the *torque coefficient*, which is an approximate factor, but commonly used to calculate resultant preload in a torqued bolt system.

For a specific thread type (fixed – α – value) the k-value is affected by changes in the friction coefficients, thread diameter and thread pitch, which are represented by the $\tan\lambda$ value.

Calculations show that a 10% reduction of thread friction coefficient μ_t , bearing (under head) friction coefficient – μ_b –, pitch diameter d_p , and pitch (lead) value L , results in changes of the k-value of -4%, -5%, +1%, and -1%, respectively. There are various approaches to find an approximate value for the relationship between the torque of the nut and the resulting shank tension, and two of them are based on the standard DIN 946, the German VDI 2230 [25], the work of Motosh [26], and Bickford [27] (Equation (33)).

$$T_{in} = F_p \left[\frac{P}{2\pi} + \frac{\mu_t r_t}{\cos\beta} + \mu_n r_n \right] \quad (33)$$

Equation (34) is based on DIN 946 / VDI 2230.

$$M_A = F_v \left[0.159 \times P + 0.578 \times d_2 \times \mu_G + \frac{D_{Km}}{2} \times \mu_K \right] \quad (34)$$

These two expressions, (33) and (34), are equal when $\beta = 30^\circ$, $\mu_t = \mu_G$, $r_t = d_2/2$, $\mu_n = \mu_K$, $r_n = D_{Km}/2$, $F_p = F_v$, and $T_{in} = M_A$, which give:

	Equation 33:	Equation 34:
First term	$F_p [P/2\pi]$	$F_v [0.159 \times P]$
Second term	$F_p [\mu_t \times r_t / (\cos\beta)]$	$F_v [0.578 \times d_2 \times \mu_G]$
Third term	$F_p [\mu_n \times r_n]$	$F_v [\mu_K \times (D_{km}/2)]$

The angle – β – is the angle between the thread side and an imaginary plane perpendicular to the bolt shank axis, and the value of $\beta = 30^\circ$ corresponds with most V-threads, including ISO, NTP and UTS. With the given assumptions, [Equations \(33\)](#) and [\(34\)](#) are equal. [Equation \(35\)](#) is presented in [Paper VII](#):

$$\begin{aligned} T &= \frac{F_p}{2} \left[\frac{(\mu_n \times d_n)}{\sin 30} + 1.155 \times \mu_t \times d_t + \frac{P}{\pi} \right] \\ &= F_p \left[\frac{P}{2\pi} + 0.578 \times d_t \times \mu_t + \frac{\mu_n \times r_n}{\sin 30^\circ} \right] \end{aligned} \quad (35)$$

The calculations above show that the expression in [Equation \(35\)](#) is identical with the two previous, [Equation \(33\)](#) and [Equation \(34\)](#), as long as $d_t = d_2$, with the only exception of the $\sin 30^\circ$ value, which represents the coned contact area between the locking nut and the main nut.

2.5 Strain gauges, strains, and stresses

Normal stress calculations based on theoretical values:

The normal stress in a bar in axial tension, as illustrated in [Figure 2.7](#), can be calculated according to the [Equations \(36\) – \(39\)](#), from Norton [\[24\]](#):

$$\sigma = \frac{F}{A}, \quad (36)$$

where – F – is tension force, and – A – is the minimum cross-sectional area of the bar.

When the minimum cross-sectional area is through a threaded area, the cross-sectional area can be expressed by [Equation \(37\)](#):

$$A = \frac{\pi}{4} \times \left[\frac{d_p + d_r}{2} \right] = \frac{\pi}{4} \times [d - 0.93815 \times p]^2 \quad (37)$$

where d_p – is the pitch diameter, d_r – the minor diameter, d – the mayor diameter, or pin diameter, and p – is the pin thread pitch.

For ISO threads the following relationships are given:

$$d_p = d - 0.649519 \times p \quad (38)$$

$$d_r = d - 1.226869 \times p \quad (39)$$

The tensile area is reduced compared to the area represented by the pitch diameter. Studies indicate that an average between the pitch and minor diameters represents better the tensile area.

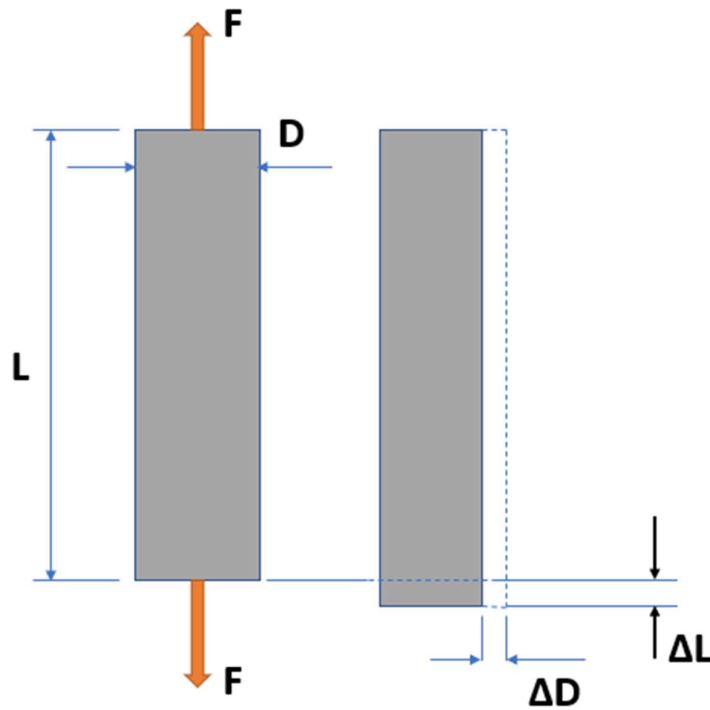


Figure 2.7. An illustration of a bar in axial tension

Strain gauges are widely used to register strains due to external load, heating or cooling etc, and further to calculate the resulting stresses. In a pin or bolt it can be of interest to measure strains due to radial shear loads or axial tension loads. The normal stress – σ [N/mm²] – from pure axial tension of a bar, as illustrated in [Figure 2.7](#), can be expressed as [Equation \(36\)](#). The change of length of the bar – ΔL – due to the axial tension – F – is shown in [Figure 2.8](#), and can be expressed with [Equation \(40\)](#):

$$\Delta L = \frac{FL}{AE} \quad (40)$$

where – L – represents the loaded length of the bar, and – E – represents the Young's modulus for the material.

Strain – ε [-] – can be expressed as the elongation in x-direction, over the original length, as shown in [Equation \(41\)](#) and the force required to reach a specific elongation is indicated in [Equation \(42\)](#):

$$\varepsilon = \varepsilon_x = \frac{\Delta L}{L} = \frac{\left(\frac{F \times L}{AE}\right)}{L} = \frac{F}{A \times E} \quad (41)$$

$$F = \varepsilon_x \times A \times E \quad (42)$$

In addition, the bar elongated in x-direction will also contract in transversal direction, which can be calculated with the actual Poisson's ratio, typically with an absolute value around 0.3 for steel.

The relationship between the tensioning or force applied on a bar and its change in cross-sectional area, is vital in how strain gauges work.

The basic configuration of strain gauge contains typically a supporting foil, resistance wires, connections, adhesive joint, and object of measurement, often a mechanical component like a load pin. When the object of measurement is exposed to a load, it will deform, and the cross-sectional area of the resistant strain gauge wire will then also be changed

and thereby also the ohmic resistance, or its resistance to the flow of electric current measured in ohms. Such changes in ohmic resistance are recorded and the required strain for reaching the change in resistance, defined.

A schematic view of strain gauge strings measuring *shear strains* in a pin cross-section is illustrated in Figure 2.8. The strings are positioned at $\pm 45^\circ$ angle to the load, F . One set of strings gets elongated, and the other compressed, as shown.

The average shear stress τ_a over the pin cross-section, for a pin as illustrated in Figure 1.10 can be expressed as the force F divided by the total cross-sectional area A , as shown in Equation (43).

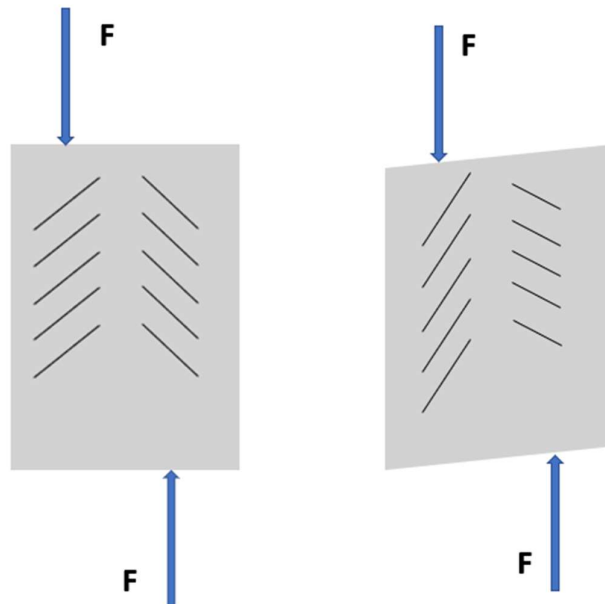


Figure 2.8. An illustration of strain gauge strings under deformation

$$\tau_a = \frac{F}{A} \quad (43)$$

The strain values measured at $\pm 45^\circ$, $-\varepsilon_{45^\circ}[-]$, may be taken to calculate the average shear stress $-\tau_a-$ over the pin cross-section, as shown in [Equation \(44\)](#).

$$\tau_a = 2 \times \varepsilon_{45^\circ} \times G, \quad (44)$$

where $-G-$ represents the shear modulus.

The equations developed and presented in this chapter are applied and cited to, later in this thesis.

3 Research Methodology and Materials

3.1 General

Different research approaches were applied to accomplish the defined objectives of this thesis, such as (a) *questionnaire-based surveys* among relevant stakeholders, (b) *experimental tests*, and (c) *literature studies* on modelling techniques for mechanical joints, fretting fatigue and wear, in addition to self-loosening of bolts. In addition, some (d) *analytical approaches* and *numerical analysis* of type FEA were conducted.

A typical and generalized procedure to reach the defined objectives can be described as:

- (i) Identifying the research area of interest
- (ii) Defining the research objectives
- (iii) Performing a literature study
- (iv) Selecting data collection techniques
- (v) Collecting the desired and required data
- (vi) Analysing the collected data, and define the results
- (vii) Discussing the results
- (viii) Drawing conclusions from the results
- (ix) Presenting the results

3.2 Questionnaire-based survey

This chapter relates to the work presented in [Paper I](#) and [IV](#). The main questionnaire-based survey gave an excellent opportunity to communicate directly with a wide range of stakeholders related to the specification, design, calculation, production, assembly, use and service/repair/maintenance of heavy machinery with clearance fit and expanding pin systems. The survey was sent as pdf file by e-mail to 256

potential stakeholders, where 140 were based in Norway and 116 in other countries. The questionnaire contained various questions organized in six main sections:

- (1) Size of company
- (2) Company profile
- (3) How long the company applied, specified, or worked with expanding pin technology
- (4) On which type of market and equipment the company applied the technology
- (5) Whether the company is using own designed expanding pin or from others
- (6) Effects and consequences of applying expanding pin solutions

Sections 4 and 6 contained the main questions, where section 4 contained 9 segments regarding types of machines and equipment used by the different industries. Section 6 contained 15 segments with options for effects and consequences of use of expanding pins compared to standard clearance type of pins. The complete questionnaire is added in Appendix A.

A minor survey among a few energy companies placed in Norway was also performed in relation to a safety study involving equipment and personnel at the Norwegian shelf, as presented in [Paper IV](#). The main survey was implemented according to the generalized procedure indicated above. The options for answers were given in the questionnaire (closed-ended answers), but with an additional option for comments, or open-ended answer.

- (i) Identify the research area of interest:

The research area of interest was defined from the beginning of the PhD study named “Effect and consequence analysis regarding expanding PIN-technology in various types of heavy machinery”. One way to get

such information was to perform a questionnaire-based survey among certain stakeholders with a close relationship to the technology in question. They summarize the information needed to be extracted from the defined stakeholders.

(ii) Define the research objectives:

The research objectives, both general and specific, are listed in Chapter 1.1.4 and The corresponding research questions are presented in Chapter 1.2

(iii) Perform a literature study:

A short literature study on questionnaire surveys [11-13,28-31] was performed to learn more about the background, history, techniques, advantages and disadvantages of such surveys, before starting up the survey itself.

(iv) Select data collection techniques:

At the time of selecting the data, the pandemic COVID-19 broke out, and companies both in Norway, Europe and many other countries started to relocate their employees, typically to home office solution, making them take outstanding vacation days, reducing their presence at the office, or even terminate their contracts. The best, and almost only way to go forward with the survey at that point was by running an e-mail-based dispatch of the questions, in addition to some phone-based follow up activities. The specific stakeholders of interest were defined from the company Bondura's client lists, partner's contact information, and web searches on companies with relationship to heavy machinery, in addition to contact information received during the survey.

(v) Collect the desired and required data:

The questionnaire was sent to the potential responders in pdf format, by e-mail, and most of those who responded also responded by filling out

the questionnaire and e-mailed it back, but a few persons preferred to deliver the required information by phone, or as a written “story” in an e-mail without the pdf attachment.

(vi) Analyse the collected data, and define the results:

All data received as feed-back from the responders were put into a excel sheet with all survey sections on the horizontal axis and responders on the vertical axis. In combination with filter functions, it became possible to analyse the received data and find possible correlations between the sections.

(vii) Discuss the results:

Based on the analysis referred to in (vi) the results could be discussed, see also Chapter 4 (Results and Discussions).

(viii) Draw conclusions from the results:

Based on the analysis referred to in (vi) and discussions referred to in (vii), some conclusions could be drawn, see also Chapter 5 (Conclusions and Future Outlook).

(ix) Present the results:

The results of the questionnaire-based survey were published in [Paper I](#) and [Paper IV](#), in addition to this PhD Thesis.

There are, according to Batinic et al. [11], four traditional sources of error in questionnaires or sample surveys:

- *Coverage error*: This is a mismatch, differences or not being a one-to-one correspondence between the target population or potential respondents, and the sampling frame. For example, suppose a researcher is using LinkedIn to determine the

Norwegian voters' opinion about the energy crisis in Europe. Because not all voters are LinkedIn users and not all LinkedIn users are voters, there will be a mismatch that results in coverage errors.

- *Sampling error*: This is a kind of error that occurs when the sample used is not representative for the whole population, and the obtained results could then differ from the results that would be obtained from the entire population. For example, the researcher in the previous example asks only those who have bought a Tesla car, which are just a small segment of the total potential voters. Increasing the sample size and use of more random sampling can reduce the problem.
- *Measurement error*: Such errors can typically be caused by interviewers, respondents, data processors, or other personnel participating. It could be poor question wording, poor interviewing, survey mode effects etc.
- *Nonresponse error*: Error due to people from the sample not responding to the survey, who, if they had responded would have provided different answers and different final survey results.

3.3 Experimental tests

Several of the articles in this PhD thesis are based on experiments performed both at the UiS premises, and at external locations, and those can be found in:

- (a) [Paper II](#) - An investigation of the effects and consequences of combining Expanding Dual Pin with radial spherical plain bearings
- (b) [Paper III](#) - A novel technique for temporarily repair and improvement of damaged pin joint support bores

- (c) [Paper V](#) - Study of Bondura® Expanding PIN System – Combined Axial and Radial Locking System
- (d) [Paper VI](#) - Experimental and Numerical Studies of Stress Distribution in an Expanding Pin Joint System
- (e) [Paper VII](#) - Comparative study on loosening of anti-loosening bolt and standard bolt system

Different experiments were performed for different studies, as described in Chapters 3.3.1 – 3.3.5 below, to achieve the different research objectives described in Chapter 1.1.4. The five tests are mainly experimental, with some numerical and analytical analysis included.

3.3.1 An investigation of the effects and consequences of combining Expanding Dual Pin with radial spherical plain bearings

This chapter relates to the work presented in [Paper II](#). The objective of this research was to investigate possible changes in the required rotational moment between the two bearing rings, due to shape and diameter changes of the inner ring of a radial spherical plain bearing (RSPB), and as a function of the expanding pin's tightening torque. The expansion of the inner ring was measured by a CMM, and the rotational moment of the bearing with two separate hydraulic jacks, the first loaded the bearing and the second forced the bearing inner ring to rotate.

The expansion of the inner rings and the required rotational moment of the bearings were measured for four different test configurations, (i) two inner rings mounted on two expanding sleeves (one inner ring on each sleeve) without external load, and (ii) one single inner ring mounted on two expanding sleeves (one inner ring on both) without external load, (iii) two complete bearings mounted on two expanding sleeves (one

bearing on each sleeve) with external load, and (iv) one complete bearing mounted on two expanding sleeves (one bearing on both) with external load, as illustrated in [Figure 3.1](#).

Expansion of the inner rings in configurations (i) and (ii) are achieved by torquing the pin, and measure with CMM. The rotational moments in (iii) and (iv) are achieved by external loads on the U-blocks, force the distribution bar to lift, measure the required force and calculate the required moment.

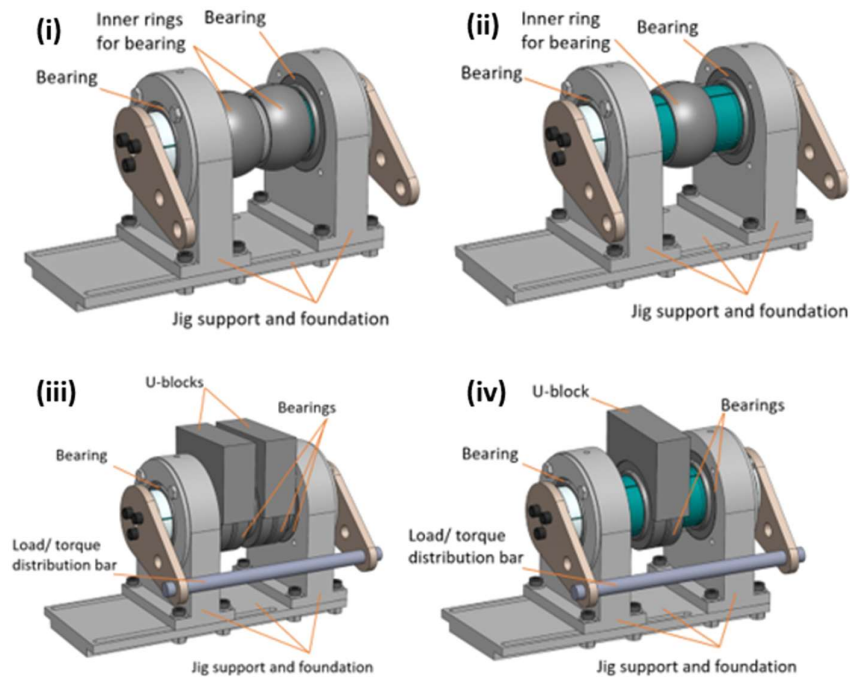


Figure 3.1. Test configuration (i) expansion of two rings with two sleeves - Test 1a (non-lubricated & lubricated), (ii) expansion of one ring with two sleeves – Test 1b (non-lubricated & lubricated), (iii) rotation with two rings on two sleeves – Test 2a, and (iv) rotation with one ring on two sleeves – Test 2b

Materials used:

The experimental test of each pin and bearing system has the following items, as partly illustrated in [Figure 3.1](#):

Test material – configuration (i):

- Separate inner rings of RSPB, type GE 80 ES (steel/steel), 2 pcs
- Complete RSPBs of type GE 80 ES (steel/steel), 2 pcs
- Bondura Expanding Pin System of type Dual 66 (1 load bearing pin, 2x2 sleeves, 2 end plates, set screws, inner sleeve tightening screws and outer sleeve tightening screws), 1 pc
- Distance rings (small), 3 pcs

Test material – configuration (ii):

- Separate inner ring of RSPB, type GE 80 ES (steel/steel), 1 pc
- Complete RSPBs of type GE 80 ES (steel/steel), 2 pcs
- Bondura Expanding Pin System of type Dual 66 (1 load bearing pin, 2x2 sleeves, 2 end plates, set screws, inner sleeve tightening screws and outer sleeve tightening screws), 1 pc
- Distance rings (wide), 2 pcs

Test material – configuration (iii):

- Complete RSPBs of type GE 80 ES (steel/steel), 4 pcs
- Bondura Expanding Pin System of type Dual 66 (1 load bearing pin, 2x2 sleeves, 2 end plates, set screws, inner sleeve tightening screws and outer sleeve tightening screws), 1 pc
- Distance rings (small), 3 pcs
- U-blocks, 2 pcs

Test material – configuration (iv):

- Complete RSPBs of type GE 80 ES (steel/steel), 3 pcs

- Bondura Expanding Pin System of type Dual 66 (1 load bearing pin, 2x2 sleeves, 2 end plates, set screws, inner sleeve tightening screws and outer sleeve tightening screws), 1 pc
- Distance rings (wide), 2 pcs
- U-block, 1 pc

The same complete test jig was used for all four tests. In addition, a CMM (Zeiss) machine was used to measure the radial expansion of the inner rings, for the tests with configuration (i) and (ii). For the tests with configuration (iii) and (iv) a 100 metric tonnes capacity hydraulic load cylinder (Enerpac) was applied to put load on the U-blocks (as external loads), and a 10 metric tonnes jack with transducer was applied to put force to the crossbar (Load / torque distribution bar) and make the pin assembly to rotate, and also measure the required force.

Experimental setup and test procedure:

The experimental tests were performed at two different locations, at two different points of time. The tests with configuration (i) and (ii) were performed first (at UiS), and thereafter (iii) and (iv) (at external premises), according to the following procedures:

Configuration (i) for Test 1a:

- The test setup illustrated in [Figure 3.1 \(i\)](#) was installed into the CMM and fixed to the table to avoid any relative movements between the jig and the machine.
- The tightening screws at each pin end were torqued from 10 to 70 Nm, in steps of 5 Nm when the sleeves *were not lubricated*, and torqued to 10, 20, 30, 50 and 70 Nm *when lubricated*.
- The diameters of the inner rings were measured and recorded for each 10° angular distance around the ring, at 4 different ring sections, at -25 mm, -5 mm, +5 mm, and +25 mm compared to the ring centre (lubrication hole centre). The sections were named (a), (b), (c) and (d), respectively, illustrated in [Figure 3.2](#).

Configuration (ii) for Test 1b:

- The test setup illustrated in [Figure 3.1 \(ii\)](#) was installed into the CMM and fixed to the table to avoid any relative movements between the jig and the machine.
- The tightening screws at each pin end were torqued from 10 to 40 Nm, in steps of 5 Nm, and thereafter to 50, 60 and 70 Nm when the sleeves were not lubricated, and torqued to 10, 20, 30, 50 and 70 Nm when lubricated.
- The diameters of the inner rings were measured and recorded for each 10° angular distance around the ring, at 4 different ring sections, at -25 mm, -5 mm, +5 mm, and +25 mm compared to the ring centre (lubrication hole centre). The sections were named (a), (b), (c) and (d), respectively, illustrated in [Figure 3.3](#).

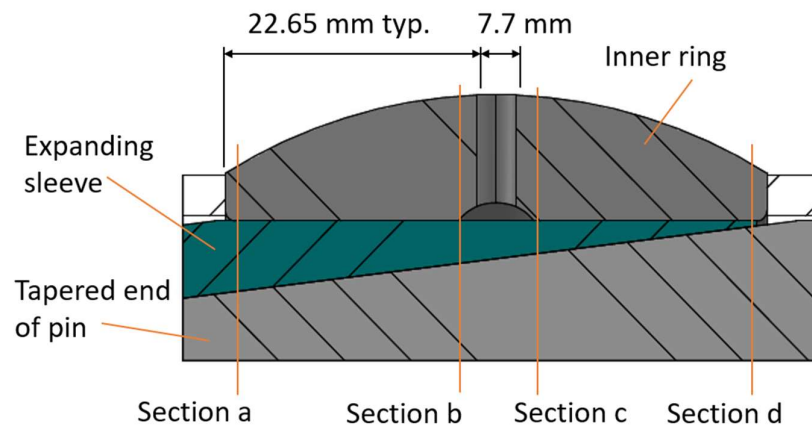


[Figure 3.2](#). Inner ring on single sleeve, with sections (a) to (d), from configuration (i)

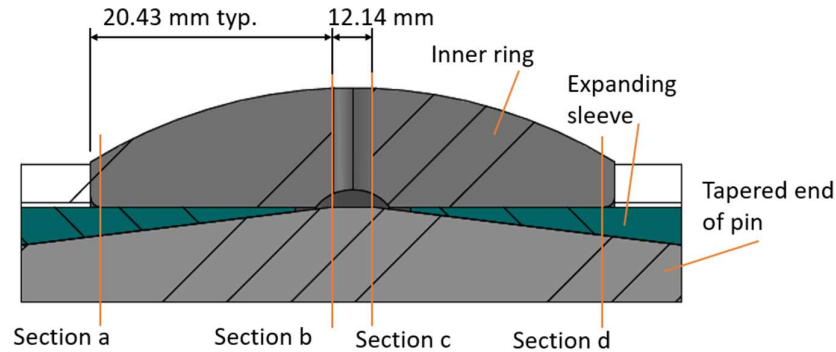


Figure 3.3. Inner ring on double sleeve, with sections (a) to (d), from configuration (ii)

Configuration (iii) for Test 2a:

- The test setup illustrated in [Figure 3.1 \(iii\)](#) was installed into a 100 metric tonnes capacity hydraulic cylinder, to load the bearing with an external vertical load.
- The hydraulic cylinder loaded each centre bearing from 0 to 400 kN (0 – 800 kN in total for both bearings), in steps of 50 kN, but dependent of torque values.
- For each external load level, included 0 kN, the tightening screws of the expanding pin was torqued, and the sleeves introduced an outward radially directed force into the bearing inner ring.
 - o From 0 to 400 kN the pin was torqued to 5 Nm
 - o From 200 kN to 400 kN the pin was torqued to 25, 45 and 65 Nm
- For each combination of external load level and torque level, a 10 metric tonnes capacity hydraulic cylinder was applied to force the distribution bar to move upwards, and the maximum forces required to turn the bearing were measured and recorded for calculation of the required rotational moment.

Configuration (iv) for Test 2b:

- The test setup illustrated in [Figure 3.1 \(iv\)](#) was installed into a 100 metric tonnes capacity hydraulic cylinder, to load the bearings with an external vertical load.
- The hydraulic cylinder loaded the centre bearing from 50 to 400 kN, in steps of 50 kN.
- For each external load level, the tightening screws of the expanding pin was torqued, and the sleeves introduced an outward radially directed force into the bearing inner ring. Then the pin was torqued from 5 to 65 Nm, in steps of 10 kN.
- For each combination of external load level and torque level, a 10 metric tonnes capacity hydraulic cylinder was applied to force the distribution bar to move upwards, and the maximum forces required to turn the bearing were measured and recorded for calculation of the required rotational moment.

Detailed cross-sections through bearing centre for configurations (iii) and (iv) are illustrated in [Figure 3.4](#). The (a) shows only one of the bearing-sleeve connections, for simplicity purpose.

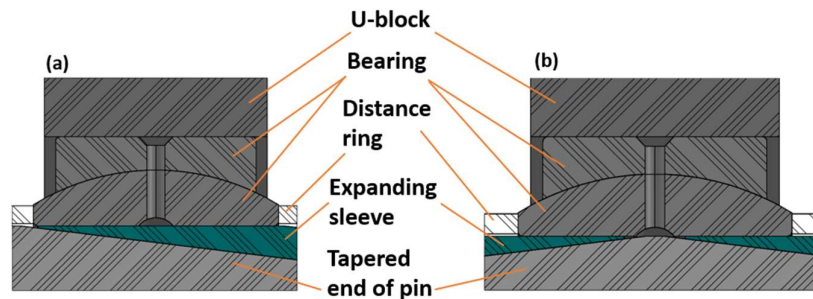


[Figure 3.4](#). Bearings with U-blocks on expanding sleeves, (a) configuration (iii), and (b) configuration (iv)

3.3.2 A novel technique for temporarily repair and improvement of damaged pin joint support bores

This chapter relates to the work presented in [Paper III](#). The objective of this research was to investigate a new technique for temporarily repair of worn and damaged support bores where standard cylindrical pins have been applied ([Figure 3.5 \(a\)](#)) by comparing possible options for further operation, including use of expanding pin systems ([Figure 3.5 \(b\)](#)). Increasing clearance between the pin and the support bores results in larger movements relatively between pin and supports in radial direction, but also often in axial direction in addition to possible rotational movements. The initial installation clearance from the first installation of a fabric new pin in new support bores increases over time and the process could be accelerating. Repairing damaged supports are time consuming and involves direct costs in repair and materials, and indirect costs in unwanted and often unplanned downtime.

The worn or damaged support bore was 3D scanned and a temporarily repair insert was 3D printed ([Figure 3.5 \(c\)](#)), installed, and tested in a hydraulic load machine. Strain gauges were attached to both a standard cylindrical pin and an expanding pin to measure strains under external loads.

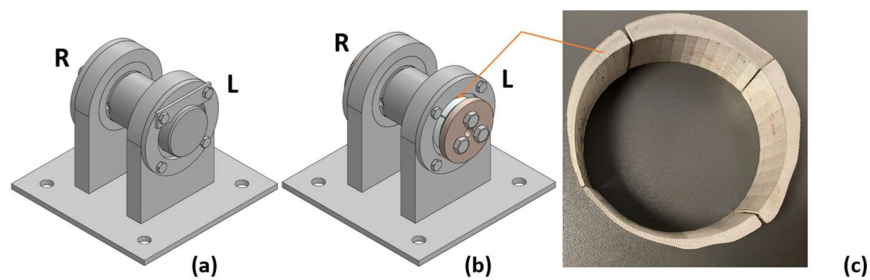


Figure 3.5. Test equipment, with (a) the cylindrical pin, (b) expanding pin, and (c) 3D printed boss at left (L) support of the expanding pin

Materials used:

The experimental test of each expanding pin system has the following items, as partly illustrated in [Figure 3.5](#).

Expanding pin system:

- 1 pc of load bearing pin, Ø88 mm diameter, h7, R_a 3.2, with weakening grooves and prepared surface for strain gauges, R_a 0.4. Pin material was of material quality EN 1.4418 – high strength stainless steel. Sleeves and endplates were of material quality S355, and the tightening screws 8.8.
- 2 pcs of expanding end sleeves to fit the pin conical ends
- 2 pcs of endplates
- 6 pcs of tightening screws
- 4 pcs of strain gauges of type FCA-1-11-1LJB (fish bone type) with corresponding cables

Standard cylindrical pin:

- 1 pc of load bearing pin, Ø88 mm diameter, h7, R_a 3.2, with weakening grooves and prepared surface for strain gauges, R_a 0.4. Pin material was EN 1.4418 – high strength stainless steel.
- 1 pc of positioning/locking plate, for preventing the pin from rotating, S355 material.
- 4 pcs of strain gauges of type FCA-1-11-1LJB (fish bone type) with corresponding cables

In addition, the following were used:

- A test jig as shown in [Figure 3.5 \(a\)](#) and [\(b\)](#)
- 1 pc of 3D printed repair insert of material Inconel 625 for the expanding pin system
- 1 additional expanding sleeve, oversize, for the expanding pin system

- The glue was of type CN Single component room-temperature-curing (Cyanoacrylate)
- The strain gauge measurement system was equipped with an amplifier of the type QuantumX MX1615B, and data is processed by a CATMAN software
- The load tests were performed in a jig with a Enerpac CLP 100-ton capacity hydraulic cylinder, and a RTN 470-ton capacity load cell
- In addition, a handheld scanner of model HandySCAN 700TM was used for the scanning purpose, a CAD program (Autodesk Inventor®) for processing digitally the scanned information and convert the data into the required drawing of STL file format, and a 3D printer machine and sintering machine were of brand Markforged.

Experimental setup and test procedure:

The quality of the functionality of the repaired pin joint was investigated by comparing measured strains at the joint, in 5 different test cases:

Test 1: a standard cylindrical pin with even distributed wear (0.9 mm play at the diameter, at each end)

Test 2: a cylindrical pin with additional severe wear and ovality at one end (0.9 mm play at one end, and up to 5.9 mm at the other)

Test 3: an expanding pin with even distributed wear (0.0 mm play at the diameter, at each end)

Test 4: an expanding pin with additionally severe wear and ovality at one end (0.0 mm play at one end, and up to 5.0 mm at the other)

Test 5: an expanding pin with repaired support at the damaged end (0.0 mm play at the diameter, at each end)

The strain gauges were placed at the groove weakening sections, which were 6 mm wide with a 3 mm radius, and 7.5 mm depth. The minimum cross-sectional diameter at the centre of each groove was 73 mm, as illustrated in Figures 3.6 and 3.7. In total there were 4 strain gauges per pin, two at each end, placed at 180° distance, named (a), (b), (c), and (d).

The standard cylindrical pin was installed into the test jig and locked into position with the position plate. The expanding pin system was installed into the test jig and wedge-locked to the support bores by torquing the tightening screws, which pushed sleeves to move axially and expand radially.

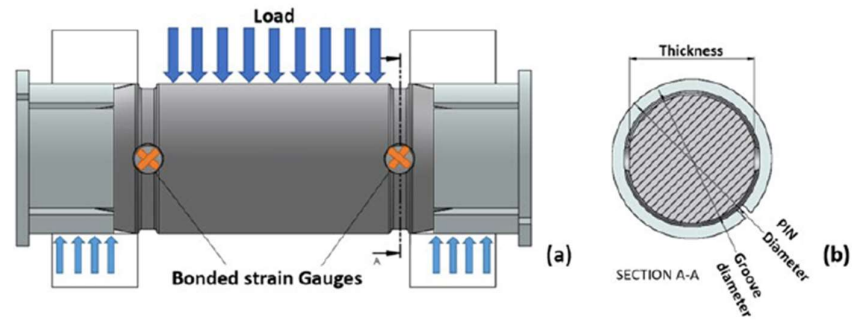


Figure 3.6 Strain gauges on loaded expanding pin, (a) at 0° position, and (b) cross-sectional area at grooves

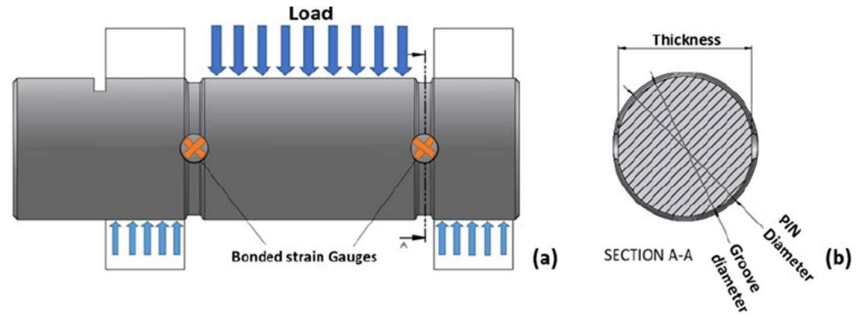


Figure 3.7 Strain gauges on loaded cylindrical pin, (a) at 0° position, and (b) cross-sectional area at grooves

The pins were loaded externally above each weakening groove, with the above-mentioned hydraulic cylinder, to achieve shear only, and avoid any strains from bending of the pins. The external load was applied in steps of 100 kN tons, from 100 to 500 kN, and the strains measured. The strains at each of the 4 strain gauges were measured, at 0° and 15° pin positions. The 0° position was defined as “when the external load was perpendicular to the plan with the 4 strain gauges”.

3.3.3 Study of Bondura® Expanding PIN System – Combined Axial and Radial Locking System

This chapter relates to the work presented in [Paper V](#). The objective of this research was to investigate the maximum possible preload achieved with the combined axial and radial locking pin and evaluate the shear capacity of a parallel plate, or joint, or joint in connected flanges, using that pin system (Norwegian patent number 344779), which combines the preload bolt and expanding pin characteristics, also illustrated in [Figure 3.8](#). The results were compared with theoretical values by use of standard preloaded bolts.

The *axial preload* bolt capacity creates surface contact pressure between the parallel plates, in addition to the contact pressure between bolt head and plate, and nut and plate. The *radially expanding* pin capacity locks the pin assembly to each of the parallel plates and prevents or reduces the possibility of sliding of the plates relatively to each other, in addition to eliminate the possibility of sliding, radially, axially, or rotationally between bolt head – plates – nut ([Figure 3.9](#)).

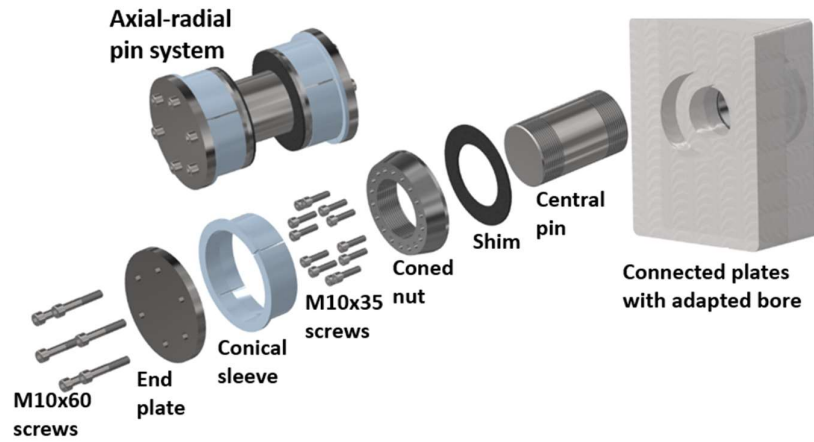


Figure 3.8. Exploded view of an axial-radial pin assembly

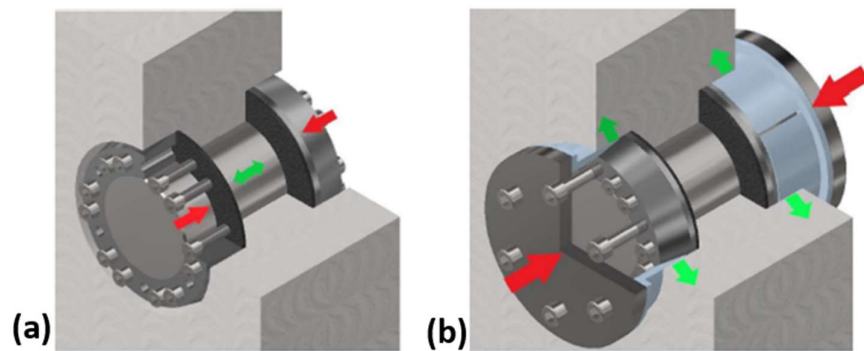


Figure 3.9. Function of tightening screws for achieving; a) preload, and b) radial locking

Materials used:

The experimental test of each axial-radial expanding pin system has the items given in [Table 3.1](#), as partly illustrated in [Figure 3.8](#):

Table 3.1. Material properties of items used in axial-radial tests

<u>Description</u>	<u>Ø50</u>		<u>Ø80</u>	
	<u>Quantity</u>	<u>Material property, R_m [MPa]</u>	<u>Quantity</u>	<u>Material property, R_m [MPa]</u>
<u>Central pin</u>	<u>1</u>	<u>1083</u>	<u>1</u>	<u>1081</u>
<u>Shims</u>	<u>2</u>	<u>1858</u>	<u>2</u>	<u>1858</u>
<u>Conned nuts</u>	<u>2</u>	<u>1494</u>	<u>2</u>	<u>1494</u>
<u>Conical sleeves</u>	<u>2</u>	<u>540</u>	<u>2</u>	<u>500</u>
<u>End plates</u>	<u>2</u>	<u>547</u>	<u>2</u>	<u>505</u>
<u>Tightening screws M10x35</u>	<u>14</u>	<u>1625</u>	<u>24</u>	<u>1625</u>
<u>Tightening screws M10x60</u>	<u>14</u>	<u>1293</u>	<u>24</u>	<u>1312</u>

In addition, 1 pc of hand wrench of type USAG 40-200 Nm and 1 pc of steel test jig (tensile min. 450 MPa) were used for both tests, 2 pcs of strain gauges of type KLY41 / HBM for each pin and 2 pcs as dummies, data acquisition system (DAQ), measurement electronic gadget (Spider8), computer with software (Catman® professional), and required cables. All threads were lubricated with Molykote P74.

All tightening screws were of type ISO 4762 / strength class 12.9 but hardened additionally to 16.9 (M10 × 35). The shims and coned nuts were also hardened additionally to reach the strength indicated above.

Experimental setup and test procedure:

The maximum possible preload was measured by installing the axial-radial pin solution in a test jig simulating a flange joint, as illustrated in [Figures 3.9 and 3.10](#), torquing the bolts as shown in [Figure 3.9\(a\)](#), and in parallel measure the corresponding strains at the surface of the central pin, shown in [Figure 3.11](#).

The expanding pin systems were preloaded and expanded by the following procedure:

- 1) The central pin was installed into the flange joint bore, and the strain gauges were glued to the pin.
- 2) One shim was installed on each side of the central pin.
- 3) One threaded coned nut was installed and turned by hand on each side of the threaded central pin, until the end of the threads.
- 4) The M10 × 35 tightening screws were torqued in steps of 20 Nm, from 40 Nm to 140 Nm, and a final step of 20 Nm where one the screw broke. They were torqued following a cross-pattern.
- 5) Strain was measured by two strain gauges per pin, for each step.
- 6) The conical sleeves were installed, thereafter the end plates, and the tightening screws M10 × 60.
- 7) The M10 × 60 screws were torqued directly to 140 Nm, and strains at the central pin were measured.

The measured strain values were used as input to further calculations and analysis.



Figure 3.10. Test jig for measuring maximum preload



Figure 3.11. Central pin with two strain gauges at 180° distance

3.3.4 Experimental and Numerical Studies of Stress Distribution in an Expanding Pin Joint System

This chapter relates to the work presented in [Paper VI](#). The objective of this research was to study the stress distribution and the magnitude of stresses exerted to the equipment supports when an expanding pin solution is installed and in normal use, as illustrated by [Figure 1.11](#). One support was substituted with a test boss with constant thickness, inner and outer diameter, as illustrated in [Figure 3.12 \(a\)](#), to make it possible to measure the strains at the boss' outer surface as it expands radially, as result of torquing the tightening screws and pushing the sleeve into the boss. Radial and tangential (hoop) stresses were calculated from the measured strains, and the results compared with corresponding FEA results.

Materials used:

The experimental test of each expanding pin system contains the items listed in [Table 3.2](#), and as partly illustrated in [Figure 1.11](#) and [Figure 3.12](#). In addition, 1 pc of hand wrench of type USAG 40-200 Nm and 1 pc of steel test jig (tensile min. 450 MPa) were used for the test, and 3

Table 3.2. Test material:

Description	Quantity	Material property, R_m [MPa]
Pin Ø88.9	1	1074
Conical sleeves	2	547
End plates	2	547
Test boss	1	583
Tightening screws M16	6	8.8

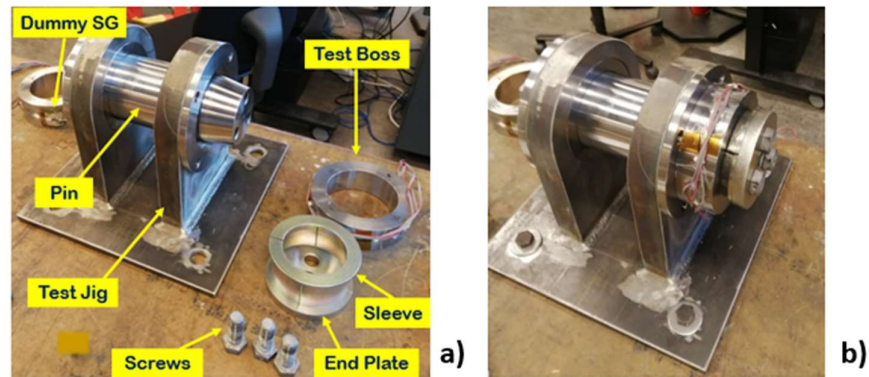


Figure 3.12. Test setup, (a) separate parts, and (b) installed

pcs of strain gauges of type LY4-1-5 /120 / HBM (half-Wheatstone bridge configuration) for the test boss. In addition, 3 active dummy gauges on a similar boss, data acquisition system (DAQ), QuantumX amplifier / HBM, computer with software (Catman 4.5) and required cables. All threads were lubricated with Molykote P74.

Experimental setup and test procedure:

The strains in the test boss were measured by installing a Bondura® Expanding Pin in a test jig but replace one of the supports with a boss with constant thickness, inner and outer diameter, and expand the sleeve by torquing the screws. The measured strain values were used as input

to further calculations and analysis, and the expanding pin system was torqued and expanded by the following procedure:

- 1) The pin was inserted into the test jig together with one sleeve, one endplate and three tightening screws.
- 2) The tightening screws at the opposite pin end, compared to the test boss, were torqued to wedge-lock the sleeve, and restrain any movement, and not loosened until the end of the test.
- 3) The tightening screws at the test boss pin end were torqued to 140 Nm, each time through the test.
- 4) The test boss with strain gauges, one sleeve, one end plate and three tightening screws were installed at the other pin end, and the screws were only hand tightened as a starting point. The test boss was restricted to move axially.
- 5) The test boss with three strain gauges was rotated 90° after each strain measurement (measuring at 0°, 90° and 270°) for 3 different layouts, (1) non-lubricated partly cut sleeve, (2) lubricated partly cut sleeve, and (3) lubricated completely cut sleeve.
- 6) The sleeve in the test boss was placed in positions $\pi/4$, $5\pi/4$, and $7\pi/4$, while the test boss strain gauges were placed at $\pi/2$, π , and $3\pi/2$ for the two layouts, (1) non-lubricated partly cut sleeve, (2) lubricated partly cut sleeve. This gives a relative angular distance of $\pi/4$ between each strain gauge and its closest sleeve cut.

3.3.5 Comparative study on loosening of anti-loosening bolt and standard bolt system

This chapter relates to the work presented in [Paper VII](#). The objective of this research was to investigate the function and capabilities of a newly developed anti-loosening pre-loaded bolt system, designed to operate separately or in combination with expanding pin systems. In addition, the anti-loosening bolt system called Vibralock® was compared with

standard HV bolt system when it comes to resisting bolt loosening, due to vibrations or oscillating transversal forces.

Transversal direction for vibrations, displacements and forces are normally seen as the most critical direction, when it comes to self-loosening of pre-loaded bolt systems, and a so-called Junker test was performed, in addition to an axial directional test with preload and oscillating loads. The Junker test setup with transversal loads is illustrated in Figure 3.13, and Figure 3.14 shows the corresponding tested bolt solution. The test with axially directed loads is illustrated in Figure 3.15. The standard HV bolts were tested with 1 nut each. The Vibralock® bolts were all tested with 1 main nut and 1 locking nut each.

For all *tensioned versions*, the bolt shank was tensioned by a hydro-electrical tensioner tool to an axial force representing approximately 90% of its material yield value, the main nut was manually tightened, and the tensioner tool was released. The resulting bolt shank tension was around 70% of its yield, which was the pre-defined value to get the required final bolt pre-load, or clamp load. The locking nuts on the Vibralock® bolts were always torqued by a hydro-electrical torque tool, to a predefined value.

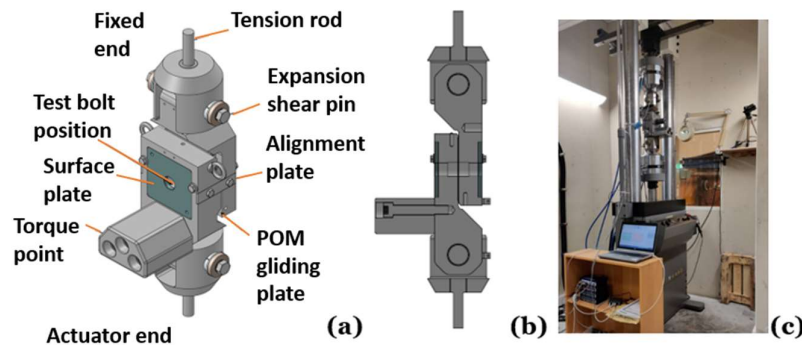


Figure 3.13. Test setup transversal loads, (a) test jig schematics, (b) cross-section view, and (c) jig installed in hydraulic test jig

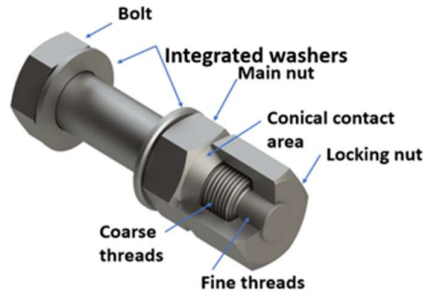


Figure 3.14. Test bolt of type Vibralock® for tensioning of the shank

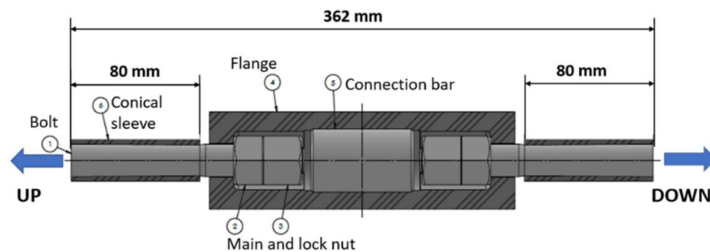


Figure 3.15. Test setup for the anti-loosening M20 bolt system

For all *torqued versions*₂, the bolt shank was tensioned by applying torque on the nuts, both on main nuts, and on locking nuts for the Vibralock® bolts. Different bolt sizes required different tensioning and torque tool sizes.

Materials used:

The experimental test of each pin system has the following items, as partly illustrated in Figures 3.13 – 3.15:

Test material – Vibralock® M30, tensioned (4 in total), and torqued (1 in total):

- One complete bolt system includes:

- 10.9 quality HDG bolt with head and two-size shank, M30/M16 with pitch 3.5 / 1.5 mm, respectively
- Main nut with additional outer conical contact surface, made of 10.9 steel material
- Locking nut with inner conical surface, long nut for tensioned version (i), and short nut for torqued version (ii), both made of 10.9 steel material
- Washers integrated in bolt head and main nut
- 2 pcs strain gauges – full bridge, placed at each side of the bolt at a horizontal plane with angular distance of 180°, with cables, to measure the clamp force as function of transverse displacement cycles (to calculate the loss of clamp force)

Test material – Vibralock® M42, tensioned (1 in total), and torqued (1 in total):

- One complete bolt system consisting of:
 - 10.9 quality HDG bolt with head and two-size shank, M42/M24 with pitch 4.5 / 2.0 mm, respectively
 - Main nut with additional outer conical contact surface, made of 10.9 steel material
 - Locking nut with inner conical surface, long nut for tensioned version, and short nut for torqued version, both made of 10.9 steel material.
 - Washers integrated in bolt head and main nut.
 - 2 pcs strain gauges – full bridge, placed at each side of the bolt at a horizontal plane with angular distance of 180°, with cables, to measure the clamp force as function of transverse displacement cycles (to calculate the loss of clamp force)

Test material – HV bolt M30, tensioned (4 in total), and torqued (1 in total):

- One complete bolt system consisting of:
 - o 10.9 quality HDG bolt with head and shank, M30 with pitch 3.5 mm
 - o Nut Class 10
 - o Washers used for torqued version only
 - o 2 pcs strain gauges – full bridge, placed at each side of the bolt at a horizontal plane with angular distance of 180°, with cables, to measure the clamp force as function of transverse displacement cycles (to calculate the loss of clamp force)

Test material – HV bolt M42, tensioned (2 in total), and torqued (0 in total):

- One complete bolt system consisting of:
 - o 10.9 quality HDG bolt with head and shank, M42 with pitch 4.5 mm
 - o Nut Class 10
 - o Washers used for torqued version only
 - o 2 pcs strain gauges – full bridge, placed at each side of the bolt at a horizontal plane with angular distance of 180°, with cables, to measure the clamp force as function of transverse displacement cycles (to calculate the loss of clamp force)

In addition, all threaded surfaces and bearing surfaces between nuts and surface plates (flanges) were lubricated with Molykote P74 to minimize the friction coefficients. The fatigue test machine applied for bolt tests was an MTS 809 Axial/Torsional Test System, model 319.25, as illustrated in [Figure 3.13 \(c\)](#). Two displacement measuring units – LVDT – were used to measure the real imposed amplitude or transversal displacement of the contact surfaces between bolt head / surface plate

(flange) and nut / surface plate (flange). The real displacement differs from the imposed from the software, due to play in the expansion shear pin joints.

Test material – Vibralock® M20 (3 pcs in total):

- One complete bolt system consisting of:
 - 10.9 quality bolt without head and two-size shank, M20/M16 with pitch 2.5/1.5 mm, respectively, with conically machined shank and blueing threaded threads
 - A two-part sleeve with inner conical surface to fit the pin shank, and outer cylindrical surface to join the fatigue machine clamps.
 - Main nut with outer conical contact surface against the locking nut, of Class 10
 - Locking nut with inner conical surface against the main nut, unthreatened surfaces
 - No washers included

In addition, a flange system with a connection bar was designed to test two different bolt solutions at the same time, as illustrated in [Figure 3.15](#). The flange system contained two hollow-bars with inner threads, and one bar with outer threads, to connect the two hollow-bars.

Experimental setup and test procedure:

All tests were performed at UiS test facilities, and they can be divided into two main types of tests, (a) transversally loaded M30 and M42 bolts, and (b) axially loaded M20 bolts, where all bolts were preloaded in axial direction and exposed to oscillating forces in transverse and axial directions, respectively.

Before running experimental tests with transversal loads and displacements:

- The test jig was mounted and installed into the hydraulic test rig, MTS 809, as shown in [Figure 3.13 \(c\)](#), with one end connected to the rig fixed (upper) end, and the another to the actuator (lower) end. The M30 and the M42 bolts require different sizes of test jigs.
- Two displacement measuring units were mounted to measure the real relative displacements between the two parts of the test jig, which were joined by the preloaded bolts, and represent flanges.
- The alignment plates were removed after each bolt had been preloaded, but before any transversal oscillating load was added.
- The MTS test machine control unit and computer were prepared to log the actuator's forces and displacements, and the data from the strain gauges and displacement transducers were logged by a HBM QuantumX data acquisition device via Catman AP software.
- Each bolt with corresponding strain gauges was installed into the test bolt position, preloaded by either tensioning, or torquing of main nut, and torquing of locking nut for the Vibralock® bolts.

Experiment type (a) – HV standard bolt, M30, tensioned

- The bolt with strain gauges was installed into the test bolt position, and cables for strain gauges and displacement transducers were connected to a separate computer, for registration of measured values.
- The required preload was achieved by applying a tension tool on the shank. The final pretension which represented 70% of material yield was reached by first applying a preload of 90% of material yield, and then release the tensioning tool. Necessary adjustments of the tension level were taken, when required, to reach the predefined bolt preload.
- The transversal oscillating loads on the bolt assembly were introduced by activating the hydraulic test rig.

- The frequency was set to 1 Hz, and the displacements increased stepwise until the preloaded bolt had lost 90% of its clamp load (due to turning of the nut) within the range of 200 – 400 cycles.
- The following values were recorded:
 - o Imposed and real displacement values [mm]
 - o Number of load cycles [-]
 - o Frequency of load cycles [-]
 - o Bolt preload as function of the number of cycles [kN]
 - o Transvers load [kN]

Experiment type (a) – HV standard bolt, M30, torqued

- As for “HV standard bolt, M30, tensioned”, but with some adjustments, as described below.
- The required preload which represented 70% of material yield was achieved by applying a torque tool on the nut. Necessary adjustments of the torque level were taken, when required, to reach the predefined bolt preload.

Experiment type (a) – HV standard bolt, M42, tensioned

- As for “HV standard bolt, M30, tensioned”, but with bigger jig and tool.

Experiment type (a) – HV standard bolt, M42, torqued

- As for “HV standard bolt, M30, torqued”, but with bigger jig and tool.

Experiment type (a) – Vibralock® bolt, M30, tensioned

- The bolt with strain gauges was installed into the test bolt position, and cables for strain gauges and displacement transducers were connected to a separate computer, for registration of measured values.

- The required preload was achieved by applying a tension tool on the shank. The final pretension which represented 70% of material yield was reached by first applying a preload of 90% of material yield, and then release the tensioning tool. Necessary adjustments of the tension level were taken, when required, to reach the predefined bolt preload.
- After having applied tensioning tool to reach the required pretension of the bolt, the locking nut was torqued to a predefined value.
- The transversal oscillating loads on the bolt assembly were introduced by activating the hydraulic test rig.
- The frequency was set to 1 Hz and the displacement value obtained from the test “HV standard bolt, M30, tensioned” was applied as input.
- The test was run for 3000 cycles, and loss of clamp load was calculated. In addition, the same values as for “HV standard bolt, M30, tensioned” were recorded.

Experiment type (a) – Vibralock® bolt, M30, torqued

- As for “Vibralock® bolt, M30, tensioned”, but with some adjustments, as described below.
- The required preload which represented 70% of material yield was achieved by applying a torque tool on the main nut, instead of tensioning tool. Necessary adjustments of the torque level were taken, when required, to reach the predefined bolt preload.
- The displacement value applied was taken from the “HV standard bolt, M30, torqued” run.

Experiment type (a) – Vibralock® bolt, M42, tensioned

- As for “Vibralock® bolt, M30, tensioned”, but with bigger jig and tool.
- The displacement value applied was taken from the “HV standard bolt, M42, tensioned” run.

Experiment type (a) – Vibralock® bolt, M42, torqued

- As for “Vibralock® bolt, M30, torqued”, but with bigger jig and tool.
- The displacement value applied was taken from the “HV standard bolt, M42, torqued” run.

Experiment type (b) – Vibralock® bolt, M20, in tension

- The main nut was turned by hand into its predefined location on the bolt for the upper location, and the locking nut was torqued to 200 Nm towards the main nut. The bolt shank was slightly conical shaped with bigger diameter at its end.
- The relative position of the two bolts to each other, and their position relative to the bolt shank were marked with red colour.
- The bolt end without nuts was installed into the upper half of the flange, until the main nut met the flange inner surface.
- The same procedure for the second bolt on the lower half of the flange.
- Both upper and lower flange were turned onto the threads of a connection bar, as illustrated in [Figure 3.15](#).
- The sleeves were slightly conical on their inner surface to fit the conical bolt shanks and installed on the free end of each bolt.
- The bolt ends, bolt A and B, with sleeves were installed vertically into the fatigue machine and locked to its upper and lower clamps.
- Bolt A (lubricated threads, with Molykote P74) and B (unlubricated threads) were loaded axially to 100 kN, and an oscillating load of +/- 15 % were added, with frequency 10 Hz, until 498.000 cycles.
- The test setup was dismantled, and a control was performed to check if any of the nuts had rotated relatively to the other nut, or to the bolt shank.

- Thereafter the same procedure was applied for Bolt C (lubricated) and B (unlubricated).
- Bolt C and B were exposed to the same axial load, oscillating load amplitude, and frequency, but they were run until Bolt B broke at 668.000 cycles.
- Pictures and SEM images of the broken areas and surfaces were taken, as illustrated in [Paper VII](#), Figure 7, 8, and 9 [7].

3.4 Analytical approaches and numerical analysis

This thesis is compounded by 9 papers in total, where different effects and consequences on pins, supports, and associated equipment are investigated, in addition to experimental work, surveys and literature studies. None of the papers are solely dedicated to analytical or numerical analysis, but those analyses are used as additional tools, mainly in relation to the experimental work.

A generalized description of the development of the most important formulas used in the analytical approaches is given in Chapters 2.1 to 2.5. In this chapter, the specific formulas applied in the different papers will be presented and explained, together with the numerical analysis applied as follows: (a) An investigation of the effects and consequences combining expanding dual pin with radial spherical plain bearings, (b) A novel technique for temporarily repair and improvement of damaged pin joint support bores, (c) Study of Bondura® Expanding PIN System – Combined Axial and Radial Locking System, (d) Experimental and Numerical Studies of Stress Distribution in an Expanding Pin Joint System, and (e) Comparative study on loosening of anti-loosening bolt and standard bolt system.

3.4.1 An Investigation of the Effects and Consequences of Combining Expanding Dual Pin with Radial Spherical Plain Bearings

[Paper II](#) describes an investigation where the effects of combining an expanding pin solution with Radial Spherical Plain Bearings (RSPBs) were studied. The paper contains mainly experimental tests, with a few analytical analyses based on thick cylinder theory.

The inner rings of 3 pieces RSPBs of type SKF GE 80 ES were separated from the complete bearings, installed on an expanding pin, and loaded radially outwards. The expanding pins were torqued stepwise from 0 to 70 Nm, which resulted in stepwise increased internal load on the rings. The diametrical changes of each ring were measured for each increase of internal load, with a CMM. Illustrations of test setup are given in [Figure 3.1](#).

By use of thick cylinder theory and the measured radial changes – u – in the tested rings, the ring inner pressure – p_l –, and tangential, or hoop stress – σ_θ – were calculated, for both dry and lubricated sleeves, see [Figures 3.2](#) and [3.3](#) for sections where diametrical changes were measured, and stresses calculated.

All the calculated stresses for Test 1a and 1b, for sections (a), (b), (c) and (d), for torque 15 and 30 Nm (non-lubricated) and 30 Nm (lubricated), are shown in [Table 2 \[2\]](#) and [Table 3 \[2\]](#), respectively. [Equations \(10\)](#) and [\(11\)](#) were used to calculate the radial and tangential stresses at the ring outer surfaces, respectively, where the calculated change in radius, u , is given by [Equation \(45\)](#).

$$\begin{aligned}
 u = u_{open\ end} = & \left(\frac{r}{E \times (b^2 - a^2)} \right) \\
 & \times \left[(1 - \nu) \times (p_1 a^2 - p_2 b^2) \right. \\
 & \left. + \left(\frac{(1 + \nu) a^2 b^2}{r^2} \right) \times (p_1 - p_2) \right], \quad (45)
 \end{aligned}$$

where E – represents the elasticity modulus (210 GPa), ν – Poisson’s ratio (0.3), p_2 – external pressure (0), a – ring inner radius (40 mm), b – ring outer radius at 4 sections, r – radius where stresses were calculated, and p_1 – internal pressure (calculated).

The radial and tangential stresses were calculated at the rings outer surfaces, where $r = b$, at each calculated section (a) to (d) in [Figures 3.2](#) and [3.3](#). With defined values for all variables in [Equation \(45\)](#), except for internal pressure p_1 , this variable was changed until the calculated change of the ring radius u was equal to the changes measured by CMM. The internal ring pressure p_1 value that gave identical values for calculated and measured change in ring radius u was applied to calculate the ring surface radial σ_r and tangential σ_t stresses, from [Equations \(10\) – \(12\)](#).

3.4.2 A novel technique for temporarily repair and improvement of damaged pin joint support bores

[Paper III](#) is a study where the use of expanding pin is applied in combination with 3D printed metal insert, to investigate its capability to temporarily repair a damaged pinned support bore. Normally, when a support has experienced major wear or damage to its bore surface the clearance between the operating pin and the support bore increases, and the quality of the pinned joint decreases.

Five different tests were performed on two different pin types, (a) a standard cylindrical pin, and (b) an expanding pin system.

For pin type (a), two tests were performed, Test 1 with evenly distributed wear on both support bores, and Test 2 with additional heavy wear on one of the bores. For pin type (b) three tests were performed where Tests 3 and 4 had the same wear pattern as Test 1 and 2 for pin type (a), and additionally Test 5 was performed where the 3D printed repair insert was applied.

Four strain gauges was applied for each pin test, two at each side of the pin at the weakening grooves, and at the pin's neutral axis for vertical bending. The strain values at each cross-section at each weakening groove were both measured and calculated. Since the four strain gauges were not placed exactly at the minimum pin cross-section, but with a slightly offset by error, as illustrated in [Figure 3.16](#), the actual cross-sectional area was recalculated for the two cross sections and taken into the calculations. The average pure shear stress at each real cross-section was calculated as the real force divided by the actual cross-sectional area, and the maximum shear stress was assumed to be $4/3$ of the average value, acc. to Budynas and Nisbett [32], see also [Figure 3.17](#).

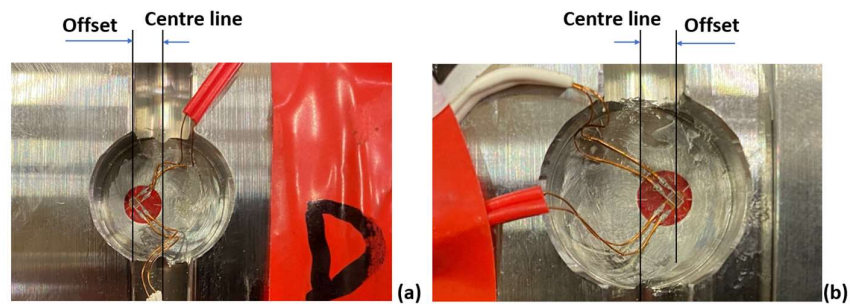


[Figure 3.16](#). Examples of strain gauge offsets from pocket centre line for (a) the cylindrical pin, and (b) the expanding pin

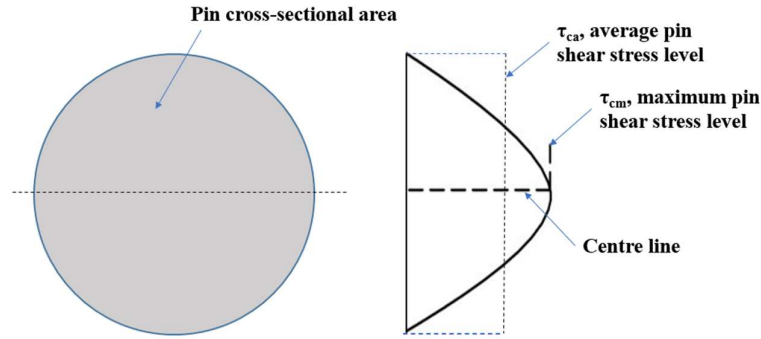


Figure 3.17. Examples of strain gauge offsets from pocket centre line for (a)

The measured strain values – ε_{45° – were compared to the calculated average and maximum values, – ε_{ca} – and – ε_{cm} –. The average strain values were calculated from Equation (46), also presented as Equation (1) [3], based on Equation (44), and the calculated maximum strain is 4/3 of the calculated average.

$$\varepsilon_{ca} = \frac{\tau_a}{2 \times G} = \frac{F}{2 \times A \times G}, \quad (46)$$

where – F – represents the total external load on the pin [N], – A – the sum of the total shear areas [mm^2], and – G – the shear modulus [N/mm^2].

The comparison was made between measured, calculated average, and calculated maximum strains for all 5 tests when the pins were placed at 0° position and turned 15° compared to the first measurements. The measured and calculated values at 500 kN external load are presented in Table 3 [3] and Table 4 [3]. For each of the Tests 2 and 4 one of the ends of each pin was resting fully on one support bore, and the other end was fully, partly, or not at all resting on the other support bore, due to the severe wear and corresponding clearance. Thus, the calculations become inaccurate for those tests, but it could be indicated theoretical minimum

and maximum strain values, based on the calculated values for Tests 1 and 3.

3.4.3 Study of Bondura® Expanding PIN System – Combined Axial and Radial Locking System

Paper V describes a study of a patented pin solution which combines radial locking of a pin, as for expanding pin solutions, with axial loading, as for preloaded bolts. Normally, flange connections are joined by use of preloaded standard bolts, which create shear capacity, or a contact pressure between the flanges sufficiently high to prevent any relative radial, axial, or rotational displacements between the flanges. Any such displacement would accelerate the loosening of the bolts and nuts, and could lead to failure of the joint, with the risks such failures imply.

The equation for the relationship between the applied torque on a bolt and the resulting preload, or clamp load, is developed in Chapter 2.4 “Bolts, nuts, and threads”, and expressed in Equations (31) and (32).

The k – value is called the torque coefficient and is affected by the thread pitch value, thread diameter, thread angle, thread friction factor, and bolt head friction factor. In this paper, for the further calculations, the torque coefficient was set equal to 0.18, but can vary maybe up to +/- 30%. It is often considered to be in the range of 0.18 – 0.22. In Table 3 [5], the theoretical clamp loads – F_i – were calculated based on the Equation (31), with the same torque values – T_i – which were applied for the experimental test. The mayor thread diameter – d – was set to 9.78 mm for the M10 tightening screw. The clamp loads were presented as *Preload per screw* in the corresponding table.

Based on the *theoretical clamp loads* per tightening screw, the theoretical preloads for the Ø50 mm and Ø80 mm pins were calculated, called *Max. preload* in the same table. The Ø50 mm pin had 7 tightening screws at each end, and the Ø80 mm pin had 12. Based on the maximum

preload of the two pin systems, the corresponding theoretical normal stresses were calculated, called *Normal stress*, calculated from the formula:

The *measured strains* for each torque level, presented in Table 2 [5], were used to calculate the real *Normal stress from measured strain* for the two pin sizes, Ø50 mm and Ø80 mm, included in Table 4 [5], and the percentage differences between real and theoretical stress levels were also included. The relationship between the measured strain value – ε – and the corresponding clamp force – F – is given in Equation (42), and is affected by the pin material, or elasticity modulus – E –, and the smallest cross-sectional area – A –, often at the threaded part.

The minimum cross-sectional area of the pin is given in Equation (37), and it is affected by the thread pitch size – p –. The normal stress at each pin size were calculated according to Equation (36). The theoretical maximum preloads for the axial-radial pin solutions, Ø50 mm and Ø80 mm, were compared to the calculated theoretical maximum preloads for standard bolts, M50 and M80. The preloads of the standard bolts were calculated based on their ultimate strength and minimum cross-sectional area at the threads. The values for the tested axial-radial pins and calculated values for standard bolts were thereafter compared, as shown in Table 5 [5].

Based on the results above, the axial-radial pin solutions were optimized to yield better results. The sizes and number of tightening screws were optimized to maximize the pin preloads, as illustrated in Table 6 [5] and the maximum shear capacity of the corresponding joints were compared in Table 9 [5]. The flange shear capacity with standard bolts is given in Equation (5) [5] and with the axial-radial pin system, Equation (6) [5].

A visualization of how the axial-radial pin and the standard bolt systems are joining two flanges are illustrated in Figure 7 [5]. A simple comparison was made between the two methods of joining flanged joints, by use of FEA, as illustrated in the Figures 8 and 9 [5]. A cut-out

of two flange connections, one with axial-radial pin fastener and the other with a standard bolt fastener, were compared when they were exposed to equal radial stress. All results are discussed in Chapter 4.

3.4.4 Experimental and Numerical Studies of Stress Distribution in an Expanding Pin Joint System

Paper VI describes an investigation that reports a study conducted on the stress distribution and magnitude exerted into the equipment support bore. Both experimental and numerical methods were applied in the investigation, and the experimental part were described in Chapter 3.3.

The FEA was performed in Abaqus/CAE which is a powerful and user-friendly standalone interface for FEA pre- and post-processing, simplification, and advanced meshing. To achieve a more realistic simulation of the behaviour of the EPS joint, *true stress* and *true plastic strain* relations were applied in the FE analysis, and they were determined by the Equations (47) and (48).

$$\sigma_{true} = \sigma_{eng} \times (1 + \varepsilon_{eng}) \quad (47)$$

$$\varepsilon_{true} = \ln(1 + \varepsilon_{eng}), \quad (48)$$

where – σ_{eng} – represents the engineering stress [MPa], – ε_{eng} – the engineering strain [-], and – ε_{true} – true strain [-].

The engineering stress – σ_{eng} – and engineering strains – ε_{eng} – are measured in tensile tests, where engineering stress is the applied load divided by the original cross-section area of the test specimen. True stress is defined as the applied load divided by the actual and reduced cross-sectional area, which changes over time. Strains corresponding to ultimate strength is set to be 1/3 of the strain value corresponding to the A5 value representing the rupture for the test material. The plastic true

strain is equal to the difference between true strain and the elastic strain, as shown in [Equation \(49\)](#).

$$\epsilon_{pl.true} = \epsilon_{true} - \epsilon_{elastic} = \epsilon_{true} - \frac{\sigma}{E} \quad (49)$$

At small strain values, the difference between engineering and true strains are small, but for bigger strain values the difference increases significantly. The conversions from engineering to true material properties for the pin sleeve are shown in [Table 3.3](#) below, based on the following material characteristics and calculations:

Table 3.3. Conversion from engineering to true material properties for pin sleeve

Description	Yield strength / at stress point, R_c [MPa]	Ultimate strength / at stress point, R_m [MPa]	Elongation, A5 [%]	Source
Sleeve material, σ_{eng}	404	547	25.6	Material tests
Engineering stress, σ_{eng}	404	547		Material tests
Engineering strain, ϵ_{eng}	0.0019	0.0853		σ_{eng}/E , 1/3 of A5
True stress, σ_{true}	404.77	593.66		Equation (47)
True strain, ϵ_{true}	0.0019	0.0819		Equation (48)
True plastic strain, $\epsilon_{pl.true}$	0.000	0.0800		Equation (49)

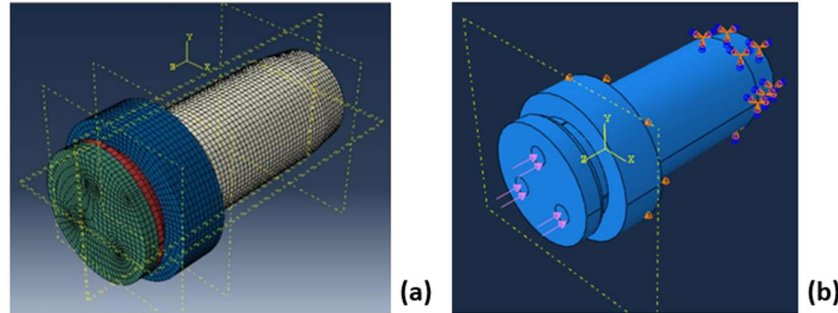


Figure 3.18. EPS model in Abaqus/CAE, with (a) mesh model, and (b) boundary conditions

The EPS parts for the actual test were, in addition to the test jig itself are, 2 end plates, 2 sleeves, 1 test boss, 1 pin, and 6 tightening screws. All EPS parts were modelled as 3D homogeneous solid, and the assembly of each part was according to the procedure for the experimental set-up. The EPS mesh model is illustrated in Figure 3.18(a), and the boundary conditions are shown in (b).

The quality of the mesh element affects the accuracy of the simulation result, and the C3D8R element was used for the EPS parts, which is a continuously three-dimensional, eight-node linear brick, reduced integration, and hourglass controlled element, and uniform 4 mm size. To simplify the EPS 3D model, the tightening screws which are torqued in the experimental test were replaced with equivalent axial loads. This resulted in a reduced number of contact surfaces, and thus reduced complexity of the model. The remaining contact surfaces were modelled with Coulomb friction, with friction coefficient $\mu = 0.2$.

The test boss had a shape as a thick-walled cylinder, with a positive inner pressure and zero outer pressure. In this case the Equations (10), (11), and (12) can be applied to calculate the theoretical values for the radial stress $-\sigma_r-$ and the tangential hoop stress $-\sigma_\theta-$ over the test boss wall thickness, in addition to the inner pressure $-p-$.

Hoop strains were measured at the test boss outer surface, and by applying Equations (50), (51), and (52) the corresponding stress components including radial, hoop, and axial stresses were calculated. The outer surface did not experience any external force, and no movements, as the inner surface due to its contact with the expanding sleeve. The axial stress at the boss inner surface is described in Equation (8) [6].

$$\varepsilon_r = \frac{1}{E} [\sigma_r - \nu(\sigma_\theta + \sigma_z)] \quad (50)$$

$$\varepsilon_\theta = \frac{1}{E} [\sigma_\theta - \nu(\sigma_r + \sigma_z)] \quad (51)$$

$$\varepsilon_z = \frac{1}{E} [\sigma_z - \nu(\sigma_r + \sigma_\theta)] = \text{constant}, \quad (52)$$

were E and ν represent the modulus of elasticity and Poisson's ratio for the test boss, respectively.

Hoop stresses were calculated on the test boss inner surface in situation (i) non-lubricated partly cut sleeve, (ii) lubricated partly cut sleeve, and (iii) lubricated completely cut sleeve, from Equation (5) [6], and Equations (10) - (12). In addition, hoop stresses were calculated on the test boss outer surface in situation (iii), and radial stresses on the test boss inner surface in situation (i), and (iii). The results are shown in Figures 5, 6, and 7 [6], and Figures 4.30, 4.31, and 4.32.

3.4.5 Comparative study on loosening of anti-loosening bolt and standard bolt system

Paper VII describes a comparative study between an anti-loosening preloaded bolt system with pending patent application called Vibralock®, and a standard preloaded HV bolt system. The study

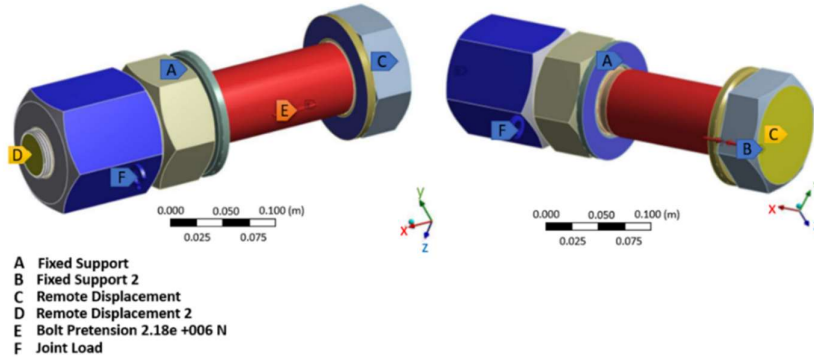


Figure 3.19. FEA boundary conditions for the M72 Vibralock® bolt

contains mainly experimental tests, which includes (a) Test 1 with 3 sets of M20, and (b) Test 2 with 5 sets of M30, and 2 sets of M42 anti-loosening bolt systems, in addition to 5 sets of M30, and 2 sets of M42 standard HV bolt systems. In addition, a FE analysis was performed on a M72 anti-loosening bolt system. The FE analysis were performed by an external company [33] with the aim to investigate the structural integrity of the bolt system, especially in the threads.

The ANSYS 19 R2 program with 3D elements was used for the FEA, prior to Test 2. Both (i) linear and (ii) non-linear models (with quadratic element order for the 3D elements and linear element order for the axisymmetric model) were checked to verify the structural integrity of the anti-loosening bolt system. For the complete analysis the friction factor for threads was set to 0.12, and between the two nuts 0.35. The contact surface between the two nuts had an angular distance of 30° to the bolt axis, with a production tolerance of 0.5°.

(i) Linear material model:

- Non-linear geometry (large deformation theory) and contacts
- First stage: Pre-tension of bolt shank to 2.180 kN
- Second stage: Torquing of locking nut up to pre-tension 930 kN, which was reached after 51.3° rotation

- (ii) As for (i) but with a non-linear material model. The analyses were conducted with the following conditions, as illustrated in [Figure 3.19](#):
- Boundary conditions: Identical boundary conditions for (i) and (ii). The washers were set fixed outside the 78 mm diameter jig bore. The bolt head and nut end centres were locked against rotation, and against displacement in the YZ plane, which were placed perpendicular to the bolt axis.
 - Geometry and material: The coarse threads for both (i) and (ii) were set to $M72 \times 6$, and the fine threads $M48 \times 3$. The clamp length between washers was 157 mm. For the linear model (i) Young modulus – E – was set to 210 GPa and Poisson’s constant 0.3. For the non-linear model (ii) a bilinear isotropic hardening was assumed.
 - Contact conditions: Normal Lagrange formulation was employed on all frictional surfaces for (i) the linear analysis, as it allows no contact surface penetration. The friction coefficient between washers and nut/head was set to 0.2. For the non-linear analysis (ii) the conditions were the same, with the exception that the augmented Lagrange formulation was applied instead of the normal, which is accepted when the penetration is insignificant.
 - Mesh: Linear analysis (i): Linear and full integration elements were applied due to the complexity of the analysis, and the meshed model had a total number of 1 157 297 nodes and 5 792 650 elements. For the non-linear model (ii), linear and full integration elements were also used, and the number of nodes and elements were reduced to 532 513 and 2 460 415, respectively. In addition, the models were meshed using default element sizes of 0.0022 mm and 0.001 mm for the linear and quadratic element, respectively.

4 Results and Discussions

4.1 General

This thesis is based on nine published articles or papers which focus mainly on experimental tests and questionnaire-based survey, but also some numerical (FEA) and analytical analysis are included.

The results with corresponding discussions are presented thematically, including some unpublished results from the investigations. Summary of the appended articles are presented at the end of this section and the complete questionnaire for the study reported in Paper I is added in Appendix A.

4.2 Thematic area-based discussion of results

The results achieved with this PhD study have been divided into 3 main thematic areas, as listed below, which correspond well with the previously specified general and specific objectives (Chapter 1.1.4) for this study.

- (i) Results from questionnaire-based survey, presented in [Paper I](#) and [IV](#)
- (ii) Results from study of traditional expanding pin solutions, based on [Papers II](#), [III](#), and [VI](#), and
- (iii) Results from study of newly developed pin solutions, based on [Papers V](#), and [VII](#)

No results are defined nor discussed based on the two literature studies in [Paper VIII](#), and [IX](#).

4.2.1 Results of questionnaire-based survey (Papers I and IV)

The main survey was answered by 58 persons within different companies, or product areas, called stakeholders, and they were from 10 countries, and 3 continents, which represented 23% response rate compared to the total that could have responded. The main group of those who responded came from Norway (67%), with Scotland (10%) and Sweden (9%) as second and third, but also Finland, The Netherlands, Greece, Germany, Canada, USA, and Brazil were represented.

The overall distribution of responders divided into Norwegians and non-Norwegians is illustrated in Figure 4.1. Based on the percentage response rate for the two groups, the *overall reaction rates* were defined, as indicated in Table 3 of Paper I [1]. The overall reaction rates represent the *willingness to respond* to the survey.

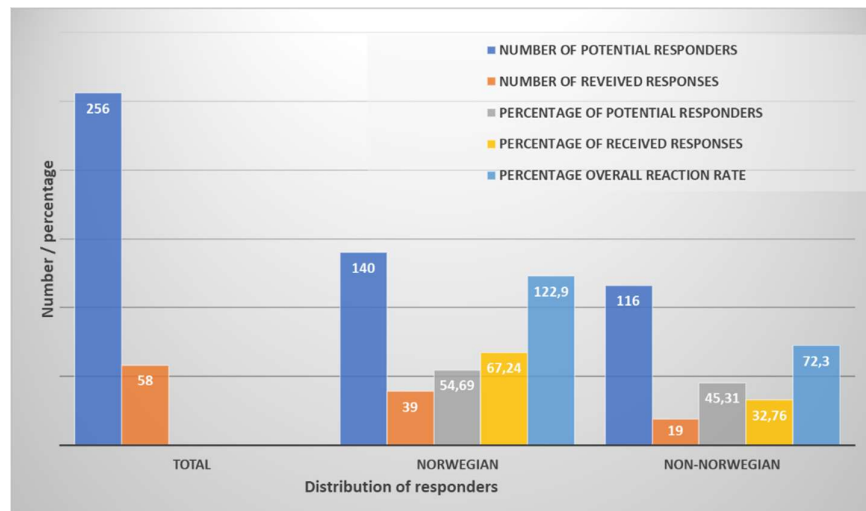


Figure 4.1. Overall distribution of responders

An overall reaction rate of 1.00 means that the relationship between number of received responses from one group to the total responses, is the same as potential responders from the same group, of the total potential. A value > 1.00 means higher willingness to respond, and a value < 1.00 means lower willingness. The Norwegian based companies had an average overall reaction rate of 1.23 (67.24% / 54.69%), where the number 67.24% represents the received responses from the Norwegian based companies (39) compared to the total received responses in the survey (58) (response rate), and 54.69% represents the number of Norwegian based companies (140) which had received the request, compared to the total survey request (256) (distribution rate). The non-Norwegian based companies had an overall reaction rate of 0.72.

These numbers indicated a higher willingness from the Norwegian based companies (+70 %) to respond to this specific survey, compared to the other companies. The study didn't state exactly why the Norwegian based companies had a higher willingness to respond, but as indicated in [Paper I](#), the long relationships between the biggest markets, maritime and offshore oil&gas, and company Bondura Technology, the University of Stavanger, and the Norwegian Research Council, could have influenced these rates.

The company size (CS) for each company was divided into three alternatives, CS1 ≤ 20 employees, CS2 21-100, and CS3 > 100 , and the distribution is illustrated in [Figure 4.2](#). The company profile is describing the stakeholder's main activity. One company can have responded as more than one stakeholder, but then within different product areas. The company profile distribution per location is shown in [Figure 4.3](#).

The company *size and profiles*, per geographical location, are illustrated in [Figures 4.2 and 4.3](#), and they show that 52 % of all companies that have responded were of the bigger size, which means they had over 100

Results and Discussions

employees, and the rest was equally divided between “21 – 100” and “below 21” employees, for the complete survey.

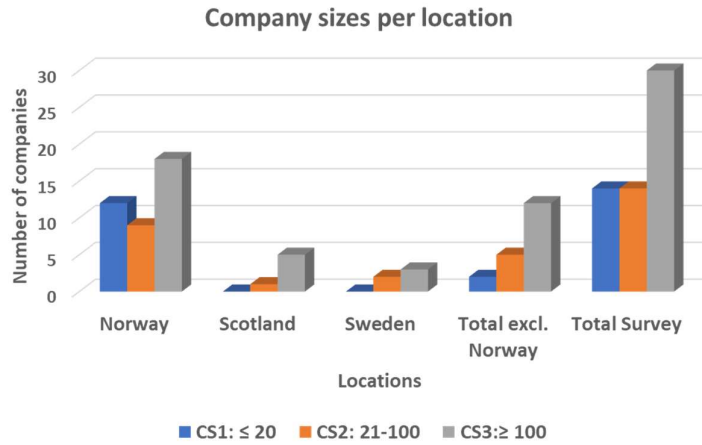


Figure 4.2. Distribution of company size

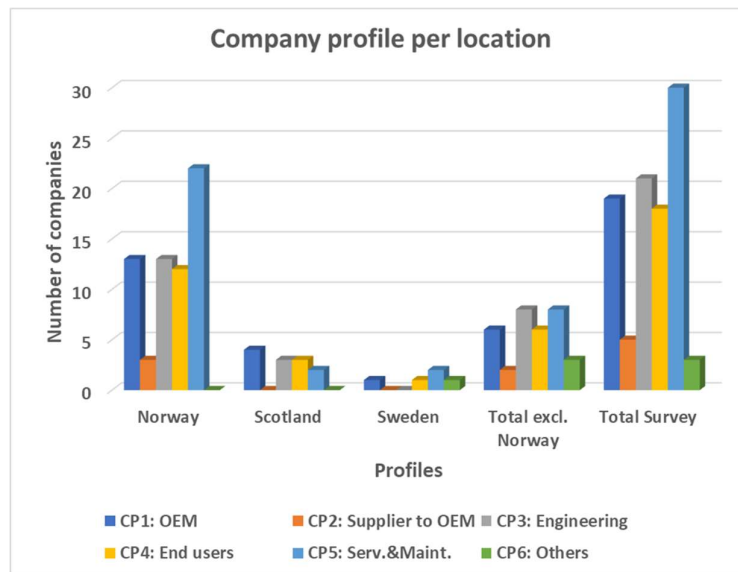


Figure 4.3. Distribution of company profile

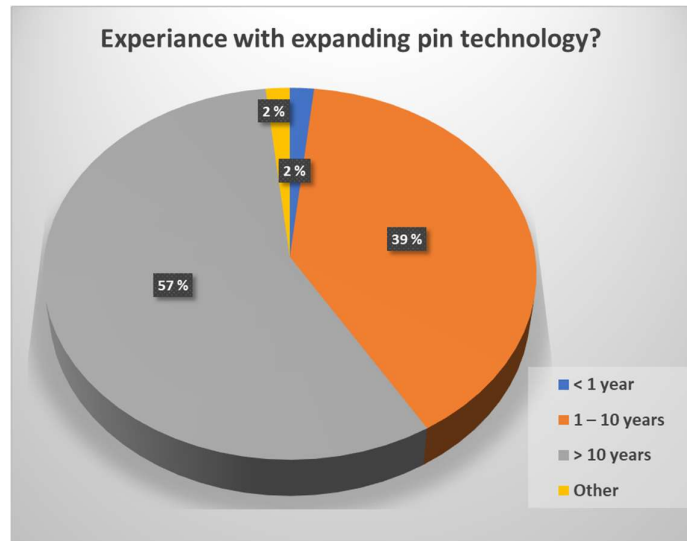


Figure 4.4. Experience with expanding pin solutions

For the Norwegian and non-Norwegian based companies, the corresponding values are 46 %, 23 %, 31 %, and 63 %, 26 %, 11 %, respectively. This shown that the non-Norwegian based companies had an over-representation of companies from the biggest size segment, compared to the Norwegian based (factor 1.37), while the Norwegian based had an over-representation of the smallest size segment (factor 2.9). The company profile distribution, which shows which area the stakeholders operate and where they have their activities, is almost identical for the two groups, but with higher percentage participation of companies within Service & Maintenance for the Norwegian based companies, which might be connected to the over-representation of smaller companies for this group compared to the non-Norwegian based.

The stockholder's length of experience with expanding pin solutions is shown in Figure 4.4. The periods are divided into three, with (i) less than 1 year, (ii) 1-10 years, and (iii) over ten years, in addition to (iv) which has an unclear length of knowledge.

Results and Discussions

All 58 stakeholders are represented within one or more segments, which are defined as: (a) Offshore oil&gas, (b) Maritime/ships, (c) Subsea-ROV/str., (d) Dredging, (e) Mining, (f) Construction and earth moving, (g) Specialized machines, (h) Steel and paper, and (i) Other. The 58 stakeholders have confirmed activities with expanding pins in a total of 106 times in the 9 different segments, which indicates that each stakeholder have activities in 1.83 segments, in average.

Many of the stakeholders also confirmed to us or have used expanding pins in several different machines and equipment within the different segments, with an average of 2.4 machines per stakeholder within the total of 9 segments, as shown in Table 7 in Paper I. The *distribution* of equipment where expanding pins were used, between Norwegians and non-Norwegians based stakeholders, within the “Offshore” and “Maritime” segments (42 and 32 responders, respectively), is illustrated in Figures 4.5 and 4.6.

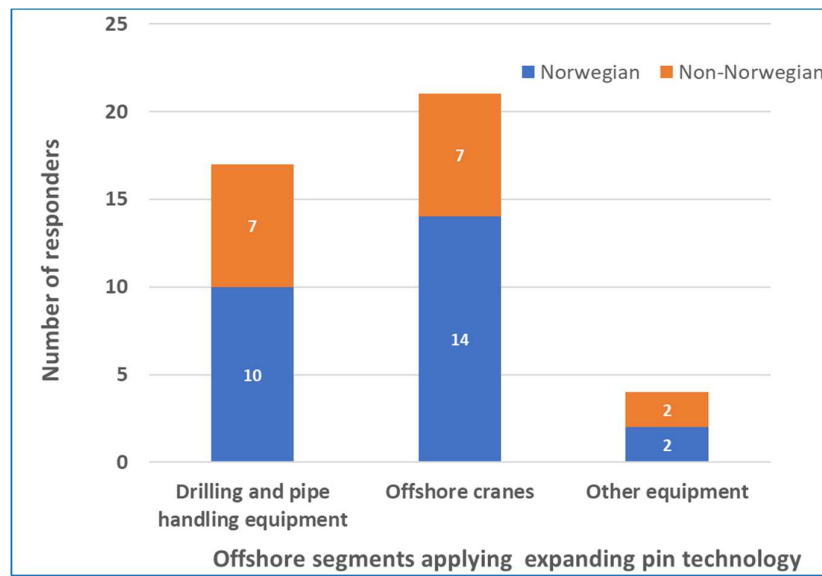


Figure 4.5. Distribution of responders within the Offshore oil&gas segment

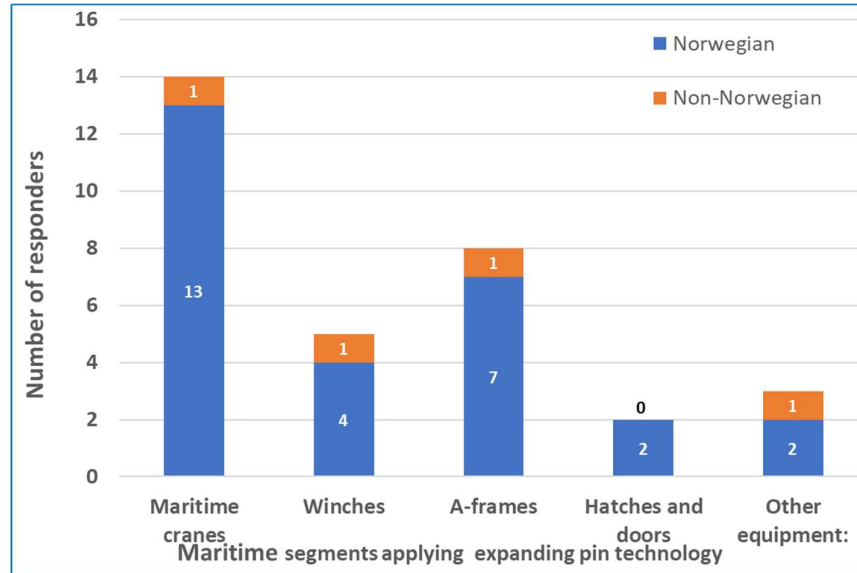


Figure 4.6. Distribution of responders within the Maritime segment

Within “Offshore”, 90 % of the expanding pins are applied in Drilling and Pipe handling equipment, and Offshore cranes. Within “Maritime” 84 % is distributed into Maritime cranes, Winches, and A-frames. The next segments are “Construction & Earth moving” and “Mining”, with 18 and 14 responders, respectively.

Many of the survey responders, 87 %, confirm that the expanding pin solutions they have applied were sourced from *external suppliers*, and the rest (13 %) indicated that they had used their *own design* for expanding pins applied for their own products, as illustrated in Figure 4.7. The numbers for “own design” were 14 % and 10 %, for the Norwegian and non-Norwegian based stakeholders, respectively. Analysing all the 8 Norwegian based companies applying their own expanding pin design, 75% belonged to the bigger size segment (CS3 > 100 employees), and 75 % belonged to the segment with longest experience with expanding pin solution, (> 10 years), and 50 % belonged to both groups at the same time (big with long experience). These 8

Results and Discussions

companies all work within the sectors “Offshore”, “Maritime”, and “Construction & Earth moving”. If a company design, apply, or sell a product which is identical or based on information they have received from their suppliers over several years, that could be an infringement according to the law. In this case, it can be seen that those who designed their own expanding pin solutions belonged to the biggest companies with longest experience with the products in question, within huge industries.

On the question “What is the reason for your company to choose or work with expanding pin technology?”, four closed-end answers were given, in addition to one open-end:

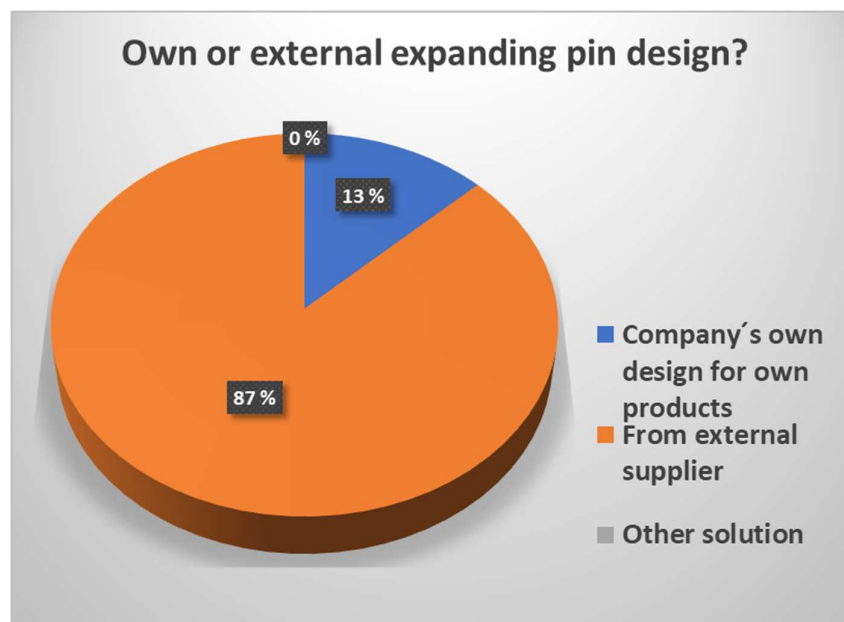


Figure 4.7. Source of expanding pin design

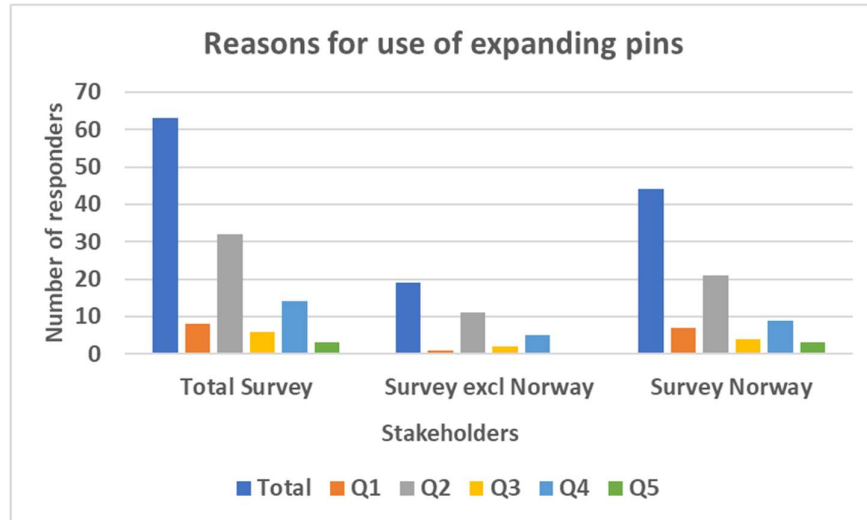


Figure 4.8. Reasons for use of expanding pins

(Q1) It is a strong wish or requirement from our clients, (Q2) It is based on our previous experience, (Q3) It is new for us, and we want to test it, (Q4) The pins come with the equipment when we receive it, and (Q5) Other reasons. The reason why the total number of responders (63) is higher than the previous defined number of responders (58) is because some have responded on more than one of the five options.

Both the Norwegian and non-Norwegian based companies gave the same *main reasons* for their use of expanding pins, being (Q2) “It is based on out previous experience”, and (Q4) “The pins come with the equipment when we receive it”, with 51 % and 22 %, respectively, as illustrated in Figure 4.8. This indicates that this pin solution has worked as expected or better (Q2), and the procure was repeated based on previous experiences, for those who are in the position to select and procure themselves. The numbers also show that the expanding pin solution comes installed into the equipment, from OEMs (Q4), and there is no choice for the receiving part to choose pin solutions. Around 13 % stated that their reasons for using this technology was (Q1) “It is strong wish or

requirement from our clients”, which is typically the result of a push-pull strategy, where the pin suppliers are pushing the OEMs to include the expanding pin solution into their products, and their clients are pulling at the same time, to reach the same goal.

In [Paper IV](#) only segments (a), (b), (c), (d), and (f) were analysed, and the segments (e) Mining, (g) Specialized machines, and (h) Steel and paper were not taken into consideration. The results from [Figure 4.9 – 4.17](#) are taken from [Paper IV](#), where the stakeholders are divided into 6 groups, (i) OEMs, (ii) Supplier to OEMs, (iii) Engineering companies, (iv) End-users, (v) Service & maintenance companies, and (vi) Others, and from [Paper I](#), where the stakeholders are divided into Norwegian and non-Norwegian based. The stakeholders’ *perceptions and experiences* have been illustrated through questions and responses regarding *Safety, Wear, Breakage, Installation and Retrieval time, and Economic impact*, as described below.

Safety:

[Figure 4.9 \(a\)](#) visualizes the stakeholder groups’ view on the importance of having safe and secure pin solutions in their operations, in general, while [\(b\)](#) illustrates their opinion on safety level when comparing expanding pins against standard cylindrical pin solutions. The *importance of safety* for personnel and equipment was highly valued by the stakeholders, as shown in [Figure 4.9 \(a\)](#). Only 4 % stated that the safety was “Not important”, while the rest, representing 96 %, was almost equally divided between “Important” and “Crucial and decisive”, which represent well the general perception of the attitude towards safety in the industries in question. Approximate 60 % of the stakeholders in each of the three groups, (i) OEMs, (ii) Supplier to OEMs, and (iii) Engineering companies, confirmed safety as “Crucial and decisive”.

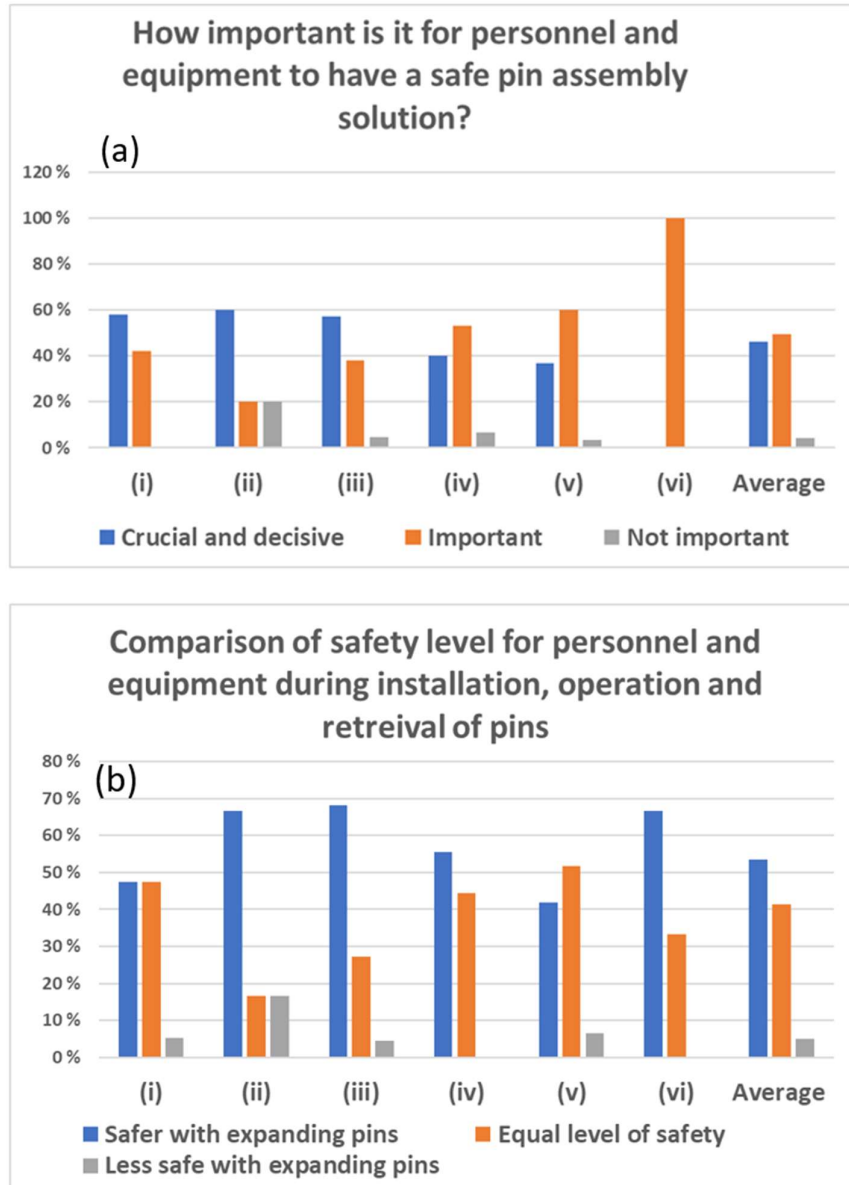


Figure 4.9. Expanding pin regarding safety level, (a) importance, and (b) comparison

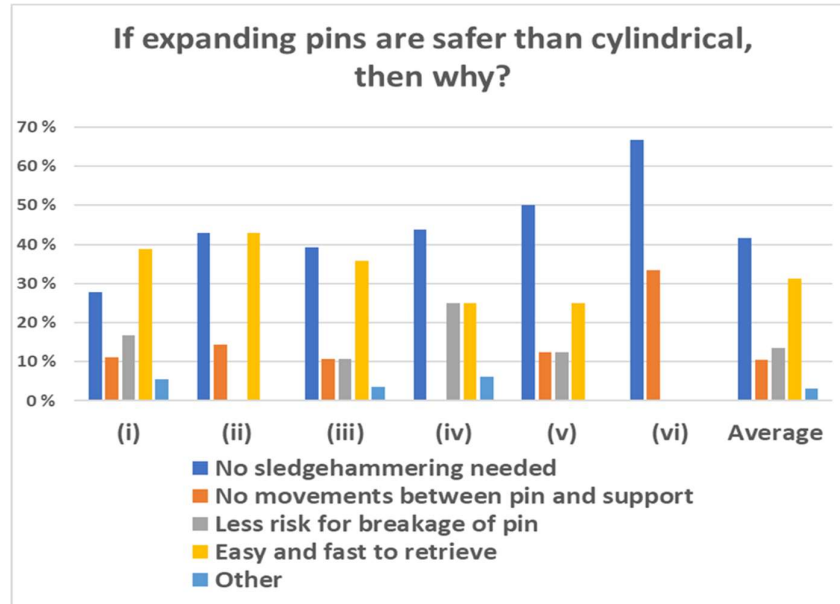


Figure 4.10. Expanding pin – reasons for safety level

In relation to the question about the stakeholders' opinion on the importance of safety, they were also asked to give their *comparison of safety level* between expanding pins and standard cylindrical ones. From Figure 4.9 (b) it can be seen that 54 % had the opinion of expanding pin solutions being better during operations (installation, operation, and retrieval) than the standard cylindrical one, while only 5 % indicated the opposite. The highest value on “Safer with expanding pins” (68 %) was given by the (iii) Engineering companies, and the highest value on “Less safe with expanding pins” (17 %) came from (ii) Suppliers to OEM's. In addition to the four optional answers, an additional question was given for those who reported expanding pins to be safer, “If expanding pins are safer than cylindrical, then why?”, as illustrated in Figure 4.10. The all-over average values show that there are two main reasons for the “then why” question, “No sledgehammering needed (for installation of pins)” with 42 %, and “Easy and fast to retrieve” with 31 %. The groups (iv) End-users, and (v) Service & Maintenance companies had relative high

scores on “No sledgehammering needed” with 44 % and 50 %, respectively.

It can be expected that these two groups in general have good experiences with installing standard cylindrical pins and have first-hand knowledge with the most common issues and problems related to such work. In Figure 4.9 (b) it is illustrated that over 50% of the stakeholders confirm that the expanding pin system is a safer solution than the cylindrical, and the reason why is seen in Figure 4.10.

Wear:

Figure 4.11 visualizes well the stakeholders’ opinions about wear issues when comparing the two pin types, and as indicated, all stakeholder groups show a clear tendency to have experienced *less tear and wear* (at pin and supports) with expanding pins, compared with standard pins.

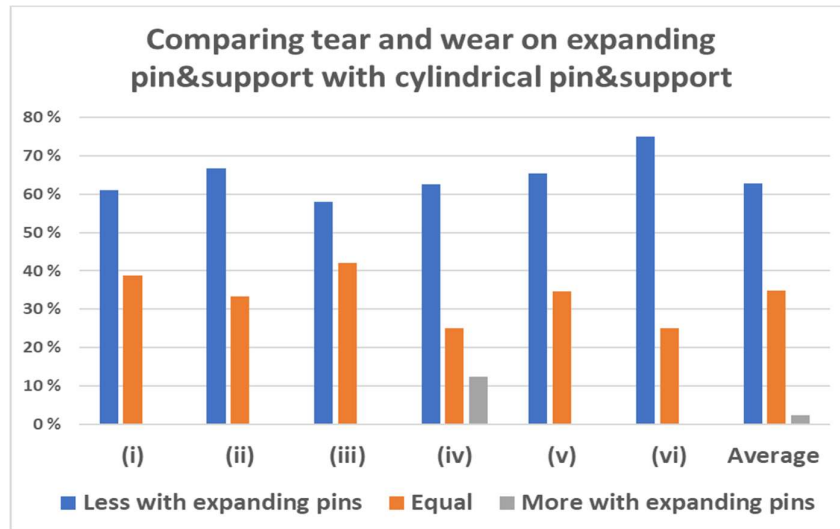
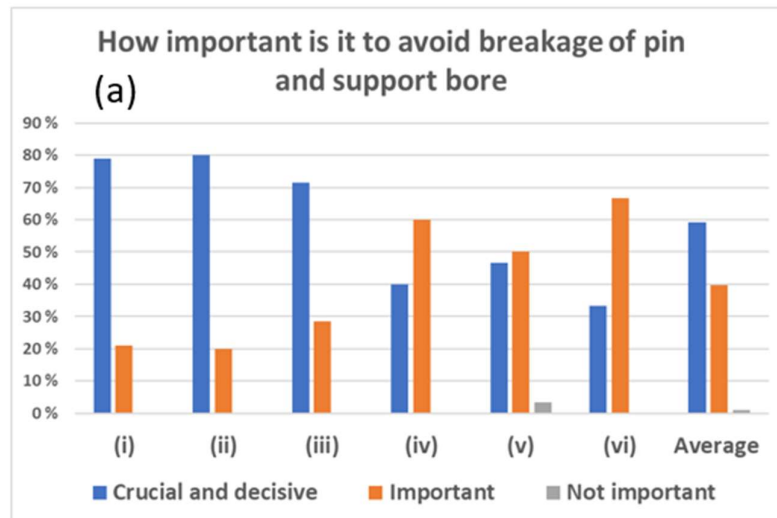


Figure 4.11. Comparison of tear and wear between expanding pin system and cylindrical pins

The average values show a score of 63 % in favour of “Less with expanding pins”, 35 % stating “Equal” and only 2 % “More with expanding pins”, with the latter coming from the End-users group. A correctly installed expanding pin system will not move relatively to the supports due to the wedge effect, so no wear issues should be present, but if the pin assembly is incorrectly installed and tightened up, relative movements could occur, and wear could happen.

Breakage:

Figure 4.12 (a) gives a view over the stakeholders’ *opinion of the importance* of avoiding pin and support breakage in their machines and equipment, while 4.12 (b) illustrates the stakeholders’ *opinions when comparing* expanding pins with cylindrical ones. The information in Figure 4.13 is presented in Paper I, and represents Figures 11 and 12 (b), where the responses are distributed between Norwegian based and non-Norwegian based companies, or stakeholders.



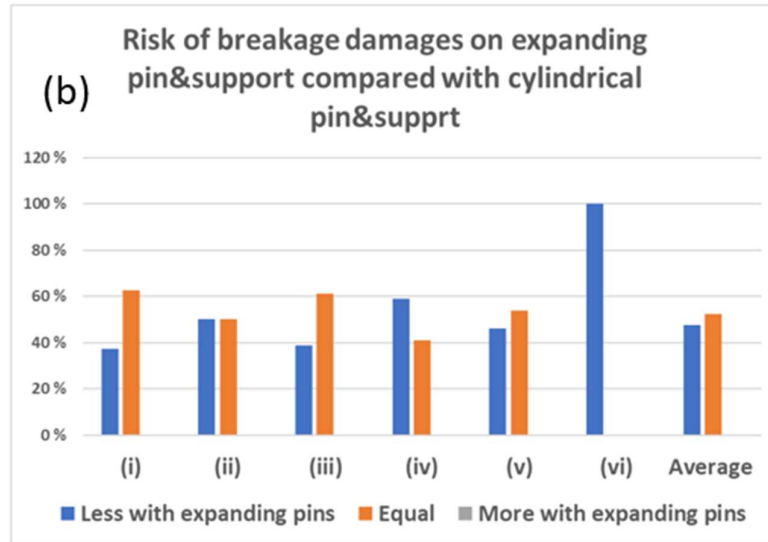


Figure 4.12. Expanding pin regarding breakage, (a) importance, and (b) comparison

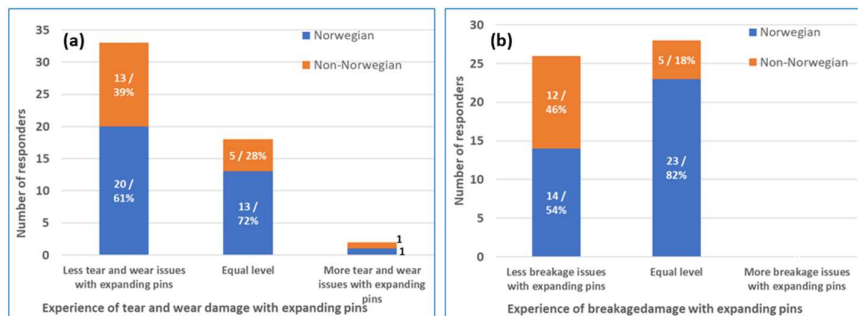


Figure 4.13. Experiences with expanding pins, distributed per location, (a) tear and wear, and (b) breakage

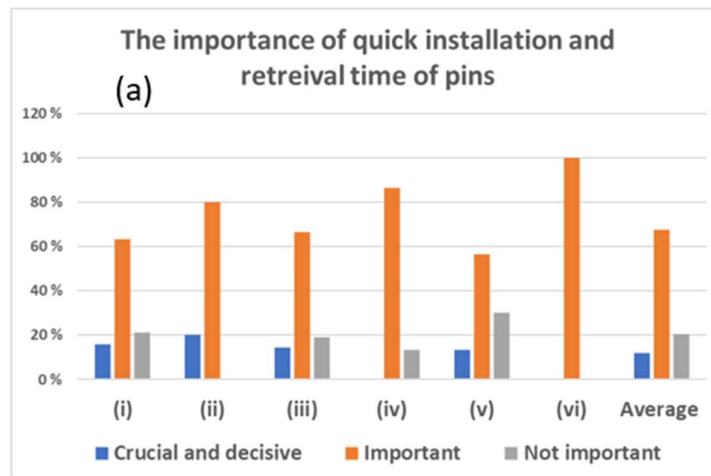
The stakeholders were first asked about the *importance to avoid breakage* of pin and support, and subsequently about their opinion of the risk of breakage when comparing expanding and cylindrical pins, see Figure 4.12. An average of 59 % confirmed that it is “Crucial and decisive” to avoid breakage damages, with 70-80 % for the three groups,

(i) OEMs, (ii) Suppliers to OEMs, and (iii) Engineering companies. For the three other groups, (iv) End-users, (v) Service & Maintenance, and (vi) Others, the attitude changed more against “Important” rather than “Crucial and decisive”, and even 1 company within (v) stated “Not important”. This change of attitude could maybe be related to who must pay and who gets work and paid when such accidents occur.

There were 0 % stating a higher *risk of breakage* with expanding pins, and 48 % who stated reduced or less risk with expanding pins. These results coincide well with experiences where expanding pins are wedged to the supports with zero clearance, and standard cylindrical pins create increasing clearance between pin and support over time. Increased clearance results in increased accelerations in the joint, and therefor also increased reaction forces, which can provoke pin breakage.

Installation and retrieval time:

The stakeholders’ opinions about the importance of quick installations and retrievals, and their view on how an expanding pin solution act on installation and retrieval compared to a standard cylindrical pin are illustrated in [Figure 4.14](#).



Results and Discussions

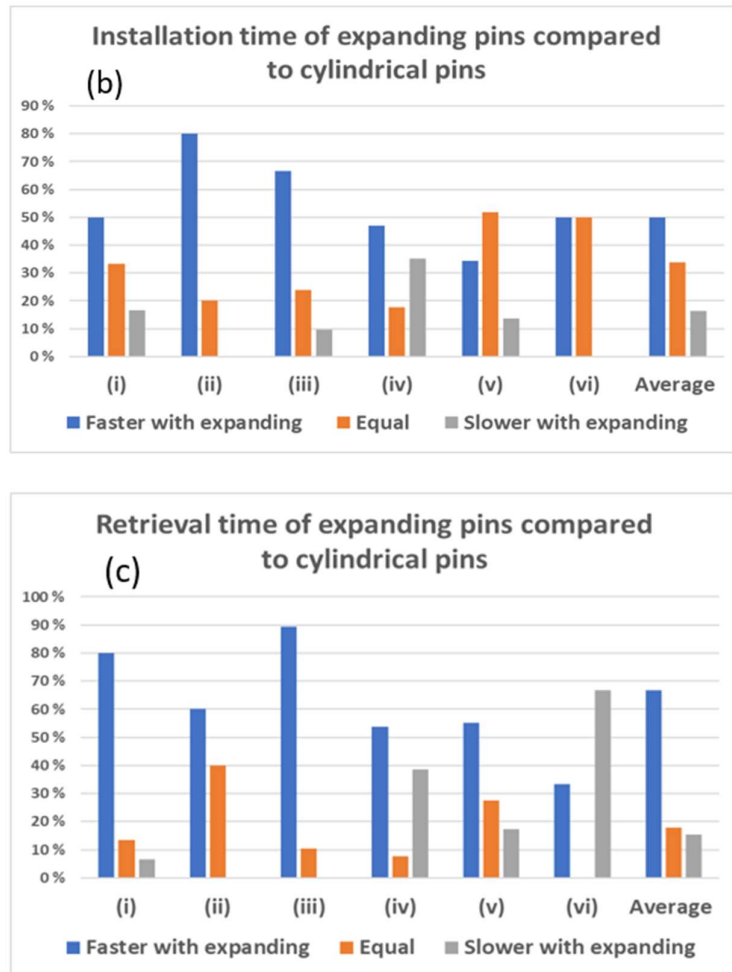


Figure 4.14. Expanding pin regarding quick installation and retrieval, (a) importance, (b) comparison on installation time, and (c) comparison on retrieval time

Results and Discussions

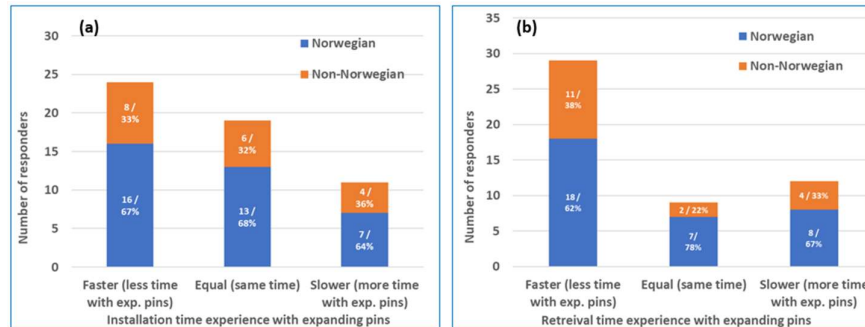


Figure 4.15. Experiences with expanding pins, distributed per location, (a) installation time, and (b) retrieval time

The information in Figure 4.15 is presented in Paper I and represents Figures 14 (b) and (c), but the responses are distributed between Norwegian based and non-Norwegian based companies. The *importance of quick installation and retrieval* time of pins and the stakeholders' comparisons of the two pin types, are illustrated in Figure 4.14. It can be seen that 80 % of the total responders are of the opinions that a quick installation and retrieval process is important, or very important (crucial and decisive), with 20 % saying that it is not important, with Service & Maintenance as the highest score (30 %). As for Breakage above, it could be a relationship between who must pay and who gets work and paid when such pin solutions have to be installed or retrieved. The Service, repair, and maintenance companies often get paid for the hours spent, so their interest will not necessarily be working with on quick solutions which could reduce their scope of work and turn-over.

The stakeholders' *actual experiences and opinions* on expanding pins vs cylindrical pins, when it comes to installation and retrieval time, is illustrated in Figure 4.14 (b) and (c). A majority of the total survey stated that the process with *installation and retrieval* of pins go faster when the pins are of expanding type, with 50 % and 67 %, respectively. The corresponding scores for "Slower with expanding" pins are 16 % and 15 %.

Regarding *Installation time*, the stakeholder groups (i) OEMs, (ii) Suppliers to OEMs, and (iii) Engineering companies, have the highest scores on “Faster with expanding” pins, with 50 %, 80 % and 67 %, respectively. The two first are also the groups that actually install the required pins into new equipment before deliver to their clients and should have valuable experience and competence within that area. The End-user group has the highest score of all groups on “Slower with expanding” with 35 %, although its score on “Faster with expanding” is even higher (47 %). End-users are not necessary the most experienced with the installation, compared to OEMs and Service companies, which could maybe explain the high score.

Regarding *Retrieval time*, the differences are even greater, in favour of “Faster with expanding” pins. The stakeholder groups (i) OEMs, and (iii) Engineering companies, have the highest scores, with 80 % and 89 %. From [Figure 4.15 \(b\)](#) it can be read that the non-Norwegian based companies have a shift from “Equal” towards “Faster with expanding” pins, compared to the Norwegian based companies. As for Installation, the End-user group also here had a high score (38 %) on “Slower with expanding”, and the explanation is probably the same.

Economic impact:

The specific question in the survey was “What are the *economic effects and consequences* for your company and/or your clients when using expanding pin technology, instead of standard cylindrical pins?”. The scores and numbers on Economic impact are presented in [Figure 4.16](#) (divided into Norwegian and non-Norwegian based location), and [Figure 4.17](#) (divided into stakeholder groups). It can be seen that 85 % of the total number of responders state that the expanding pin solution is Important or Crucial and decisive for them, divided into 64 % and 21 %, respectively.

Results and Discussions

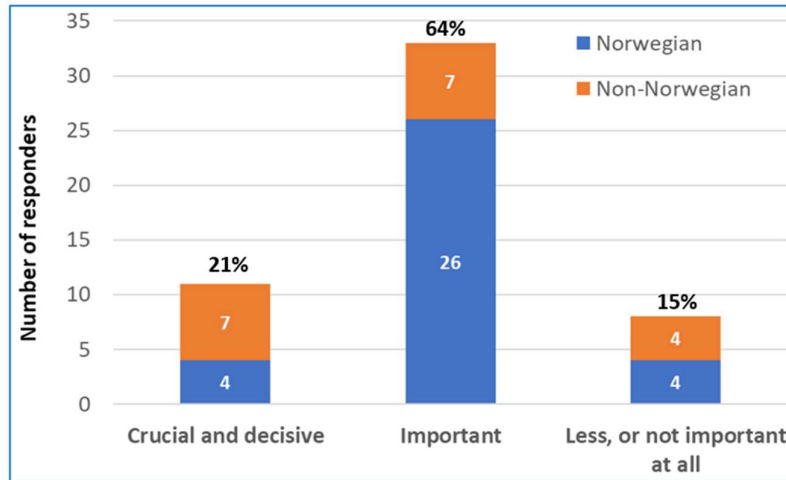


Figure 4.16. Economic impact of use of expanding pins compared to standard cylindrical pins, per location

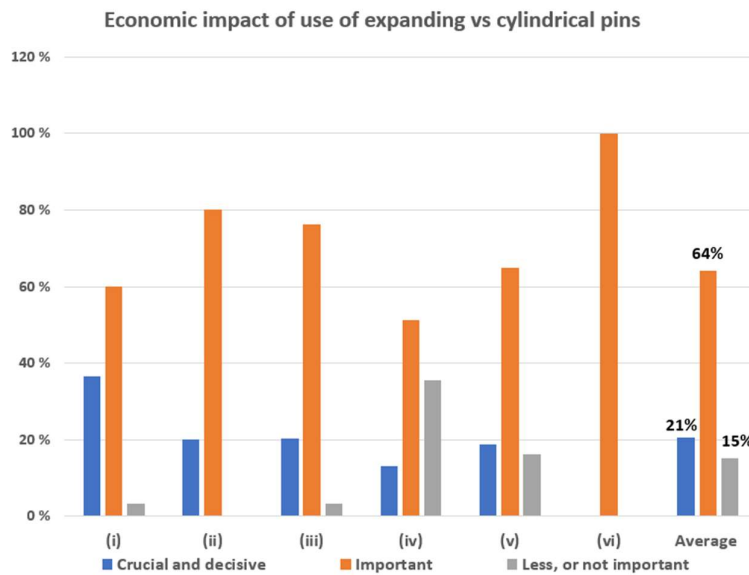


Figure 4.17. Economic impact of use of expanding pins compared to standard cylindrical pins, per stakeholder group

A group representing 15 % of the total responders is of the opinion that the expanding pin solution is of Less importance, or Not important at all. This last group is equally divided between Norwegian and non-Norwegian based companies, and 7 of the 8 companies belong to the Service, Repair, and Maintenance, and End-users. These groups could have a negative attitude towards the expanding pin solution because it represents a more efficient solution which could reduce their scope of work and income, as shown in [Figure 4.11](#) (less tear and wear), [Figure 4.12](#) (less risk of breakage), [Figure 4.14](#) (shorter installation and retrieval time), and [Figure 4.17](#) (economic impact for OEMs). It can also be noticed that 4 out of the 8 companies that stated that the expanding pin was not important from an economic point of view, also represent the group which receive the OEM equipment / machines with pins already installed. It can also be seen that 3 out of the same 8 companies have confirmed that expanding pins are faster to install and retrieve, and at the same time confirming the economic impact to be low, or zero. The OEMs, suppliers to OEM, and Engineering companies have a score of 99-100 % on expanding pin solutions being Important or Crucial and decisive from the economic point of view.

4.2.2 Results of studies of traditional expanding pin solutions ([Papers II, III, and VI](#))

These analysis of traditional bondura® expanding pin systems include an experimental study of combining expanding dual pin with radial spherical plain bearings ([Paper II](#)), an experimental study of applying expanding pin with 3D printed repair kit for worn supports ([Paper III](#)), and experimental and numerical studies of the stress distribution in an expanding pin joint ([Paper VI](#)).

In [Paper II](#), the values of diameter changes of the bearing inner ring were measured, when exposed to the radial expansion of the expanding dual pin, as illustrated in [Figures 4.18 – 4.21](#). The 4 figures correspond

with the test set-ups illustrated in [Figure 3.1 \(i\)](#) and [\(ii\)](#) with non-lubricated and lubricated sleeves. An expanding dual pin was first installed into *two bearing inner rings* ([Figure 3.1 \(i\)](#)), and subsequently into *one single inner ring* ([Figure 3.1 \(ii\)](#)). Both tests were performed with dry and lubricated sleeves and in both cases complete bearings were installed in the supports. In addition, similar tests were performed but with *two complete bearings* ([Figure 3.1 \(iii\)](#)), and *one single complete bearing* ([Figure 3.1 \(iv\)](#)). In these two last tests (2a and 2b), the bearings were loaded additionally stepwise with external load, and the required moment to turn the pin on bearing inner ring relatively to the bearing outer ring was measured and calculated. The bearings were lubricated internally, and the sleeves were dry and clean.

In Test 1a and 1b, the dual pin was torqued, and the inner rings were loaded radially outwards, and changes in diameter at 4 sections (a, b, c, and d, as shown in [Figures 3.2](#) and [3.3](#)) were measured by CMM. The measured values for Test 1a, non-lubricated and lubricated, are illustrated in [Figures 4.18](#) and [4.19](#). Section – a – in [Figure 3.2](#) represents the entrance side for the sleeve. Section – a – and – d – in [Figure 3.3](#) represent the entrance sides for the sleeves.

Both the non-lubricated and lubricated Test 1a ([Figures 4.18](#) and [4.19](#)), where each ring is mounted on its own single sleeve, indicate that the bearing rings opens up, or increase its outer radii, at sections – a – and – b –, and decrease at – c – and – d –, as the expanding sleeve enters the ring, with highest radius increase at entrance section – a –. This was also found in [Paper VI](#) where the sleeve radial stresses and pin-sleeves contact stresses were analysed by FEA.

The measured values for Test 1b, non-lubricated and lubricated, are illustrated in [Figures 4.20](#) and [4.21](#). The zero-point is a soft torque moment of 5 Nm, and the values shown in the corresponding figures are the increase of expansion compared to the defined zero-point torque.

Results and Discussions

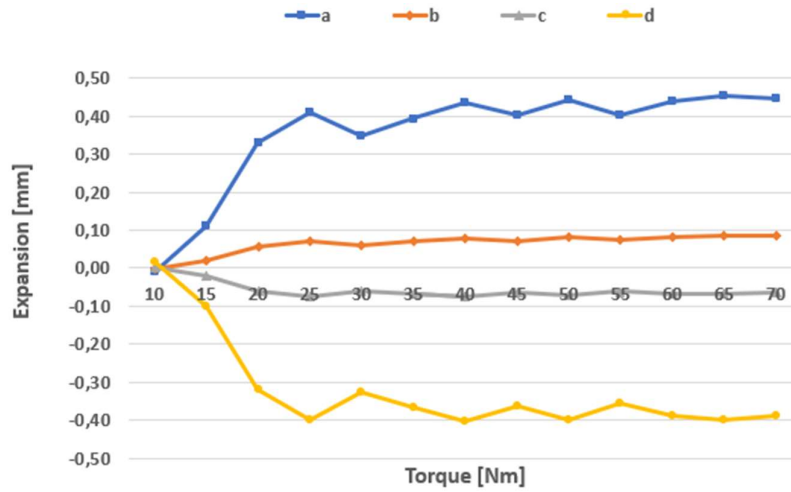


Figure 4.18. Test 1a – ring deformations on non-lubricated single sleeve

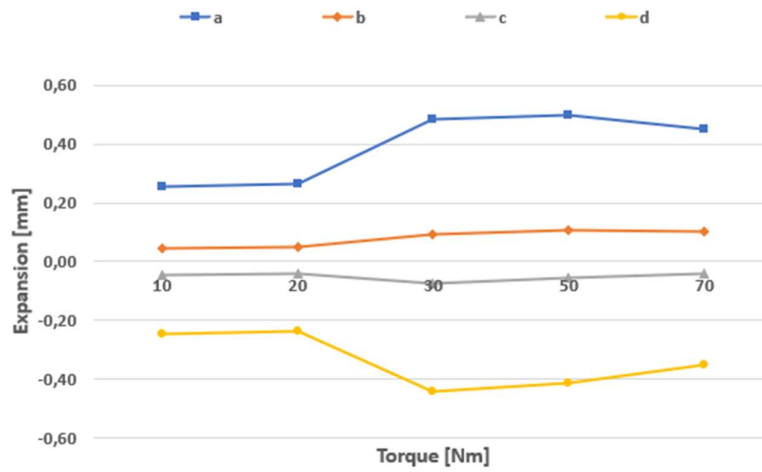


Figure 4.19. Test 1a – ring deformations on lubricated single sleeve

Results and Discussions

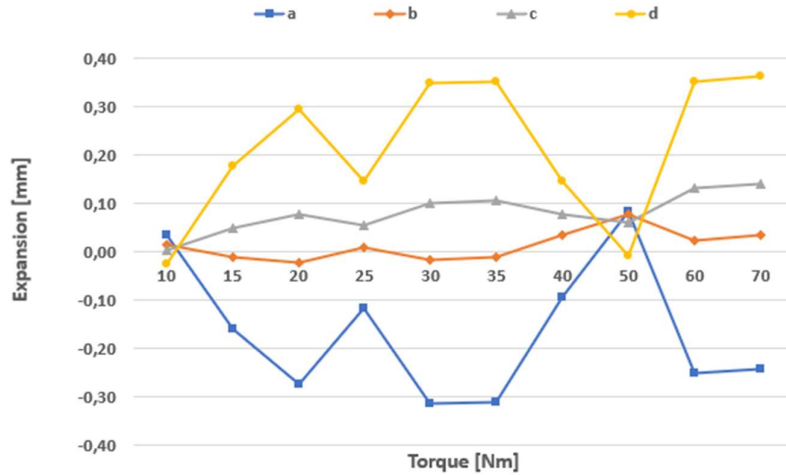


Figure 4.20. Test 1b – ring deformations on non-lubricated double sleeve

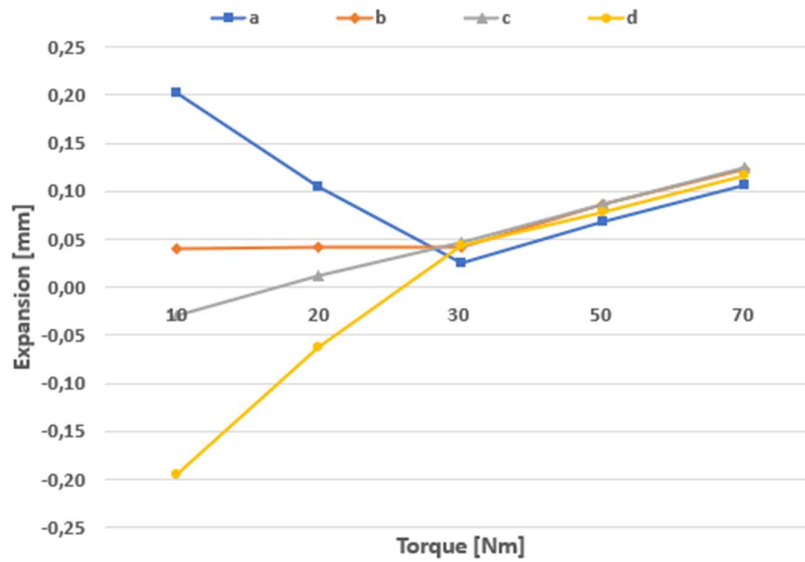


Figure 4.21. Test 1b – ring deformations on lubricated double sleeve

When comparing the *Test 1a* non-lubricated version (Figure 4.18) with the lubricated (Figure 4.19) it becomes clear that deformation pattern and

the maximum ring radius changes are almost identical, + 0.45 to + 0.50 mm and – 0.40 to – 0.42 mm, but with some differences at the lower torque values. The sleeve in the non-lubricated version didn't slip at 10 Nm torque, probably due to friction, and the ring didn't deform. After torquing to maximum value of 70 Nm, the ring remained deformed with increased entrance diameter (section *a*) and reduced radius on the opposite side.

When comparing the *Test 1b* non-lubricated version (Figure 4.20) with the lubricated (Figure 4.21) it becomes clear that the behaviour of the two versions were quite different. In this test one ring is mounted on two sleeves at the same time (Figure 3.1 (ii), and 3.3), so each of the sections – *a* – and – *d* – represent an entrance side, and the centre sections – *b* – and – *c* – are placed at the unsupported area at the middle of the ring.

The un-lubricated version shows a much more serrated shape than the lubricated, for both sides of the ring, but with opposite changes, where – *d* – generally has increased (up to +0.35 mm) and – *a* – generally has decreased (down to - 0.30 mm), over the complete torque range. The only exception is at 50 Nm torque where the – *a* – section has increased and the – *d* – section has decreased. The strongly serrated shape shown at section – *a* – is probably the effect of the entrance of the sleeve at the opposite side, at section – *d* –, and overcome the accumulated/hysteresis surface stresses with increasing torque.

The lubricated version though has a completely different deformation pattern, with increased – *a* – section diameter (+0.20 mm) and reduced – *d* – section (down to – 0.20 mm) at lowest torque of 10 Nm. At torque level 30 Nm both sides or sections had increased identically to approximately +0.04 mm, and further torque resulted in further identical deformation behaviour, with 50 Nm / + 0.07 mm, and 70 Nm / + 0.12 mm.

The two tests, *Test 1a* and *Test 1b*, both with non-lubricated and lubricated versions, gave 4 different bearing inner ring behaviours when

exposed to radial expansion from the expanding dual pin. It is assumed that the effects from the expanding sleeves will give the same deformation pattern on the inner ring when they are installed in a bearing on an expanding pin, when the radial clearance between the inner ring and outer ring is still not reduced to zero, and the bearing is not exposed to external loads.

The behaviour of complete bearings exposed to the combination of an expanding pin and external loads are illustrated in [Figures 4.22](#) (Test 2a) and [4.23](#) (Test 2b), both with internal lubrication of the bearings but dry sleeves, and the contact configurations are shown in [Figure 3.4](#). The figures indicate the rotational moment required to turn the pin assembly in the bearings as internal torque and external load increases.

The pin in *Test 2a* was torqued to following values; 0 Nm, 5 Nm, 25 Nm, 45 Nm, and 65 Nm, with external loads in steps of 50 kN, from 0 kN to 400 kN. The pin in *Test 2b* was torqued from 5 kN to 65 kN in steps of 10 kN, with external loads of 50 kN, 100 kN, 200 kN, 300 kN, and 400 kN.

In *Test 2a* ([Figure 4.22](#)), the highest rotational moments were measured for the lowest and the highest torque values, 5 Nm, and 65 Nm, respectively. The two torque values 25 Nm and 45 Nm had an average of 25-35% lower rotational moments compared to 5 Nm and 65 Nm torques, in the upper range of external loads (250 – 400 kN). This test was performed with internal lubrication of the bearings, but dry and clean sleeves.

Results and Discussions

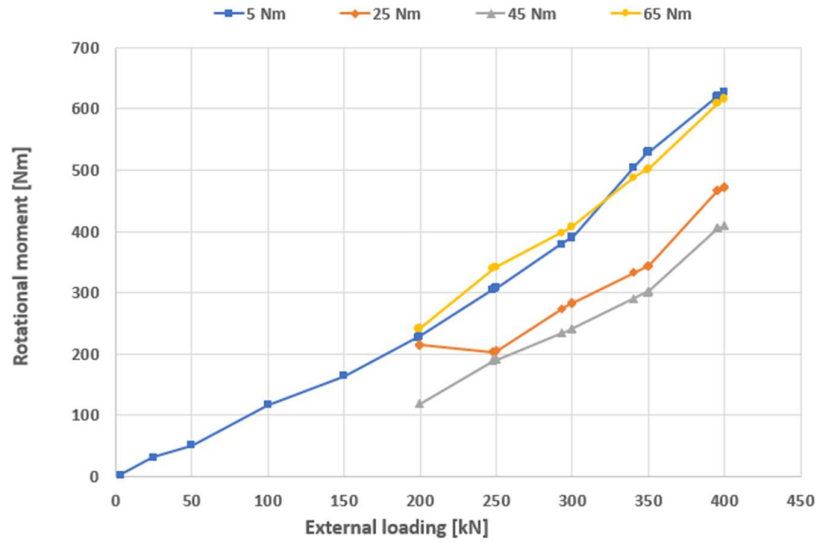


Figure 4.22. Test 2a – total rotation moment per bearing, on single dry sleeve

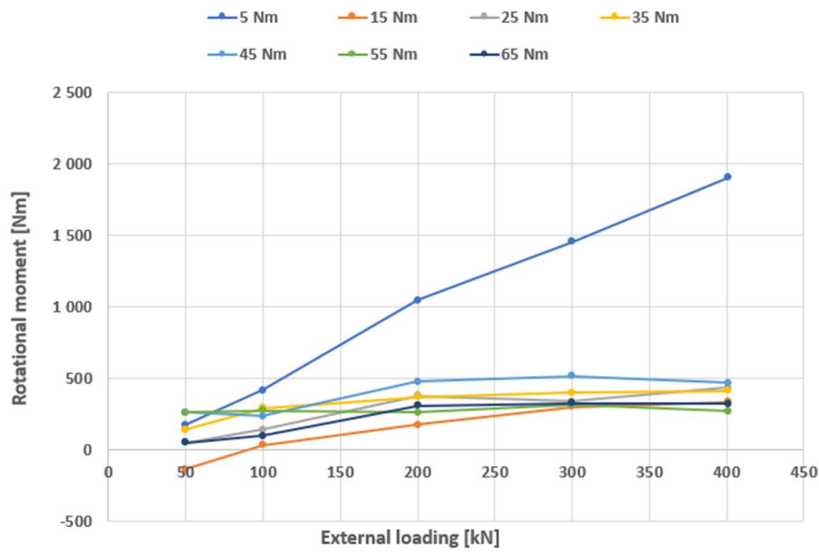


Figure 4.23. Test 2b – total rotation moment per bearing, on double dry sleeves

The reasons or explanations for the measured results could be:

- At lowest torque, 5 Nm, the expansion of the inner ring was close to zero at all sections, as illustrated in [Figure 4.18](#), thus inner surface kept its cylindrical shape, and the clearance between the inner and outer rings was positive as for a fabric-new bearing. This relatively wide clearance results in a relatively small contact pressure area between the rings, and a corresponding high contact pressure with possible accelerated loss of oil film, which is the situation represented by the curve for 5 Nm torque in [Figure 4.22](#). It is assumed that a curve with a standard cylindrical pin would be very much like the one for the 5 Nm torque.
- At medium torques, as for 25 and 45 Nm, the inner ring took a conical-cylindrical shape at zero external load ([Figure 4.18](#)), but with increasing external loads the shape was pushed back from conical-cylindrical to more cylindrical, which means less difference between the sections – *a* – and – *d* –. The inner ring has expanded (as illustrated in Fig. 12a in [Paper II](#)), but less than the fabric-new tolerance. This expansion of the inner ring increased the contact area between the rings in the bearing, reduced the contact pressure and loss of oil film, and resulted in reduced required rotational moment (compared to the 5 Nm torque curve), as shown in [Figure 4.22](#).
- At the maximum torque, 65 Nm, the rotational moment curve became almost identical with the one for the lowest torque. The average expansion over the inner ring was still lower than the fabric-new tolerances (as illustrated in Fig. 12a in [Paper II](#)), but the shape was conical-cylindrical with a maximum expansion of 0.45 mm which is 3 – 6 times higher than the fabric-new tolerances. It is assumed that the external load was not able to push back the inner ring from a conical-cylindrical to a cylindrical shape, and therefore it was produced a high contact

pressure between the rings, at the – a – section side of the inner ring.

In *Test 2b* (Figure 4.23), the lowest pin torque, 5 Nm, gave an elevated rotational moment for the pin assembly, compared to the other torque values, over almost the complete range of external loads (100 to 400 kN). The 6 torque values 15 to 65 Nm with steps of 10 Nm, had a variation of rotational moment from approx. 0 - 300 Nm at 50 kN load to 266 – 466 Nm at 400 kN load, while for the 5 Nm torque the corresponding values were approx. 200 Nm and 1903 Nm. This test was performed with internal lubrication of the bearings, but dry and clean sleeves. The reasons or explanations for the measured results could be:

- The curve for the 5 Nm torque can be explained as for Test 2a.
- The difference between Test 2a and 2b is that for 2b both ring ends were forced to expand, and by that continuously forcing the inner ring shape to work towards the cylindrical shape, and not the conical-cylindrical shape, also for the highest torque value. The increasing external load will also push the inner ring towards the cylindrical shape. The average ring deformation (as described in Fig. 13a in Paper II) is below the absolute minimum fabric-new tolerances up to around 55-60 Nm torque, and most probably also at the 65 Nm torque.

In Paper III a novel technique for repair of damaged pin joint supports was investigated and presented, by experimental techniques. The damaged support area was 3D scanned and the collected data was used to 3D print a repair insert which was installed as the “new bore surface” or contact surface against the expanding pin sleeve.

The study contains experimental test results from 5 different tests as described in Table 1 in Paper III, as illustrated in Figure 3.5, (test 1) cylindrical pin with equally distributed wear on both supports (clearance 0.9 mm on L+R), (test 2) cylindrical pin with additional wear on one side (clearance 0.9 – 5.9 mm on L), (test 3) expanding pin with equally

Results and Discussions

distributed wear on both supports (clearance 0.0 mm on L+R), (test 4) expanding pin with additional wear on one side (clearance 0.0 – 5.0 mm on L), and (test 5) expanding pin with repair insert at the side with additionally wear (clearance 0.0 mm on L+R). The test set up is illustrated in [Figure 4.24](#) and strain gauges were applied to measure strains during external loading of the pins, as shown in [Figure 3.6](#) and [3.7](#).

The results achieved are visualized through [Figures 4.25 – 4.29](#), which are representing the 5 experimental tests that were performed. The results from all tests are showing both (a) measured strains at each pin end at 0° position, and (b) percentage change of strain value when turning the pin 15° . The strains measurements from *Test 1* are illustrated in [Figure 4.25](#). The measured results in *Test 1* (standard cylindrical pin with identical and evenly distributed wear at each support bore) showed an increasing difference between the measured strains at the two ends (R, L), both in strain and percentage values, as the external load increased.

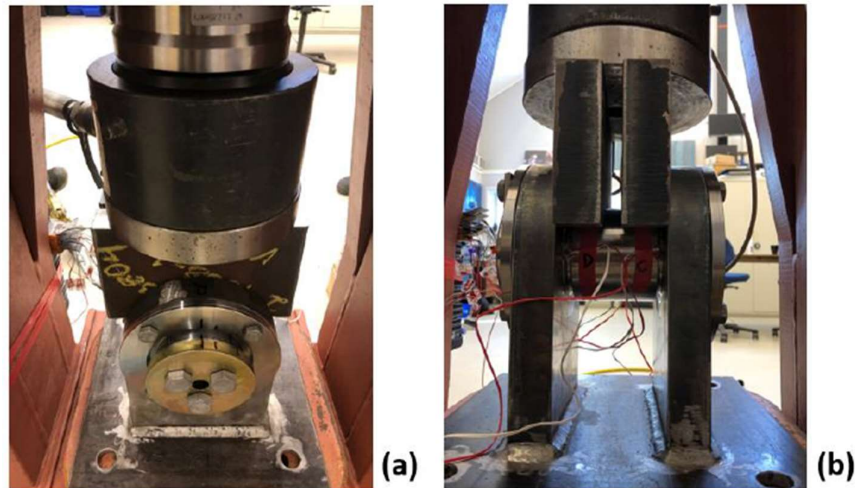


[Figure 4.24](#). Test setup with (a) expanding pin, and (b) standard cylindrical pin

Results and Discussions

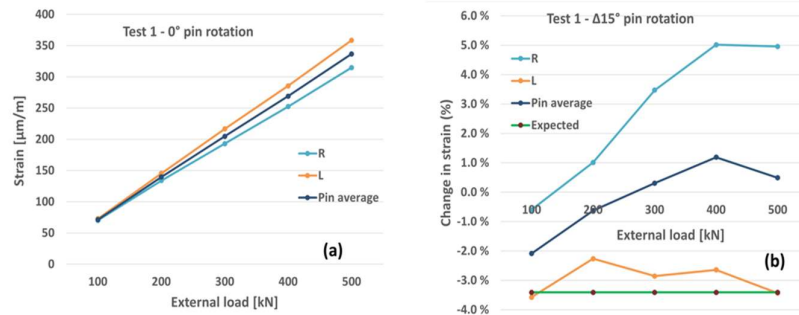


Figure 4.25. Test 1, (a) strains at 0° , and (b) percentage change, from 0° to 15°

The differences between the two pin ends at 0° position increased from 1.7 % at lowest load to 6.5 % at highest load, and when turning the pin 15° the average change of strain value increased 0.5 % instead of decrease 3.4 % as expected, which gave a difference of 3.9 %. The differences between the two pin ends at 15° position also increased with increasing external load, but less, or well below the half of the 0° values.

There could be several reasons and explanations why there are measured changing percentage differences between the pin ends at different external loads, and deviations between the measured average percentage change in strains, compared to the expected. Such reasons, or combinations of those, could be quality and type of strain gauges and glue, exact location of strain gauges, accuracy of the test jig and test performance, residual stresses in the steel etc.

The strains measurements from *Test 2* are illustrated in Figure 4.26. The results from Test 2 (same pin as in Test 1 but with additional severe wear at one support) were slightly different from Test 1, with highest percentage difference (8.4 %) at lowest external load and lowest (5.2 %) at highest load. In this test the, when turning the pin into the 15° position, the average strain value stayed at a higher level than for Test 1, with value +1.8 % at maximum load, compared to expected -3.4 %, which resulted in a *difference of 5.2 %*, compared to 3.9 % for Test 1. The

Results and Discussions

additional wear (+5 mm) at one side of the supports (L) made the pin turn a little also in the axial direction (approx. 3°) which could have affected the measurement negatively.

The measured results in *Test 3* (expanding pin wedged at both supports – [Figure 4.27](#)) showed lower differences in measured strains between the two pin ends, with 0.5 % at lowest external load and 2.8 % at highest, or only 43 %, compared to *Test 1*. When turning the pin into the 15° position, the average strain value at maximum load was -1.7 %, compared to the expected -3.4 %, which resulted in a *difference of 1.7 %*, which is 43 % of the corresponding value at *Test 1*. The strains measurements from *Test 4* are illustrated in [Figure 4.28](#).

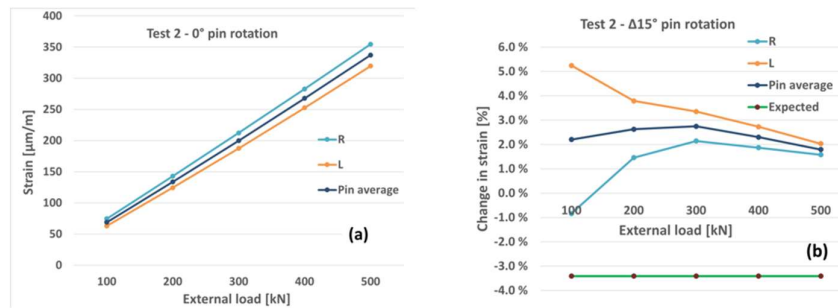


Figure 4.26. Test 2, (a) strains at 0° , and (b) percentage change, from 0° to 15°

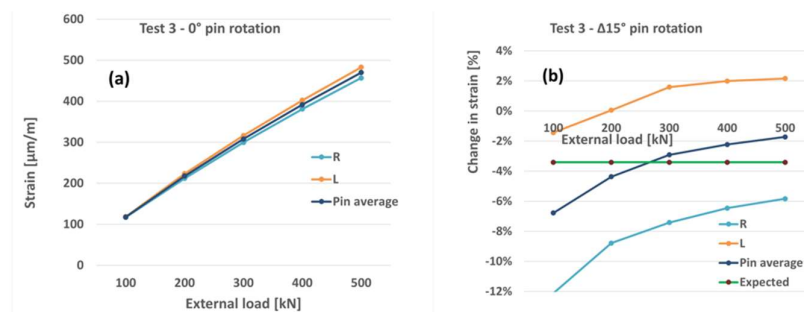


Figure 4.27. Test 3, (a) strains at 0° , and (b) percentage change, from 0° to 15°

Results and Discussions

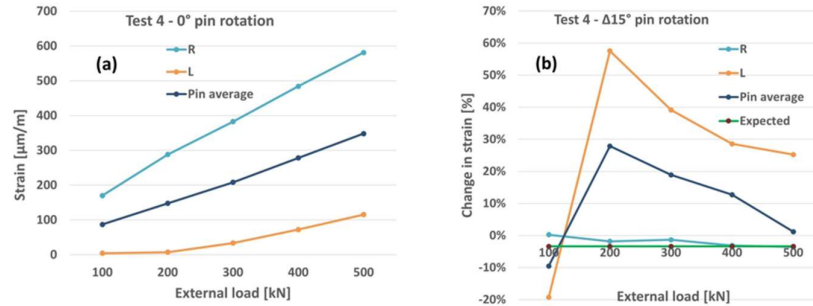


Figure 4.28. Test 4, (a) strains at 0° , and (b) percentage change, from 0° to 15°

Test 4 (expanding pin wedged at (R) side and free hanging at (L) side due to major wear at support) had very deviant values, as indicated in Figure 4.28. There was a major difference in measured strain values between the two sides (R) and (L), with highest values at the (R) side. Because of the major wear at the (L) side this end of the pin was “hanging free” and the (R) took all the load, until the external load reached 200 kN. At maximum external load (500 kN) the strain value at the (R) side was 6 times higher than at the (L) side, which indicate that the (L) end of the pin probably did not bend enough to touch the support.

The results from *Test 5* (expanding pin wedged to both supports with a repair insert at the (L) side to compensate for severe wear) are illustrated

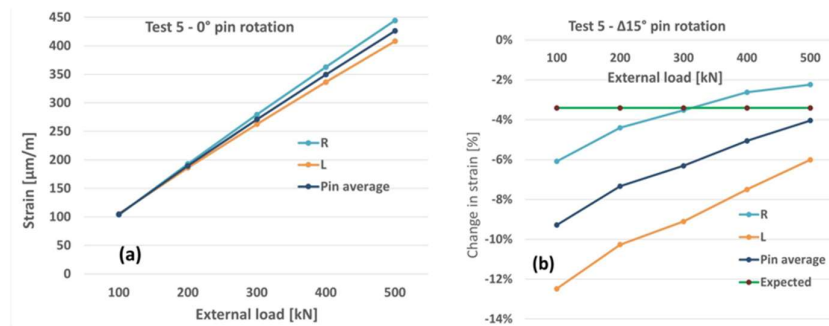


Figure 4.29. Test 5, (a) strains at 0° , and (b) percentage change, from 0° to 15°

Results and Discussions

in Figure 4.29. The differences in measured strains between the two pin ends were between the corresponding results from Test 1 and 3, with 0.9 % at lowest external load (1.7 % and 0.5 %, respectively) and 4.3 % (6.5 % and 2.8 %, respectively). When turning the pin into the 15° position, the average strain value at maximum load was -4.0 %, compared to the expected -3.4 %, which resulted in a *difference of 0.6 %*, which is the minimum difference of the 5 tests.

The measured and calculated strain values at both (R) and (L) sections, for all 5 tests, at 500 kN external load, are shown in Tables 4.1 and 4.2. Exact values for Test 2 and 4 could not be calculated, but their theoretical min./max. limits were given. The percentage relationship between maximum calculated values and measured values are also given.

In addition, the theoretical average and maximum strain values were calculated for each section (R) and (L), for each Test 1 – 5, at external load 500 kN, and compared with the measured ones. These values are shown in Tables 4.1 and 4.2. The calculated maximum values were compared with the measured values, and the differences are +26 %, -3 %, and +8 % at the 0° pin position for Test 1, 3 and 5. For the 15° pin position, the values were +21 %, -4 %, and +8 %, respectively.

Table 4.1. Measured and calculated strain values at real cross-sections for 0° pin rotation and 500 kN external load

Test No.	Pin End	Measured Strain Values, ϵ_{as} ($\mu\text{m}/\text{m}$)	Calculated Values:		
			For Average Shear Strains, ϵ_{ca} ($\mu\text{m}/\text{m}$)	For Max. Shear Strains, ϵ_{cm} ($\mu\text{m}/\text{m}$)	Max. to Measured Average Strain (%)
1	R	315	333	444	+26
	L	359	303	404	
2	R	355	> 333	>444	
	L	320	< 303	<404	
3	R	457	326	435	-3
	L	483	360	480	
4	R	581	> 326	>435	
	L	115	< 360	<480	
5	R	444	326	435	+8
	L	408	360	480	

Results and Discussions

Table 4.2. Measured and calculated strain values at real cross-sections for 15° pin rotation and 500 kN external load

Test No.	Pin End	Measured Strain Values, ϵ_{45° ($\mu\text{m/m}$)	Calculated Values:		
			For Average Shear Strains, ϵ_{α} ($\mu\text{m/m}$)	For Max. Shear Strains, ϵ_{cm} ($\mu\text{m/m}$)	Max. to Measured Average Strain (%)
1	R	330	322	429	+21
	L	346	293	391	
2	R	360	>322	>429	
	L	326	<293	<391	
3	R	430	315	420	-4
	L	493	348	464	
4	R	560	>315	>420	
	L	144	<348	<464	
5	R	434	315	420	+8
	L	384	348	464	

The measured values should (theoretically) be between the calculated average and maximum, and closer to the maximum, due to the strain gauge locations at the pins. The calculated values with expanding pins in Tests 3 and 5 correspond well with the measured maximum values, with -3 % and +8 % for 0° position, and -4 % and +8 % for 15° position. The corresponding values for the cylindrical pin were +26 % and +21 %.

Both the measured and calculated values are highly dependent on the exact location of the strain gauges, which affects the real cross-section area where the strains were measured and calculated.

In Paper VI, the stress distribution in the pin joint (bore and pin) was studied both experimentally and numerically, and the test setup is illustrated in [Figure 3.12](#). The pin end-sleeve had one cut-through and three partly cut-throughs, for expansion purposes. The complete cut-through was set into 4 different positions, $\pi/2$, $5\pi/2$, $7\pi/2$, and $\pi/4$, and the strains were measured by strain gauges, for both unlubricated and lubricated sleeves. In addition, a test was performed with a sleeve with 4 complete cut-throughs, and lubrication. Three different tests were performed with the following configurations, (1) *Unlubricated* sleeve with 3 x partly cut and 1 x fully cut-through, as presented in [Figures 4.30](#), [4.31\(a\)](#), and [Table 4.3](#), (2) *Lubricated* sleeves with 3 x partly cut and 1 x

fully cut-through, as presented in Figure 4.31(b) and Table 4.3, and (3) Lubricated sleeves with $4 \times$ fully cut-through, as presented in Figure 4.32. Only measured values at the inner surface of the test boss are given in Figure 4.30 (a)-(c), but additionally outer values in (d).

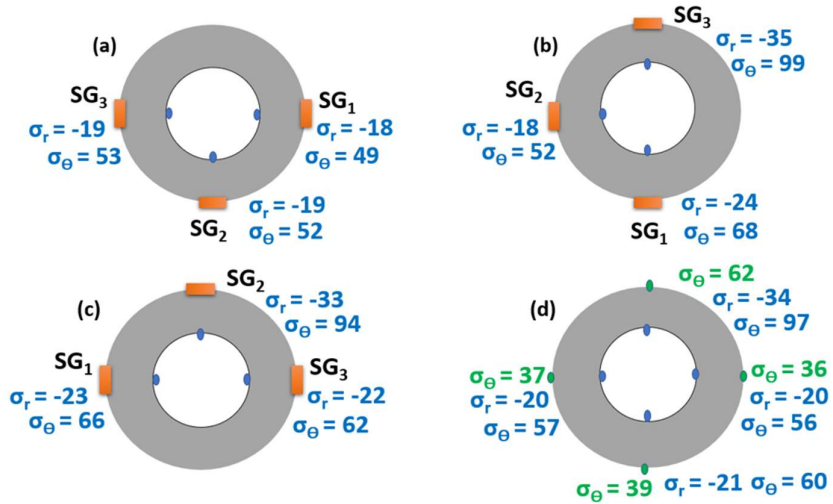


Figure 4.30. Hoops and radial stresses with unlubricated sleeve and 1 complete cut-through at $\pi/2 + 3$ partly cut-throughs, and strain gauge positions (a) 1, (b) 2, (c) 3, and (d) average values

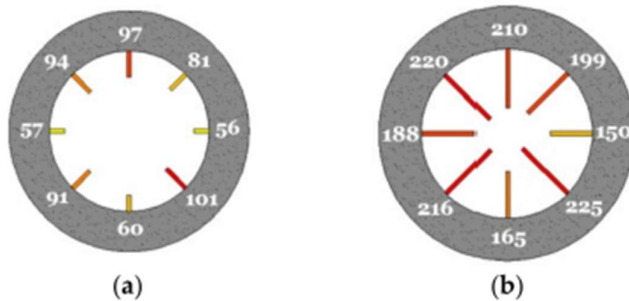


Figure 4.31. Hoop stresses at test boss inner surface with (a) unlubricated, and (b) lubricated sleeve, both for complete cut-through at $\pi/2$ position

Results and Discussions

Table 4.3. Calculated Hoop stresses on inner test boss surface, with one complete cut through and three partly cut throughs

Test Layout	Strain Gauge Nr. (Locations)	Position of Complete Cut-Trough			
		$\pi/2$	$5\pi/4$	$7\pi/4$	$\pi/4$
Unlubricated	No SG (0)	56	-	-	-
	SG 3 ($\pi/2$)	97	107	102	100
	SG 2 (π)	57	85	104	79
	SG 1 ($3\pi/2$)	60	88	76	93
Lubricated	No SG (0)	150	-	-	-
	SG 3 ($\pi/2$)	210	236	212	237
	SG 2 (π)	188	216	209	220
	SG 1 ($3\pi/2$)	165	203	181	230

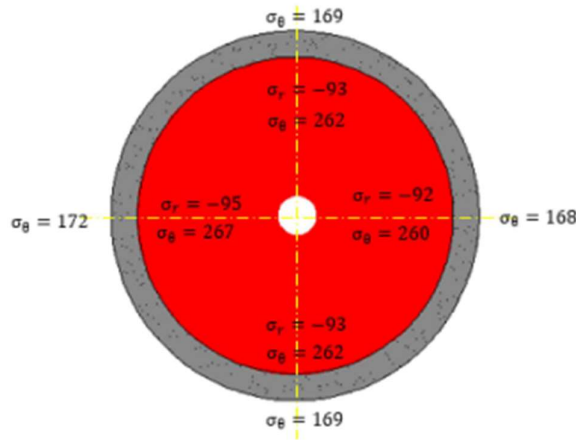


Figure 4.32. Hoop stresses at test boss inner surface with sleeve with 4 complete cut-throughs

Based on the measured strains values, the Hoop stresses were calculated, as illustrated in Figures 4.30, 4.31, Table 4.3, and Figure 4.32. Figure 4.30 shows the calculated Hoop and radial stresses on the inner surface of the test boss, in addition to the Hoop stresses at the outer surface, for positions 0, $\pi/2$, π , and $3\pi/2$.

The average Hoop stresses on the test boss inner surface from Figure 4.30 (d) are illustrated at Figure 4.31 (a). The calculated Hoop stresses on the test boss inner surface, Figure 4.31 (a) and (b) were placed into Table 4.3, at $\pi/2$ position, together with the corresponding calculated values for sleeve complete cut-through at $5\pi/2$, $7\pi/2$, and $\pi/4$, for both lubricated and non-lubricated situations.

It can be seen from tests (1) and (2) that the stress distribution at the inner surface of the test boss is not uniform. The hoop stress along the inner surface of the test boss is higher at the single fully cut-through, for both the dry and lubricated test, compared to the partly cuts, with 68 % and 25 % higher, respectively. In addition, the hoop stresses between all cuts are higher than at the stress at the partly cuts, with 60 % and 28 % higher, respectively. At test (1) the lowest hoop stress value (56 MPa) is 55 % of the highest (101 MPa), and at an angular distance of $\pi/4$. For test (2), the value is 67 %, and the angular distance between the minimum stress (150 MPa) and the maximum (225 MPa) is the same, and in addition the angular distance between the complete cut and the minimum and maximum stresses are the same ($\pi/2$ and $3\pi/4$). In test (3) there are 4 fully cut-through with almost identical hoop stress values (+/- 1.3 %).

When comparing the calculated hoop and radial stresses from the three different conditions, it can be concluded that there are losses due to friction and expansion of sleeve, during torquing. The average of hoop stresses in the lubricated condition (2) is 2.54 times greater compared with the non-lubricated condition (1), and the condition with 4 fully cut-through (3) is 3.48 times higher.

By comparing the lubricated fully cut-through (3) with the unlubricated partly cut sleeve condition (1), it becomes clear that 71.3 % of the total **applied** energy has been *dissipated into*, (a) to deform the sleeve in the elastic region of the material, and (b) to overcome the friction force, or elastic hysteresis. The percentage is calculated by comparing the loss (3.48 – 1.00) to the original value (3.48), which gives 71.3 %. The

remaining part of 28.7 % of the total **applied** energy was spent to *expand* the test boss elastically.

By comparing the lubricated partly cut sleeve condition (2) with the unlubricated partly cut sleeve condition (1), it was found that 60.6 % of the **dissipated** energy was required to overcome (b) the friction, which represents 43.2 % of the total applied energy. By comparing (2) and (1) it could also be calculated that 39.4 % of the **dissipated** energy was required to overcome (a) the elastic expansion or deformation of the sleeve, which represents 28.1 % of the total **applied** energy.

The energy used to expand the sleeve is the energy that remains in the clamped system in the form of residual contact pressure. [Figure 4.33](#) illustrates visually the distribution of the total applied energy (of a non-lubricated sleeve with three partly and one complete cut) by torquing the tightening screws, into dissipated energy and expansion of the test boss. In addition, it shows how the dissipated energy is distributed between expansion of the sleeve and friction resistance.

Sleeves with partly cuts could require more energy to expand, and therefor increase the level of dissipated energy, and reduce the energy applied to clamp the pin to the supports. If the sleeves are lubricated, that would reduce the energy required to overcome the friction and by that reduce the level of dissipated energy, which would increase the clamping pressure.

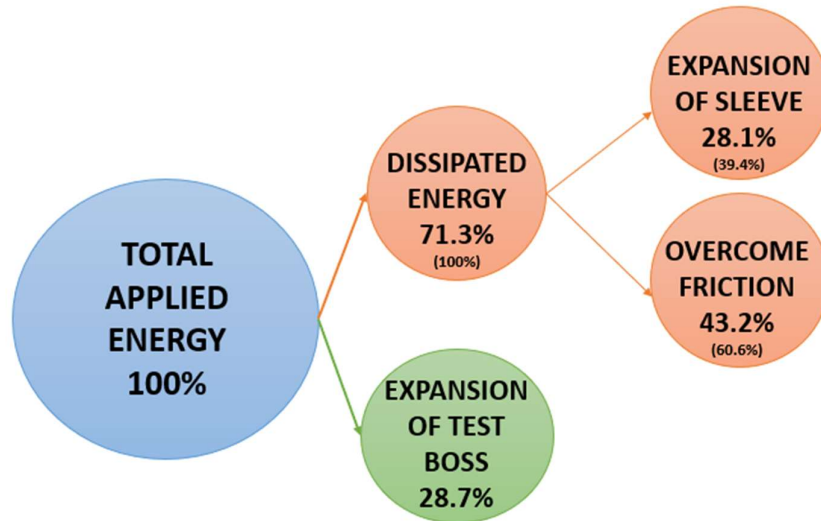


Figure 4.33. Distribution of applied energy into a pin joint with non-lubricated sleeve, with three partly and one complete cut

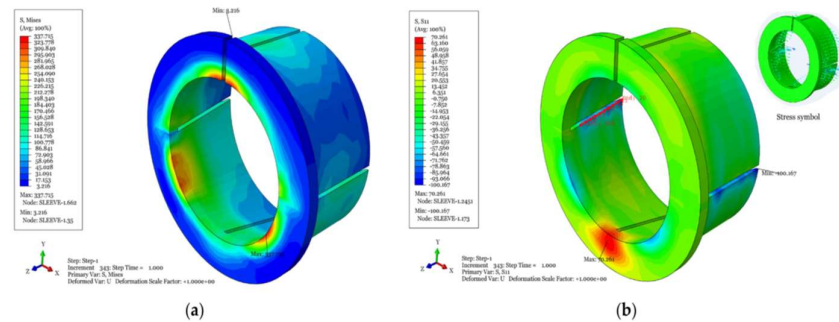


Figure 4.34. Sleeve stress at 200 Nm torque, (a) von Mises, and (b) X-direction (S11).

The FE results from the Abaqus simulations for the sleeve and the pin were compared with the theoretical formulas of Andrzejuk et al. [15], while the FE results for the test boss were compared with the experimental results. Figure 4.34 (a) illustrates the von Mises stress distribution in the sleeve, and (b) the axial stresses (S11 / x-dir.), where the X=0 is placed at the thinnest end of the sleeve. Figure 4.35 shows the

Results and Discussions

comparisons between the FE and theoretical sleeve results, while Figure 4.36 shows the axial (S11) stress distribution in the pin itself, at 200 Nm torque. The FE and theoretical pin radial stresses are compared in Figure 4.37 (a), and pin and sleeve contact pressure compared with the theoretical in (b).

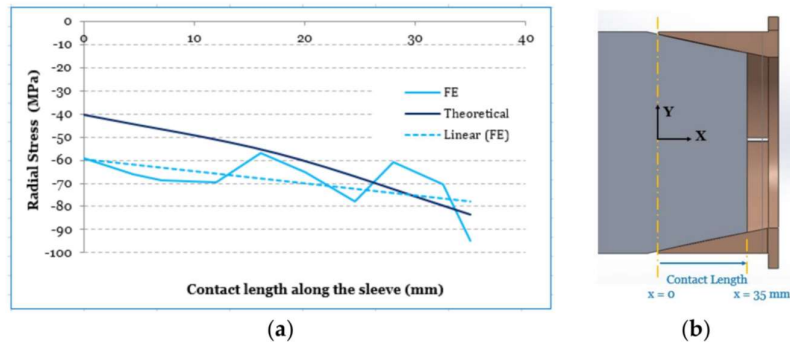


Figure 4.35. Sleeve radial stress at 200 Nm torque, (a) comparison FE with theoretical, and (b) illustration of contact length

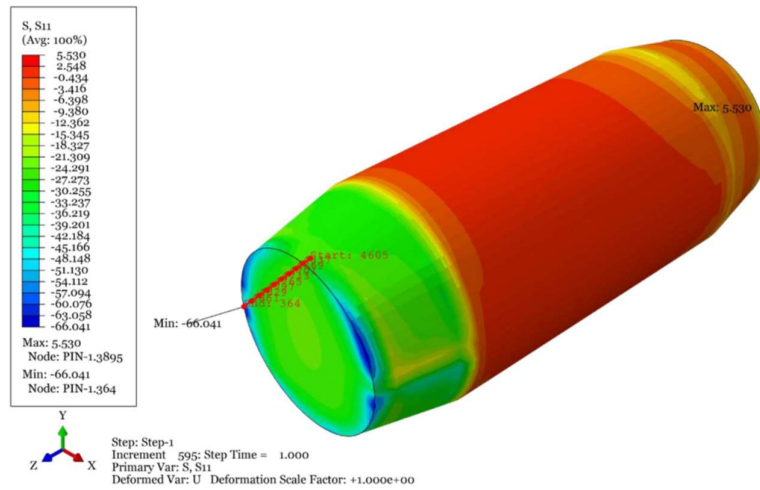


Figure 4.36. Stress distribution at 200 Nm torque (S11 / X-direction)

Results and Discussions

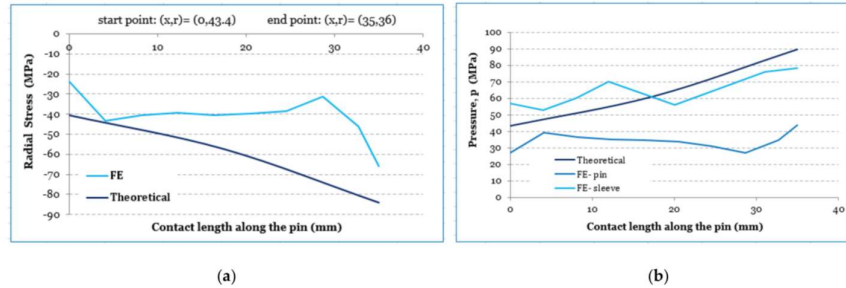


Figure 4.37. Pin stress at 200 Nm torque, (a) radial stress comparison between FE and theoretical values, and (b) pin and sleeve contact pressures compared with theoretical values

The FEA results for the sleeve, Figure 4.34 and 4.35, were very close to the calculated values based on the formulas for reference from Andrzejuk et al. [15], which was a coned sleeve without any cuts. The FEA results for the test boss, Figures 4.38 and 4.39, were also in good agreement with the experimental results, where the differences most likely were due to assumptions and simplifications during FE modelling. However, the FEA results for the pin were not in good agreement with the corresponding theoretical formulas, as indicated in Figures 4.36 and 4.37, and one of the reasons could be problems due to mesh size and discreteness of the contact.

Since there were performed experimental tests on the test boss it was possible to compare those results with the FE results. The FE von Mises stress distribution is shown in Figure 4.38, and the comparison of Hoop stresses between experimental and FE values, at outer and inner boss surface, for the 4 angular positions 0 , $\pi/2$, π , and $3\pi/2$, are illustrated in Table 4.4. The FE axial stress in the test boss is illustrated in Figure 4.39. The comparison of experimental and FE stress on the boss inner surface is illustrated in Table 4.5.

Results and Discussions

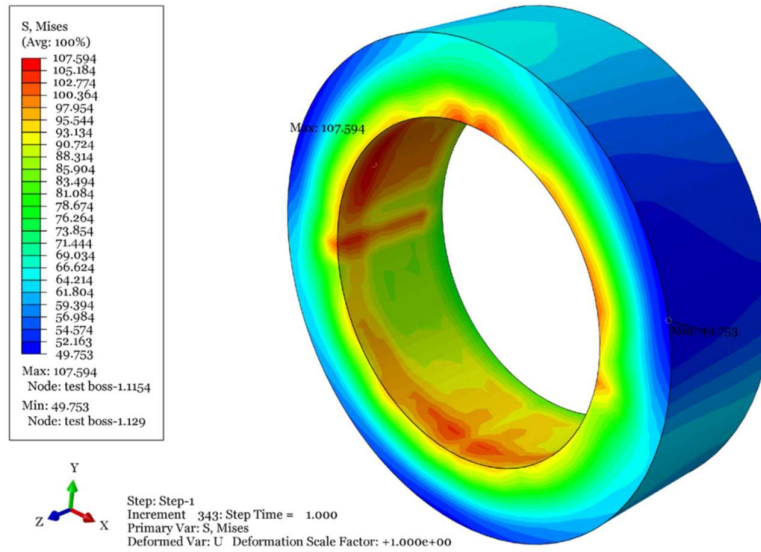


Figure 4.38. FE von Mises stress distribution in the test boss at 200 Nm torque

Table 4.4. Comparison of Hoop stress in the test boss inner and outer surface

Angular Position [rad]	Inner Surface			Outer Surface		
	Experimental [MPa]	FE [MPa]	Error [%]	Experimental [MPa]	FE [MPa]	Error [%]
0	55.93	85.9	53.58	36.12	51.59	42.83
$\pi/2$	96.82	75.77	-21.74	62.37	50.97	-18.28
π	57	84.85	48.86	36.75	49.44	34.53
$3\pi/2$	60.19	83.82	39.26	38.83	48	23.62

Table 4.5. Comparison of radial stress in the test boss inner surface

Angular Position [rad]	Inner Surface		
	Experimental [MPa]	FE [MPa]	Error [%]
0	-19.86	-19.07	4.14
$\pi/2$	-34.37	-27.91	23.15
π	-20.24	-18.65	8.53
$3\pi/2$	-21.37	-15.84	34.91

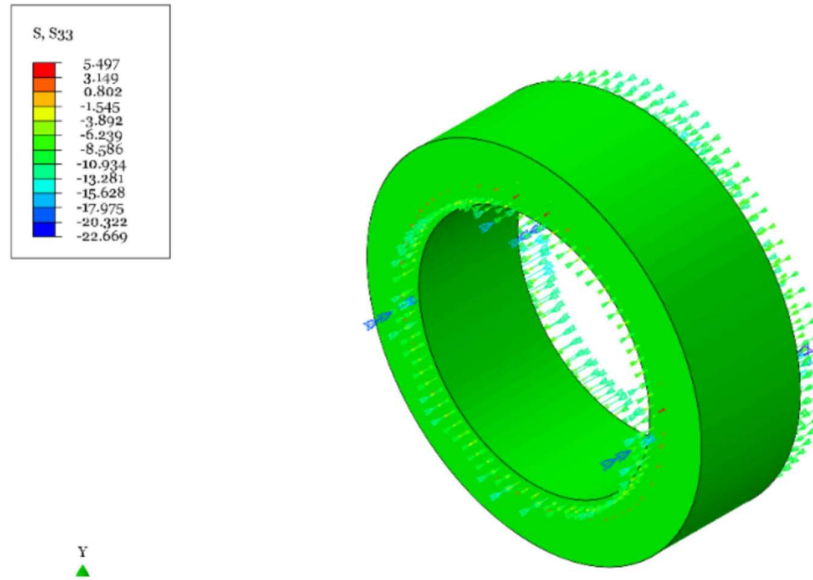


Figure 4.39. FE axial stress distribution in the test boss at 200 Nm torque

A hoop stress comparison was made between experimental and FE results on the inner and outer boss surfaces and presented in Table 5 in Paper VI, and the differences were in the range of 18 – 54 %. Similar comparison was made for radial stress on the boss inner surface, and the differences were a little lower, and in the range of 4 – 35 %.

The FEA results did not predict higher hoop stress at the complete cut-through compared to the partly cuts, as measured, but the measurements could be affected by the changing locations of the tightening screws relatively to the cuts. In the FE analysis, the tightening screws were located at almost exact the same positions as the maximum hoop stress, as indicated in Figure 4.34 (a), at $\pi/2$, $5\pi/4$, and $7\pi/4$.

4.2.3 Results of studies of newly developed pin solutions (*Papers V, and VII*)

The two pin solutions presented in the two publications (Paper V and VII) are the PhD candidate’s inventions. The pin solution with combined axial and radial locking system (**Paper V**) has been granted patent in Norway and has pending patent in the EU. The anti-loosening pin system (**Paper VII**) has pending patents in the USA, EU, and Norway.

The combined axial and radial locking system described in **Paper V** contains 7 different parts, as illustrated in **Figure 3.8**, for both Ø50 mm and Ø80 mm pin diameter sizes. The maximum possible preloads that could be achieved for different torque levels for both pin dimensions were calculated based on, (a) bolted connection theories, as described in **Equations (31) and (32)**, and (b) measures strains, as shown in **Table 4.6**.

Based on (a) and (b), maximum normal stresses were calculated for both pin dimensions, in addition to theoretical maximum preloads, and tightening screw preloads, as shown in **Tables 4.7 and 4.8**, and the results were compared as indicated in **Figure 4.40**.

Table 4.6. Measured strains in the central pin for different levels of applied torque

Torque levels [Nm]	Measured strain [$\mu\text{m/m}$]	
	Ø50 pin system	Ø80 pin system
0	0	0
40	368	222
60	609	312
80	873	416
100	1104	585
120	1366	676
140	1538	790

Table 4.7. Theoretically calculated values of preload per M10 screw, max. pin preloads, and normal stress for both axial-radial pin dimensions

Results and Discussions

Torque level [Nm]	Preload per screw [kN]	Ø50 mm pin		Ø80 mm pin	
		Max. Preload [kN]	Normal stress [MPa]	Max. Preload [kN]	Normal stress [MPa]
0	0	0	0	0	0
40	22.7	159.1	91.0	272.7	58.3
60	34.1	238.6	136.4	409.0	87.4
80	45.4	318.1	181.9	545.3	116.6
100	56.8	397.6	227.4	681.7	145.7
120	68.2	477.2	272.9	818.0	174.8
140	79.5	556.7	318.4	954.3	204.0
149.2	84.8	593.4	339.3	1017.3	217.4

Table 4.8. Calculated values of normal stress from measured strains, and difference with theoretical stress, for both axial-radial pin dimensions, with M10 screws

Torque level [N]	Ø50 mm pin		Ø80 mm pin	
	Normal stress from measured strain [MPa]	Difference from theoretical stress [%]	Normal stress from measured strain [MPa]	Difference with theoretical stress [%]
0	0	0	0	0
40	77.4	-14.9	46.5	-20.2
60	127.9	-6.3	65.4	-25.2
80	183.4	+0.8	87.4	-25.0
100	231.8	+1.9	122.8	-15.7
120	286.9	+5.1	142.0	-18.8
140	322.9	+1.4	165.8	-18.7

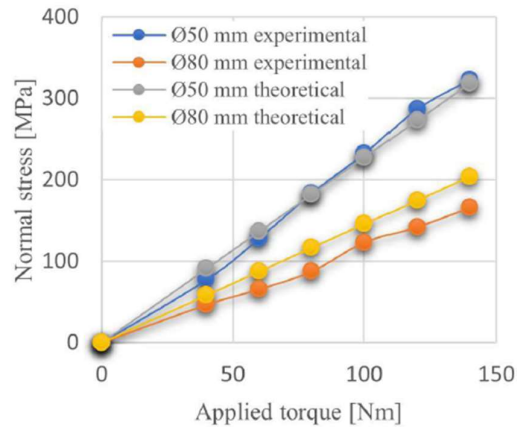


Figure 4.40. Theoretical and experimental normal stresses vs applied torque for both pin dimensions, with M10 screws

By comparing the calculated theoretical preloads for the standard bolts with the tested axial-radial pins systems with M10 screws, it shows that the tested axial-radial pin solutions Ø50 and Ø80 reached lower preload levels, with 44.4 % and 62.9 % lower, respectively, as indicated in [Table 4.9](#). To improve the axial-radial pin solution when it comes to its maximum preload, calculations were made with the maximum possible number of screws in different sizes, as indicated in [Table 4.10](#). The maximum preloads were reached with 7 screws of M12 at each side for the Ø50 pin, and 10 screws of M14 for the Ø80 pin, with 840.5 kN and 1645.1 kN, respectively. By increasing the diameter of the tightening screws the number of screws decreases linearly (approximately) with the diameter of the screws, but the screw cross-section area increases with the square of the diameter (approximately), which increases the maximum possible preload in the axial-radial pin solution.

In [Table 4.11](#), the maximum preload values were compared for the standard bolts, the tested axial-radial pins (with M10 screws) , and improved axial-radial pins (with M12 and M14 screws). It was possible to improve the axial-radial pin preloads with 41.6 % for pin Ø50, and 61.7 % for pin Ø80, compared to the tested pin versions. Still the pin preloads were lower than the ones for the standard bolts, with 21.3 %, and 40.0 % lower.

[Table 4.9](#). Comparison of maximum calculated theoretical preload values for the tested axial-radial pin systems with M10 screws, and standard bolts

Fastener size [mm]	Standard bolts [kN]	Tested axial-radial pins [kN]	Difference [%]
50	1067.6	593.4	- 44.4
80	2741.1	1017.3	- 62.9

Results and Discussions

Table 4.10. Maximum calculated theoretical preload values for screws and improved axial-radial pin systems, for different screw sizes and number

Size	Thread diameter [mm]	Max. torque [Nm]	Preload per screw [kN]	Ø50 mm pin system		Ø80 mm pin system	
				Max. no. of screws	Preload [kN]	Max. no. of screws	Preload [kN]
M8	7.78	74.0	52.8	11	581.0	18	950.8
M10	9.78	146.9	83.5	9	751.2	14	1168.6
M12	11.73	253.5	120.1	7	840.5	12	1440.9
M14	13.73	406.6	164.5	-	-	10	1645.1

Table 4.11. Comparison of maximum possible preload for standard bolt system with tested (M10 screws) and improved axial-radial pin systems (different screw sizes and numbers)

Fastener size [mm]	Improved axial-radial pin preload [kN]	Difference [%] of Improved axial-radial pin vs:	
		Standard bolts	Tested axial-radial pins
50	840.5	- 21.3	+41.6
80	1645.1	- 40.0	+61.7

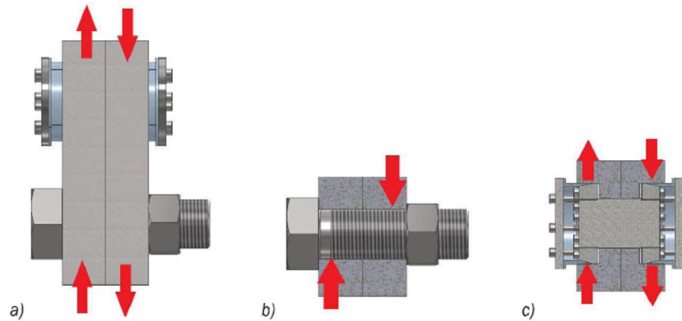


Figure 4.41. Application of loads, (a) radial on the connected flange, (b) radial on a standard bolt, and (c) radial on an axial-radial pin system

The comparisons of maximum possible preload in standard bolts and axial-radial pin solutions are shown above, and the maximum possible flange shear capacities with the different bolting solutions were also investigated, theoretically. The application of the loads is illustrated in [Figure 4.41](#).

The shear capacity of a flange connection with standard bolts can be represented by [Equation \(53\)](#), and for an axial-radial pin, by [Equation \(54\)](#). The safety factor – ks – was set to 1.00 for comparison's purposes, the friction factor – μ – 0.3, and – τ_y – 450 MPa.

$$Q_{pb} = \frac{F_i \times \mu}{ks} \quad (53)$$

$$Q_{pp} = \frac{F_i \times \mu + \tau_y \times A_t}{ks} \quad (54)$$

where – Q_{pb} – represents the shear capacity per bolt of a bolted flange system, – Q_{pp} – the shear capacity per bolt of axial-radial pin system, – F_i – the bolt or pin tension load, – μ – the friction coefficient on contact surfaces, – τ_y – the yield limit of the pin material, – A_t – the pin minimum cross-sectional area, and – ks – the safety factor.

The flange shear capacities when applying standard bolted systems were calculated and are listed in [Table 4.12](#), and the change of shear capacity from M50 to M80 increased with the square of the diameter increase; $80/50 = 1.6$, and $822.3 / 320.3 = 2.56 = (1.6)^2$. The flange shear capacity, when applying the axial-radial pin solution, is more complex and depends in addition to the clamp force, also on the pin shear capacity, which is different from the bolted situation. The flange shear capacity for the axial-radial pin system also increases approximately with the square of the pin diameter increase, but it is considerably higher than for the bolted solution.

Results and Discussions

As shown in Table 4.13, the theoretical flange shear capacities with the axial-radial pin system are over 3 times higher the values from the bolted system, or the shear capacity increases were 225.7 % and 216.1 % of the M50 and M80 values, respectively. With a standard bolted flange system there will always be a clearance between the bolt and the flange hole, and the flanges can slide or move relatively to each other if the contact shear capacity has not been reached. In an axial-radial pin flange system, the flange contact shear capacity and the pin shear capacity will be activated *at the same time*, thus, the sum of them must be overcome before sliding of flanges can occur. In addition to reach a considerable higher shear capacity ($\times 3$), the axial-radial pin systems require a considerably lower torque to reach its maximum preloads, as illustrated in Table 4.14, with only 2.5 % for the Ø50 dimension and 1.0 % for the Ø80, compared to the required torque for the M50 and M80 bolts.

Table 4.12. Theoretical flange shear capacity per bolt, with M50 and M80 standard bolts

Standard bolts	Max. possible preload [kN]	Shear capacity [kN]
M50	1067.6	320.3
M80	2741.1	822.3

Table 4.13. Theoretical flange shear capacity per bolt, with Ø50 and Ø80 axial-radial pins, and comparison with standard bolt solutions

Pin size [mm]	Max. preload [kN]	Tensile area [mm ²]	Shear capacity [kN]	Shear capacity increase [%]
Ø50	840.5	1748.7	1043.0	225.7
Ø80	1645.1	4679.1	2599.1	216.1

Table 4.14. Required torque for optimized axial-radial pin systems and standard bolts to reach maximum preloads

	Fastener	Required torque [Nm]
Axial-radial pin system	Ø50 mm / M12	235.5
	Ø80 mm / M14	406.6
Standard bolts	M50	9505.7
	M80	39106.8

Paper VII is a comparative study on loosening between an anti-loosening bolt concept called Vibralock®, and a standard HV bolt system. The anti-loosening bolt system was tested in two different experimental tests, Test 1 with M20 bolts, and Test 2 with M30 and M42 bolts, in addition to a FE analysis of an M72 bolt.

The test setup for *Test 1* is illustrated in [Figure 3.15](#), with two bolts systems tested at the same time, in vertical position. Three bolts without washers were tested with axially directed load of 100 kN (60 % of yield) and +/- 15 kN oscillating load at 10 Hz frequency, A – lubricated / 498×10^3 cycles, B – unlubricated / 498×10^3 cycles, and C – lubricated / 668×10^3 cycles.

The test with A and B bolts was run until first failure, which was material fatigue with bolt breakage of bolt B, as illustrated in [Figure 4.42](#). Bolts A and C did not experience breakage. The nuts were controlled for rotation during testing, and no rotation occurred.

The *Test 2* setup is illustrated in [Figure 3.13](#), and transversal displacements of the flange plates with standard HV bolts were forced into the joint, until the loss of clamp loads were reduced with at least 90 % of its original preload, before reaching 400 cycles. The same level of displacements was applied also for the anti-loosening bolt system which

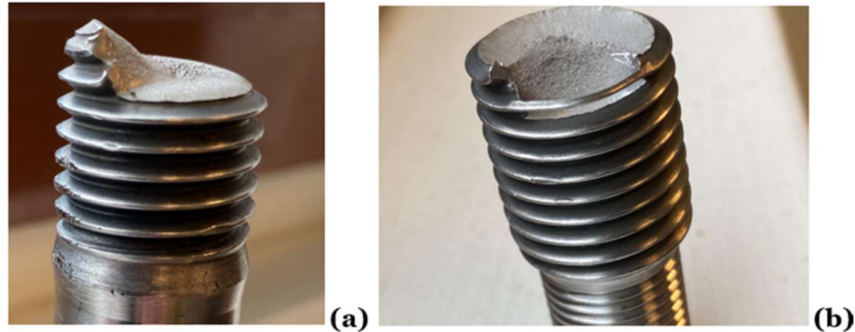


Figure 4.42. Breakage of bolt B, (a) threads not engaged with main nut, and (b) threads engaged

were then run for at least 3000 cycles. Different levels of displacements were required for different bolt sizes. The test results of the M30 bolt runs are illustrated in [Figure 4.43](#), and the M42 results in [Figure 4.44](#).

The test results of the M30 and M42 bolts give a clear answer on how the two different bolt systems react on the test. The standard HV bolt systems, both torqued and tensioned, lose 90 % of their original clamp load level within 200 to 400 cycles, with the specific flange plate displacements, while the Vibralock® anti-loosening bolt system, exposed for identical displacements, loose in the range of 4 – 8 % of their clamp load over 3000 cycles.

Since none of the nuts of the anti-loosening bolt system start to turn, the clamp load loss of 4 – 8 % must occur due to elastic compression of the loaded steel parts and asperities (if the compression continues into or during the test), plastic deformations of asperities, residual stress release in the shank, and elastic deformations of threads.

Results and Discussions

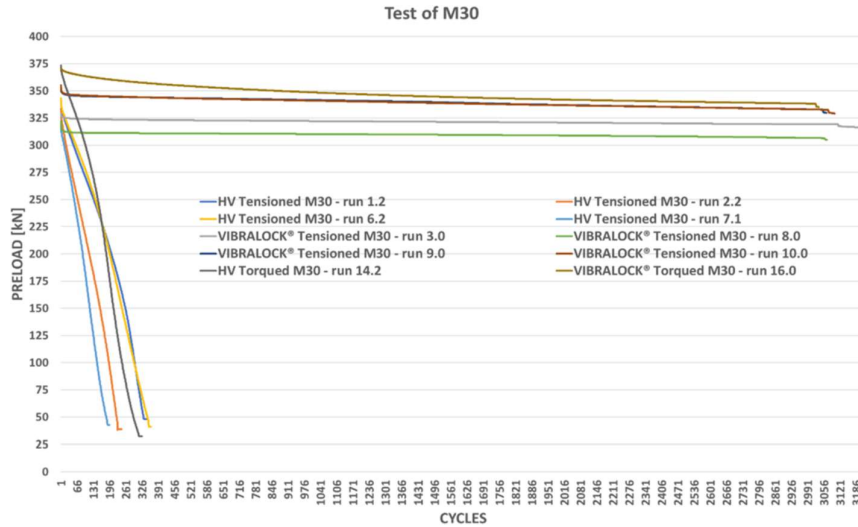


Figure 4.43. Loss of clamp load M30 bolts, Vibralock® and HV

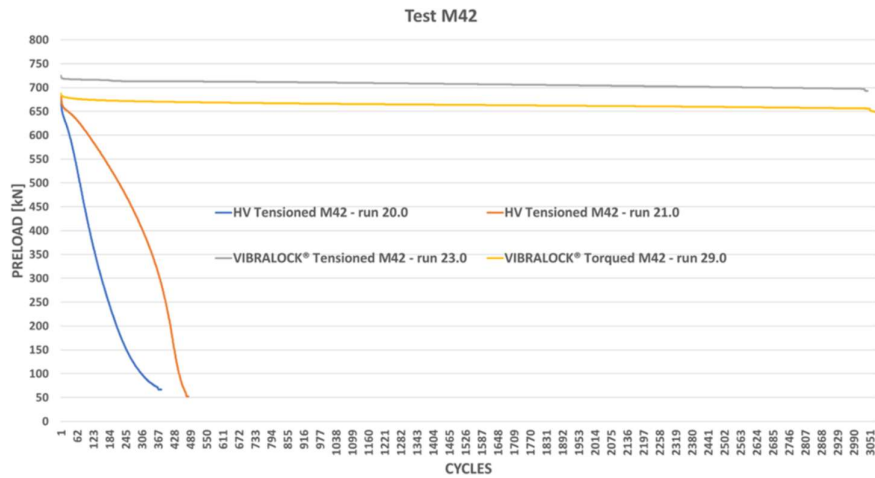


Figure 4.44. Loss of clamp load M42 bolts, Vibralock® and HV

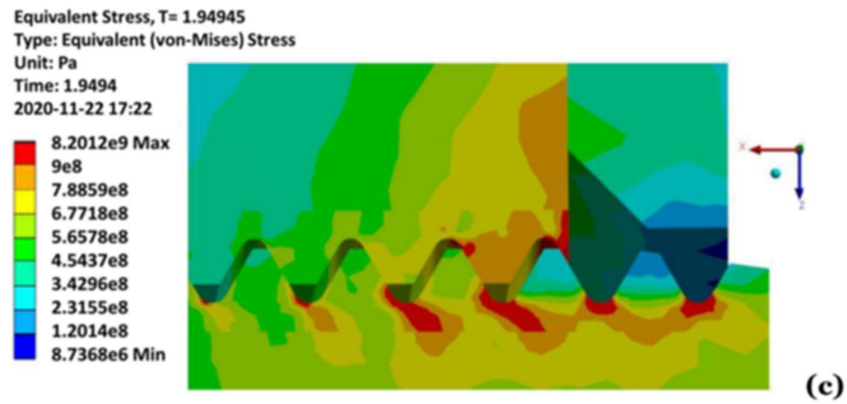
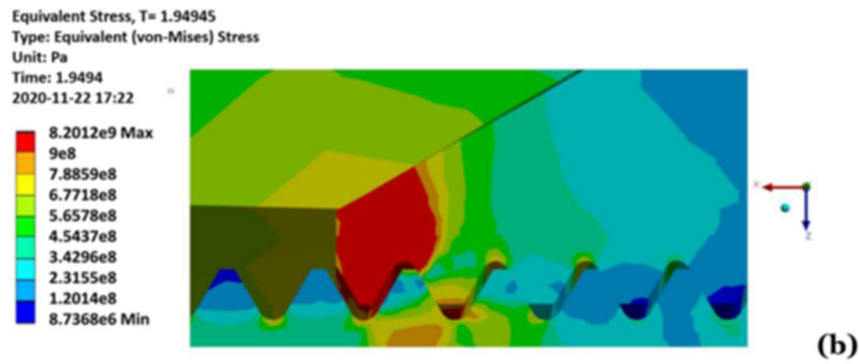
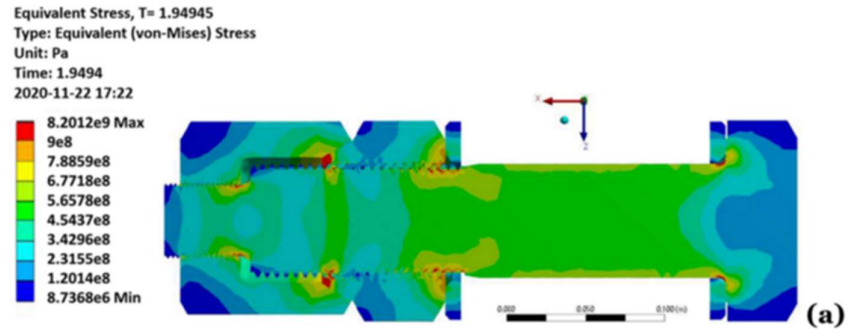
The situation for the standard HV bolts would most likely be the same, but in addition the turning of the nut generate a massive continuously loss of clamp load, as measured in the test. The FE analysis was performed by an external company, on a M72 anti-loosening bolt system,

which is a bigger size than the experimental tests of M20, 32 and 40 bolts. It was performed a linear and a non-linear analysis, to investigate the structural integrity of the threads in the bolt and nuts, where the pre-defined clamp loads were 2180 kN in the main shank, and 930 kN in the minor shank.

With the linear analysis ANSYS gave a torque value of 29967 Nm to reach the clamp load of the minor shank, which was almost identical to the value calculate from Equation (35) of 29440 Nm. With the non-linear analysis the corresponding values were 32105 Nm, and 32890 Nm calculating with the same equation. The reason for different results using the same Equation (35) is that for the linear analysis, a fabrication tolerance of 0.5° was introduced on the nut contact areas, which reduced the effective contact diameter. The von Mises stresses from the linear and non-linear FE analysis are illustrated in Figures 4.45 and 4.46. When comparing the two models, it can be seen that the stress pattern is almost identical. The linear analysis resulted in the maximum stress level of 820 MPa at the main nut contact area against the locking nut, and at the first engaged coarse bolt threads, in addition to the first engaged fine bolt threads. In the non-linear analysis, the over-all stress level is approximately the same as for the linear analysis, also at the most stressed areas, where the stress level is in the range of 788 – 900 MPa. A very small portion of the main nut to locking nut contact area shows an increased stress level of 900–1350 MPa.

Though the FE simulation was done on a bigger bolt size (M72) compared to the others (M20, 30, and 42), the plots in Figures 4.45 and 4.46 coincide well with the fracture condition of bolt B in Test 1, which occurred at or close to the first engaged thread against the main nut (Figure 4.42) and reflects the description from literature [34]. In general, the combination of physical tests and FEA, and the combination of 4 different bolt dimensions is meant to give a wider *proof of concept* of the bolt locking system.

Results and Discussions



Results and Discussions

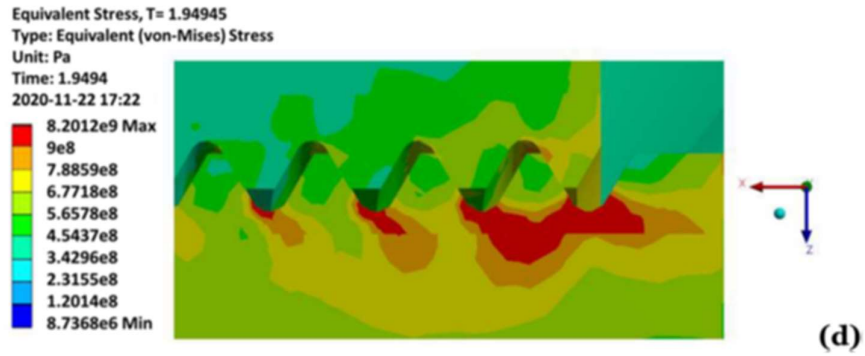
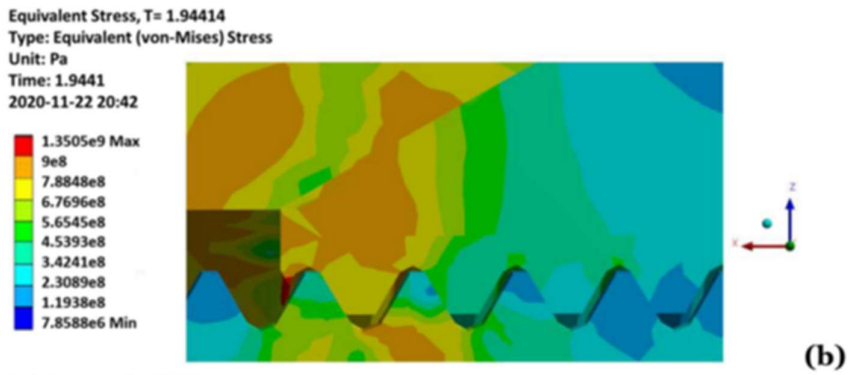
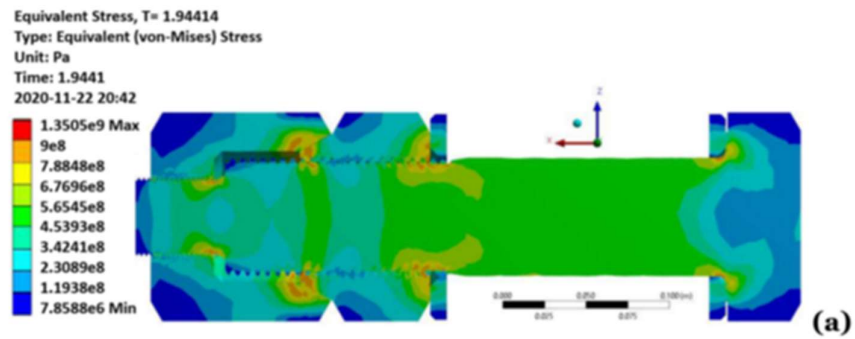


Figure 4.45. von Mises stress from the linear FE analysis, (a) overall view, (b) conical contact area, (c) coarse threads, and (d) fine threads



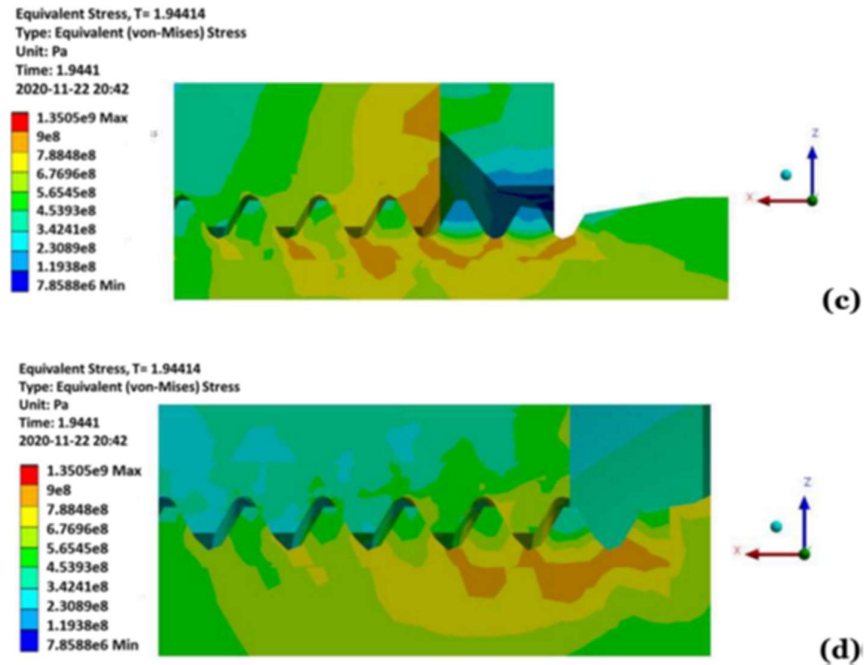


Figure 4.46. von Mises stress from the non-linear FE analysis, (a) overall view, (b) conical contact area, (c) coarse threads, and (d) fine threads

4.3 Summary of appended papers

The thesis comprises 9 papers, of which 6 are journal papers and 3 are conference proceedings. In this section, the corresponding summaries of these 9 papers are presented, and the contribution of each paper to the overall study is highlighted.

4.3.1 Paper I: Questionnaire-based survey of experiences with the use of expanding PIN systems in mechanical joints

In this paper, the results of a questionnaire-based survey are presented, performed within a wide range of industries and geographical areas. The

purpose of the survey was to develop better understanding of the perception of the expanding pin system in the national Norwegian, and global market.

Six different sections are highlighted: Size of company, Company profile, Experience with expanding pins, Market and equipment, Pin source and Effects and consequences of applying expanding pin solutions. The responses on the survey came from 10 different countries, with the main segments being Offshore oil & gas, Maritime/ships and Construction / earth moving. In total 256 potential responders received the questionnaire, divided into 140 Norwegian based companies and 116 non-Norwegian.

The study starts with a general description of different pin connection types, with a comparison of contact stresses between new and used standard cylindrical pin solutions, and the expanding pin type. In addition, some background information on the latter pin system is given and continues with the questionnaire-based survey. There are several methods of how to assemble mechanical components using shear pins in pinned joints, such as: (1) shrink fit, (2) press fit, (3) clearance fit, and (4) expanding pin. By using the more complex radially expanding pin, challenges related to high energy activities (heating or cooling at (1)), high pressure requirements (hydraulic pressure at (2)), and wear, fretting and breakage problems (due to a loose pin as in (3)), can be reduced or avoided.

The expanding pin concept is illustrated in [Figures 1.11](#) and [1.12](#), and various examples of its applications are illustrated in [Figures 1.1 – 1.9](#) and [1.13](#), and in addition typical mechanical properties for typical pin and support materials (heavy machinery) are presented in [Table 1 \[1\]](#). A questionnaire-based survey was performed to reveal stakeholders' experiences with the use of expanding pins in mechanical joints, in various machines and equipment, where the questions were divided into six sections: (i) Size of company, (ii) Company profile, (iii) Experience

with expanding pins, (iv) Market and equipment, (v) Pin source, and (vi) Effects and consequences of applying expanding pin solutions.

The stakeholders in this study are divided into the six following groups: (a) OEMs, (b) Suppliers to OEMs, (c) Engineering companies, (d) End-users, (e) Service/repair/maintenance, and (f) Others. By analyzing the feedback data from these stakeholders, a better understanding of the perception of the expanding pin system in the market is possible. The pin system's strengths and weaknesses can be identified to further optimize design, develop effective market approach, and improve procedures for installation, operation, and retrieval of the pins. In total, 256 potential responders received the questionnaire, 140 (55%) Norwegian based and 116 (45%) non-Norwegian based. A total of 58 responded, which gives an *overall response rate* for the survey of 23%, coming from 10 different countries at 3 different continents, where 39 were Norwegian based, and 19 others, see [Figure 4.1](#). The *willingness to respond* is called *reaction rate* and is here defined as the relationship between the percentage *response rate* and the percentage *request rate*.

The study reveals various important opinions and perceptions of the stake holders' relationship to expanding and standard pins. [Figures 4.5](#) and [4.6](#) indicate in which equipment expanding pins are installed for the two major segments, Offshore and Maritime, and corresponding distribution between Norwegian and non-Norwegian based companies, where Drilling equipment (40%) and Offshore cranes (50%) are important in the Offshore segment, and Maritime cranes (44%) and A-frames (25%) in the Maritime segment.

On the question "Why choose expanding pins?" ([Figure 4.8](#)) a majority (51%) of the total survey stated, Q2 "It is based on our own previous experience" as the most important reason, followed by Q4 "The pins come with the equipment when we receive it" (22%), and Q1 "It is a strong wish or requirement from our clients" (13%). A comparison of *Installation time* and *Retrieval time* for expanding pins to standard

cylindrical pins is shown in [Figure 4.15](#), which indicates that both the installation and retrieval time are reduced by use of expanding pins, compared to cylindrical ones, confirmed by 44% and 58% of the responders, respectively.

Similar comparisons are presented for:

- Tear and wear damages
- Breaking damages
- Importance of safe pin solution (in general)
- Safety for personnel and equipment
- If expanding pins are safer, then Why?
- Other effects and consequences
- Economic impacts

When summarizing all, it becomes clear that most of the respondents have a positive experience with, or an excellent perception of expanding pin systems, when it comes to installation, operation, retrieval, safety for personnel and equipment, and economic advantages for their company and clients. The complete paper with additional results [\[1\]](#) is attached.

4.3.2 *Paper II: An Investigation of the Effects and Consequences of Combining Expanding Dual Pin with Radial Spherical Plain Bearings*

In this paper, experimental tests were conducted together with some analytical studies on how radial spherical plain bearings act in combination with expanding dual pins. The standard cylindrical pin in a moveable joint as illustrated in [Figure 1 \[2\]](#) can be of many different designs, with different advantages or disadvantages.

The aim of the study reported in this paper is to investigate the effects and consequences of locking an expanding *bondura*[®] Dual Pin to the inner ring of a Radial Spherical Plain Bearing (RSPB) and compare that

with the use of a standard cylindrical pin, for both dry and lubricated contact surfaces. As part of the experimental work, the bearing inner ring is separated from the outer ring and loaded separately with a pressure load acting radially outwards, and its deformations are measured by a Coordinate-Measuring Machine (CMM) to find the relationship between the radial load and the corresponding ring deformation. In addition, the complete bearing with lubricated internal surfaces was installed on a Dual pin and then loaded stepwise with combinations of radial outward force from the expanding sleeve and external inwards radial load representing operational loads. The assembly was then forced to turn, and the required static moment at the exact moment of turning was observed. The bearings were of type Radial Spherical Plain Bearings (RSPBs), GE 80 ES, steel/steel, and loaded externally up to their maximum dynamic load limit of 400 kN, per bearing.

The Dual expanding pin solutions, illustrated in Figure 3 [2], are applied in various types of industrial equipment and machines often where the pins interact with bearings, such as cranes offshore or onshore, ports, drilling and pipe handling equipment, rotating sheaves, amusement equipment, A-frames, flood dike gates, etc. In such applications, the bearings can typically be of spherical plain type of bearings. The inner sleeve expands outwards towards the inner surface of the inner ring of the bearing but creates normally less contact pressure compared to what the outer sleeve does against the support bore. The contact pressure between the bearing and the expanding sleeve is enough to prevent the bearing inner ring from rotating but must not be high enough to disturb the bearing's function by expanding the inner ring and eliminate the bearing's radial inner production tolerance. Figure 3(b) [2] illustrates a dual pin assembly, and Figure 3(c) [2] illustrates a dual pin where one half is shown with an exploded view.

The following two main experimental tests were conducted: *Test no. 1* (a) and (b): tests of bearing inner rings installed on a dual expanding pin. *Test no. 2* (a) and (b): tests of complete bearing ass. installed on a dual

exp. Pin, with the test set-ups are detailed in Table 1 [2]. Figures 3.2 and 3.3 show the contact area between pin, sleeve and bearing inner ring for Test 1 and Test 2, with one inner ring on one sleeve and one inner ring on two sleeves, respectively. The radially expansion – u – was measured by CMM at the 4 sections indicated in the figure.

Thick-walled cylinder theory was applied to consider the relationship between the inner and outer pressure, and radial displacement between the inner and outer surface of the cylinder thickness. The radial and tangential (hoop) stresses σ_r and σ_θ were calculated by use of the expressions in Equations (10) – (12). The – u – value in Equation (45) represents the radial expansions measured with the CMM, and by introducing the measured values – u – for radial expansion into the Equation (45) the value for inner pressure – p_1 – were determined, since the remaining factors are all known.

Test 1:

With one specific value – p_1 –, for each measured value – u –, the radial and hoop stresses were calculated, from Equations (10) and (11). Tables 2 [2] and 3 [2] show the calculated values for the inner pressure and hoop stress at the four sections indicated in Figures 3.2 and 3.3, for some specific values of the radial expansion. Figures 4.18 - 21 show the relationships between torque and expansion, at the different ring cross-sections. The test configurations for Test 1 are shown in Figure 3.1 (i) and (ii).

Test 2:

Test 2a comprises of two complete RSPBs as shown in Figure 3.1 (iii) and (iv). The results from loading the bearing stepwise with internal and external loads and the measure of the required moment to turn the outer ring relatively to the locked inner ring of the bearing on single sleeve are shown in Figure 4.22. Test 2b is performed in a similar way as Test 2a but with one single bearing at the assembly mid part, expanded by two

separate sleeves, and the highest rotational moment was clearly only at the lowest tightening torque, 5 Nm, as illustrated in [Figure 4.23](#), and the remaining torque values in the range of 25–65 Nm did not give any major scattering in moment values.

As a conclusion for this study, for both Test 2a and Test 2b the required rotational moment was considerably reduced when the torquing level increased, from 5 Nm. For the first of the two tests the rotational moment increased again for the highest torque value, 65 Nm. The rotational moment in Test 2b was reduced from 1900 Nm at the lowest torque (5 Nm) and highest external load (400 kN), with a drop of 75-86 %. More information and results are included in the original and published article attached [\[2\]](#).

4.3.3 *Paper III: A novel technique for temporarily repair and improvement of damaged pin joint support bores*

This study investigates and compares five options when a joint with a cylindrical pin has reached a severe level of wear and ovality, outside its planned service stop. The work involved testing the viability of 3D scanning of the damaged bore surface, 3D printing of a metal bushing, and inserting the bushing into the damaged joint. In addition, two pin solutions, i.e., standard cylindrical pin and an expanding pin type were installed into the repaired joint, loaded and the strain on the pin ends close to the supports were measured. For the sake of comparison, the supports had both smooth circular bore and severe wear and ovality.

The five tests, representing the options are:

- *Test 1*: a standard cylindrical pin with evenly distributed wear / pin-bore clearance at each end (which represents wide original tolerances or further operations after repair of bores by line boring to a bore diameter greater than original diameter),

- *Test 2*: a cylindrical pin with additional severe wear and ovality at one end (which represent unevenly distributed wear between the two bores, compared to test 1),
- *Test 3*: an expanding pin with evenly distributed wear / original pin-bore clearance at each end (which is eliminated by the expanding effect),
- *Test 4*: an expanding pin with additionally severe wear and ovality at one end (which is only partly eliminated by the expanding effect, compared to Test 3)
- *Test 5*: an expanding pin with repaired support at the damaged end, and therefor reduced bore diameter (where clearances in both bores were eliminated by the expanding effect)

The tests are also specified in Table 1 [3], the test setup with 3D printed repair insert is illustrated in Figure 3.5, and Figure 4.24, and the pins are illustrated in Figure 3.6 (expanding pin), and Figure 3.7 (cylindrical pin). The strains were measured using strain gauges, placed at the pin weakening grooves section, close to the contact areas between pin and supports. The pin grooves are 6 mm wide, with a 3 mm radius and 7.5 mm deep which gives a minimum cross-sectional diameter of 73 mm.

For each of the tests (Tests 1–5) the pins were loaded from 0 to 500 kN in steps of 100 kN, and readings were taken after each loading. The pins were loaded three times at each step. All tests were first loaded at 0° position with all four strain gauges placed in a plan in parallel with the external load direction, and then rotated into a 15° position, loaded again and the results were recorded to see the effect of the rotation, on the measured values. The measured strain values were corrected because of variations in the cross-sectional area under the strain gauges, due to offsets compared to the ideal location of strain gauges with minimum cross-sectional area, as illustrated in Figure 3.16.

The results from Test 1 – 5 are illustrated in Figures 4.25 – 4.29, respectively, where (a) strains at 0° position, and (b) percentage change

of strains when turning the pins from 0° to 15° position. Based on the tests and analysis performed in this investigation, it can be concluded that the repair procedure of a damaged support bore including the installation of a 3D printed bushing can be a viable solution. It is relatively easy to perform, and the 3D printed insert seems to fit very well with both the damaged bore and the expanding pin. In addition, based on the results of this investigation the tests of the pin with the repair insert (Test 5) does not show any negative or weak results compared to the other tests.

4.3.4 *Paper IV: Safety related study of Expanding Pin systems application in lifting and drilling equipment within Construction, Offshore, and Marine sectors*

This paper is based on the survey from the Paper I “Questionnaire-based survey of experiences with the use of expanding PIN systems in mechanical joints” [1], in addition to a short literature study on onshore cranes, in addition to a short view on how some Norwegian and foreign energy companies in the Stavanger region (Norway) relate to the required and statutory laws, regulations and standards in the petroleum industry. The main purpose of this study is to analyze the importance of use of expanding pins, related to safety for personnel, equipment, and environment, on cranes, drilling equipment, and other heavy machinery, and the types of involved companies are OEM (i), supplier to OEM (ii), engineering (iii), end-user (iv), service & maintenance (v), or others (vi).

The responders in the original survey were from 10 different countries with companies from Norway as the main group (67%). In addition, there are companies from Sweden, Canada, Scotland, Greece, Brazil, Finland, The Netherlands, USA, and Germany. The different responders operate in various markets as, (a) Offshore Oil&Gas, (b) Maritime, (c) Subsea, (d) Dredging, (e) Mining onshore & offshore, (f) Construction & earth

moving, (g) Specialized machines and equipment, (h) Steel and paper industry, and (i) Other. In this study, only the following segments are included: (a), (b), (c), (d) and (f), and some of the companies have activities in more than only one of the segments. The survey was directed to persons and positions with responsibility related to pin solutions, or related machines and equipment.

Lifting and hoisting equipment such as cranes are often subject to strict rules and certifications due to the nature of the operations they are performing, and the risks involved. A floating structure such as a ship can have six degrees of movement; a) heave, b) sway, c) surge, d) roll, e) pitch, and f) yaw, which all can affect negatively lifting and loading operations. Without a compensation system, such uncoordinated relative movements can generate high dynamic and shock loads into the equipment and specially into the pinned joints, who can suffer friction wear, corrosion wear, fretting wear, and deformations which again can result in increased play in the joint, see [Figure 1.10](#) and [1.11](#), or even breakage of the pin.

Any heavy lifting equipment within any industry involving standard cylindrical pins will be exposed to a relative movement between pin and support with the wear issues it brings, due to the diameter difference between the pin and the support bore, typically for installation purposes. The expanding pin system [\[14,35\]](#) has got the ability to expand towards the support bore surfaces and lock the pin with a radial wedge pressure, and by that eliminate the wear issues at the pin – bore contact surfaces, and normally, the pin material is of higher steel quality than the support material, and typical material qualities are described in [Table 1 \[4\]](#).

This survey reveals how the involved companies value safety for personnel and equipment in general, how safe the expanding pin solution is compared to the standard cylindrical pin, and their capabilities when it comes to tear, wear, breakage and easiness of installation and retrieval. The types of involved companies are OEM (i), supplier to OEM (ii),

engineering (iii), end-user (iv), service & maintenance (v), or others (vi). The questionnaire-based survey gives some interesting relationships between the participants view on safety, and the different pin solutions, divided into which area they belong. Around 54% aimed at the expanding solution as the safest, and only 4% stating this pin as less safe. The stakeholder (ii), (iii), (iv) and (vi) clearly indicate this with a 65% average score on *Safer with expanding pins*. The reasons for *why* the expanding pin is considered safer, there are two main reasons given, (1) *No sledgehammering needed*, and (2) *Easy and fast to retrieve*.

The risk to be exposed to wear for the expanding pin solution and for a cylindrical one is different, and both are shown in [Figure 1.14](#). For all the participants, the *importance of avoiding breakage* is naturally highly valued, and when it comes to the *risk of having pin/support breakage*, there is no one (0%) indicating that expanding pins are more exposed to breakage, than the std pin. It is relatively equally divided between *Less with expanding pins* and *Equal*, with 48% and 52% as total values, respectively.

Analysing the tear and wear comparison between expanding pins and cylindrical ones, it shows that within each of the stakeholder segments (i) – (vi) it exists a clear opinion and experience that there are less wear issues with expanding pins compared to standard pins, with 63% and 35%, respectively. Only 2% see more wear issues with expanding pin solutions. When comparing *installation and retrieval time* for expanding and cylindrical pins, [Figure 4.14 \(b\)](#) and [\(c\)](#), respectively, most of the stakeholder segments responds that the expanding pins are the fastest to install, and the total average states 50% for expanding pins as fastest, 34% as equal, and 16% stating standard pins as fastest. For the retrieval time the stakeholder segments (i) – (v) respond that the expanding pin is the fastest to retrieve, and the corresponding numbers for the total average are 67%, 18% and 15%, respectively.

Expanding pin solutions seems to be recognized as a safer pin solution compared to standard cylindrical pins, specially within the Offshore and Maritime segments, where the safety is valued highly by all the stakeholders. The stakeholders in this survey are both OEM, suppliers to OEM, Engineering companies, End-users, and Service companies. The fact that there is, in general, no need for sledgehammering to get the pin in or out of the joint, given its capability to expand after installation and contract before retrieval, makes the solution score high on safety compared to the cylindrical solution. The expanding pin can be installed and retrieved easily without hammering, flame-cutting, welding and line-boring, which is recognized by the stakeholders as important regarding safety for both personnel and equipment. In addition, the stakeholders also recognize that the wear problem is considerably less with expanding pins, as also for breakage of pins and supports. The statistics from the survey can be seen in [Figures 4.09 – 4.12, 4.14, and 4.17](#), and more information can be found in the published article attached [\[4\]](#).

4.3.5 *Paper V: Study of Bondura® Expanding PIN System – combined axial and radial locking system*

In this paper, a combined axial and radial locking pin is investigated. The most common way of connecting huge flanges is by pretensioned bolts where the level of pretension or preload in the bolt shank is directly affecting the connection's shear capacity to resist relative displacements or movements between the flanged surfaces in contact, or between bolt head – nut and flanges. The use of standard bolt systems is well known, relatively easy with standardized tools available, both for torquing and tensioning. A drawback with this solution is that all clamping force and joint shear capacity are heavily dependent on the bolt preloads.

The combined axial-radial locking system has got Norwegian patent (number 344799) and combines preload in the pin to pulling the connecting flanges together, with radially locking the pin system with wedges to the two flanges. Figures 3.8 and 3.9 show the different parts the pin system contains, and how the pin system works. The separate parts are, (i) the central pin with threaded ends, (ii) shims to protect the surface of the connected plates, or flanges, from the M10×35 screws, (iii) coned nuts to transfer the pin tension created by torquing the M10×35 screws, into the flanges, (iv) M10×35 screws to create pin tension and flange compression, (v) conical sleeves to lock the pin system to the flanges radially, and prevent any relative movements between pin and flanges, (vi) endplates to transfer the axial tightening force created by torquing the M10×60 screws, into the conical sleeve, and (vii) M10×60 screws to create the axial force to push the conical sleeve into position between the coned nut and the flange bore and create the wedge force.

Figure 4.47 illustrates the difference between the design approaches to eliminate the failure of a flange connection by both fastener systems, standard and axial-radial pin system. For the standard bolt and nut system, the restriction of both the axial and radial movements depend on the preload in the bolt. If the preload is not sufficient, or reduced over its functional period, that would result in loss of contact pressure, which consequently could lead to failure of the connection.

Whereas, for the axial-radial pin system, the restriction of the radial movements between the flanges does not entirely depend on the central pin's preload. The expanded conical sleeve between the pin and flanges, transfers the radial load to the central pin and for a failure to occur due to radial movements, the external radial load must have the magnitude enough to surpass the shear yield strength of the central pin.

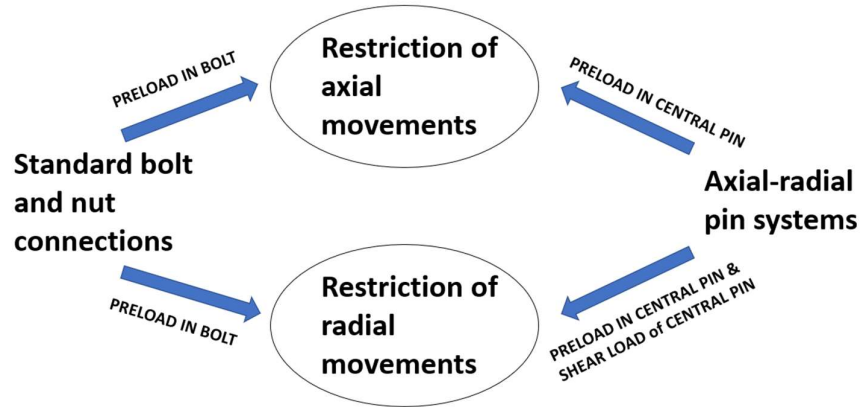


Figure 4.47. Design approaches for axial- radial pin system and standard bolt in terms of restricting axial and radial movements

Preloads were calculated and verified by experimental tests to observe and understand the normal stress in the central pin. The calculations were performed for both standard bolts (M50 and M80) and the axial-radial locking system ($\text{Ø}50$ and $\text{Ø}80$ mm). Instead of a real, two-part flange, a one-part test jig with inspection holes was applied as shown in Figure 3.10. The material properties are given in Table 1 [5], where the M10×35 bolts (tightening screws) have been additionally hardened and strengthened from 12.9 up to 16.9.

The theoretical values of preload per screw, max preload, and normal stress for both axial-radial pin sizes were calculated, and the measured strains were used to calculate values of average normal stress in the tested pins, as shown in Tables 4.6 – 4.8. Figure 4.40 shows the correlation values between the theoretical and experimental normal stresses vs applied torque for axial-radial pin solutions $\text{Ø}50$ mm and $\text{Ø}80$ mm. The calculated maximum preloads based on the measured strains for the tested pins are lower than the theoretical preloads for the standard bolts, as shown in Table 4.9, and therefore an optimization of tightening screw size and number for the axial-radial pins was done, see Table 4.10.

The maximum *experimental* preload value for Ø50 mm pin (593.4 kN) was achieved by 7 pcs of M10 screws, and for the Ø80 mm pin (1017.3 kN) by 12 pcs of M10, at each end for both. The maximum *theoretical calculated* preload value for Ø50 mm pin (840.5 kN) was achieved by 7 pcs of M12 screws, and for the Ø80 mm pin (1645.1 kN) by 10 pcs of M14, at each end for both.

Figure 4.41 illustrates the two different pin types (standard and axial-radial) installed in a flange, exposed to transversal forces, or relative radial movements. The shear capacity, Q_{pb} , of a flange joined by *standard bolts* is expressed by Equation (53), and the shear capacity, Q_{pp} , of a flange joined by *axial-radial pins* is expressed by Equation (54).

When the external radial load exceeds the shear capacity, Q_{pb} , of the bolt-flange or flange-flange connection, the joint fails, and increases the risk of cut-off the bolts. The bolthead and nut are not fixed to the flanges and can therefor act like movable joints when shear capacity has been overcome. When it comes to the tested axial-radial pin system, the pin ends are fixed to each flange plate, and the pin's material strength adds to the total shear capacity, Q_{pp} , which can be expressed as Equation (54), where τ_y represents the yield limit for the pin material, and A_t is the total pin shear area. Table 4.11 compares the calculated maximum shear capacity between a standard bolt and an optimized axial-radial pin solution, for both pin dimensions.

Summarizing the study, it can clearly be seen that by fixing the pin ends to the flange plates, as for the axial-radial pin solution, the joint shear capacity increases to a level more than 3 times the shear capacity for the standard bolts. In addition, the axial-radial pin solution requires a considerably lower torque to reach its maximum preload and shear capacity, as indicated in Table 4.14. The complete study is attached [5].

4.3.6 *Paper VI: Experimental and Numerical Studies of Stress Distribution in an Expanding Pin Joint System*

This article reports the study conducted on the stress distribution and the magnitude of stresses exerted to the equipment support when an expanding pin system (EPS) is installed on the machine, and both experimental and finite element (FE) methods were used. Pin joints are widely used mechanisms in different industrial machineries such as aircrafts, cranes, ships, and offshore drilling equipment providing a joint with possibility of relative rotation about one single axis. Due to the tolerance needed for insertion of a standard cylindrical pin in the equipment support bore, the pin is prone to relative displacement inside the bore or slip between surfaces in contact. The amplitude of this relative displacement usually increases as time passes and since the material of the support often has lower quality grade than the pin, it leads to creation of slack in the equipment and malfunctioning of the machine, over time, and costly repairs might be required.

An EPS can be a solution to this problem where the split sleeve expands to eliminate the gap as the expanding pin is torqued, as illustrated in [Figure 1.11](#). The expanding sleeve locks to the support bore at a 360° contact area and thus provides a better stress distribution and reduces or eliminates stress localizations. In the EPS, normally both ends of the pin are tapered and a pair of expansion sleeves are fitted at both ends of the pin followed by end plates or load transfer elements. As the tightening screws or bolts are tightened, the expansion sleeves are forced over the tapered ends of the pin creating a wedge force and contact pressure between the pin and the support holes, which locks the EPS into the pivot.

The experimental results show how much of the applied energy to the EPS in the form of torque is spent to expand the split sleeve and to overcome friction. This study was conducted by using both experimental

and numerical methods, where the experimental setup is illustrated in [Figure 3.12](#). A test boss (ID 89 mm and OD 129 mm) was manufactured for the experiment and equipped with 3 strain gauges on its outer diameter surface for measuring the external hoop stresses, with active-dummy gauge compensation method for unplanned temperature variations.

To investigate the stress distribution the strain measurements were taken by moving the relative position of the boss, with the strain gauges, to the cut sleeve, by rotation. The test boss was restricted from moving axially during the test. Three different scenarios were checked:

- (1) Non-lubricated partly cut sleeve
- (2) Lubricated partly cut sleeve
- (3) Lubricated completely cut sleeve

The purpose of doing a test with lubricated partly cut sleeve in layout (2) was to evaluate the effect of friction, compared with the non-lubricated part, and to analyse how much of applied torque dissipates by friction. In addition, the point of interest for performing tests on lubricated completely cut sleeve in layout (3) was to analyse how much of the applied torque to the joint system is merely used to expand the sleeve elastically. The friction coefficient for the non-lubricated test was set to $\mu = 0.2$, and 0 for the lubricated tests.

The resulting stresses were determined using thick-walled formulas [\[36\]](#), where the inner and outer radii of the test boss are “*a*” and “*b*”, respectively, and the radial and hoop stresses are presented as [Equations \(10\), \(11\) and \(12\)](#). The calculated hoop stresses on the inside surface of the boss based on the outside strain measurements for the lubricated and unlubricated partly cut sleeve cases can be seen in [Table 4.3](#). The average Hoop stress values for the two above mentioned cases can be seen in [Figure 4.31](#), and for the lubricated and completely cut sleeve case in [Figure 4.32](#), while [Table 4.4](#) gives Hoop stresses on the inner and outer boss surfaces calculated from measured strains, in addition to FE results

and percentage difference between the two methods, for the lubricated case with partly cut sleeve.

The calculated Hoop stress at the test boss inner surface was 68% higher at the sleeve full cut through compared to the three partly cuts, for the (1) non-lubricated case with partly cut sleeve. The comparative values for the second case, (2) lubricated with partly cut sleeve, was +25%. For the last case, (3) lubricated with completely cut sleeve, the differences between the most and least loaded cut were below 3%, both at the inner and outer surface of the test boss.

The average Hoop stress at the inner surface of the test boss was 2.54 times higher for the (2) lubricated case with partly cut sleeve compared to the (1) non-lubricated case with partly cut sleeve. The average stress for the (3) lubricated case with completely cut sleeve was 3.48 times higher than the case (1). By making a comparison between the cases (1) and (3), it can be concluded that 71.3 % of the *total applied energy* by torquing is dissipated into friction of sleeve (elastic hysteresis), and deformation of sleeve (when expanding), see Equation (55). The remaining energy, 28.7%, is applied to create the *clamp force* or pressure between the pin assembly and the support, or test boss in this case.

$$\frac{\text{Loss of applied energy} = \text{Energy case (3)} - \text{Energy case (1)}}{\text{Energy case (3)}} = \frac{3.48 - 1}{3.48} = 71.3\% \quad (55)$$

By making a comparison between the cases (1) and (2), it can be concluded that 60.6% of the total dissipated energy was to overcome friction between the sleeve and bore/pin, and the remaining 39.4% was due to elastic deformation of the sleeve. Compared to total applied energy these losses are 43.2% and 28.1%, respectively. The distribution of applied energy into the joint is illustrated in Figure 4.33. Further results and analysis can be found in the attached article [6].

4.3.7 Paper VII: Comparative study on loosening of anti-loosening bolt and standard bolt system

This paper describes a comparative study between the novel Vibralock® anti-loosening bolt concept and a standard HV bolt system. The most important factor in relation to reliability and functionality of bolted joints is the clamping force, where both friction and torque are important factors. Vibrations in mechanical systems can result in loss of clamp forces in preloaded bolts, whose effect depends on vibration type and level, preload level, contact surface and size, reduction and loss of asperities, thread type and size, thread pitch, lubrication of threads, etc. After fatigue, self-loosening of bolts is one of the most common causes of failure in bolted connections. Grabon et al. [37] indicated that surveys from the USA show that up to 23% of all car service problems were related to loosening fasteners, and even for new cars around 12% had this problem.

Generally, there are two methods of generating the required pretension in bolts: (1) by torquing the nut directly by hand torquing tool or torquing tools with external energy source, or (2) by hydraulic tensioning of the shank [38,39] followed by a light torquing of the nut, pressure release and disconnection of the hydraulic tool thereafter. In both cases, with direct torquing or hydraulic tensioning, the nuts are exposed to vibrations and possible fatigue and fretting problems over time, which again can lead to nut turning and self-loosening.

Re-tightening of standard bolts at critical positions, for instance, for floating Offshore Wind Power systems, as illustrated in Figure 4.48, has become a high-cost activity that the system owners and operators both want and need to minimize. Vibrations and oscillating loads in both axial and transverse directions will often lead to self-loosening of the bolted systems, and therefore a yearly re-tightening schedule of a certain amount of the bolts, typically 10%, is normally introduced. Vibrations tend to deform and reduce the height of asperities at the contact surfaces,

and a high pre-load could lead to material yield at the first engaged threads. Both lead to reduced clamp force and increased risk of nut turning, which generate further clamp force loss and possibly total failure of the bolted system.

The first author of this paper has designed a new anti-loosening bolt solution, as illustrated in [Figure 3.14](#), where all three parts; bolt, main nut and locking nut, are designed to work together to reduce any self-loosening effects of the bolt assembly, and by that reduce or prevent the need for re-tightening pretensioned bolts in critical positions. Such a reduced need for re-tightening bolts would have a great cost-impact, especially at Offshore Wind Power sites, where the cost for re-checking and re-tightening is substantial, see [Figure 4.48](#).

The aim of this study was to investigate how the anti-loosening bolt concept reacts and resists on external axial and transverse loads including loads due to vibrations. To conduct the study, two different experiments

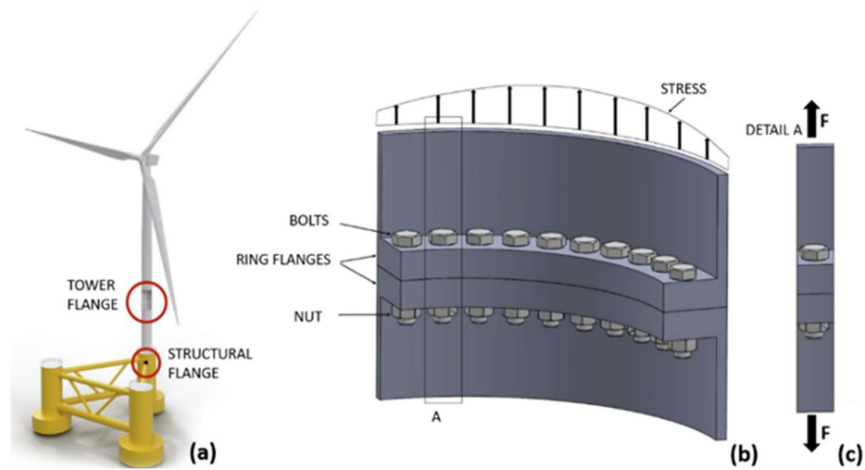


[Figure 4.48](#). Wind turbine tower, (a) floating system, (b) flange details, and (c) force directions

and one Finite Element Analysis (FEA) were conducted, all on different bolt sizes. The two experiments are designated as Test 1 and Test 2, where:

- Test1: M20 bolts were used, but without the bolt head, to make it possible to install and test two bolt systems at the same time. The aim of the test is to investigate whether the nuts were exposed to self-loosening during the *axial* dynamic loading, and if there were dimensional and surface changes at the contact surfaces, like the threads and nut cones.
- Test 2: M30 and M42 bolt systems were exposed to *traversal* dynamic loads and any loss of clamp load were measured. The FE analysis was performed to analyse the structural integrity of the experimental test, but on bigger pin diameter, M72.

Many investigations have been conducted to get more knowledge about self-loosening of bolted joints, often based on studies by Junker [40] regarding criteria for self-loosening of fasteners under vibrations. At the first stage of self-loosening, there is no relative rotation between the bolt and the nut, but there could be a local cyclic plasticity near the engaged thread roots, typically the three first threads, which will also result in a fastener elongation. The second stage is characterized by relative rotation of the nut to the bolt, due to loss of clamp load as described above. The anti-loosening effects will increase with:

- Increased bolt preload
- Decreased load amplitude
- Lubrication of threads with MoS₂ based paste
- Finer threads, or smaller thread pitch sizes
- Improved or reduced surface roughness

It is a near linear relationship between the preload and the self-loosening resistance, according to an experimental study performed by Jiang et al. [41]. The plastic deformation of asperities is large under high excitations amplitude, which can result in reduction and possibly complete loss of

clamp force over time. Transverse loads in oscillation represent the type of external exposure that generate most self-loosening issues in preloaded bolt system, where elongation beyond the elastic limit of the threads and microslip on the thread and bearing surfaces are the two basic loosening mechanisms.

The experimental setup for *Test 1* is illustrated in [Figure 3.15](#). Two M20 bolts with nuts were tested simultaneously, with axial loading an oscillation. Each bolt system, A, B and C, was loaded with 100 kN axial tension, and oscillating (amplitude) load of ± 15 kN, which gives a utilization level of approximately 60% to material yield, at 10 Hz frequency and without washers. The bolts are made of material quality 10.9, and the locking nut was torqued with 200 Nm against the main nut. There was no turning of nut relatively to each other, or relatively to the bolt shank during the test.

The experimental setup for *Test 2* is illustrated in [Figure 3.13](#). M30 / M16 (3.5 mm and 1.5 mm pitch) and M42 / M24 (4.5 mm and 2.0 mm pitch) anti-loosening bolt systems were tested in a 260 kN dynamic standard test rig (MTS), as a Junker test with transverse oscillating displacements, of ± 1.0 mm and ± 1.5 mm, respectively. The bolt systems were tested both for torqued and tensioned versions, both preloaded to 70% of material yield (10.9 grade). According to the DnV defined test procedure the Vibralock® should be tested with the same load that provoked 90% loss of preload in the standard HV bolt system, within 200 – 400 load (displacement) cycles, but the anti-loosening system were to run minimum 3000 cycles. The torqued bolt systems had washers include, while the tensioned had not.

The following parameters were logged; amplitude, clamp load at start, clamp load at end, number of cycles, while the loss of preload over the duration of the test was calculated. All loads were given in kN and the losses of preload were in addition given in percentage values.

The tests of the M30 and M42 bolt locking systems showed a superior resistance to self-loosening compared to the HV reference bolts of same sizes, see [Figure 4.43](#) for the M30 results, and [Figure 4.44](#) for the M42 results. The HV reference bolts lost 86-92% of their preload before 400 cycles, while the bolt locking systems had a loss of 3-9% before 3000 cycles, for the same tests. Based on the test and simulation results, the following main conclusions was made regarding the new bolt locking system:

- The bolt system is superior to standard bolt-nut systems when it comes to anti-loosening resistance
- It experiences a minimum of preload loss over time.
- No turning of nut relative to bolt takes place.
- It is easy to preload and disarm, if required.

4.3.8 *Paper VIII: Fretting fatigue and wear of mechanical joints: Literature study*

In this paper, fretting fatigue and wear of mechanical joints are discussed, as an extension of the first paper, and a complementary literature study, which look deeper into previous studies and investigations on the mechanisms of damages that occur in interference fitted connections of mechanical systems. In general, with increasing transmitted power, mechanical connections are exposed to increasing loads and the risk for damages at contact areas is therefor also increasing. It is focused on fretting fatigue, its causes, and what can be done to prevent or avoid life reducing factors of components and system.

The second chapter focus on different mechanical connection techniques, whereas the third chapter elaborates around fretting fatigue in the different types of connections. There are many different connection types and designs, often depending on their operational situation, which varies between different industries and equipment,

climate zones, type and level of loads, materials etc., where different combinations of the beforehand mentioned variables lead to different capability to resist fretting, wear, corrosion, surface damages, and shortened lifetime. Damages on surfaces in contact, exposed to vibrations from dynamic forces, can lead to crack initiation and propagation, and possibly fretting fatigue and reduced fatigue life.

A standard cylindrical pin, or a mechanical radial expanding pin, as illustrated in [Figure 1.11](#), could be applied in a joint that require a shear pin, where the standard shear pin is installed into the joint with a certain radial clearance while the expanding pin is eliminating that clearance after installation. There are a variety of expanding pin solutions, but in general they have a load bearing pin with tapered ends, complementary axially partly or completely cut sleeves for making the radially expansion possible and tightening screws or bolts to force the sleeve axially and then to expand radially. This pin system can have between one and four expanding sleeves, depending on its required function. The expanding sleeves act as wedges between the load bearing bolt and the support bores, and its interference fit level depends on the torquing level, in addition to tapered angle, contact area between the surfaces in contact, lubrication etc.

In general, fatigue is a well-known issue in mechanical joints and structures, and it is described by The American Society for Testing and Material (ASTM) [\[42,43\]](#) as “The process of progressive localized permanent structural change occurring in a material subjected to conditions that produce fluctuating stresses and strains at some point or points and that may culminate in cracks or complete fracture after a sufficient number of fluctuations”, “A small-amplitude oscillatory motion, usually tangential, between the solid surfaces in contact”, and “The progress of crack formation at a fretting damage site, progressive crack growth, possibly culminating in complete fracture, occurring in a material subjected to concomitantly fretting and fluctuating stresses and strains”.

The process of fatigue is typically divided into three stages, (i) Initial fatigue damage with crack nucleation and initiation, (ii) Cyclic growth of the crack, or crack propagation, and (iii) Fracture of the remaining cross-section. In general, fretting can be treated as three interrelated problems, (a) Fretting wear, (b) Fretting corrosion, and (c) Fretting fatigue.

Fretting wear could arise as a combination of fretting and corrosion, as described in Figure 3 [8]. It is a microscopic dynamic process induced by a short amplitude sliding motion, where debris from a wear process could be trapped between the contact surfaces and play an important role in the further wear process. Fretting wear is an important reason for failures of key components and can reduce the fatigue life considerably.

Different bodies in a joint could have different geometrical shapes, and therefore also different contact shapes, and then act differently under loading. The different areas in the joint can be defined as: (i) stick zone, (ii) slip zone, and (iii) open zone, were:

- (i) There are no relative movements in the stick zone between the two surfaces, and therefore wear will not occur.
- (ii) It will be some relative movements in the slip zone, and fatigue and abrasive wear will occur.
- (iii) No contact between the surfaces in the open zone, and therefore no wear will occur.

This paper also investigates previous studies of *railway axles* with interference fit connections, and aircraft structure and fuselage with riveted or pinned connections. Railway axles have typically interference fit connection between the wheel seat and wheel hub, which represent critical parts due to long-time exposure to crack initiation, because of fretting fatigue. Typical actions taken to eliminate or reduce the problem are (a) optimizing the contact pressure / interference fit level, (b) finding better surface treatments / palliatives, (c) optimizing stress relief groves, (d), improving material strength, and more. *Aircraft structures* and

fuselage are normally connected by rivets, introduced into skin plate holes that often are cold expansion threaded first, and connected by interference fit. *Cold expansion* is a cold forming process to deform the bore wall in the plastic region to make it more fatigue resistant, due to reduced stress amplitudes. Interference fit levels up to 2% increases the fatigue life [20-22], but further increase of the interference fit level don't seems to increase the fatigue life further.

This study revealed that fatigue, in general, have caused many severe accidents over the years. A world-wide survey of aircraft accidents [44] in the period 1934-79 revealed 306 fatal accidents with 1803 fatalities, were fatigue played an important role. Accidents like the Alexander L. Kielland hotel platform, and several helicopter accidents working on the Norwegian shelf, showed all fatigue as an important reason for failure.

The article concludes with the fretting problems being a source for concerns in most industries and must be taken seriously. The mechanical radial expanding pin solution is not sufficiently well known and applied in investigations, but its advantages when it comes to installation, retrieval, elimination of the need for heat/cold, and the possibility to quickly adjust the interference fit level, makes it worth investigate further. More information can be found in the original paper [8].

4.3.9 Paper IX: On modelling Techniques for Mechanical Joints: Literature Study

This paper is a literature study and elaborates around modelling techniques, methods and models typically applied for mechanical joints, to study the evolution of contact profiles, to predict fretting fatigue and wear, crack initiation and growth, stresses and deformations, and other important issues related to mechanical joints. The review and analysis reported are based on study of a wide range of reported literature during the last 25 years.

In most mechanical systems, there are needs for power or force transmissions and connecting techniques between connecting moveable parts, and such joints could be of different types, like riveted, interference fitted (press or shrink fitted), clearance fit pins and pre-loaded bolts, in addition to the less known *expanding pin* solution. The latter one consists of a load-bearing pin with coned ends where corresponding coned expanding caps, or sleeves, are placed. The *sleeves* have four cuts in axial direction which enable a radially expansion as they are forced to displace in axial direction due to torquing of the bolts, typically called *tightening screws*. The sleeves work as wedges and lock the pin assembly to the support bore with an adjustable contact pressure. The use of such expanding pins could be called a mechanical *radial expansion technique* [35]. In addition to the radial expansion technique for mechanical joints, there are several other mechanical connection techniques, typically such as:

- (i) Press fit, also known as friction fit, which is a type of interference fit, where one part (the biggest) is pushed into a second part (the smallest) and by that it creates a contact pressure on the contact surfaces.
- (ii) Shrink fit, which is another type of interference fit, where the inner part is cooled down, and/or the outer part is heated up before joining them, and when the heat treated parts get back to the ambient temperature they connect, and it creates a contact pressure on the contact surfaces.
- (iii) An open hole, or clearance fit, connection with shear pins has no surface contact pressure on the contact surfaces, apart from the pin's own dead weight, and external operational loads.
- (iv) The pre-loaded bolt which consists of a bolt with threaded shank and a head, and at least one threaded nut. The bolt is pre-loaded by torquing the nut, or hydraulic tension of the shank.

A research problem is a statement of a concern, and an investigation will include a model of the problem, where in modelling of mechanical joints, the two main techniques can be categorized as either (a) *stochastic* (also called probabilistic), or (b) *deterministic* [45]. The category (a) refers to a system whose behavior is intrinsically non-deterministic and has a random probability distribution, which can be analyzed statically from observed historically data. The category (b) is a technique using both analytical and numerical models and methods, where the analytical methods are typical Newton's law of motion, Laplace transformation methods, Lagrange differential equations, D'Alembert's principle of virtual work, Hamilton's principle, Fourier series and transform, Duhamel's integral and Lamé's equations. Analytical modelling techniques can be considered as the basis of the development of computer simulations of mechanical joints, such as finite element methods (FEM).

Although analytical approaches are widely used to model mechanical joints, it is not always possible to find an exact analytical solution, especially for high order nonlinear equations with complex coefficients. In such situations, the numerical methods are needed to give approximations, rather than exact answers, as they are mathematical representations of physical behaviors, based on some relevant hypothesis and simplified assumptions.

This study presents some previous research with focus on type of numerical study and objective / methodology. ABAQUS and ANSYS seems to be common software for performance of numerical analysis, but other as FRANC2D® and ADINA are also used. The objectives for these analysis' are typically to, (1) simulate evolution of contact profiles, (2) predict fretting fatigue crack initiation, (3) investigate stress relief groove shape effects on fretting fatigue, (4) study the influence of elevated temperature on crack propagation lifetime, (5) in combination with fretting fatigue experiments under cyclic contact loading, (6) verify and compare results, as crack growth in shrink-fit assembly subjected to

rotating bending, (7) compare deformations and stress in shrink-fitted hub-shaft joint with Lamé's equations, (8) predict fretting fatigue and compare with test results, (9) investigate the fatigue damage evolution at a fastener hole, treated by cold expansion [46,47], and (10) investigate the effect of interference fit level on fretting fatigue.

In addition, some typical experimental models and methods are highlighted, where the objective is typically to investigate around fatigue. In general, the fatigue life can be defined as the sum of the crack formation (or initiation) and the crack propagation, where fatigue life is dependent on the cycle history of the loading magnitude, since a higher stress level is required for the crack initiation, compared with the propagation. Typical types of fatigue can be mechanical, creep, corrosion, thermo-mechanical and fretting, where fretting fatigue seems to be a repeated problem in many industries when it comes to mechanical joints. Supplementary information with discussions and conclusion can be found in the attached article [9] in Part II.

Results and Discussions

5 Conclusions and Future Outlook

Expanding pin solutions of various types and shapes have been commercially available for use in machines, cranes, and different equipment for around 30 years, but they are still not as well-known and comprehensively applied as the case in more standard cylindrical pin solutions. There are currently 2 – 4 companies on the global arena supplying such specialized pin solutions, in addition to several smaller companies supplying to their local or national market, or to their own use in own machines.

This PhD study has focused on the effects and consequences of applying expanding pin solutions in heavy machinery, and the theoretical background, research methodology, and results are presented in nine published papers that are appended, in addition to the previous chapters of this thesis, and both the general objectives (1) – (3) and specific objectives (i) – (v) specified in Chapter 1 have been fulfilled.

The results from the *questionnaire-based survey* (Specific objective (i), and RQ1 and RQ2), with corresponding discussions, were presented in Chapter 4.2.1, based on responses from stakeholders with some, or comprehensive, knowledge and experience with one or more types of expanding pin solutions.

The majority, or 85 % of the respondents, stated that the economic impact of use of expanding pins compared to standard pins was important or very important for them and their clients. The reasons for the economic importance with expanding pins, compared to standard cylindrical ones, were expressed as:

- Considerable shorter installation and retrieval time because expanding pins were considered easy and fast to work with, and no sledgehammering needed. The short and easy installation and

retrieval time was considered as important for the majority of the responders.

- Considerably less levels of tear and wear when using expanding pins, with one respondent only stating the opposite.
- About half of the respondents claimed that there were less risk of pin or support breakage with expanding pins, and no one claimed a higher risk with such pins.
- More than half of the respondents stated that it was / is safer for personnel and equipment during installation, operation, and retrieval of pins when applying expanding pins, and a very small percentage claimed the opposite.

The results regarding the studies of *traditional expanding pins* (Specific objectives (ii), and (iv), and RQ3), with corresponding discussions, were presented in Chapter 4.2.2, which is based mainly on experimental tests. It could clearly be observed that when applying an expanding pin in a radial spherical plain bearing, the rotational moment needed to turn the outer ring relatively to the inner ring was considerably reduced, compared to the lowest torque value, for all values of external load. This effect happened for all torque values for the configuration with two expanding sleeves on one bearing, and for all torque values except the highest for the configuration with one expanding sleeves on one bearing.

The expanding pin solution was also combined with a 3D printed repair insert in worn and damaged supports, to minimize the downtime of the equipment and its operations. The specific combination was compared with four other options and strain measurements indicated that the combination of expanding pin and 3D printed repair insert could work well.

When a standard expanding pin is used in a support it introduces stress into the support material. A test boss with fixed length, and outer and inner diameter was equipped with strain gauges and the measured results

were used to calculate Hoop and radial stresses over the thickness of the boss. Measurements were performed with both with lubricated, non-lubricated, sleeve in one piece, and sleeve cut into four pieces. The results indicated that only around 29 % of the total applied energy into the sleeve (by torquing the pin screws) went to create clamp force or pressure between the pin assembly and the support, while the rest, about 71 %, was dissipated energy which went into overcome friction (43 %) and expansion of the sleeve (28 %).

The results regarding the studies of *newly developed pin solutions* (Specific objectives (iii), and RQ4), with corresponding discussions, were presented in Chapter 4.2.3, which is based mainly on experimental tests. A pin solution which combined preloaded and expanding pin capabilities was investigated and showed interesting results. The axial preload was achieved by torquing a number of smaller bolts (tightening screws) instead of one bigger nut (as for normal bolt-nut systems), and the radial expanding locking was achieved as for “normal” expanding pin solutions, with axially cut sleeves. The maximum achievable preload, and flange shear capacity, with this pin solution was less than the theoretically value when applying standard bolts of the same dimension. The difference was the radial locking or wedging capacity between pin and support, which theoretically increased the shear capacity by including the shear capacity of the pin material itself, not only the shear capacity of the flange surfaces in contact. When optimizing the number and sizes of the tightening screws, the axial-radial pin solution reached a total shear capacity of over 3 times compared to the standard bolt systems, with considerably lower tightening torques, only 1 – 2.5 %.

A newly developed anti-loosening bolt concept was tested and compared with standard HV bolt systems by measure clamp load losses during transverse loading, also called a Junker test, for Ø30 and Ø42 mm bolt systems. The anti-loosening bolt has a locking nut that goes on smaller thread pitch and diameter compared to the main nut, and their contact

Conclusions and Future Outlook

surface is coned. The bolt was either torqued or tensioned for the main nut and torqued for the locking nut. The standard bolts were exposed to such a transverse amplitude that the (main) bolt turned and 90 % of the preload was lost within 200 – 400 cycles, and the same amplitude was applied for the anti-loosening bolts. The results for the newly developed anti-loosening bolts showed no nut turning at all, and a clamp loss of only 4-8 % over 3000 cycles, where the HV bolts lost over 90 % during maximum 400 cycles because of considerable nut turning and self-loosening.

It can be concluded that the expanding pin system in general is very well appreciated by those who have experiences with it, and it has an important economic impact, both when it comes to safe handling the pins and during operation and repairs of machines and equipment. This pin solution can improve the functionality of a bearing, reduce downtime due to repairs, increase shear capacities of flanged connections, and eliminate self-loosening of bolts.

Future studies on expanding pins could investigate further and more in depth regarding several of the issues presented here. More detailed information about the economic impact and safety of applying expanding pin solutions could be important to have available for decision makers, both when choosing bolt/pin systems for new-built machines, cranes, and equipment, but also for after-market in relation to maintenance, repair, and overhaul. In addition, it could be both interesting and important to perform more FE analysis, especially in relation with testing the combination of expanding pin and different types and sizes of bearings, to ensure better and wider basis when decisions are taken. It would also be important to perform a full-scale test with the combination of expanding pins and 3D printed repair inserts, in different operational situations to verify its functionality. Both the axial-radial pin solution and the anti-loosening bolt system could be experimentally tested on full-scale huge flange connections, and analysed numerically, to achieve more knowledge about their advantages and weaknesses. This thesis has

Conclusions and Future Outlook

not included any experimental tests of pin or bolts of stainless-steel materials, which could be of interest for future investigations.

6 Scientific and Practical Contribution

The contribution of a PhD research should be to create new knowledge within, and add scientific value to, the specific field of study with the aim to improve quality of life for humans, animals, and all living creatures. To improve quality of life, common factors like the environment must be protected, and our work processes must be based less on short time profit, and more on sustainability over time. Even industrial machines and equipment used to create, maintain, or improve quality of life must be protected and improved. Although wear, breakage, and failures of such machines and their processes create jobs for humans within repair and maintenance, it is a destructive process for the society and its prosperity of good life. Even today, many OEMs choose lower quality on many parts, such as pins and bolts, to maintain the lowest possible production cost of their machine or crane and leave the future problems and costs to their customers and the end-users. Such attitudes might seem to be profitable for the company at short term, but not for the society at a long-term view.

This thesis with its corresponding published papers has presented both scientific and practical contribution to society, mainly through questionnaire-based survey and experimental tests, with some additional finite element analysis. Through the published papers and this thesis, both the scientific society and the different industries are invited to learn more about how to reduce their unnecessary high risks and losses, by use of expanding pin systems instead of cylindrical pins. Such risks and losses occur typically because of rough and long handling time, typically during installation and retrieval of pins which could require sledgehammering, nitrogen freezing, flame cutting, welding, line boring etc. Both planned and unplanned downtime due to repairs of wear, breakage, or cracks of pins, bolts, supports, or machine parts can be substantially reduced by use of expanding systems. In addition, different pin and bolt solutions have been investigated and presented with

capabilities to: (i) reduce the rotational friction of radial spherical plain bearings during operation with external loading, (ii) potentially reduce drastically downtime of machines due to repair of worn or damaged support bores, and (iii) increase huge flange shear capacity by prevent nut rotation and clamp load loss, and by include the bolt shear capacity into the total flange shear capacity.

The principles of scientific work should always be based on honesty, curiosity, objectivity, openness, and being critical and responsible. This thesis is done based of these principles, and future investigations around the same pin and bolt technologies, applying the same principles are wished welcome.

References

- [1] Ø. Karlsen og H. G. Lemu, «Questionnaire-based Survey of Experiences with the Use of Expanding PIN Systems in Mechanical Joints,» *Results in Engineering*, 2 March 2021.
- [2] Ø. Karlsen og H. G. Lemu, «An Investigation of the Effects and Consequences of Combining Expanding Dual Pin with Radial Spherical Plain Bearings,» *Applied Mechanics*, vol. 2022, nr. 3(2), pp. 573-589, 2022.
- [3] Ø. Karlsen, H. G. Lemu og I. Berkani, «A novel technique for temporarily repair and improvement of damaged pin joint support bores», *Applied Mechanics*, 2022.
- [4] Ø. Karlsen og H. G. Lemu, «Safety related study of Expanding Pin Systems application in Lifting and Drilling Equipment within Construction, Offshore, and Marine sectors», in *COTech&OGTech 2022*, Stavanger, 2021.
- [5] M. M. Akhtar, Ø. Karlsen og H. G. Lemu, «Study of Bondura® Expanding PIN System – Combined Axial and Radial Locking System», *Strojniski Vestnik / Journal of Mechanical Engineering*, pp. 625-634, 01 December 2021.
- [6] S. Salahshour, Ø. Karlsen og H. G. Lemu, «Experimental and Numerical Studies of Stress Distribution in an Expanding Pin Joint System», *Applied Mechanics*, pp. 46-63, 30 December 2021.
- [7] Ø. Karlsen og H. G. Lemu, «Comparative study on loosening of anti-loosening bolt and standard bolt system», *Engineering Failure Analysis*, vol. 2022, nr. 140, p. 106590, 2022.

- [8] Ø. Karlsen og H. G. Lemu, «Fretting fatigue and wear of mechanical joints: Literature study», i *COTech 2019*, Stavanger, 2019.
- [9] Ø. Karlsen og H. G. Lemu, «On Modelling Techniques for Mechanical Joints: Literature Study», in *IWAMA 2019: Advanced Manufacturing and Automation IX*, Plymouth, UK, 2020.
- [10] Britannica, “Encyclopedia Britannica,” Encyclopædia Britannica, [Online]. Available: <https://www.britannica.com/>. [Accessed 23 June 2022].
- [11] B. Batinic, U.-D. Reips, M. Bosnjak og A. Werner, Online Scosial Science, Seattle WA: Hogrefe & Huber Publishers, 2002.
- [12] E. Martin, «Survey Questionnaire Construction», *Survey Methodology*, vol. 2006, nr. 13 , 2006.
- [13] S. Roopa og M. S. Rani, «Questionnaire designing for a survey», *Journal of Indian Orthodontic Society*, vol. 2012, nr. 46(4), pp. 273-277, 2012.
- [14] I. Berkani, Ø. Karlsen og H. G. Lemu, «Experimental and numerical study of Bondura® 6.6 PIN joints», in *COTech 2017*, Stavanger, 2017.
- [15] A. Andrzejuk, Z. Skup og R. Zalewski, «Analysis of a conical sleeve with pivot joint loading of axial force», *Journal of Theoretical and Applied Mechanics*, vol. 2014, nr. 52, 2014.
- [16] K. Ning, J. Wang, P. Li, D. Xiang og D. Hou, «Multi-objective intelligent cooperative design for interference fit of the conical sleeve», *Journal of Mechanical Science and Technology*, vol. 2021, nr. 35(8), pp. 3569-3578, 2021.

- [17] X. Q. Zhao og P. Shang, «Exact solution of stresses of tapered interference fit», *Applied Mechanics and Materials*, vol. 2014, nr. 556, pp. 4284-4287, 2014.
- [18] P. R. N. Childs, *Mechanical Design Engineering Handbook*, San Diego: Elsevier Science & Technology, 2018.
- [19] N. L. Pedersen, «On optimization of interference fit assembly», *Structural and Multidisciplinary Optimizatio*, vol. 54 (2), pp. 349-359, 2016.
- [20] T. N. Chakherlou, M. Mirzajanzadeh, B. Abazadeh og K. Saeedi, «An investigation about interference fit effect on improving fatigue life of a holed single plate in joints», *European Journal of Mechanics-A/Solids*, vol. 2010, nr. 29(4), pp. 675-682, 2010.
- [21] K. Iyver, G. T. Hahn, P. C. Bastias og C. A. Rubin, «Analysis of fretting conditions in pinned connections», *Wear*, vol. 1995, nr. 181-183 (Part 2), pp. 524-530, 1995.
- [22] K. Iyver, C. A. Rubin og G. T. Hahn, «Influence of interference and clamping on fretting fatigue in single rivet-row lap joints», *Journal of Tribology*, vol. 2001, nr. 123(4), pp. 686-698, 2001.
- [23] J. A. Collins, H. Busby og G. Staab, *Mechanical Design of Machine Elements and Machines, a failure prevention perspective*, Hoboken: John Wiley & Sons, Inc., 2009.
- [24] R. L. Norton, *Machine Design. An integrated approach*, Upper Saddle River, New Jersey, USA: Prentice Hall, 2014.
- [25] VDI Verein Deutscher Ingenieure e.V., «VDI», [Online]. Available: <https://www.vdi.de/en/home>. [Accessed 19 July 2022].

- [26] N. Motosh, «Development of Design Charts for Bolts Preloaded up to the Plastic Range», *Journal of Engineering for Industry*, vol. 1976, nr. 98(3), pp. 849-851, 1976.
- [27] J. Bickford, *Introduction to the Design and Behavior of Bolted Joints*, Boca Raton: CRC Press, 2008.
- [28] Galton, «English Men oif Science», [Online]. Available: <https://galton.org/books/men-science/index.html>. [Accessed 21 July 2022].
- [29] P. Lietz, «Research into questionnaire design: A summary of the literature», *International journal of market research*, vol. 2010, nr. 52(2), pp. 249-272, 2010.
- [30] K. Olson, «An Examination of Questionnaire Evaluation by Expert Reviewers», *Field methods*, vol. 2010, nr. 22(4), pp. 295-318, 2010.
- [31] E. M. Ikart, «Survey questionnaire survey pretesting method: An evaluation of survey questionnaire via expert reviews technique», *Asian Journal of Social Science Studies*, vol. 2019, nr. 4(2), p. 1, 2019.
- [32] R. G. Budynas og J. K. Nisbett, *Shigley's Mechanical Engineering Design*, Ninth Edition, New York: McGraw-Hill, 2011.
- [33] Stavanger Engineering AS, «Stavanger Engineering» [Online]. Available: <https://staveng.no/>. [Accessed 19 August 2022].
- [34] W. Wang og K. M. Marshek, «Determination of the load distribution in a threaded connector having dissimilar materials and varying thread stiffness», *J. Eng. Ind.*, pp. 1-8, 1995.

References

- [35] Bondura, «Bondura», [Online] Available: www.bondura.no. [Accessed 28th April 2022].
- [36] E. Ventsel og T. Krauthammer, Theory, Analysis, Applications, New York: Routledge, 2001.
- [37] W. A. Grabon, M. Osetek og T. G. Mathia, «Friction of threaded fasteners», *Tribology International*, vol. 2018, nr. 118, pp. 408-420, 2018.
- [38] Enerpac, «Enerpac,» Enerpac, [Online]. Available: <https://www.enerpac.com/en-us/training/e/tensioning>. [Accessed 23 March 2020].
- [39] Torq/Lite Europe AS, «Torq/Lite», [Online]. Available: <https://www.torqlite.eu/>. [Accessed 21 June 2022].
- [40] G. H. Junker, «Criteria for self loosening of fasteners under vibration», *Aircraft Engineering*, p. 1, January 1973.
- [41] Y. Jiang, M. Zhang, T. W. Park og C. H. Lee, «An experimental study of self-loosening of bolted joints», *J Mech*, pp. 925-31, Dec. 2004.
- [42] ASTM, *ASTM, Standard Terminology relating to Fatigue and Fracture Testing*, 2013.
- [43] ASTM, *ASTM, E2789: Standard guide for fretting fatigue testing*.
- [44] G. S. Campbell, «A note on fatal aircraft accidents involving metal fatigue», *International Journal of Fatigue*, vol. 1981, nr. 3(4), pp. 181-185, 1981.
- [45] Y. Amir, S. Govindarajan og S. Iyyanar, «Bolted joints modeling techniques, analytical, stochastic and FEA comparison», in *ASME*

References

International Mechanical Engineering Congress and Exposition, Proceedings (IMECE), Houston, 2012.

- [46] T. N. Chakherlou og J. Vogwell, «A novel method of cold expansion which creates near-uniform compressive tangential residual stress around a fastener hole», *Fatigue and Fracture of Engineering Materials and Structures*, vol. 27 (5), pp. 343-351, 2004.
- [47] T. N. Chakherlou og J. Vogwell, «The effect of cold expansion on improving the fatigue life of fastener holes», *Engineering Failure Analysis*, vol. 10 (1), pp. 13-24, 2003.

Part II: Appended Papers

Appended Paper I

Questionnaire-based survey of experiences with the use of expanding PIN systems in mechanical joints

KARLSEN, Ø.; LEMU, H. G.

Results in Engineering, 2021, vol. 9, p. 100212

<https://doi.org/10.1016/j.rineng.2021.100212>



Questionnaire-based survey of experiences with the use of expanding PIN systems in mechanical joints



Ø. Karlsen^{*}, H.G. Lemu

Department of Mechanical and Structural Engineering and Materials Science, University of Stavanger, Stavanger, Norway

ARTICLE INFO

Keywords:

Expanding pins
Heavy equipment
Tear and wear
Downtime
Safety

ABSTRACT

In this paper, experiences with the use of expanding pins in mechanical joints in different equipment are investigated through a questionnaire-based survey, where six different sections are highlighted; Size of company, Company profile, Experience with expanding pins, Market and equipment, Pin source and Effects and consequences of applying expanding pin solutions. The responses on the survey came from 10 different countries, with the main segments being Offshore oil & gas, Maritime/ships and Construction/earth moving. In total 256 potential responders received the questionnaire, divided into 140 Norwegian based companies and 116 non-Norwegian. Expanding pin systems are clearly seen as technically better pin solutions which protect better both people and equipment, and the non-Norwegian companies are reporting better experiences with expanding pins, in general, compared to the Norwegians, and recognize more the importance of the economic effects of applying expanding pins, compared to standard cylindrical pins.

1. Introduction

Pins or bolts are involved in almost any mechanical joint, moveable or fixed, in order to transfer power or forces/reaction forces from one part to another. For heavy equipment and machinery like cranes, drilling equipment, dumpers etc., the most common pin solution would be of cylindrical type, with a specific length and a uniform diameter over the whole length, and often with a locking plate at the end. Such pins normally come with the equipment from the OEM (Original Equipment Manufacturer), and pin spare parts are normally delivered from the same OEM as a part of their business philosophy. The end-user of that equipment is often obliged to buy the OEM spare parts to maintain the equipment guarantee, and then often to a relative high price.

There are typically 4 ways of assembling mechanical components using pinned joints:

1) *Shrink fit*: a type of fit where an oversized pin is fitted by cooling the pin or by heating the support bore surface [1]. When the temperature of the assembled pin and bore reach to the same ambient temperature level either by expansion of the pin or contraction of the bore, an interface contact pressure between pin and support bore wall is produced. The contact pressure keeps the pin in its position during

service and operation and prevents any relative movements between the pin and the support, being axial, radial, or rotational.

- 2) *Press-fit*: in this case, an oversized pin is forced into the bore by an axial load and by that the necessary interference fit is produced. The contact pressure keeps the pin in its position during service and operation, like the case with shrink fitted pin, and is given by elastic modulus, interference fit level, solid shaft diameter, and hollow hub inner and outer diameters. Fig. 1 [1] shows a principle sketch of a press fit.
- 3) *Pin joint with locking plate*: in this joint a pin with a slightly smaller diameter than the bore is inserted and locked to the supports with locking plate to avoid rotation or axial displacement. The radial movements depend on the installation tolerance between pin and support. The tolerance level would typically depend on the OEM's preferences regarding the installation, operation/service, and retrieval processes. A very tight tolerance could be ideal for service and operation, but difficult or impossible for installation and retrieval.
- 4) *Pin joint with expanding pin technology*: this is a joint where an expanding type of pin system is introduced [2–4] which will typically have an installation tolerance or clearance as in 3), and then expands and locks to the bore wall much like as cases 1) and 2). The contact

^{*} Corresponding author.

E-mail address: oyvind.karlsen@uis.no (Ø. Karlsen).

pressure due to the interference fit between the pin and the supports prevents any relative movements.

When shrinking a pin into position by cooling (1) or forcing it to produce the interference fit (2), it may become complicated and expensive to remove it, if required. It cannot necessarily be done at site due to restrictions on heat/cold work, or hydraulic pressure limitations due to personal and equipment safety restriction. The most common pin solution for heavy equipment is, therefore, the standard cylindrical one with a slightly smaller diameter than the bore in the joint, which theoretically is easier to install and retrieve than the standard interference fit solutions, due to the installation tolerances on the pin diameter.

A pin lying loose in a joint will always move around during service and operation since its diameter is slightly smaller than the support bore diameter. Such movements of the pin in combination with load, vibrations and punches will create tear, wear and ovality in the bore, and possible wear of the pin depending on the steel quality, which again results in a bigger play and reduced contact area between pin and support. A reduced contact area will increase the contact pressure, and the risk of accelerating wear, although the surface might be hardened due to the previous plastic deformations, and increased risk of pin breakage.

Pin breakage or malfunction can have serious consequences, not only of mechanical and operational nature, but also injuries or fatal consequences for personnel. Ahmed and Gu [5] described failure modes, causes, consequences and prevention methods in an analysis of marine boilers, where bolt failures due to incorrect tightening torque or loose joints can ultimately result in personnel injuries. Such bolt and joint issues can also result in loose boiler or low steam pressure due to pressure loss, with fire and explosion as consequences. Major accidents onboard, or breakage of bolts in the rudder system, can lead to loss of control over the ship, collision and loss of personnel, cargo, and major negative impact on the marine environment, as happened with the infamous accident of the Exxon Valdez [6]. Haute and Pire [7] did a case study regarding maintenance intervals for MP-TP bolted connections for offshore windfarms. Due to the increasing size and number of bolts, maintenance has become a cost and health, safety and environment (HSE) issue that must be considered up against the risk of self-loosening of the installed bolts, which again is a serious risk. Corrosion of steel is often a great problem within a wide range of industries and activities, and liquids like drilling mud contain normally highly corrosive additives which negatively also affect the bolt connections. Many investigations are performed to develop corrosion inhibitors, as discussed in Akintola et al. [8].

The expanding pin system is more complex design-wise than a standard cylindrical pin design, but it has a range of advantages compared to the other solutions, like the pin shrink fitted by cooling, press-fit to interference and standard cylindrical solutions. This investigation will analyse the feedback and experiences from various stakeholders, who have different experiences and interests when it comes to expanding pin systems. Some of the typical interests of the relevant stakeholders considered in the study are listed below:

- **OEMs:** These produce and deliver complete systems (crane, vehicle, etc) often without having operational activities themselves and therefore not suffering the negative consequences regarding the choice of type of pins, apart from possible pre-installation issues, typically under controlled conditions. Their choice of pin types could be affected by requirements from their customers. Normally the OEMs would require their customers to buy spare part pins to maintain the product guarantee. Some OEMs are producing and delivering their own pin designs, and others are supplying from external producers, but according to OEM's requirements.
- **Sub-suppliers to OEMs:** These are supplying complete or part of the systems to the OEM, and the choice of pin types would typically be according to OEM's requirements.

- **Engineering companies:** These can design pin systems according to strict requirements from their customers or implement own design. Some engineering companies also run projects for their clients and could have more freedom when it comes to choosing pin systems, and some engineering companies are part of an OEM group.
- **End-users:** An end-user (of the OEM equipment) will always receive the equipment with the pins already installed, and normally with restrictions when it comes to changing pins. They are normally committed or obliged to buy the OEM's pin solution to maintain the equipment guarantee.
- **Service/repair/maintenance:** Such companies can be part of an OEM, or a freestanding company often with a certain level of liberty to propose pin type system.
- **Pin producers:** These would have their own pin design often with a general interest in reaching all possible decision makers at all stakeholders.

Upon analysing the feedback data from the above-listed stakeholders to the distributed questionnaire, the purpose of this study is to develop better understanding of the perception of the expanding pin system in the market, identifying its strength and weaknesses in order to optimize the design, develop effective market approach and improve procedures for installation, operation, maintenance and retrieval of pins and pin systems. In addition, the survey result will assist in new developments to satisfy needs in the market. The survey is part of a study on technical and economic consequences of using the expanding pin (i.e. type 4 joint in the above list) for heavy duty machinery.

2. Backgrounds and applications of expanding PIN system

Pins used in heavy machinery and industrial equipment have normally a smaller diameter than the support bore, but a higher strength and harder surface. Typical support materials can be high yield strength structural steel plate S355J2 (EN 10025), where J2 indicates -20 °C temperature impact test, or S420 (EN10025). The physical properties of both materials are given in Table 1. Steel grade S420, is a high strength weldable structure fine grain steel quality. It can reach high impact properties for certain grade variations even at temperatures as low as -50 °C.

2.1. Background

The pin is normally exposed to high loads, often oscillating, dynamic or exposed to shocks, and it serves as the critical connection element between different parts of the machine. The pin material is therefore normally of a higher strength steel grade than the supports, often of quality 42CrMo4 Q + H, 34CrNiMo6 Q + H or 30CrNiMo8 Q + H, 17-4 PH, and S165 M/1.4418, whose physical properties are given in Table 1 [11].

Table 1
Physical properties of pin and support materials for heavy machinery [9,10].

Steel grade	Yield strength, R _{p0.2} [MPa]	Tensile strength, R _m [MPa]	Valid diameter size range [mm]
S355 (EN 10025-2/-5)	355	470	40-80
S420 (EN10025 -2/-6)	360	520-680	63-80
42CrMo4 Q + H (EN10083)	650	900	≤ Ø100
34CrNiMo6 Q + H (EN10083)	800	1000	≤ Ø100
30CrNiMo8 Q + H (EN10083)	900	1100	≤ Ø100
S17-4 PH D1150/1.4542	725	930	-
S165 M/1.4418	700	900-1100	-

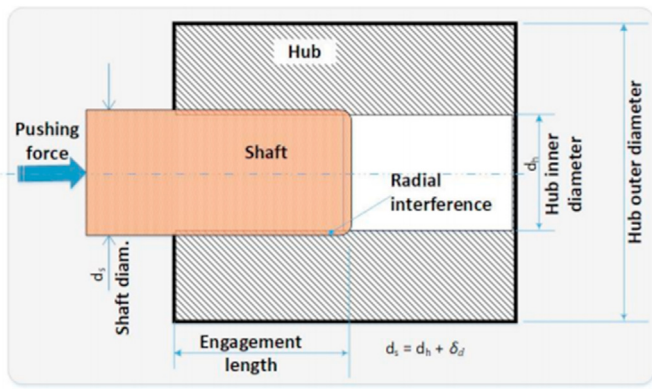


Fig. 1. Principle sketch of a press fit.

A standard pin would create a contact pressure with the support bore only because of the external load, and the contact surface would be less than 180°, depending on the installation tolerances, or diameter differences between the pin and the bore. An increased, or wider, tolerance would result in a reduced contact area and increased radial contact pressure as a result.

The contact stresses between the support bore with diameter $D_2 (= 2r_b)$ and pin with diameter $D_1 (= 2r_a)$ (Fig. 2) can be calculated by using

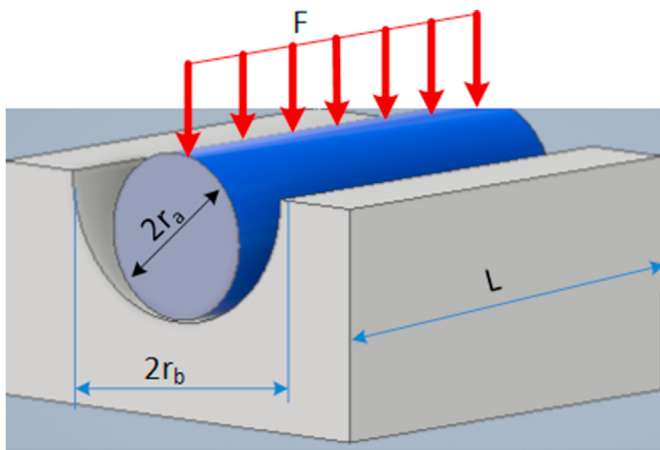


Fig. 2. An illustration of the pin in support.

the Hertz contact formula,

$$a = \sqrt{\frac{2F \left(\frac{1-\nu_a^2}{E_a} + \frac{1-\nu_b^2}{E_b} \right)}{\pi L \frac{1}{2} \left(\frac{1}{r_a} - \frac{1}{r_b} \right)}}, p_{max} = \frac{2F}{\pi a L} \text{ and } p_{av} = \frac{F}{A_{contact}} = \frac{F}{2aL}$$

where a represents half the contact width between the two contact surfaces, the support bore and the pin, and F , L , r_a and r_b represent the applied load, contact length and radius of the pin and the support hole, respectively. E and ν represent the Young's modulus and the Poisson's ratio respectively. The surfaces in contact can be cylinder in cylinder, cylinder against cylinder, cylinder on flat surface, and combinations with a ball, as analysed by Brezeanu [12], and Purushothamam and Thankachan [13].

A standard cylindrical pin would have a tolerance, or play, against the bore during installation, but with an increasing play over time, due to wear because of the repeating relative movements between the pin and the bore. The increased wear results in a decreased contact width $-2a$, which increases the contact pressure and accelerates the wear effects.

An expanding pin assembly, on the other hand, would create a 360° radial contact pressure between the contact surfaces of the pin and the support bore due to the wedge force introduced by the expanding sleeves when torquing the tightening screws, which prevent the relative movements between the pin and the supports and thereby also any wear. In addition, the external load ($F_{ex} = 2 \cdot F$) increases the radial contact pressure over 180° contact surface of the pin assembly itself. The surface contact area on the opposite side of the loaded pin side will have an increased surface contact stress level, and the surface contact area on the same side will have a reduced surface contact stress level (Fig. 3). It could be expected that the increased and decreased surface contact stress can be described by the formulas for P_{max} and P_{av} , as for a cylindrical pin in a support.

Half the contact width $-a$, max and average Hertz contact pressure, P_{max} and P_{av} , respectively are given in Table 2. The input variables that resulted in the values given in the table are: nominal pin and bore diameter Ø80 mm, bore and pin tolerances H7/h7 for the new cylindrical pin and wear value of 2 mm on diameter for the old cylindrical pin connection and zero for the expanding pin connection. Bore and pin contact length is 40 mm for the cylindrical pins and 35 mm for the expanding one. The load F is applied on each support. All pins are made of material 34CrNiMo6+QH, and the supports are made of S355J2. The pin material has a typically minimum yield strength of 800 MPa, and the support material strength is 355 MPa.

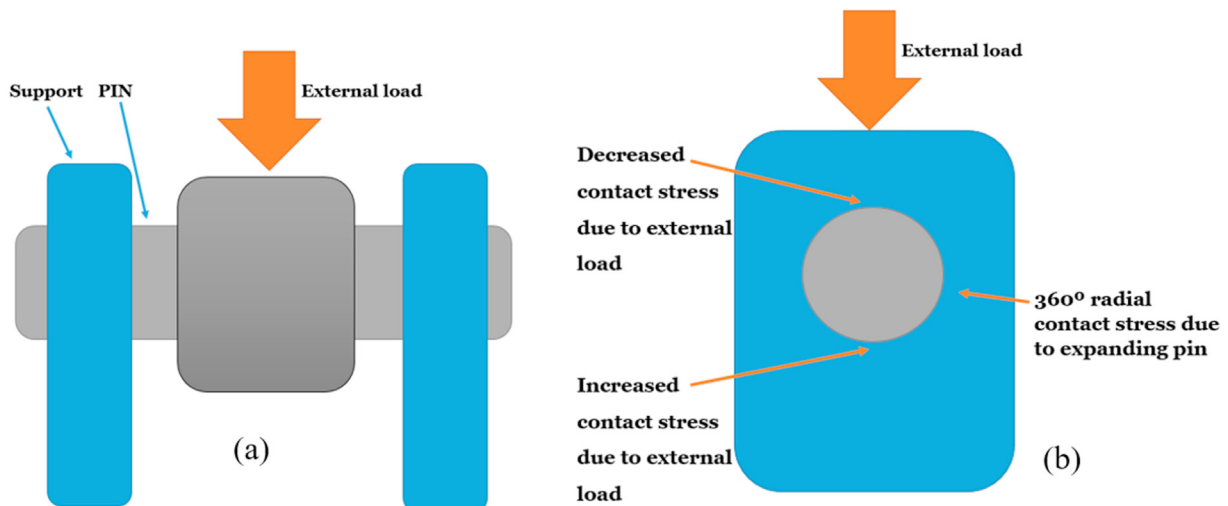


Fig. 3. Contact stresses in expanding pin solution with external load.

Table 2
 “a” value, max and average contact pressure as function of external load F on each support.

F [kN]	New cylindrical pin			Used cylindrical pin			Expanding pin – new and used		
	“a” [mm]	P _{max} [MPa]	P _{av} [MPa]	“a” [mm]	P _{max} [MPa]	P _{av} [MPa]	“a” [mm]	P _{max} [MPa]	P _{av} [MPa]
150	33	72	56	8	294	231	63	43	34
300	47	102	80	11	416	327	63	87	68
450	58	125	98	14	510	400	63	130	102
600	66	144	113	16	589	462	63	174	136
750	74	161	126	18	658	517	63	217	170
1.000	86	186	146	21	760	596	63	290	227

It can also be noted that when the cylindrical pin has worn to a play greater than 0.23 mm, its contact pressure surpasses the contact pressure of the expanding pin solution at load 1.000 kN, and greater than 0.11 mm at load 600 kN. At load 220 kN and a play of 2 mm the contact pressure for the cylindrical pin reaches the yield limit of the support steel, i.e. 355 MPa.

It can be seen from Table 2 that by increasing the external force F, the different “a” value for the new and used cylindrical pin increases, as expected, but for the expanding pin the “a” value is constant. The expanding pin solution is designed to work in all operational situations with full contact between the pin and the bore, independent of the load F, which means a maximum and constant “a” value all the time. When the “a” value is constant the P_{max} and P_{av} values are linear with the force F. If the F is doubled from 150 kN to 300 kN, the max and average contact pressure is also doubled. If the “a” value is not constant, but dependent of the F, the max and average contact pressure is increasing less than the double, due to the increased “a” value.

In addition, there could be tangential tension stress, the Hoop stress, on the bore surface and compression stress on the pin surface depending on the interference level and friction coefficients for the surfaces. An approximate indication of this stress can be found by applying an analytical approach with the Lamé’s equations (elasticity theory for thick walled cylinder), often applied when calculating deformations and stresses at interference fit connections [14,15].

An expanding pin system [2–4] (Fig. 4) combines some of the advantages from the other pin joint categories such as shrink fitted pin, the press-fitted pin and the standard cylindrical pin, while it also avoids their main disadvantages.

Shrink fitting by cooling is a way of achieving an interference fit of the pin and taking advantage of its thermal contraction before assembly, and a typically cooling medium can be liquid nitrogen at –196 °C [16]. After assembly, when the pin returns to an ambient temperature, the thermal expansion results in a strong contact pressure between the pin and its contact surfaces. Although there are many advantages with shrink fitting a pin in a moveable joint, there are certain disadvantages. It requires a system for cooling to extreme low temperatures and it might be complicated or impossible to retrieve the pin, if required, due to the complicated process involving high or low energy situations. To install

the bolt in mobile machines such as excavators, the machine will have to be transported to a distant workshop because such a process might not be possible at to perform at the machine operation site. The installation tolerance would be as wide as necessary to get the pin installed and depending on the cooling process the operation tolerance will be reduced to zero. Many investigations have been performed with the aim to learn more about the different effects involved in the process. McMillan et al. [17] studied the slip at the interface surfaces between a circular shaft and a hub exposed to axial load, where the slip was measured by drilling a small diameter hole through the assembly. The profile of the hole was then measured by a Talysurf profilometer, with an accuracy of 1–2 µm. Mouaa et al. [18] presented an analytical model analysing the stresses in an assembly with a solid shaft and hub, within the elastic-plastic range, while Toma [19] studied a new construction method “shrink fitting method by high-frequency induction heating”. Gutkin and Alfredsson [14] investigated the growth of fretting fatigue cracks in a shrink-fitted joint subjected to rotating bending.

Press-fitting a pin into a joint is another method of achieving an interference fit without applying high temperature or cooling of any of the involved parts. A commonly used method would be to use a pin with a diameter slightly greater than the joint bore and load the pin axially to force it into correct position. The interference fit level in a press-fitted joint can be defined as [20].

$$I = \frac{D - d}{d} \times 100\%$$

where D is the pin diameter, and d is the bore diameter.

As for the shrink fitting by cooling, the press fitting technique creates a solid and firm interference fit but could as well be very complicated both to insert and retrieve if required. The installation tolerance would be negative but forced to zero which then would be the operation tolerance. As for shrink fit connection by cooling, a press fit joint could be complicated or impossible to disarm and retrieve outside a well-equipped workshop, often distant from the actual operation area of the machine. Murcinková et al. [21] studied dimensional parameters of the press fit bearing-shaft joint, by analytical and numerical approach, and Strozzi et al. [22] investigated the stress concentrations at the rounded edges of the hub in an interference fit with a solid shaft, subjected to bending. Lee

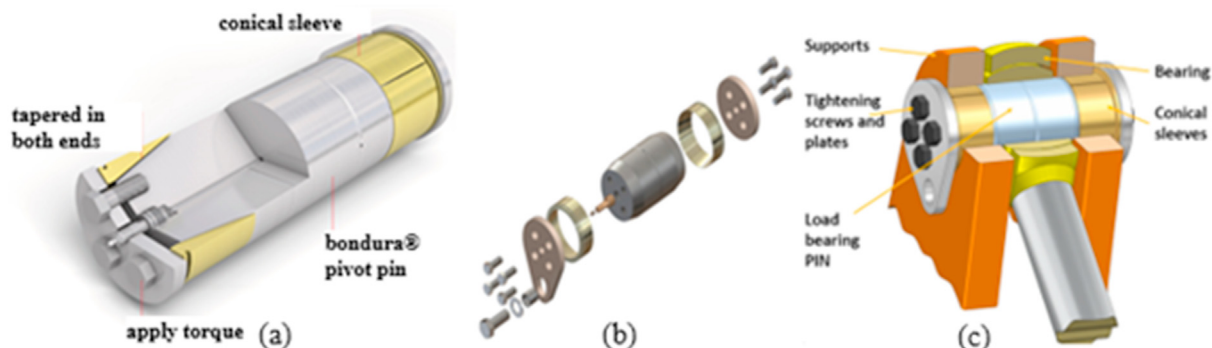


Fig. 4. Expanding pins - (a) pin assembly, (b) exploded view, (c) pin installed in joint.



Fig. 5. Std cylindrical pins - (a) and (b) play due to tear and wear of supports, (c) cold welded pin.

at al [23]. studied fatigue damage in a press-fitted shaft under bending. An experimental attempt was made to understand better the fretting damages in press-fitted connections using a rotating bending fatigue machine under constant amplitude cyclic loading. Song et al. [24] also investigated rotary bending fretting fatigue damage, of railway axles.

A standard cylindrical pin will normally have a slightly smaller diameter than the hole where to enter. This tolerance can vary depending on the pin size, weight, length, complexity of the installation process etc. Typical tolerances on the pin and bore are defined in ISO-2768, which is a geometrical tolerance standard with the intention to simplify drawing specifications for mechanical tolerances [25]. Although the standard cylindrical pin often is an easy solution when it comes to the installation process it might result in damaging wear on the supports during operation or cold welding between pin and support, as shown in Fig. 5.

2.2. Applications of expanding pin systems

The expanding pin system [2,4] can operate with any required installation tolerance, like the standard cylindrical pin. The end-sleeve at an expanding pin works as a wedge between the tapered end of the pin and the support bore wall and prevent any relative movement between the surfaces in contact; pin/sleeve and sleeve/bore wall. The wedge force is produced when torquing the tightening screws or nut, which again pushes the end-sleeve in between the tapered end of the pin and the bore wall. This function allows the expanding pin to operate with an interference fit towards the support bore, much like the shrink-fit pin and the press-fit do. It is easy and straight forward to retrieve an installed expanding pin system. The tightened screws or nuts must be loosened, the sleeve is removed by special tool if required, and the pin can be retrieved easily. The retrieval process of an expanding pin system is therefore different compared to the same process for a shrink fit pin by cooling or a press fit pin.

The development of more sophisticated expanding pin solutions started in the late 80's and early 90's as solutions to smaller excavators and other agricultural equipment suffering major tear and wear problems in the moveable joints. Later, these solutions were introduced into the Oil&Gas and maritime industry, in addition to high volume OEM vehicles for agriculture, forestry, mining etc. The expanding pin technology is still in little use compared to the use of standard cylindrical pins, and it is not as well-known as shrink fit and press fit are. However, the knowledge about this solution is increasing and it can be found in various industries in various countries.

The expanding pins come in various forms, sizes, and material qualities, depending on.

- the type of industry, equipment, and joints where to be installed,
- the exposure to corrosive environments, loads and vibrations,
- issues and problems to be solved,
- patents and other intellectual property (IP) restrictions, stakeholders' preferences and much more.

The expanding pin solution resolves various issues and problems which other pin solutions cannot resolve easily. In addition to the previous mentioned tear, wear and ovality problems that often occur (Fig. 5), the expanding pin can:

- Easily be installed and retrieved in situations with heavy pins with requirements to minimum installation tolerances in combination with complicated joint positions.
- Prevent situations where the cylindrical pin could get cold-welded or contact-welded to the bore, and difficult or impossible to disassemble unless destructive methods such as flame cutting, welding and line boring are used. The cold-welding is a solid-state welding process without heating, where similar metals strongly adhere when the atoms in contact "recognize" each other. The cold-welding could overlap with galling, fretting, sticking, and adhesion.
- Provide a higher grade of safety for personnel and equipment during installation and retrieval of the pin
- Reduce the risk of breakage of the pin because of reduced reactions forces, or accelerations, due to prevention of relative movements between the pin itself and the supports it is connected to, ref Fig. 6, compared to a standard cylindrical pin solution.
- Reduce both the planned and unplanned down-time due to better control and less unwanted issues.

Expanding pin solutions are applied in a wide range of machines within many industries and geographical areas, but still not equally known in the different markets and segments as the standard cylindrical pins. Expanding pins are normally applied in positions and joints where there are known to be some specific issues in the past or expected to be in the future, or where it is needed to ease the process of installation and retrieval (Fig. 7). Such issues involve typically heavy loads, vibrations, accelerations, punches/hammering, tear and wear, ovality, breakage of pins, requirements of a minimized operational tolerance between pin and supports, long installation and retrieval time of pins, damage of bearings, unwanted mechanical noise, corrosion, etc., and such expanding pin solutions can often be found in:

- Offshore, onshore and mining drilling and pipe handling equipment
- Offshore, maritime and port handling cranes, in addition to tower cranes
- Earth moving equipment and vehicles, both onshore, mining and for dredging
- Steel and cellulose fabrication machines
- Many more

3. Research methodology

To investigate the stakeholder's experiences and opinions regarding the use of expanding pin technology, a questionnaire was developed and sent to 323 contacts. The selected contacts (companies) for the questionnaire are those assumed to have a certain knowledge of the

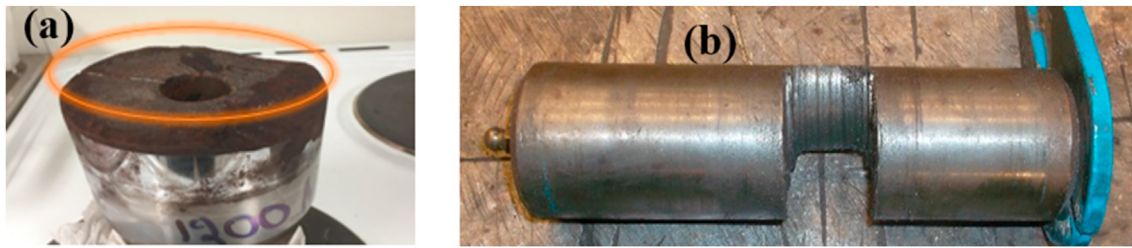


Fig. 6. Std cylindrical pins - (a) breakage of pin, (b) wear damaged pin.

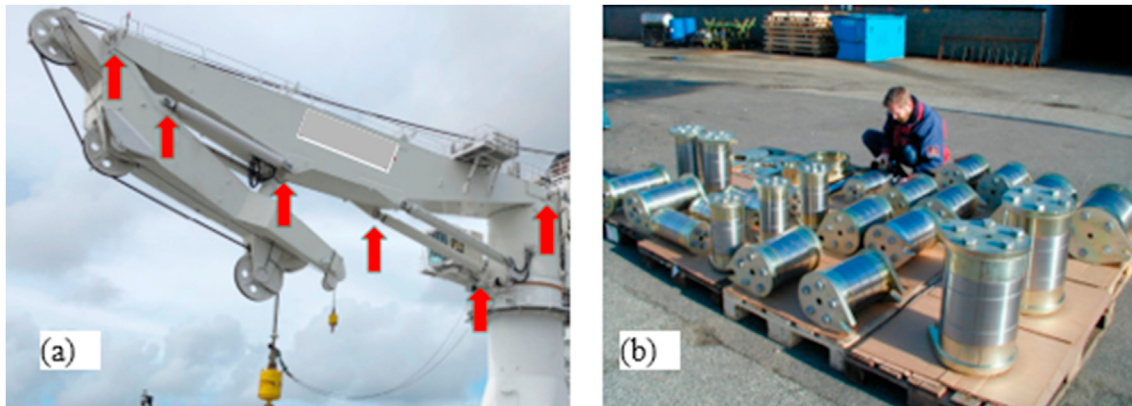


Fig. 7. Expanding pins (a) installed in a maritime crane, (b) pins prepared for offshore cranes.

expanding pin technology. Among these, 22 failed delivery messages, and 45 stated immediately to have no knowledge of the technology. Of the remaining companies, 23% responded positively by filling in the questionnaire or giving comments apart.

The questionnaire was distributed to potential respondents by e-mail with the questionnaire attached as an editable pdf file. 41% answered by typing directly into the pdf file, 52% answered by manually filling in a printing out copy and 7% did not answer the Questionnaire directly but gave written comments in e-mail reply. The original Questionnaire version was made in English, but some respondents asked for a Norwegian version, which was delivered.

The Questionnaire contained diverse questions organized under six sections as listed below.

- (1) Size of the company
- (2) Company profile
- (3) How long the company applied, specified, or worked with expanding pin technology
- (4) On which type of market and equipment the company applied the technology
- (5) Whether the company is using own designed expanding pin or from others
- (6) Effects and consequences of applying expanding pin solutions

These questions are designed to collect required data from the personnel, companies or respondents that are intended to fall under three main categories: (i) characteristics and profile of the companies – sections (1) and (2), see Chapter 4.2; (ii) type and period of usage of expanding pin technology by the companies – sections (3)–(5), see Chapter 4.3 and (iii) effects and consequences of using expanding pin technology experienced by the companies – section (6), see Chapter 4.4. While the questions under category (i) are intended to provide some background information, questions under category (ii) and (iii), particularly questions under section (4) and (6) represent the main sections of the investigation about market/equipment and the effects and consequences of applying expanding pins respectively. In section (4), each

segment a) to i) contains options of questions regarding type of equipment and machines used by the industry, and in section (6) each segment a) to o) contains choices for effects and consequences.

4. Analysis and discussion of results

4.1. Distribution and feedback rate of the questionnaire

The survey was distributed to 323 contacts in various companies, where 22 were returned as error messages and 45 reported to have no experience or knowledge to the products and therefore declined to participate. This leaves 256 potential respondents and among these 140 (55%) are Norwegians and 116 (45%) are from other countries. In this survey a company is defined as Norwegian when the responses are coming from its Norwegian location, and not because of ownership or global main office location. The overall response rate for the survey is defined as the number of responses compared to the number of mailings, and for this survey it is 23%, or 58 responses out of 256 potential responders, who received the questionnaire as an editable pdf file, added to an e-mail.

Comparing the distribution of the feed-back from the survey with the distribution of all the receivers of the survey (Fig. 8), it can be observed that it is a relatively higher response rate from the Norwegian companies compared to the remaining companies. The Norwegian companies represent 55% of the total potential responders, and 67% of the total received responses, which gives an overall relative reaction rate of 1.23 (i.e. total number of received Norwegian responses [%] divided by the total number of potential Norwegian responders [%]). For the non-Norwegian respondents, the value is 0.72. The overall relative reaction rate of the Norwegian companies is then 70% higher than for the others.

The reaction rates are calculated as indicated in Table 3. The overall reaction rates indicate the relationship between each group's (Norwegian or non-Norwegian companies) response willingness in %-age, and the same groups share of the requests (mailings) for participating in the Survey (total rate for potential responders). The segment relative reaction rates are calculated by the response willingness per segment,

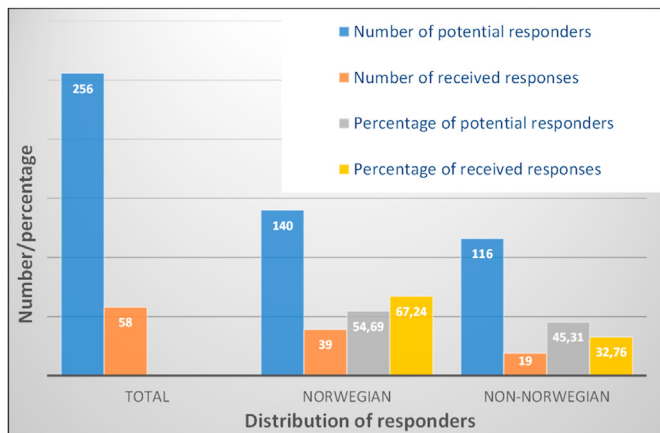


Fig. 8. Overall distribution of responders.

compared to the same total rate for potential responders, as for the overall reaction rates, as indicated in Table 4.

4.2. Location and profile of responding companies

As shown in Table 5, the total number of respondents in this Survey is 58, where 39 (67%) come from Norway and the remaining 19 (33%) come from 9 other countries in three different continents, with a total distribution of Europe 55 (95%), North America 2 (3%) - and South America 1 (2%). The second and third dominant responders are Scotland with 6 (10%) and Sweden with 5 (9%). Percentages are with respect to the total responders.

The responses received on the Questionnaire would be a combination of the perception of the responding person and the actual company's experience. Though only single responses were received from most companies, a few bigger companies have responded with more than one Questionnaire, in which case the answers and comments are coming mainly from different areas within the company that are often working with different types of equipment and therefore having different experiences. Responses from different persons with different experiences on the same product area or department within the same company are therefore expected to increase the Survey's accuracy on the company's experience.

The size distribution and profile of respondents are given in Table 6.

Table 3
Overall reaction rate structure.

	Received responses			Relative reaction rates	
	Total, No. (%)	Norwegian No. (%)	Non-Norwegian No. (%)	Norwegian (-)	Non-Norwegian (-)
Total received responses	58 (100)	39 (67)	19 (33)	1.23*	0.72
Total potential responders	256 (100)	140 (55)	116 (45)		

* Calculation of exact overall reaction rates; Norwegian: $67.24\%/54.69\% = 1.23$ and Non-Norwegian; $32.76\%/45.31\% = 0.72$.

Table 4
Segment wise overview of received responses and calculated relative reaction rates.

Segment	Received responses			Relative reaction rates	
	Total, No.	Norwegian, No. (%)	Non-Norwegian, No. (%)	Norwegian (-)	Non-Norwegian (-)
a) Offshore Oil&Gas	30	20 (67)	10 (33)	1.22	0.74
b) Marine - ships	19	16 (84)	3(16)	1.54	0.35
c) Subsea - ROV/str.	5	5 (100)	0 (0)	1.83	0.00
d) Dredging	7	7 (100)	0 (0)	1.83	0.00
e) Mining	12	9 (75)	3 (25)	1.37	0.55
f) Construction and earth moving - onshore	17	16 (94)	1 (6)	1.72	0.13
g) Specialized machines	5	5 (100)	0 (0)	1.83	0.00
h) Steel and paper ind.	5	1 (20)	4 (80)	0.37	1.77
i) Other	6	3 (50)	3 (50)	0.91	1.10

Table 5
Location of responder companies.

Responders' locations	Distribution of locations	
	No of respondents	%
Total	58	100
Europe	55	95
Norway	39	67
Scotland	6	10
Sweden	5	9
Finland	2	3
The Netherlands	1	2
Greece	1	2
Germany	1	2
North America	2	3
Canada	1	2
USA	1	2
South America	1	2
Brazil	1	2

The company size distribution is defined by the size of employees as less than or equal to 20, 21–100 and over 100. The company profile is defined as OEM, Supplier to OEM, Engineering company, End-user, Service & Maintenance, and others.

Excluding companies in Norway, almost 2/3 (63%) of the respondents indicate that their company size is represented by more than 100 employees, while the remaining are distributed between company size with 21–100 employees (26%) and less than or equal to 20 employees (11%), respectively. Both the Scottish and Swedish companies have a relatively high percentage of the bigger companies, i.e. over 100 employees; 5 (83%) and 3 (60%), respectively, compared to Norway with 18 (46%).

The companies' profile, or type of business area (Table 6) also show that 92% of the respondents from the 6 possible areas are distributed over 4 areas, namely OEM, Engineering, End-user and Service & Maintenance companies with 19 (20%), 21 (22%), 18 (19%) and 30 (31%), respectively, with Service & Maintenance being the biggest.

4.3. Type and period of usage of expanding pin technology by the companies

Some of the companies work in one segment only, while others have parallel activities in various segments. The combinations between respondents and the activities in the various segments, as obtained from the Survey results are given in Table 7. The three main segments are "Offshore Oil&Gas", "Maritime/ships" and "Construction/earth moving"

Table 6
Company size and profile.

		Norway		Scotland		Sweden		Total excl. Norway		Total Survey	
		No	%	No	%	No	%	No	%	No	%
Total		39	100	6	100	5	100	19	100	58	100
Company size	CS1	12	31	0	0	0	0	2	11	14	24
	CS2	9	23	1	17	2	40	5	26	14	24
	CS3	18	46	5	83	3	60	12	63	30	52
Total		63	100	12	100	5	100	33	100	96	100
Company profile	CP1	13	21	4	33	1	20	6	18	19	20
	CP2	3	5	0	0	0	0	2	6	5	5
	CP3	13	21	3	25	0	0	8	24	21	22
	CP4	12	19	3	25	1	20	6	18	18	19
	CP5	22	35	2	17	2	40	8	24	30	31
	CP6	0	0	0	0	1	20	3	9	3	3

CS1: No. employees ≤20; CS2: No. employees = 21–100; CS3: No. employees >100.

CP1 = OEM; CP2 = Supplier to OEM; CP3 = Engineering companies; CP4 = End user; CP5 = Service & maintenance; CP6 = Others.

Table 7
Distribution of responses on segments.

Segments (9 different):	Distribution of the 139 responses from 58 respondents, on 9 different segments			
	No. of respondents per segment	% - of total respondents (58)	No. of responses on equipment, per segment	% - of total responses (139)
Total	106		139	
a) Offshore oil&gas	30	52	42	30
b) Maritime/ships	19	33	32	23
c) Subsea – ROV/str.	5	9	6	4
d) Dredging	7	12	11	8
e) Mining	12	21	14	10
f) Constr./earth moving	17	30	18	13
g) Specialized mach.	5	9	5	4
h) Steel and paper	5	9	5	4
i) Other	6	10	6	4

with 30 (52%), 19 (33%) and 17 (30%) respondents involved, respectively, of 58 in total. In total, responses from 9 different segments were collected where 58 respondents have given 139 responses and confirming activity with expanding pins in a total of 106 times in various and

repeating segments, which indicates that each respondent has activity in an average of 1.83 segments, and is involved in an average of 2.4 different types of equipment within the selected 9 segments.

Within the “Offshore Oil&Gas” segment, which is the biggest segment, the equipment that mostly apply expanding pins are the “Drilling and pipe handling equipment” and “Offshore cranes” (Fig. 9 (a)), with 40% and 50%, respectively, of the total responses. The Norwegian based companies represent here 62% of all the segment a) responses, and specifically for the “Offshore cranes” 67%. The segment relative reaction rates for the Norwegian companies and the non-Norwegian for the segment a) are then 1.22 and 0.74, respectively, see Table 4.

For the second biggest, segment “Maritime-ships” (Fig. 9(b)), “Maritime cranes” and “A-frames” are the main equipment types for these pins, with 44% and 25% of the total responses, respectively. The segment b) relative reaction rates for this segment for the Norwegian companies and the others are 1.54 and 0.35, respectively, see Table 4. The Norwegian based companies represent here 88% of all the responses, and for “Maritime cranes” 93%, and with high participation also in the other types of equipment.

In the case of the third biggest segments, i.e. “Construction and earth moving – onshore”, expanding pins technology is mostly applied in “Vehicles” category with 56% proportion relative to the total in the segment. For this category, over 9 of 10 responses are from the Norwegian companies. The segment f) relative reaction rates for this segment for the Norwegian companies and the non-Norwegians are 1.72 and 0.13, respectively (Table 4). The different responders have different length of experience with expanding pin solutions, where the experience of Norwegian companies dominate the statistics followed by Scottish and

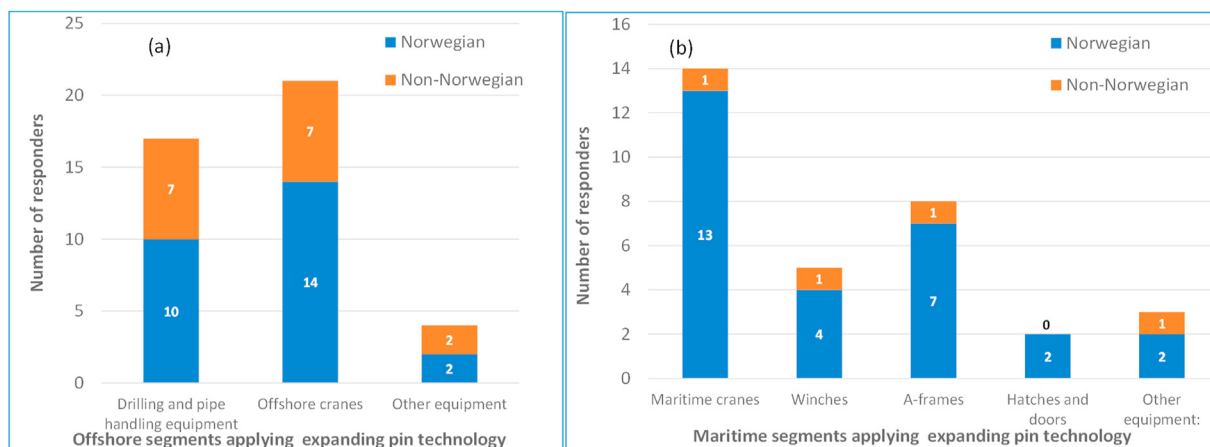


Fig. 9. Overview of respondents that apply expanding pins in (a) Offshore and (b) Maritime segments.

Table 8
Experience with expanding pin solutions.

		Norway	Scotland	Sweden	Total excl. Norway	Total Survey
		No (%)	No (%)	No (%)	No (%)	No (%)
Total		39 (100)	6 (100)	5 (100)	19 (100)	58 (100)
[years]	<1	1 (3)	0 (0)	0 (0)	0 (0)	1 (2)
	1–10	14 (36)	2 (33)	3 (60)	9 (47)	23 (40)
	>10	23 (59)	4 (67)	2 (40)	10 (53)	33 (57)
	Others	1 (3)	0 (0)	0 (0)	0 (0)	1 (2)

Swedish companies (Table 8). The survey shows also that a majority of the Norwegian companies have more than 10 years of experience in using the expanding pin solutions.

The remaining segments have lower numbers of responses, from 5 to 12 each, see Table 7. For three of these segments, namely “Subsea (ROV and structure)”, “Dredging (sea, lakes, and rivers)” and “Specialized machines and equipment” segments, only Norwegian responders were received with applications in cranes and A-frames as important equipment. The segment that is reported to have least application includes industries and equipment not included in the previous segments, NASA launch vehicles, special equipment for the metal industry, etc.

The relative reaction rates for the “Offshore Oil&Gas” segment, 1.22 and 0.74, indicate that there is a difference in the response willingness between the Norwegian based companies and the others, with 66% higher for the Norwegian companies. This could be explained by the fact that the national Norwegian and foreign Oil & Gas industry have known and applied the expanding pin technology for years. A slightly higher score from the Norwegian companies is logical since this doctoral research is being performed and supported by the company which introduced the technology into the national Norwegian oil and gas offshore market. The corresponding rates for the Maritime/ships segment, 1.54 and 0.35, are much more distant in values, with a corresponding willingness of 342% higher for the Norwegian companies. The Bondura company has delivered expanding pin systems to various bigger OEMs within the Norwegian maritime sector for the last 20–25 years, but only in minor scale to any foreign company within the same sector. This could possibly explain the huge difference in the segment relative reaction rates, for this specific segment.

The source of expanding pins for all companies is given in Table 9. Most of the respondents use an external source for expanding pins, 54 of 62, or 87%. The remaining 8 (13%) are in one way or another using their own designs for some or all of their equipment. For the Norwegian respondents 6 out of 42 (14%) claim that they apply their own designs, rather than solutions from external sources, and for the other companies the numbers are 2 out of 20 (10%). 75% of the companies applying their own expanding pin design are coming from Norway, compared to 25% from the other countries. Of all the 8 companies applying their own expanding pin design 6 (75%) belong to the bigger size, having over 100 employees, and 6 (75%) of them have worked with expanding pins for

Table 9
Expanding pin source.

Alternatives	Are the expanding pins you are using your own design, or from others?							
	Total survey		Survey excl. Norway			Survey Norway		
	No.	%-tot.	No.	%-tot.	%-alt.	No.	%-tot.	%-alt.
Total	62	100	20	100	32	42	100	68
Company’s own design for own products	8	13	2	10	25	6	14	75
From external supplier	54	87	18	90	33	36	86	67

over 10 years, 4 (50%) of the companies belonging to both groups; being big with long experience. The 8 companies work mainly in “Offshore”, “Maritime” and “Construction & Earth moving” segments, with 3, 4 and 4 companies involved, respectively.

4.4. Effects and consequences of applying expanding pin technology

The main objective of this survey is to investigate the effects and consequences of applying expanding pin solutions based on survey questionnaire divided into 20 questions with various response alternatives. The response rates for the Norwegian-based companies vs the other companies for all the questions in this section (6) are also evaluated, which resulted in an average rate of 65% and 35% respectively, out of 851 responses in total. The section relative reaction rates for this section are the same as for the over-all reaction rates for the survey, with of 1.23 for the Norwegian and 0.72 for the non-Norwegian companies.

As can be observed from Table 10, the main reason why the responders are choosing expanding pin systems is based on previous experiences (Q2) and that the pins come with the equipment (Q4) with 51% and 22% proportion of the total survey, respectively. The non-Norwegian companies have the strongest relationship between previous experience and the reason for choice of pins, with 58%. The Service & Maintenance company profile is the one where most responders are confirming the previous experience as the main reason for continue choosing expanding pins, with 20 of the 32, and 8 of those companies with more than 100 employees and 10 having more than 10 years of experience with expanding pins, independent of geographical location. Some responders (13%) state that pressure from their own clients have been the reason for choosing the expanding pins solution.

Where Q1 – It is a strong wish or requirement from our clients; Q2 – It is based on our own previous experience, Q3 – It is new for us and we want to test it, Q4 – The pins come with the equipment when we receive it and “Other reasons” - [(1) When it is urgent, but line boring is preferred if possible (2) When play is a problem and the alternative is line boring, (3) Aftermarket and repair jobs].

The importance of installation and retrieval time is valued differently between the two groups of companies, Norwegian and non-Norwegian. Around 67% of the Norwegian responders are of the opinion that installation and retrieval time is Important or Crucial and decisive, but for the non-Norwegian companies the number is close to 90%. The actual experiences of installation and retrieval time with expanding pins compared to standard pins are shown in Fig. 10. From the 11 responders claiming to have longer installation time with expanding pins, 6 belong to both “>100 employees” and “>10 years of experience with expanding pins”, and for retrieval time the corresponding numbers are 12 and 5 responders.

In total 44% confirm that Installation time is reduced by use of expanding pins, and for Retrieval time the number is 58%, with a slightly higher score for the non-Norwegian companies on Retrieval time, with 65%.

Table 10
Why choose expanding pins.

Alternatives	What is the reason for your company to choose or work with expanding pin technology?							
	Total survey		Survey excl. Norway			Survey Norway		
	No.	%-tot.	No.	%-tot.	%-alt.	No.	%-tot.	%-alt.
Total:	63	100	19	100	30	44	100	70
Q1	8	13	1	5	13	7	16	88
Q2	32	51	11	58	34	21	48	66
Q3	6	10	2	11	33	4	9	67
Q4	14	22	5	26	36	9	20	64
Other reasons:	3	5	0	0	0	3	7	100

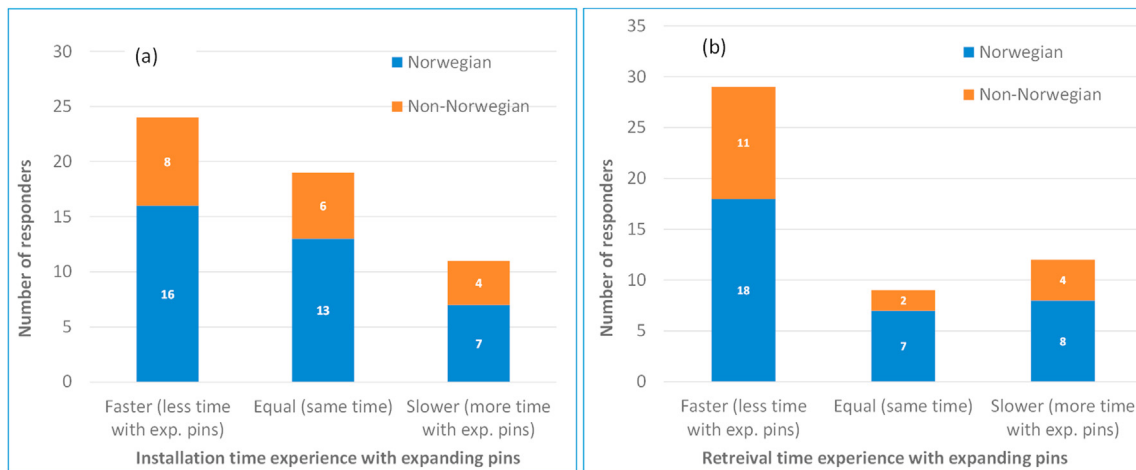


Fig. 10. Number of responders on (a) Installation time, and (b) Retrieval time.

The importance of avoiding breakage damage is highly valued by all respondents in the survey, except one, with 45% indicating that it is of “Crucial and decisive” importance. The actual experiences of tear, wear and breakage damages with expanding pins compared to standard pins are shown in Fig. 11. The study clearly shows an experienced improvement both for tear & wear and breakage problems when using expanding pin instead of standard cylindrical ones. 68% of the non-Norwegian companies claim less tear and wear issues with expanding pins, and for the Norwegian companies 59% claim the same. For breakage issues the comparative figures are 71% and 38%, showing a clearly better experience for the non-Norwegian companies. From the 12 non-Norwegian companies with experience of less breakage issues with expanding pins, 7 (58%) have more than 10 years of experience, and 6 (50%) work within the Offshore Oil&Gas industry.

Expanding pins with locking capability to bearing in addition to the supports are called Dual pins. The survey shows that only a minority of the respondents, 14%, have used that specific design, mainly because many have no need for it, or no knowledge of the design. Those who had some experience with Dual pins reported “More efficient machine or equipment” and “Longer lifetime of bearing” as the advantages.

The importance of applying safe pin solutions is highly valued by most respondents, except from two. The non-Norwegian companies have a higher score on “Crucial and decisive” than the Norwegian, with 47% vs 31%, respectively (Fig. 12 (a)). Half of the respondents believe the expanding pin solution is as safe as a standard pin, for personnel and

equipment, and 47% experience a higher level of safety (Fig. 12 (b)). The non-Norwegian companies value the expanding pin solutions as much safer than the standard solution, compared to the Norwegian, with 60% and 39%, respectively.

Those who have experienced the expanding pin solutions as safer than a standard solution have indicated their reasons as shown in Table 11. From a safety point of view for the total survey, it is highly valued that the expanding pin solution does not need sledgehammering to enter the joint (43%), together with the easiness to be retrieved when required (28%). However, there are considerable variations between the Norwegian and non-Norwegian companies, with 33% and 63% for sledgehammering and 33% and 19% for easiness of retrieval, respectively. Where Q1 - No need for sledgehammering to get the expanding pin into the joint; Q2 - No relative movements between expanding pin and supports during service/operation; Q3 - Less chance for breakage of pin during service/operation and Q4 - Easy and fast to retrieve when required.

As can be observed from Table 12, the responders confirm that they observe a number of advantages by using expanding pins compared to standard cylindrical pins, and without major differences between the Norwegian and non-Norwegian based companies. The most important advantages with expanding pins are “Less, or no wear”, “Reduced unwanted downtime”, “Longer lifetime on equipment”, and “Reduced planned downtime”, with 24%, 23%, 23% and 20%, respectively.

Where Q1 - Reduced unwanted downtime on production with expanding pins; Q2 - Reduced number and length of planned downtime

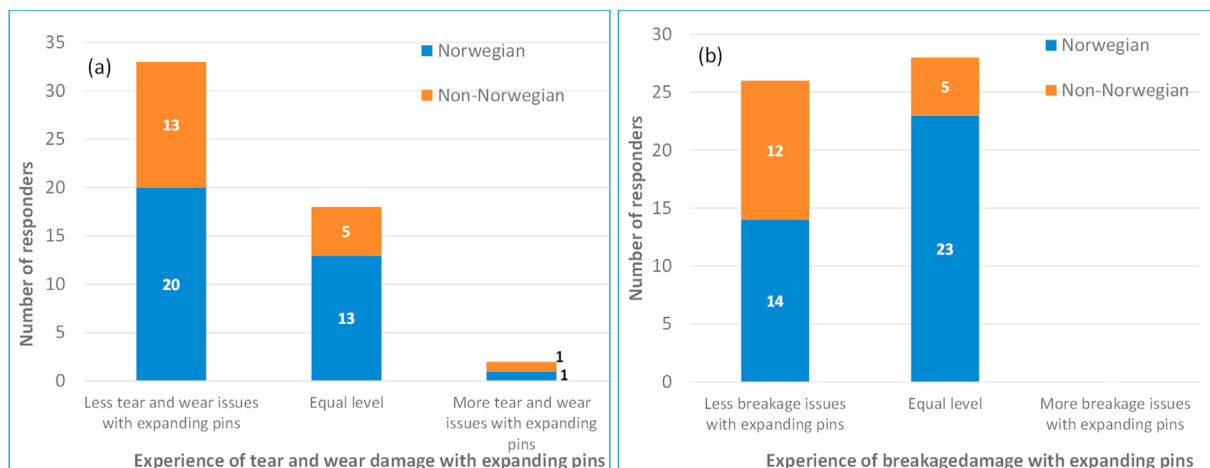


Fig. 11. Number of responders on (a) tear and wear damage, and (b) breaking damage.

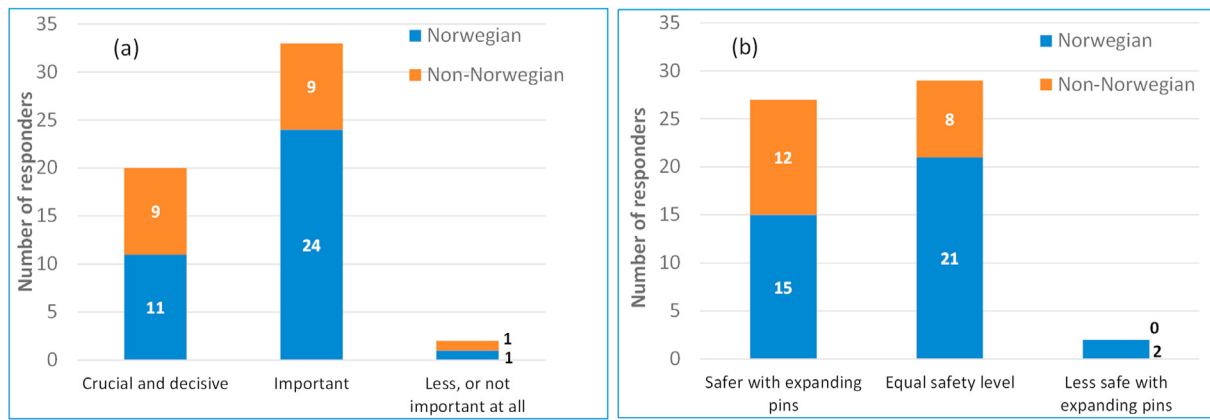


Fig. 12. (a) Importance of safe pin solution, and (b) Safety for personnel and equipment.

Table 11 Comparison of safety of expanding pins with standard pins.

Alternatives	If you marked expanding pins as safer than standard cylindrical pins in the previous question, why?							
	Total survey		Survey excl. Norway			Survey Norway		
	No.	%-tot.	No.	%-tot.	%-alt.	No.	%-tot.	%-alt.
Total	46	100	16	100	35	30	100	65
Q1	20	43	10	63	50	10	33	50
Q2	5	11	2	13	40	3	10	60
Q3	6	13	0	0	0	6	20	100
Q4	13	28	3	19	23	10	33	77
Other reasons	2	4	1	6	50	1	3	50

Table 12 Other effects and consequences.

Alternatives	Which other effects and consequences do you see for the equipment and machines in relation with repair, service, and operation, when using expanding pin solutions instead of standard cylindrical pins?							
	Total survey		Survey excl. Norway			Survey Norway		
	No.	%-tot.	No.	%-tot.	%-alt.	No.	%-tot.	%-alt.
Total	114	100	49	100	43	65	100	57
Q1	26	23	10	20	38	16	25	62
Q2	23	20	11	22	48	12	18	52
Q3	27	24	12	24	44	15	23	56
Q4	6	5	3	6	50	3	5	50
Q5	26	23	11	22	42	15	23	58
Q6	6	5	2	4	33	4	6	67

for service; Q3 - Less or no wear damage on expanding pins and supports; Q4 - Reduced corrosion on expanding pins; Q5 - Longer lifetime of equipment and machines, with expanding pins and Q6 - We don't see any specific advantages with expanding pins.

Fig. 13 shows the economic impact that the use of expanding pins may have on the responders' companies, instead of applying standard cylindrical pin solutions. The responses show that 85% of responders confirm the importance to be "Crucial and decisive" or "Important". The non-Norwegians have a clearly higher score on "Crucial and decisive" than the Norwegians with 39% vs 12%, but for "Important" it is the opposite with 39% vs 76%, respectively. At the same time, it can be noted that a relatively higher number of non-Norwegian based companies value the expanding pin solution as "Less, or not important at all", compared to the Norwegians, with 22% and 12%, respectively.

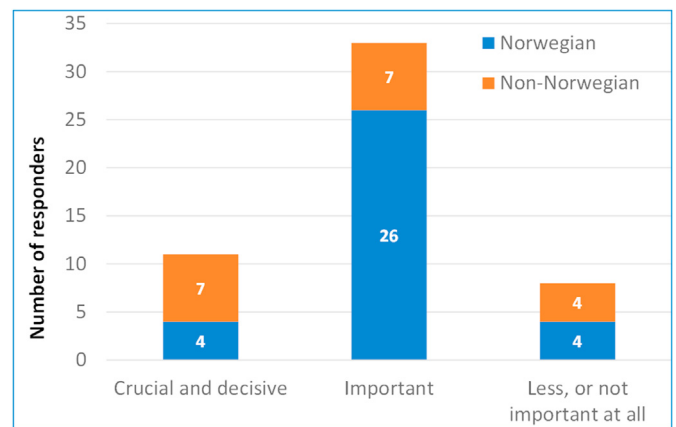


Fig. 13. Economic impact of expanding pins compared to standard pins.

5. Conclusion

In this questionnaire-based study, a total of 256 potential respondents received the questionnaire, divided into 140 Norwegian based companies, and 116 non-Norwegian. In total 58 responded, divided into 39 Norwegian based companies, and 19 non-Norwegian, with an over-all response rate of 23%, and the Norwegian based companies had a considerable higher willingness to respond, compared to the non-Norwegian based. Though not easy to conclude, it is assumed that the long and strong relationship between Bondura and the Norwegian Offshore Oil&Gas industry and Maritime sector might have influence on the willingness to respond, in addition to the participation of The University of Stavanger and The Norwegian Research Council.

Most of the respondents apply an external source for expanding pins, but 8 of the 62 responses from the 58 respondents confirm using their own design, where half of them belong to companies with more than 100 employees and having more than 10 years of experience with expanding pins. This leads us to conclude that bigger companies with long experience with the expanding pin technology have got the economic interest and self-confidence to go for their own designs, exposed to possible situations with infringements to the pin supplier companies' IP rights.

For over half of the responders, the main reason to apply expanding pin technology is because of previous experience. This can be understood that the previous experiences have been good experiences, and it can also be seen that the non-Norwegian based companies put higher value to the experience with expanding pin systems than the Norwegians. At the same time, the number of Norwegian companies who choose expanding pins is due to requirements from their own customers is three times higher, compared to the non-Norwegians. This difference can partly explain by

the market activities taken by companies like Bondura during years, to make the Norwegian OEMs' customers push the OEMs to include expanding pin technology into their products.

The responders indicate that the time required for installation and retrieval of pins, in general, is of high importance for their business and activities. Almost 90% of the non-Norwegian companies define this consumed time as "Important" or "Crucial and decisive", but only 2/3 of the Norwegian companies do the same. The majority, or 2/3, of the Norwegian companies consider the installation and retrieval time to be of less or no importance belongs to the Service & Maintenance profile, with the same share for companies having more than 10 years of experience with expanding pins, and 1/3 belonging to both groups. It is not clear why some respondents mean that the installation and retrieval time is not important, but normally the well-established Service & Maintenance companies make more business when the jobs last longer.

A majority of the responders experience that the retrieval time for expanding pins is shorter than for standard cylindrical pins, with a higher score for the non-Norwegian companies, where the majority of those have more than 100 employees and more than 10 years of experience with expanding pins. Both Norwegian and non-Norwegian companies state that there are less tear, wear and breakage issues with expanding pins and supports, compared to standard pins, where the non-Norwegian companies have the most positive experiences.

Almost all the respondents agree on the importance of having a pin solution that is safe for personnel and equipment. On the other hand, about half of the non-Norwegian companies and less than a third of Norwegian companies define it as "Crucial and decisive", only. The main reason that the expanding pin solution is safer than the standard pins is because it does not need sledgehammering to get the expanding pin into the joint. Around 90% of the Norwegian and the non-Norwegian companies agree that the use of expanding pin solutions instead of standard cylindrical pins, will reduce downtime (unwanted and planned), reduced wear damage and increase lifetime of equipment and machines. Furthermore, almost all the responders agree about the importance of the economic effects of using expanding pin systems, while only around 15% see no specific importance. The non-Norwegian companies have over three times higher score than the Norwegian ones on stating the economic effects as "Crucial and decisive".

Summarizing all, it becomes clear that a majority of the respondents have a positive experience with, or an excellent perception of expanding pin systems, when it comes to installation, operation, retrieval, safety for personnel and equipment, and economic advantages for their company and clients. There could be some sources for errors or uncertainties in this survey;

- Point of time of recollecting information regarding the global covid-19 situation.
- For the segment relative reaction rates, the segment responses are applied, and the total potential responders, not the segment potential responders.

Credit author statement

Ø. Karlsen: Conceptualization, Methodology, Investigation, Writing—original draft; H.G. Lemu: Supervision, Visualization, Resources, Writing – Reviewing and Editing, Project administration, Validation. All authors have read and agreed on the final version of the manuscript.

Funding

This research is conducted under the Industrial PhD funding provided by the Research Council of Norway and the company Bondura Technologies AS, Grant nr. 283821.

Declaration of competing interest

The authors declare that they have no known competing financial interests or personal relationships that could have appeared to influence the work reported in this paper.

Acknowledgements

The authors gratefully acknowledge the financial support provided by the Research Council of Norway and Bondura Technologies AS. The authors would like to thank the companies and individuals who provided feedback on the conducted survey.

References

- [1] Ø. Karlsen, H.G. Lemu, Fretting fatigue and wear of mechanical joints, *Literature study*, IOP Conf. Ser. Mater. Sci. Eng. 700 (2019).
- [2] Bondura, «Bondura technology,» Bondura technology, [online]. Available: [Last accessed: 23 March 2020, <https://www.bondura.no>.
- [3] I. Berkani, Ø. Karlsen, H.G. Lemu, Experimental and numerical study of Bondura® 6.6 PIN joints, IOP Conf. Ser. Mater. Sci. Eng. 276 (2017).
- [4] Nord-lock, «Nord-Lock,» [online]. Available: [Last accessed: 13 July 2020, www.nord-lock.com.
- [5] S. Ahmed, X.-C. Gu, Accident-based FMECA study of marine boiler for risk prioritization using fuzzy expert system, *Results Eng* 6 (2020) 100123.
- [6] A.R. Prabowo, D.M. Bae, Environmental risk of maritime territory subjected to accidental phenomena: correlation of oil spill and ship grounding in the Exxon Valdez's case, *Results Eng* 4 (2019) 100035.
- [7] C.V. Haute, T. Pire, Maintenance intervals for MP-TP bolted connections – a case study, *Results Eng* 5 (2020) 100064.
- [8] S.A. Akintola, M. Oki, A.A. Aleem, A.A. Adedran, O.B. Akpor, O.M. Oluba, B.T. Ogunsemi, P.P. Ikubanni, Valorized chicken feather as corrosion inhibitor for mild steel in drilling mud, *Results Eng* 4 (2019) 100026.
- [9] Eurocode, «eurocode,» [online]. Available: [Last accessed: 03 August 2020, <https://eurocodeapplied.com/design/en1993/steel-design-properties>.
- [10] ArcelorMittal, «ArcelorMittal,» [online]. Available at: [Last accessed: 03 August 2020, <https://constructalia.arcelormittal.com/en/steel-grades/s420>.
- [11] Astrup, «astrup,» [online]. Available; Last accessed: 03 August 2020, <https://astrup.no/Materialer-Produkter/Materialer/Specialstaal/Rundstaal>.
- [12] L.C. Brezeanu, Contact stresses: analysis by finite element method (FEM), *INTER-ENG* 2013, *Procedia Technol* 12 (2014) 401–410.
- [13] P. Purushothaman, P. Thankachan, Hertz contact stress analysis and validation using Finite Element Analysis, *Int. J. Res. Appl. Sci. Eng. Technol.* 2 (XI) (2014) 531–538.
- [14] R. Gutkin, B. Alfredsson, Growth of fretting fatigue cracks in a shrink-fitted joint subjected to rotating bending, *Eng. Fail. Anal.* 15 (5) (2008) 582–596.
- [15] C.E. Truman, J.D. Booker, Analysis of a shrink-fit failure on a gear hub/shaft assembly, *Eng. Fail. Anal.* 14 (4) (2006) 557–572.
- [16] W.J. Grant, Shrink fitting, *Cryogenics* 12 (4) (1972) 328–333.
- [17] M. MacMillan, J.L. Hendry, A. Woolley, M.J. Pavier, Measurement of partial slip at the interface of a shrink fit assembly under axial load, *Exp. Mech.* 58 (2018) 407–415.
- [18] A. Mouaa, N.E. Laghzale, A.-H. Bouzid, Elastic-plastic stresses in shrink fit with a solid shaft, *MATEC Web Conf* 286 (2019), 02001.
- [19] E. Toma, Optimization of rotor shaft shrink fit method for motor using "Robust design", *J. Ind. Eng. Int.* 14 (2018) 705–717.
- [20] T.N. Chakherlou, M. Mirzajanzadeh, B. Abazadeh, K. Saeedi, An investigation about interference fit effect on improving fatigue life of a holed, *Eur. J. Mech. Solid.* 29 (4) (2010) 675–682.
- [21] Z. Murcinková, P. Baron y, M. Pollák, Study of the press fit bearing-shaft joint dimensional parameters by analytical and numerical approach, *Ann. Mater. Sci. Eng. (2-a)* (2018) 1–10, 2018.
- [22] A. Strozzi, E. Bertocchi, A. Baldini, S. Mantovani, Normalization of the stress concentrations at the rounded edges of an interference fit between a solid shaft subjected to bending and a hub, *Mech. Base. Des. Struct. Mach.* 44 (4) (2016) 405–425.
- [23] D.H. Lee, S.J. Kwon, J.B. Choi, Y.J. Kim, Observations of fatigue damage in the press-fitted shaft under bending loads, *Key Eng. Mater.* 326–328 (2006) 1071–1074.
- [24] C. Song, M.X. Shen, X.F. Lin, D.W. Liu, M.H. Zhu, An investigation on rotatory bending fretting fatigue damage of railway axles, *Fatig. Fract. Eng. Mater. Struct.* 37 (1) (2014) 72–84.
- [25] I. 2768, «ISO 2768 general tolerances,» [online]. Available: [Last accessed: 13 July 2020, https://www.iso.org/search.html?q=iso%202768%20general&hPP=10&idx=all_en&p=0&hFR%5Bcategory%5D%5B0%5D=standard.

Appended Paper II

An investigation of the effects and consequences combining expanding dual pin with radial spherical plain bearings

KARLSEN, Ø.; LEMU, H. G.; BERKANI, I.

Applied Mechanics, 2022, vol. 3, no 2, p. 573-589.

<https://doi.org/10.3390/applmech3020034>



Article

An Investigation of the Effects and Consequences of Combining Expanding Dual Pin with Radial Spherical Plain Bearings

Øyvind Karlsen ^{1,2,*}, Hirpa G. Lemu ^{1,*} and Imad Berkani ²¹ Faculty of Science and Technology, University of Stavanger, 4021 Stavanger, Norway² Bondura Technology AS, 4340 Bryne, Norway; imad@bondura.no

* Correspondence: oyvind.karlsen@uis.no or oyvind@bondura.no (Ø.K.); hirpa.g.lemu@uis.no (H.G.L.)

Abstract: An expanding pin locks the pin assembly to its supports and bearings and prevents any relative movements between the surfaces in contact. In this study, the diameter changes of the bearing inner ring as a function of the expanding pin's tightening torque were studied. In addition, the required rotational moment of a set of complete bearings locked to an expanding pin solution was studied by exposing the assembly to a combination of an increasing radially outwards directed load from the bolt torquing and a radially external inwards directed load from a hydraulic jack. The bearings were of type Radial Spherical Plain Bearings (RSPBs), GE 80 ES, steel/steel, and loaded externally up to their maximum dynamic limit of 400 kN. The results indicate a major reduction in the required rotation moment of the bearing when the bearing inner ring is expanded by use of an expanding pin. The reduction of rotation moment indicates reduced contact pressure and friction force between the two bearing rings, which ultimately can have a reduced effect on ring surface wear and a positive effect on the bearing operational lifetime.

Keywords: expanding pin; dual pin; radial load; bearing capacity; spherical bearing; bearing wear; bearing lifetime



Citation: Karlsen, Ø.; Lemu, H.G.; Berkani, I. An Investigation of the Effects and Consequences of Combining Expanding Dual Pin with Radial Spherical Plain Bearings. *Appl. Mech.* **2022**, *3*, 573–589. <https://doi.org/10.3390/applmech3020034>

Received: 28 March 2022

Accepted: 6 May 2022

Published: 10 May 2022

Publisher's Note: MDPI stays neutral with regard to jurisdictional claims in published maps and institutional affiliations.



Copyright: © 2022 by the authors. Licensee MDPI, Basel, Switzerland. This article is an open access article distributed under the terms and conditions of the Creative Commons Attribution (CC BY) license (<https://creativecommons.org/licenses/by/4.0/>).

1. Introduction

A moveable joint will often contain minimum two counterparts that turn relative to each other, ideally around a center line in common. The joint can have a female part, a fork, and a male part, together with typically a bearing. Moveable joints are in use in uncountable numbers of different applications, in most industries globally and many different machines and mechanical equipment [1]. In addition, bearings are used in static joints in civil engineering and constructions. By applying a moveable joint, it is possible to transfer heavy loads of any equipment from one position to another or turn rotational movements into axial directional movements [2]. The moveable joints in general can be found in many well-known and familiar tools and furniture, like scissors, garden shears, and rotating chairs, as well as in more industrialized tools, equipment, and machines. Efficient, safe, and well-working moveable joints are indispensable in most industrial equipment and machines such as offshore and onshore cranes, drilling and pipe handling equipment, excavators, dumper trucks and other vehicles for earth moving, windmill systems, flood control gate ports, and even launch platforms for spaceships and rockets. [3]. In addition to the two counterparts that turn relative to each other [4], a third component is required to make a joint moveable, which could be a pin connection with female and male parts as shown in Figure 1a,b. The pin in a moveable joint can be of many different designs, with different advantages or disadvantages. In general, it is an advantage to have as tight tolerance as possible between the pin and the female part (supports), and against the male part during operation of the machine, to avoid any unwanted movements of a cylindrical pin (Figure 1c), which can result in mechanical wear and increased play. At the same time, it is an advantage to have wider tolerances [5] during installation and retrieval

of the pin, to avoid the pin getting stuck in the supports. The different pin designs value differently the tightness of the tolerance, either very tight to increase the quality of the joint during operation, or less tight to ease installation and retrieval of pins. It is common to lubricate the pin and the bore inner surface to reduce friction between surfaces in contact for installation and retrieval purposes [5] and to protect against oxidation, but it is not always required. Such lubrication is typically made of petroleum hydrocarbon distillate with additives to get the specific and required properties.

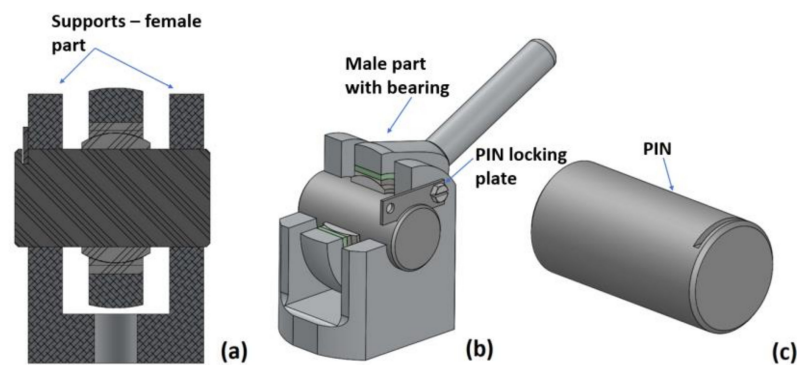


Figure 1. Pin joint illustrated as: (a) cross-sectional view, (b) isometric view, and (c) a cylindrical pin.

The aim of the study reported in this paper is to investigate the effects and consequences of locking an expanding bondura[®] Dual Pin (Bondura Technology AS, Bryne, Norway) to the inner ring of a Radial Spherical Plain Bearing (RSPB) and compare that with the use of a standard cylindrical pin, for both dry and lubricated contact surfaces. As part of the experimental work, the bearing inner ring is separated from the outer ring and loaded separately with a pressure load acting radially outwards, and its deformations are measured by a Coordinate-Measuring Machine (CMM) to find the relationship between the radial load and the corresponding ring deformation. In addition, the complete bearing with lubricated internal surfaces was installed on a Dual pin and then loaded stepwise with combinations of radial outward force from the expanding sleeve and external inwards radial load representing operational loads. The assembly was then forced to turn, and the required static moment at the exact moment of turning was observed.

2. Literature Review

Traditionally, mechanical joints for load transfer are designed with interference fitting such as shrink fitting and press fitting or using standard cylindrical pins, while expanding pin solutions are more innovative solutions with wide installation tolerances.

Shrink fitting [6] is a method to shrink a slightly oversized pin, by cooling it down with frozen nitrogen, and introduce it into the joint and let it expand back to its normal temperature, at which the interference fit is produced with the contacting support bore surfaces. This solution has a wider installation tolerance and zero operational tolerance between the surfaces in contact. Shrink fitting as a method for joining two mechanical parts has been investigated over many years, e.g., McMillan et al. [7] studied the slip between a hub and a shaft in a shrink-fit assembly subjected to axial load, and Mouaa et al. [8] reported an analytical methodology to analyze the elastic-plastic stresses in a shrink fit with a solid shaft.

Press fitting is another method of interference fitting where a slightly oversized pin is assembled into the female part by applying an axial external load. In this method, the pin is forced into correct position in the joint, reaching the interference fit with the contacting surfaces. This solution has negative/zero installation tolerance and zero operational tolerance, and the performance of this method has been studied both numerically, analytically, and experimentally over the years [9,10].

The most common solution is using a *standard cylindrical pin joint*, where a massive cylindrical dowel pin with a wide enough installation tolerance is used to install the pin without interference. This solution has a wider installation tolerance, which also is the operational tolerance and is often provided with a locking plate installed to prevent the pin from falling out over time.

The *expanding pin solution* [11,12] is less known but combines the wide installation tolerance from the standard pin solution, and often even wider, with the zero operational tolerance from the shrink fit and press fit solutions. There is a variety of different expanding pin solutions depending on the issues to be addressed, where most of them can expand to zero operational tolerance against the supports. The dual pin solution [11], however, expands in addition against the bearing, to a zero operational tolerance. The operational and damage mechanisms and the advantages of this solution are not sufficiently addressed in the literature. In the recent works of the authors, however, some research results have been reported. For instance, the expanding pin solution, as a part of a mechanical joint, has been compared to other known joint models and modelling techniques, by Karlsen and Lemu [13,14], with focus on the damage mechanisms that can occur in various connections of mechanical systems, typically such as fretting wear, fretting corrosion, and fretting fatigue. In addition, Akhtar et al. [15] reported a study on the capacities of a pin with the combination of radially expanding and axially pre-load capabilities, typically for huge flange systems. Berkani et al. [16] performed an experimental and numerical study of expanding pins with the aim of knowing more about the relation between the tightening torque and stresses generated at the contact surfaces, in addition to the effects of variations in temperature over time.

Öztürk et al. [17] performed an experimental test to determine the coefficient of static friction (COFs) for RSPBs, for polyoxymethylene (POM)/steel contact surfaces. The bearing was exposed to increasing external radial inwards directed load, and the bearing inner ring was turned relative to the outer ring and the COFs values calculated. They concluded that whereas the static friction force increased with increasing normal force, the coefficient of static friction decreased until it stabilized. Zhao et al. [18] investigated failure behaviors of RSPB joints for use in civil engineering applications, and the main findings were brittle fracture of the inner ring and brittle crack of the outer ring under uniaxial radial load, when the pin shaft bent due to overload. Under such loading conditions, the inner ring would have pressure from the outer ring at a limited width around its center line, due to difference in outer ring inner diameter and inner ring outer diameter, but reduced or missing support from the pin shaft around the same center line, due to the bending of the pin. This will result in bending of the inner ring and additional stresses and finally brittle fracture of the edges. Sun et al. [19] studied the use of RSPBs in joints in a space truss structure, subjected to tension and compression, to verify the bearing's mechanical properties and reliability. Fang et al. [20] developed a theoretical solution and a numerical model for conformal contact pressure and free-edge effects in spherical plain bearings, which varies with the bearing clearance and external load.

In the global market, only a few companies produce expanding pin solutions, and to the authors' knowledge, only one company produces the double sets of expanding sleeves, called Dual pins, for locking a second set of expanding sleeves to the bearing. The stakeholders' opinions, experiences, and the use of expanding pins on the global arena have been investigated by Karlsen and Lemu [21,22].

2.1. Expanding Pins

A typical expanding pin assembly, illustrated in Figure 2, has (1) a load bearing pin with conically machined tapered ends, (2) conically machined end-sleeves to fit the tapered pin ends, and (3) end plates and tightening screws or nuts. In addition, the assembly can have lubrication channels, if required. When torquing the screws or nuts, the end-sleeve climbs on the tapered pin end and expands until reaching a zero tolerance between the sleeve and the support bore and produces then a wedge force. The contact pressure between

the support bore and the sleeve, and between the sleeve and the pin, prevents the pin assembly from rotating or displacing axially and thereby prevents any unwanted surface wear, ovality issues, etc. The Dual expanding pin can produce a similar wedge lock against the bearing inner ring by a second inner set of expanding sleeves.

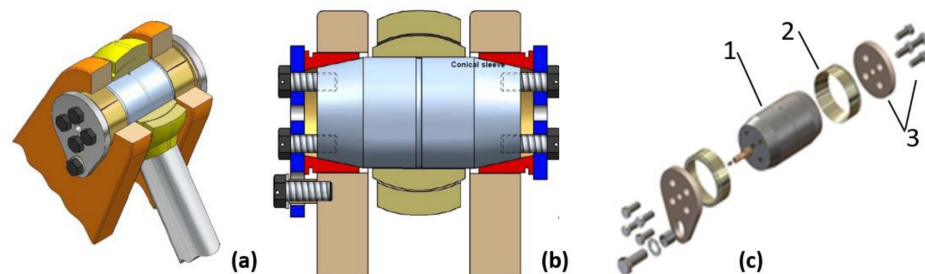


Figure 2. Expanding pin with single set of sleeves: (a) pin in joint, (b) cross-section view, and (c) exploded view.

2.2. Dual Expanding Pins

The Dual expanding pin solutions, illustrated in Figure 3, are applied in various types of industrial cranes offshore or onshore, ports, drilling and pipe handling equipment, rotating sheaves, amusement equipment, A-frames (Figure 3a), hatches on ships, flood dike gates, etc., and the pins often interact with bearings [11]. In such applications, the bearings can typically be of spherical plain or rolling type of bearings, with the latter divided into ball bearings and roller bearings. The inner sleeve expands towards the inner ring of the bearing but creates normally less contact pressure compared to what the outer sleeve does against the support bore. The contact pressure between the bearing and the expanding sleeve is enough to prevent the bearing inner ring from rotating but not high enough to disturb the bearing's function by expanding the inner ring and eliminate the bearing's radial inner production tolerance. Figure 3b illustrates a dual pin assembly, and Figure 3c illustrates a dual pin where one half is shown with an exploded view.

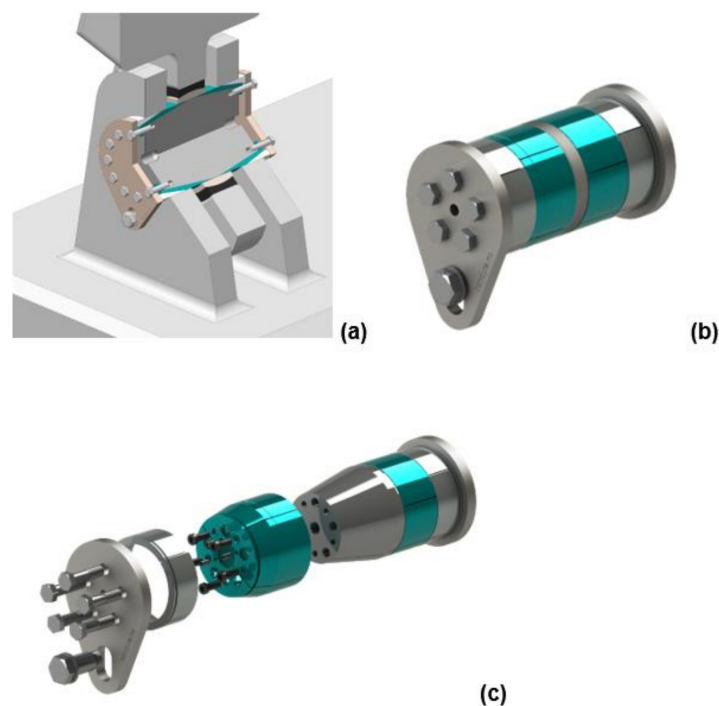


Figure 3. Dual expanding pin with two sets of sleeves: (a) pin in joint, (b) pin assembly and (c) exploded view.

3. Materials and Methods

To investigate the performance of the expanding pin solution, both experimental and analytical studies were conducted. The experiments were performed partly at University of Stavanger's (UiS) premises and partly at an external location.

3.1. Experimental Setup

The following two main experimental tests were conducted:

- (1) Test 1: tests of bearing inner rings installed on a dual expanding pin;
- (2) Test 2: tests of complete bearing assemblies installed on a dual expanding pin.

These tests are detailed in Table 1. Figures 4 and 5 show the test setups for the tests with the Dual Expanding Pin System for Test 1 and Test 2, respectively. For the experimental tests, the bearing inner rings were exposed to outwards radial expansion from an expanding pin solution, and the change of shape was measured by CMM (Zeiss, S/N 532083, Oberkochen, Germany) equipment to find the relation between the bolt tightening torque and the inner ring deformation, specifically the radial deformation.

Table 1. Test setup—pin ($\varnothing 80$ mm) and bearing combinations.

Bearing Type	Test No.	Number of Rings/Bearings
GE 80 ES (inner ring)	Test 1(a)	2/2
	Test 1(b)	1/2
GE 80 ES (complete)	Test 2(a)	0/4
	Test 2(b)	0/3

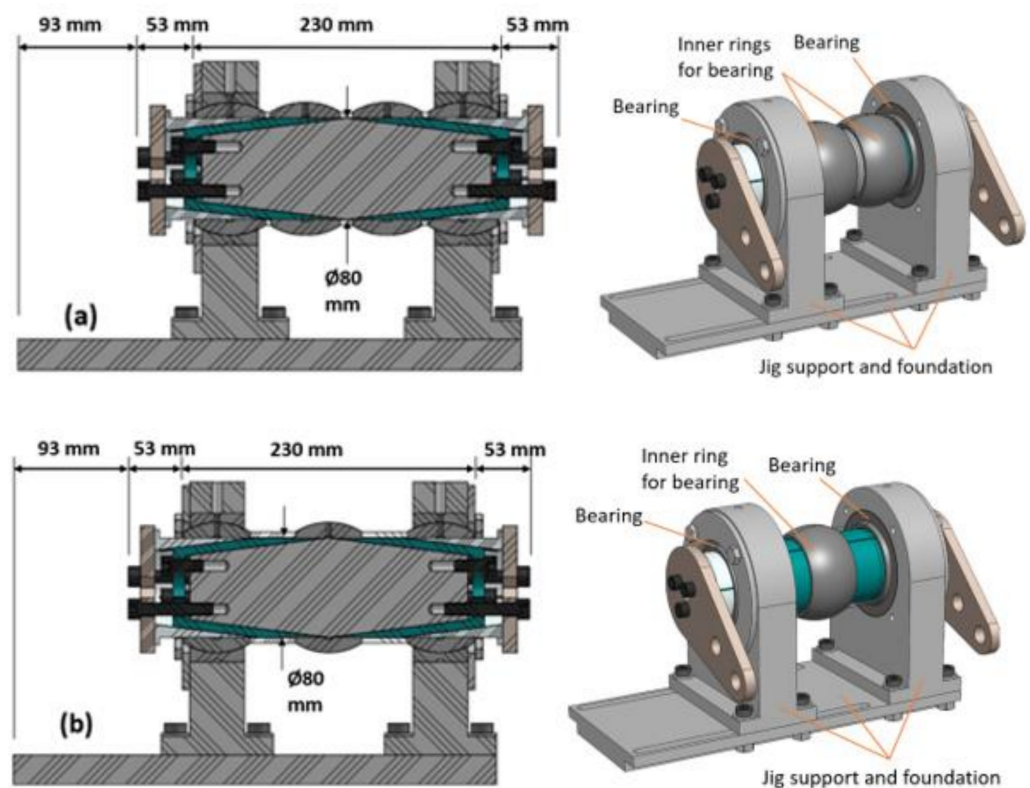


Figure 4. Test setup for Test 1: (a) Test 1a—cross sectional view (left) and isometric view with part names (right); (b) Test 1b—cross sectional view (left) and isometric view with part names (right).

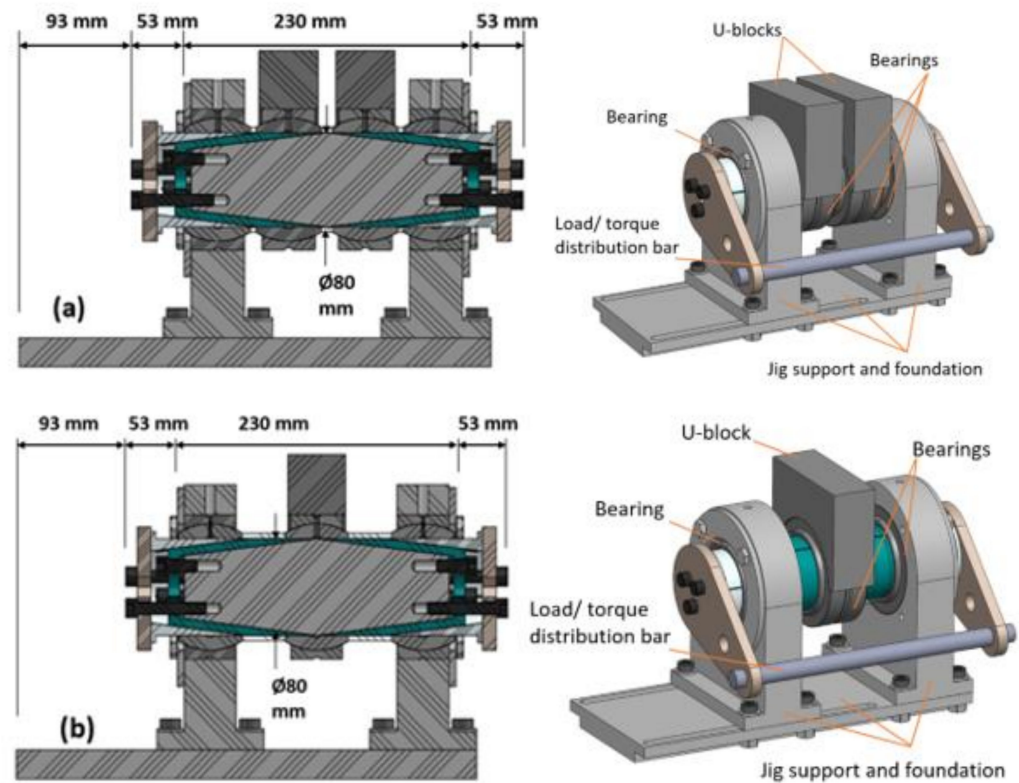


Figure 5. Test setup for Test 2: (a) Test 2a—cross sectional view (left) and view with isometric part names (right); (b) Test 2b—cross sectional view (left) and isometric view with part names (right).

The three tested inner rings were taken from the bearing SKF GE 80 ES (SKF AS, Oslo, Norway) [23] RSPBs with steel/steel surfaces and metric sizes. The complete bearing set was installed on an expanding pin solution in a test jig and loaded both radially outwards from the expanding pin, in combination with an external load from a 100 tons hydraulic load cylinder (Enerpac, S/N CLP1002E102, Ede, The Netherlands; Urdal Services AS, 4823 Nedenes, Norway). The fabric new bearing internal diameter clearance between the two rings is the range of 72–142 μm , measured perpendicular to the actual pin center axis. The required rotational moment was measured by hydraulically pushing the crossbar (Figure 5) with a 10 tons jack with a force traducer (HBM, S/N 3126849, Darmstadt, Germany) to measure the required load and investigate the effects of the two load combinations on the rotation of the bearings.

The tested GE ES bearings are made of high carbon bearing steel, typically EN 100Cr6/ISO 683-17 [24], through hardened (martensitic) to hardness 57 ± 2 (HRC), yield limit $R_{p0.2}$ of 2000 MPa, and phosphate treated surface, with Elasticity modulus of 210 GPa and Poisson's ratio of 0.3. The load bearing part of the expanding pin is made of 34CrNiMo6 + QT steel, with yield limit $R_{p0.2}$ of 1003 MPa, and ultimate R_m of 1096 MPa. The expanding inner and outer sleeves are made of 34CrNiMo6 + QT and S355J2 steel, respectively, and the latter sleeve is surface treated with yellow sink plating. The bearings are always internally lubricated to reduce contact friction and to avoid surface damages at the contacting surfaces.

By loading all 4 identical bearings in Test 2a under the same conditions and loads, the total required rotational moment for the assembly will be divided equally between the four bearings. When loading the single bearing in Test 2b, the required rotational moment generated by the two bearings in the supports are known from Test 2a, and the required rotational moment generated by the single bearing is easily calculated.

3.1.1. Bearing Inner Rings Loaded by the Expanding Dual Pin (Tests 1a and 1b)

The Tests 1a and 1b are performed on the inner rings only by introducing a radial outwards force from the expanding dual pin into the inner surface of each ring. The outward directed force is produced by torquing the tightening screws and subsequently pushing the sleeves to move axially and radially until producing a wedge force between the pin and the ring, as indicated in Figure 4. An increment of the screw torque results in an increment in the contact pressure between the sleeve and the inner ring, and the resulting ring dimension changes are measured using the CMM, which is a device that measures the 3D geometry of physical objects by sensing discrete points on the surface of the object with a probe. Various types of probes are used in different CMMs, including mechanical, optical, laser, and white light. The torque on the tightening screws is increased stepwise from zero to a maximum of 70 Nm. For each tightening step, the CMMs measure the ring surface at several points, at four defined cross-section locations, a, b, c and d, at locations -25 , -5 , $+5$, and $+25$ mm respectively, with the zero location at the bearing ring mid-point. For the Test 1a, two inner rings are supported onto one expanding pin sleeve each, giving a full contact surface, except from the lubrication channel with a width of 7.7 mm, towards the rings, as shown in Figure 6a. For the Test 1b, one inner ring is supported onto two separate expanding pin sleeves, giving partly contact surface at the mid-section, against the ring, as indicated in Figure 6b. In the latter test, the ring is not supported at its center part for a width of 12.1 mm, included the lubrication channel, due to distance between the two sleeve ends.

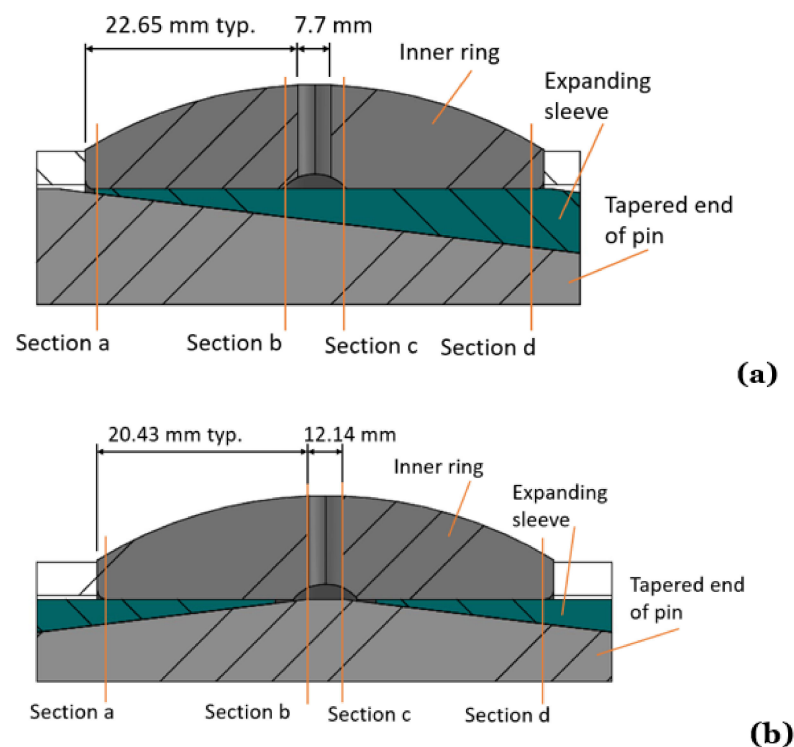


Figure 6. Ring, sleeve, and pin contact area: (a) full contact on single sleeve and (b) reduced contact at center on double sleeve.

These tests reveal how the inner ring of a complete bearing reacts and deforms when loaded by an expanding pin system, as in Test 2. Tests 1a and 1b are performed both with dry and lubricated (Molykote[®] P-74, Lindberg & Lund AS, Vestby, Norway) contact surfaces to investigate any effect on the expansion level of the rings, while the bearings in Tests 2a and 2b are performed with lubrication internally (of type SKF LGHB 2), with dry and clean expanding sleeves.

Tests 1a and 1b: The inner rings are separated from the outer rings and exposed directly to outwards radial expansion of the dual pin. One inner ring on one sleeve (Test 1a) and one inner ring on two sleeves (Test 1b). The inner ring deformations are measured by a CMM machine.

Tests 2a and 2b: Complete bearings are installed at the center part of the pin, with one additional bearing at each support. The bearings in the middle are exposed directly to combinations of internal radial tightening from the expanding pin and the external test load. The bearings at the supports are tightened up with the same expanding outwards force as the bearings in the middle.

3.1.2. Complete Bearings Loaded by the Expanding Dual Pin and External Load (Tests 2a and 2b)

The Test 2a involves 4 identical bearings of type SKF GE 80 ES in the same jig at the same time (Reference Figure 5). One bearing is installed at each support, and two are installed between the supports, in such a way that all 4 are exposed equally to the external load. The two in the middle get directly half the external load each, and the two in the supports get half the load as reaction forces. All 4 bearings are exposed to internal, outwards radial expansion from the expanding sleeves. For each step of internal load, the external load is increased stepwise from 0 to 400 and 800 kN, for Tests 2b and 2a, respectively. For each combination of internal load and external load, the required rotational moment to turn the pin connected to the 4 bearings is measured. The two bearings in the supports are exposed to identical internal, outwards radial expansion, but from the outer expanding sleeves. The loads and contact conditions are almost identical for the four bearings. The internal, outwards radial load is achieved by torquing the pin tightening screws. For the Test 2a, the two bearings are supported onto one expanding pin sleeve giving a full contact surface towards the bearings, with one bearing on each sleeve. For the Test 2b, one single bearing is supported onto two separate expanding pin sleeves, giving partly contact surface towards the bearings, with a non-contact area at its center part. The contact combinations between pin and bearing inner ring in Tests 2a and 2b are identical with those for Tests 1a and 1b (Reference Figure 6).

The required static rotational moment to turn the pin installed in the 3 or 4 bearings is measured by a 10 tons capacity hydraulic jack and cell connected to the two end plates through a crossbar, which again are connected to the pin, that is forced to turn; see Figure 7. The moment required for turning the pin is logged against the external load and the tightening screw torques.



Figure 7. Test set-up for Test 2a.

3.2. Cylinder Theory Formulas

Thick-walled cylinder theory [25] is applied to consider the relationship between the inner and outer pressure, and radial displacement between the inner and outer surface of the cylinder thickness. The inner ring of a RSPB is analyzed as an open cylinder, with a constant inner diameter but varying outer diameter along its z -axis. When analyzing a small part of the ring, which means that Δz is small, it gives a small variation in outer radius, Δb .

The strain–stress relationships for thick-walled tube with zero temperature effects are expressed as [25]:

$$\epsilon_r = \frac{1}{E} [\sigma_r - \nu(\sigma_\theta + \sigma_z)], \quad \epsilon_\theta = \frac{1}{E} [\sigma_\theta - \nu(\sigma_r + \sigma_z)], \quad \epsilon_z = \frac{1}{E} [\sigma_z - \nu(\sigma_r + \sigma_\theta)] = \text{constant} \quad (1)$$

where ϵ_r , ϵ_θ , and ϵ_z are radial, tangential, and axial strains; E is the elasticity modulus; ν is Poisson's ratio. The radial, tangential (hoop), and axial stress components σ_r , σ_θ , and σ_z , respectively, can be calculated using the expressions in Equations (2)–(4) [25].

$$\sigma_r = \frac{p_1 a^2 - p_2 b^2}{b^2 - a^2} - \frac{a^2 b^2}{r^2 (b^2 - a^2)} (p_1 - p_2) \quad (2)$$

$$\sigma_\theta = \frac{p_1 a^2 - p_2 b^2}{b^2 - a^2} + \frac{a^2 b^2}{r^2 (b^2 - a^2)} (p_1 - p_2) \quad (3)$$

$$\sigma_z = \frac{p_1 a^2 - p_2 b^2}{b^2 - a^2} + \frac{P}{\pi (b^2 - a^2)} = \text{constant} \quad (4)$$

where p_1 is internal pressure; p_2 is external pressure; P is the axial force, whose value is zero for an open cylinder; a is the inner radius; b is the outer radius; r is the radius, and the following condition is valid:

$$\sigma_r + \sigma_\theta = \frac{2(p_1 a^2 - p_2 b^2)}{b^2 - a^2} = \text{constant} \quad (5)$$

In an open cylinder analysis, with no end caps, as for the bearing inner ring, the strain and stress in the z -direction is zero, while the open-end displacement u is expressed as:

$$u_{(\text{open end})} = \frac{r}{E(b^2 - a^2)} \left[(1 - \nu)(p_1 a^2 - p_2 b^2) + \frac{(1 + \nu)a^2 b^2}{r^2} (p_1 - p_2) \right] \quad (6)$$

In these 4 tests, it is expected to have some axial stress in the inner rings due to the axially moving expanding sleeves and the distance rings possibly preventing the inner rings from moving. Tables 2 and 3 show some calculated values for internal pressure and outer surface tangential hoop stress in the bearing inner rings by setting the radially displacement $-u$ equal to the measured expansion by the CMM, from Tests 1a and 1b. The radial stress is zero and the Hoop stress is at its maximum at the ring outer surface, where $r = b$, with highest maximum stress at cross-sections locations “a” and “d”, which are at the thinnest ring sections, or sections closest to the ring ends. The calculated values are assumed to be the same for the bearing inner ring in Tests 2a and 2b as for Tests 1a and 1b, if the inner ring is loaded identically, and the bearing is not exposed to external load.

Table 2. Displacement, internal pressure, and hoop stress of inner ring, for Test 1a.

Section Locations [mm]	Non-Lubricated						Lubricated		
	Torque = 15 Nm			Torque = 30 Nm			Torque = 30 Nm		
	u [mm]	p_1 [MPa]	σ_θ [MPa]	u [mm]	p_1 [MPa]	σ_θ [MPa]	u [mm]	p_1 [MPa]	σ_θ [MPa]
a	0.112	84	508	0.347	262	1578	0.483	365	2199
b	0.020	28	82	0.059	84	238	0.091	129	365
c	-0.019	-27	-76	-0.062	-88	-249	-0.076	-108	-306
d	-0.100	-75	-453	-0.327	-247	-1488	-0.442	-344	-2012

Table 3. Displacement, internal pressure, and hoop stress of inner ring, for Test 1b.

Section Locations [mm]	Non-Lubricated						Lubricated		
	Torque = 15 Nm			Torque = 30 Nm			Torque = 30 Nm		
	u [mm]	p_1 [MPa]	σ_θ [MPa]	u [mm]	p_1 [MPa]	σ_θ [MPa]	u [mm]	p_1 [MPa]	σ_θ [MPa]
a	-0.161	-121	-731	-0.315	-238	-1434	0.025	19	114
b	-0.012	-17	-48	-0.017	-24	-68	0.042	60	170
c	0.047	67	190	0.101	144	407	0.047	67	190
d	0.176	133	801	0.350	264	1590	0.044	33	199

4. Discussion of Results

As shown in Figure 4a, Test 1a comprises an internal, radially outwards directional loading of two separate SKF GE 80 ES bearing inner rings, together with the corresponding setup for diameter deformation measurement using a CMM. Each ring was mounted on separate single expanding sleeves as illustrated in Figure 4a Figure 6a. Figures 8–11, from Test 1a and Test 1b, represent how the RSPB inner rings deform with increasing tightening screw torque. It is assumed that the effects from the expanding sleeves will give the same deformation pattern on the inner ring when they are installed in a bearing on an expanding pin, the radial clearance between the inner and outer rings is still not reduced to zero, and the bearing is not exposed to external loads.

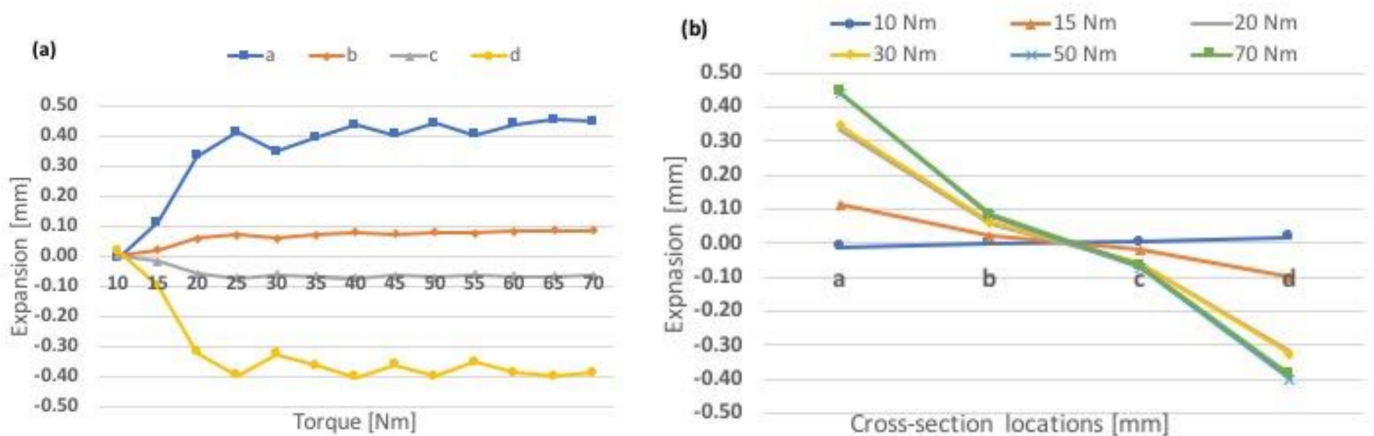


Figure 8. Test 1a—Ring deformations of non-lubricated bearing ring on single sleeve: (a) expansion as a function of torque and (b) expansion at different cross-section locations.

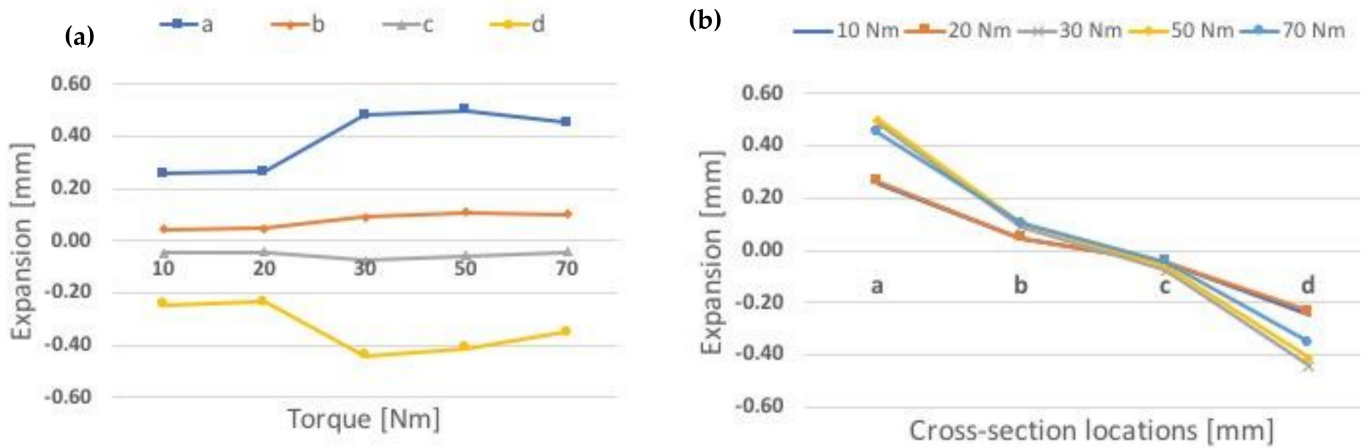


Figure 9. Test 1a—Ring deformations of lubricated bearing ring on single sleeve: (a) expansion as a function of torque and (b) expansion at different cross-section locations.

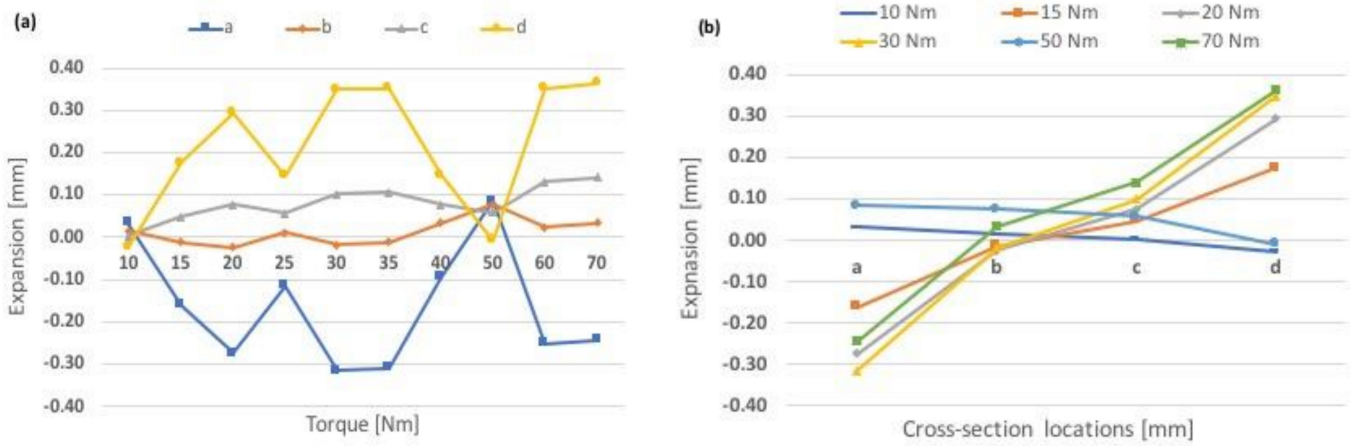


Figure 10. Test 1b—Ring deformations of non-lubricated bearing ring on double sleeve: (a) expansion as a function of torque and (b) expansion at different cross-section locations.

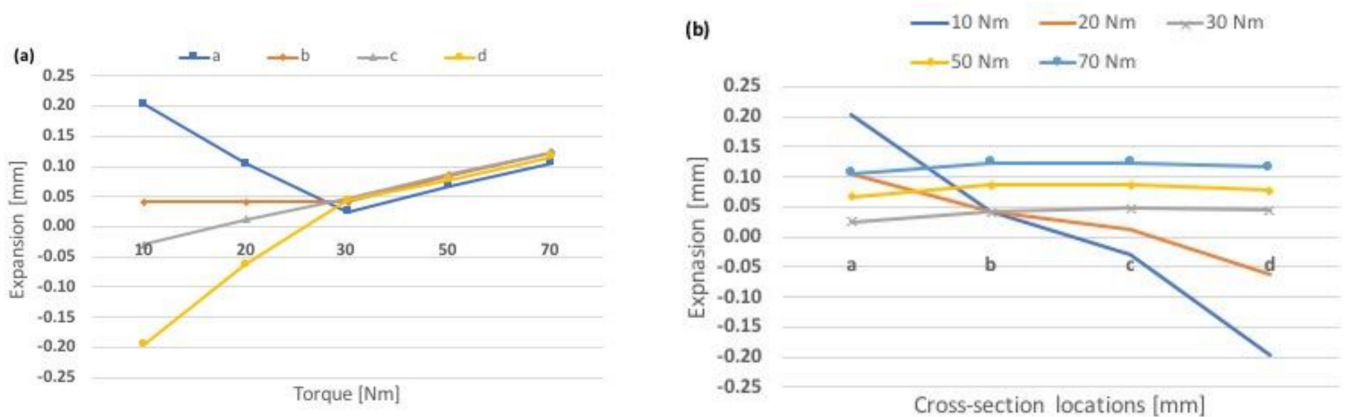


Figure 11. Test 1b—Ring deformations of lubricated single bearing ring on double sleeve: (a) expansion as a function of torque and (b) expansion at different cross-section locations.

The deformations of the ring on a single sleeve (Test 1a), for dry and lubricated sleeves, can be seen by comparing the results shown in Figures 8 and 9. In the dry case, the ring expands up to 0.410 mm (90.5% of its maximum) at 25 Nm torque, and it stays relatively constant until its maximum of 0.453 mm was reached at 65 Nm torque, at section “a”,

which is close to the ring end. At the opposite side of the ring, it contracts to slightly smaller values, or down to 90%. In the lubricated case (Figure 9), the ring expansions and contractions have increased compared to the dry case. Maximum expansion at section location “a” is 0.499 mm at 50 Nm torque, and maximum contraction at same section is 0.442 mm, at 30 Nm torque.

The contraction at the sleeve exit side is almost equal to the expansion at the sleeve entrance side, which stays at or close to 0.40 mm (expansion 347–453 μm and contraction 327–404 μm) at the torque range from 25 Nm up to 70 Nm. The maximum expansion and contraction over the torque range increased slightly with lubricated sleeves but not more than 10%. The average expansion varies up to 3 times higher for the lubricated case compared to the dry case, in the torque range of 20–70 Nm, shown in Figures 12 and 13. For Test 1a, the main expansions and contractions are seen at the ring end sections.

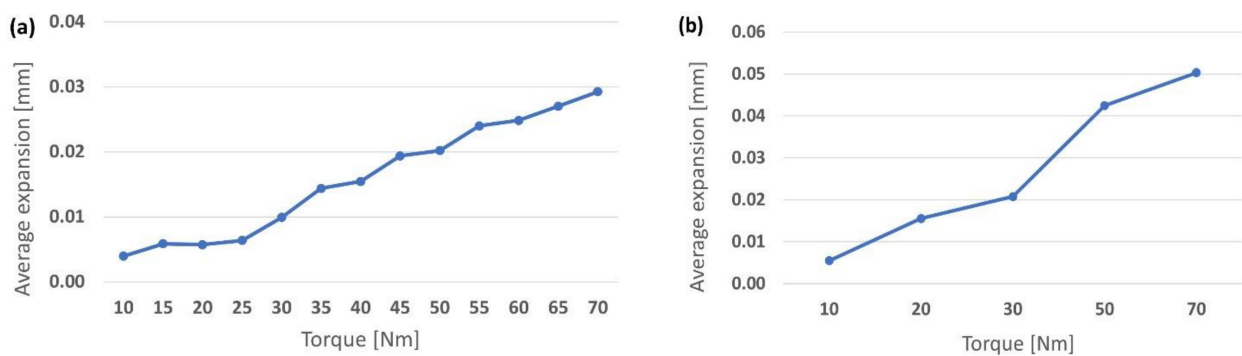


Figure 12. Test 1a—Average ring deformations of bearing rings on (a) non-lubricated and (b) lubricated single sleeve.

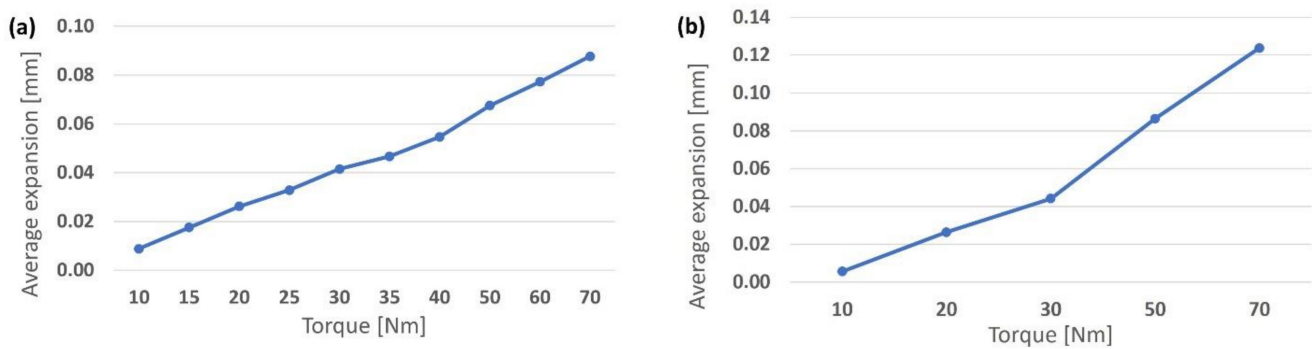


Figure 13. Test 1b—Average ring deformations of bearing rings on (a) non-lubricated and (b) lubricated double sleeve.

Test 1b was executed in a similar way as Test 1a, but the ring was supported on two separate expanding sleeves at the same time, entering at each ring end, so they leave an unsupported area at the mid part of the ring as illustrated in Figures 4b and 6b. The differences between the deformations of the ring on a double sleeve (Test 1b), for dry and lubricated sleeves, can be seen by comparing the results shown in Figures 10 and 11.

The non-lubricated case shows a serrated shaped curve where the expansion first increases and then decreases to “close to zero” when the accumulated/hysteresis surface contact stress is overcome, with increasing torque. When the ring expands by torquing the bolts and pushing the sleeves, the surface contact friction between ring and sleeve, as well as between sleeve and pin, increase and accumulate. When the torque is increased from 10 to 20 Nm, the expansion at section “d” increased from around 0 to around 0.30 mm (Figure 10a) and decreased almost equally at the opposite ring end, at section “a”. The

expansion of the sleeves changed the inner shape of the ring from perfectly cylindrical (within production tolerances) to slightly conical cylinder.

When the torque is increased further up to 25 Nm, the pushing force from the sleeves overcomes the accumulated surface contact stress; it is released, and sliding occurs, possibly between both contact surfaces (ring/sleeve and sleeve/pin) at the same time. When sliding occurs the ring tries to go back from the conical-cylindrical shape to the perfect cylindrical shape, and the contact stress gets more evenly distributed and consequently reduces the ring expansion down to “close to zero” at the “d” section and increases up to “close to zero” at the “a” section. As can be observed from Figures 8a and 10a, the same serrated shaped curve pattern can be seen when increasing the torque from 0 to 70 Nm.

In the lubricated case, it can clearly be seen that the expansion is reduced for all tightening torques, except for the lowest, and it is practically unchanged over the torques range 30–70 Nm. The maximum expansion values for 30, 50, and 70 Nm in the lubricated case are 0.047, 0.087, and 0.124 mm, respectively, compared to the fabric new bearing clearance of 0.072–0.142 mm. As can be observed from the plots in Figure 13, the average expansion varies up to 1.4 times higher for the lubricated case, in the torque range of 20–70 Nm. The lubricated case shows the highest asymmetry at the lowest torque, 10 kN, compared to the non-lubricated case where the asymmetry was around zero. The reason for this is assumed to be that in the lubricated case, the sleeves could move easier due to less friction resistance and thereby expand the ring at the sleeve entrance side that was torqued first (section “a”). When torquing the opposite side (section “d”), part of the asymmetry was eliminated, but not all, while for the non-lubricated case, the torque was lost into increased hysteresis surface contact stress and did not expand the ring until the torque was increased. When the torque increased, the accumulated or hysteresis surface contact stress was overcome, the sleeves slid, and the inner ring shape went back to its normal cylindrical shape or reduced its asymmetry as shown in Figure 11a. The effect of increasing expansion on each side of the inner ring independent of each other, from two different expanding sleeves, forces the ring into a less asymmetric shape. For Test 1b the main expansions and contractions are seen at the ring center sections.

The ring diameter changes at the 4 ring cross-section locations with non-lubricated and lubricated sleeves can be seen in Figures 10 and 11, respectively. The ring average expansion over the rings for Tests 1a and 1b are illustrated in Figures 12 and 13.

The radial expansions for different inner ring cross-sections presented in Figures 8–11 are represented by the deformation $-u$ in formula (6), and the corresponding inner pressure p_1 and tangential hoop stress σ_θ can be calculated, with the outer pressure $p_2 = 0$, whose results are given in Tables 2 and 3.

Test 2a comprises of two complete RSPBs mounted each on one single sleeve on an expanding pin and loaded both internally (i.e., radially outwards directional loading from expanding the sleeves by torquing the tightening screws) and externally (i.e., radially inwards load from the hydraulic load machine), as shown in Figures 5a and 7. The results from loading the bearing stepwise with internal and external loads and the measure of the required moment to turn the outer ring relatively to the locked inner ring of the bearing on single sleeve are shown in Figure 14. The highest rotational moments are seen at both the lowest and highest tightening torque, 5 and 65 Nm, respectively, and they increase with the increasing external load, for all torque values. The lowest rotational moments occur at 25 and 45 Nm. The reasons for this behavior are understood to be:

- At the lowest torque value, the expansion of the inner ring is zero, as illustrated in Figure 8a, as it would have been in a joint connection with a standard cylindrical pin installed. The required moment to turn the bearing is illustrated in Figure 14a,b, and these values represent fabric new bearings, with a contact surface between the bearing rings that depends on the specific bearing ring tolerance, which is in the range of 72–142 μm . A wide ring tolerance results in a reduced contact area between the two bearing rings and increased contact stresses, with possible accelerated removal of lubrication at the contact areas, followed by increased rotation moment. An increase

- of the external load increases the turning moment, as the contact pressure between the rings increases.
- When the torque level is increased to 25 and 45 Nm, the inner ring expands with a slightly serrated shape as illustrated in Figure 8a and changes the ring inner surface shape from cylindrical to conical-cylindrical, with increased opening diameter in one end and reduced opening at the other end. With increased external load, the ring shape is forced back to cylindrical shape, and the total average ring expansion can be seen in Figure 12a. The expansion of the inner ring increases the contact area between the two bearing rings and reduces the contact pressure. These expansion values are below the fabrication tolerances of the bearing, and the required turning moment is reduced, compared to the lowest torque value.
- At the maximum torque value of 65 Nm, the average expansion increases to a level still lower than the bearing internal minimum tolerances (Figure 12a), but the maximum expansion at the inner ring end is 0.45 mm (Figure 8a) which is three times over the bearing maximum tolerance. It is possible that the external load cannot push the ring back from the conical-cylindrical to the original cylindrical shape, and with high contact pressure areas between the two rings, the results show high rotation moment for high torque as well as for low torque.

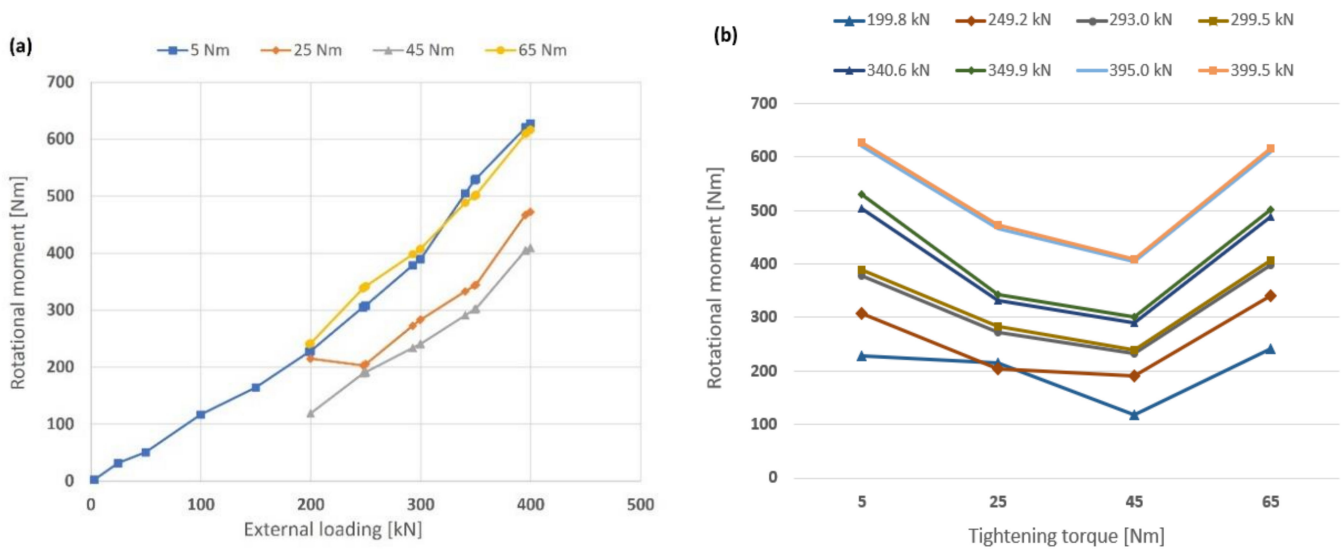


Figure 14. Test 2a—Total rotation moment per bearing, with bearing on single sleeve with (a) increasing external load and (b) increasing torque level.

Test 2b is performed in a similar way as Test 2a but with one single bearing at the assembly mid part, expanded by two separate sleeves. For the double sleeve setup (Test 2b), the highest rotational moment was clearly only at the lowest tightening torque, 5 Nm, as illustrated in Figure 15, and the remaining torque values in the range of 25–65 Nm did not give any major scattering in moment values. The rotational values are almost identical at torque value 55 Nm, for all external loads, with only a $\pm 9\%$ variation. At the maximum external load, 400 kN, the rotational moment reaches 1903 Nm with 5 Nm torque, and 266–466 Nm with torque values in the range of 15–65 Nm. The high rotational moment for the lowest torque is understood to come from the same reasons as for Test 2a. When the torque is increased to 30 Nm the asymmetry of the ring is reduced to almost zero, see Figure 11. This can be observed because all sections of the ring have increased almost identically (in the range of 0.025–0.05 mm). When the torque further increases from 30 Nm to 70 Nm, the ring stays close to symmetric over its axial length, and the ring diameter increases with increasing torque. Due to the expanding sleeves coming into the ring from both sides, in combination with increasing external load, the ring is continuously forced

back from any conical-cylindrical shape to cylindrical shape; the high contact pressure area between the two rings is avoided, and the high rotation moment does not occur for any increased torque value, within these tests.

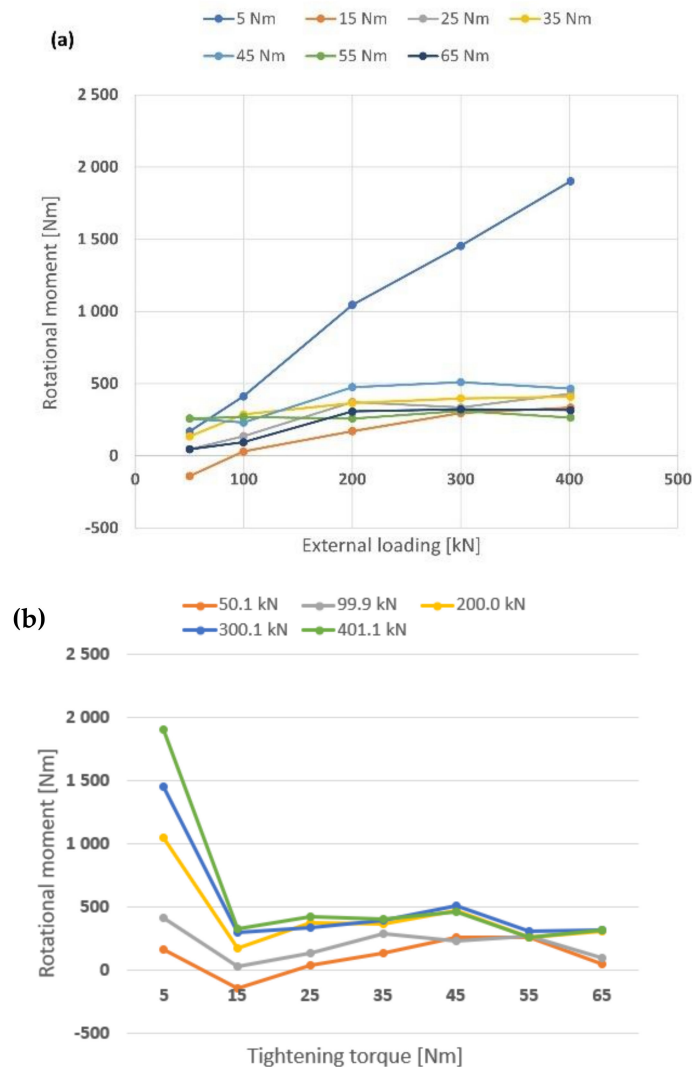


Figure 15. Test 2b—Total rotation moment per bearing with bearing on double sleeves with (a) increasing external load and (b) increasing torque levels.

A bearing mounted on an expanding pin will experience the inner ring expanding and the contact area between the inner and outer ring increasing with increasing internal load. As a result of external overload, the pin shaft could bend and then also the bearing inner ring, as described by Zhao et al. [18]. Such bending of the pin shaft could lead to increased loss of contact area between pin and inner ring at the ring center, combined with high load from the outer ring at the inner ring center area. This can lead to bending of the inner ring and subsequently brittle crack initiation at the contact areas between inner ring and pin, and inner ring and outer ring.

5. Conclusions

The setup with one bearing on two combined expanding sleeves (designated as Test 2b) clearly shows that a low tightening torque of 5 Nm results in high required rotational moment, compared to higher torques. The 5 Nm torque curve represents a rotational moment close to 1900 Nm at 400 kN external load, and for all other torques at the same external load, the rotational moments are in the range of 266–466 Nm, which is a drop in

rotational moment in the range of 75–86%. The measured rotational moments decrease substantially with only a small increase in tightening torque, due to increased inner ring expansion and reduced high contact pressure areas between the two rings, resulting in lower contact surface stresses between the two bearing rings, with improved lubrication effects. The inner ring expands when the torque levels are increased but not enough to eliminate the internal ring clearances. Thus, the ring contact pressure is reduced when the torque level is increased. For this bearing setup, it can be concluded that expanding the inner ring using expanding pin solutions will lower the total friction forces between the two rings for all external loads. The rotational moment is practically not increasing for each of the torque values within the range from 15 Nm to 65 Nm, within the higher external load range of 200–400 kN.

Following the results of this study, it is open to question whether a RSPB installed on a standard cylindrical pin shaft without the expanding effect will also suffer high friction between the rings and thereby a possibly reduced lifetime compared to the use of an expanding pin solution with a tightening torque above 5–10 Nm. The healthiest set up for the case with one bearing on two sleeves will be to apply a torque level of 20–30 Nm, which gives an equal distributed expansion of the inner ring and an expansion level within or at the lower level of the bearing inner clearance limits of 0.072–0.142 mm, where 20 Nm torque results in a 0.026 mm and 30 Nm in a 0.042 mm ring expansion with dry sleeves, and a 0.026 mm and a 0.044 mm ring expansion for lubricated sleeves, respectively.

The setup with one bearing on one single sleeve (designated as Test 2a) shows that both the lowest and highest torques, 5 Nm and 65 Nm, respectively, result in higher and almost identical rotational moments in the external load range of 200–400 kN. The reason for the high moment at low torque would be the same as in Test 2b, and the high moment at high torque is understood to come from the ring deformation shape, as shown in Test 1a. One side of the inner ring expands and encounters the outer ring and is not pushed back to its cylindrical shape, and high surface contact pressure areas are produced which increase the rotational moment. The healthiest set up for the bearing in this case seems to be with a tightening torque regime in the range of 25–45 Nm with dry sleeves with 0.006 mm and 0.019 mm ring expansion, or 20–40 Nm with lubricated sleeves, and with 0.016 mm and 0.032 mm ring expansion. When lubricating the sleeves, a higher part of the energy input (torque) goes to expand the bearing inner ring, and less is lost in overcoming friction.

Based on this study and its findings, further investigations can be recommended, especially with the use of finite element analysis (FEA) where a wider diameter range of expanding pins can be analyzed, in addition to standard cylindrical pins, in combination with extended laboratory testing. The variables of interest are diameter, bearing type, friction, torque, and external load. In addition, it could be of interest to run bearing fatigue tests with expanding pins.

Author Contributions: Conceptualization, Ø.K.; methodology, Ø.K. and I.B.; software, Ø.K. and I.B.; validation, Ø.K. and H.G.L.; formal analysis, Ø.K.; investigation, Ø.K. and I.B.; resources, Ø.K. and H.G.L.; data curation, Ø.K.; writing—original draft preparation, Ø.K.; writing—review and editing, Ø.K. and H.G.L.; visualization, H.G.L.; supervision, H.G.L.; project administration, Ø.K.; funding acquisition, Ø.K. All authors have read and agreed to the published version of the manuscript.

Funding: The research is conducted as part of Industrial PhD study funded by the Research Council of Norway, placed in Oslo, Norway, web <https://www.forskningradet.no/en/> (accessed on 27 March 2022), Grant nr. 283821. This financial support is highly acknowledged.

Institutional Review Board Statement: Not applicable.

Informed Consent Statement: Not applicable.

Data Availability Statement: Not applicable.

Acknowledgments: We are grateful for all the help, advice, and bearings received from Henrik Tveit at SKF Norway and all the support and guidance from Carl Odvar Hoel at Coba MT, in relation with the tests performed.

Conflicts of Interest: The authors declare no conflict of interest. The authors declare that they have no known competing financial interests or personal relationships that could have appeared to influence the work reported in this paper.

References

1. Myszka, D.H. *Machines and Mechanisms: Applied Kinematic Analysis*, 4th ed.; Pearson Education, Inc.: Old Tappan, NJ, USA, 2012.
2. Salahshour, S.; Karlsen, Ø.; Lemu, H.G. Experimental and numerical studies of stress distribution in an Expanding Pin Joint System. *Appl. Mech.* **2022**, *3*, 46–63. [[CrossRef](#)]
3. Ma, J.; Qian, L.; Chen, G.; Li, M. Dynamic analysis of mechanical systems with planar revolute joints with clearance. *Mech. Mach. Theory* **2015**, *94*, 148–164. [[CrossRef](#)]
4. Ambrósio, J.; Pombo, J. A unified formulation for mechanical joints with and without clearances/bushings and/or stops in the framework of multibody systems. *Multibody Sys. Dyn.* **2018**, *42*, 317–345. [[CrossRef](#)]
5. Fang, C.; Meng, X.; Lu, Z.; Wu, G.; Tang, D.; Zhao, B. Modeling a lubricated full-floating pin bearing in planar multibody systems. *Tribol. Int.* **2019**, *131*, 222–237. [[CrossRef](#)]
6. Grant, W.J. Shrink fitting. *Cryogenics* **1972**, *12*, 328–333. [[CrossRef](#)]
7. McMillan, M.; Hendry, J.L.; Woolley, A.; Pavier, M.J. Measurement of Partial Slip at the Interface of a Shrink Fit Assembly under Axial Load. *Exp. Mech.* **2018**, *58*, 407–415. [[CrossRef](#)]
8. Mouâa, A.; Laghzale, N.E.; Bouzid, A.H. Elastic-plastic stresses in shrink fit with a solid shaft. In Proceedings of the MATEC Web of Conferences EDP Sciences, 14th Congress of Mechanics (CMM2019), Rabat, Morocco, 16–19 April 2019; EDP Sciences: Les Ulis, France, 2019; Volume 286, p. 02001. [[CrossRef](#)]
9. Murčinková, Z.; Baron, P.; Pollák, M. Study of the press fit bearing-shaft joint dimensional parameters by analytical and numerical approach. *Adv. Mater. Sci. Eng.* **2018**, *2018*, 2916068. [[CrossRef](#)]
10. Lee, D.H.; Kwon, S.J.; Choi, J.B.; Kim, Y.J. Observations of Fatigue Damage in the Press-fitted Shaft under Bending Loads. *Key Eng. Mater.* **2006**, *326*, 1071–1074. [[CrossRef](#)]
11. Bondura Technology AS. Available online: <https://www.bondura.no/> (accessed on 13 April 2022).
12. Nord-lock Group. Available online: <https://www.nord-lock.com/expander-system/> (accessed on 13 April 2022).
13. Karlsen, Ø.; Lemu, H.G. On Modelling Techniques for Mechanical Joints: Literature Study. In *Advanced Manufacturing and Automation IX. IWAMA 2019; Lecture Notes in Electrical Engineering*; Wang, Y., Martinsen, K., Yu, T., Wang, K., Eds.; Springer: Singapore, 2019; p. 634. [[CrossRef](#)]
14. Karlsen, Ø.; Lemu, H.G. Fretting fatigue and wear of mechanical joints: Literature study. In Proceedings of the 2nd COTech Conference, Stavanger, Norway, 27–29 November 2019; p. 012015. [[CrossRef](#)]
15. Akhtar, M.M.; Karlsen, Ø.; Lemu, H.G. Study of Bondura® Expanding PIN System-Combined Axial and Radial Locking System. *Strojnicki Vestnik/J. Mech. Eng.* **2021**, *67*, 625–634. [[CrossRef](#)]
16. Berkani, I.; Karlsen, Ø.; Lemu, H.G. Experimental and numerical study of Bondura® 6.6 PIN joints. In Proceedings of the 1st COTech Conference, Stavanger, Norway, 28–29 November 2017; IOP Publishing Ltd: Bristol, UK, 2021; Volume 700, p. 012015. [[CrossRef](#)]
17. Öztürk, E.; Yıldızlı, K.; Memmedov, R.; Ülgen, A. Design of an experimental setup to determine the coefficient of static friction of the inner rings in contact with the outer rings of radial spherical plain bearings. *Tribol. Int.* **2018**, *128*, 161–173. [[CrossRef](#)]
18. Zhao, X.; Fang, C.; Chen, Y.; Zhang, Y. Failure behaviour of radial spherical plain bearing (RSPB) joints for civil engineering applications. *Eng. Fail. Anal.* **2017**, *80*, 416–430. [[CrossRef](#)]
19. Sun, G.; Wu, M.; Yang, Y.; Xue, S. Mechanical properties of radial spherical plain bearing (RSPB) joint with an inserted plate for building structural application—An experimental study. *Structures* **2021**, *33*, 2140–2151. [[CrossRef](#)]
20. Fang, X.; Zhang, C.; Chen, X.; Wang, Y.; Tan, Y. Newly developed theoretical solution and numerical model for conformal contact pressure distribution and free-edge effect in spherical plain bearings. *Tribol. Int.* **2015**, *84*, 48–60. [[CrossRef](#)]
21. Karlsen, Ø.; Lemu, H.G. Questionnaire-based survey of experiences with the use of expanding PIN systems in mechanical joints. *Results Eng.* **2021**, *9*, 100212. [[CrossRef](#)]
22. Karlsen, Ø.; Lemu, H.G. Safety related study of Expanding Pin systems application in lifting and drilling equipment within Construction, Offshore, and Marine sectors. In *IOP Conference Series: Materials Science and Engineering. Proceedings of the 3rd COTech Conference, Stavanger, Norway, 25–26 November 2021*; IOP Publishing Ltd: Bristol, UK, 2021; Volume 1201, p. 012026. [[CrossRef](#)]
23. SKF. Available online: <https://www.skf.com/group> (accessed on 13 March 2022).
24. OVAKO. Available online: <https://www.ovako.com/> (accessed on 13 March 2022).
25. Boresi, A.P.; Schmidt, R.J.; Sidebottom, O.M. *Advanced Mechanics of Materials*; Wiley: New York, NY, USA, 1985; Volume 6.

Appended Paper III

A Novel Technique for Temporarily Repair and Improvement of Damaged Pin
Joint Support Bores

KARLSEN, Ø.; LEMU, H. G.; BERKANI, I.

Applied Mechanics, 2022, vol. 3, no 4, p. 1206-1222

<https://doi.org/10.3390/applmech3040069>



Article

A Novel Technique for Temporarily Repair and Improvement of Damaged Pin Joint Support Bores

Øyvind Karlsen ^{1,2,*}, Hirpa G. Lemu ^{1,*} and Imad Berkani ²¹ Faculty of Science and Technology, University of Stavanger, 4036 Stavanger, Norway² Bondura Technology AS, 4340 Bryne, Norway

* Correspondence: oyvind.karlsen@uis.no (Ø.K.); hirpa.g.lemu@uis.no (H.G.L.)

Abstract: Damaged support bores due to wear and ovality can be critical for a machine and its operation, in addition to representing a safety problem and risk of pin breakage. It can be a costly operation to perform the required repairs in between planned service periods, especially because of the unplanned down time. A joint with a standard cylindrical pin will often experience wear and ovality in the support bore surfaces, and at some point, repairs will have to be performed. This study investigates and compares five options when a joint with a cylindrical pin has reached a severe level of wear and ovality, outside its planned service stop. The work involved testing the viability of 3D scanning of the damaged bore surface, 3D printing of a metal bushing, and inserting the bushing into the damaged joint. In addition, two pin solutions, i.e., a standard cylindrical pin and an expanding pin type, were installed into the repaired joint, loaded, and the strain on the pin ends close to the supports was measured. For the sake of comparison, the supports had both smooth circular bore and severe wear and ovality. It was concluded that it is possible to produce and install the 3D-printed bushing insert without major problems; the insert had satisfactory capability during test loading, and it most probably represents a good solution when it comes to the reduction in unwanted downtime during unplanned repairs of damaged joints.

Keywords: support repair; expanding pin; load pin; strain measuring; maintenance; repair procedure; 3D scanning; printing for repair



Citation: Karlsen, Ø.; Lemu, H.G.; Berkani, I. A Novel Technique for Temporarily Repair and Improvement of Damaged Pin Joint Support Bores. *Appl. Mech.* **2022**, *3*, 1206–1222. <https://doi.org/10.3390/applmech3040069>

Received: 28 August 2022

Accepted: 3 October 2022

Published: 6 October 2022

Publisher's Note: MDPI stays neutral with regard to jurisdictional claims in published maps and institutional affiliations.



Copyright: © 2022 by the authors. Licensee MDPI, Basel, Switzerland. This article is an open access article distributed under the terms and conditions of the Creative Commons Attribution (CC BY) license (<https://creativecommons.org/licenses/by/4.0/>).

1. Introduction

With increasing requirements for improved efficiency in combination with a low-cost policy of mechanical machines and equipment, the risk of failures such as wear, ovality and breakage of the joints, with pin shaft, supports and bearings involved, will increase. The supports are normally made of a lower-strength and -hardness material compared to the pin shaft [1], and therefore wear and ovality are often experienced, especially with high and alternating loads, vibrations, and shock-loads, which can be costly to repair. Increasing clearance between the pin and the support bores results in relatively larger movements between pins and supports in the radial direction, but also often in the axial direction, in addition to possible rotational movements. The initial installation clearance from the first installation of a new fabric pin in new support bores increases over time and the process could be accelerating, as described by Karlsen and Lemu [2]. Repairing damaged supports is time-consuming and involves direct costs in terms of repairs and materials, and indirect costs in unwanted and often unplanned downtime. In general, there are various methods to join the pin shaft and the supports, such as (i) with a standard, cylindrical pin, (ii) interference by press fitting, (iii) interference by shrink fitting, and (iv) interference fit by radially expanding the pin [2,3].

A standard cylindrical pin, under method (i), installed in attachment lugs (machine supports), would normally be of the clearance type, with a defined positive clearance between the pin and the bore, or a near-push-fit type (close to zero clearance, but not

interference type) [4]. Chikmath and Dattaguru [5] analyzed the stress situations by loading a joint in the pull and push directions of the lugs. A push-fit type of connection, or clearance fit, will show a region of contact/separation that changes 180° when the load is changed between pull and push, but will undergo no change of contact/separation location when the loads are pull-pull, static pull, push-push, and static push. This results in changing boundary conditions on the pin-hole interface, and the crack initiation locations are placed at $+90^\circ$ and -90° compared to the load direction.

In general, an expanding pin assembly, such as in method (iv) mentioned above (as shown in Figure 1 [6]), involves a cylindrical pin with machined tapered ends, machined sleeves with a cylindrical outer shape and conical inner shape to fit the tapered pin ends, and an endplate with tightening screws or nuts. By torquing the tightening screws or nuts, the sleeves are forced to move axially and expand radially on the tapered pin ends until the pin assembly locks via the application of wedge force to the support bore inner wall surfaces. The contact pressure between the surfaces in contact can be controlled by the torque level in the tightening screws or nuts. Any relative movements between the pin and the supports can be prevented by introducing sufficient contact pressure to the surfaces in contact. In this type of assembly, there will be no region of contact/separation due to changes in load direction. The expanding pin solution is recognized by its users as generally an easier, faster, safer, and more economical pin solution [1,7].

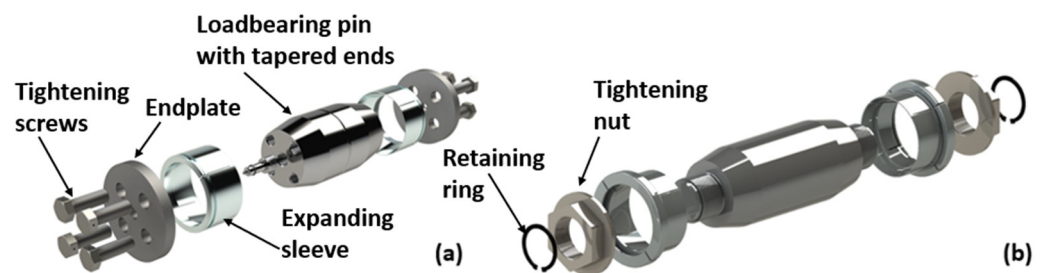


Figure 1. Expanding pin assembly (a) with tightening screws, and (b) with tightening nuts.

It can be both time-consuming and costly to perform repairs of damaged support bores, especially if this must be performed outside planned service intervals. Due to restrictions on hot-work and high-energy work, or the lack of sufficient and necessary tools, the machine or equipment might have to be dismantled and shipped to other locations for repair.

Nowadays, 3D scanning is applied for rapid product development [8] and is considered as a potential tool of production control [9,10], where the scanned digital data of the produced part are compared with the original design data. The technologies that allow RE, and the rapid design and production of prototypes (rapid prototyping (RP)) and tools (rapid tooling (RT)), by capturing three-dimensional data from physical models in digital form, are also known as 3R technologies. Javaid et al. [11] studied the use of 3D scanning for the RE, analysis, designing and measuring of complex shapes and surfaces, from an industrial perspective. The application of this technology is wide and is increasing rapidly, in fields such as automobile, aircraft, fashion, construction and healthcare, where the design of prostheses, anatomical orthoses, and a wide range of other tools are needed.

Three-dimensional printing is an additive manufacturing (AM) process [12–14], wherein a material is added through the production process and not removed as in a CNC machining process, and in many situations, it can be more cost-effective to repair partially damaged and worn parts by 3R technology than printing whole new parts. Kim et al. [15] presented a maintenance framework for such repairs to ease the task and make the process more user-friendly, and to reduce the need for expert technical support on-site, which might be difficult to get at certain locations, e.g., on ships in operation and offshore platforms. A study on how maintenance, repair, and overhaul (MRO) strategies can be optimized also presented an industrial case study [16] of a flap discs manufacturing machine with a pneumatic cylinder used to pick up and drop the final product. The conclusion was that AM

brings important advantages to MRO activities, and it offers sustainable alternatives when maintaining, repairing, overhauling, and replacing spare parts, or other components. It is necessary to determine the difference between the measured and the real part when creating a digital twin of the original part via the 3D scanning of the worn or damaged part, and this is called deviation zone estimation (DZE). Buchanan and Gardner [17] presented an article regarding a review of methods, research, applications, opportunities, and challenges related to using 3D printing construction. They stated that the AM will complement conventional production processes, rather than replace them, with a potential for hybrid solutions to achieve structural strengthening and perform repairs. Ueda et al. [18] used DZE to determine the worn and damaged area of an artificially created turbine blade, and Mortazavian et al. [19] performed a thermal–mechanical study of 3D printing for worn rail repairs. An additive material of type E71T was 3D-printed on the top of the worn rail head carbon–manganese material, and the effects of preheating on residual thermal stress at the rail/additive interface were studied. Metal additive manufacturing and repair are widely applied in both the aerospace industry and medical sector [17]. Both the Eurofighter Typhoon and Airbus 380 use 3D-printed components in non-safety-critical components, and SpaceX have built an engine chamber out of nickel superalloy. Many studies involving 3D printing have been performed within health and medical sectors. Wan et al. [20] studied bone repair by use of a biocompatible heterogeneous bone powder and 3D printing, while Zhao et al. [21] studied the 3D printing of porous titanium alloy scaffolds for bone tissue repair and reconstruction. Maroulakos et al. [22] wrote a review article on the applications of 3D printing on craniofacial bone repair, based on 43 articles (6 human and 37 animal studies). Zhu et al. [23] created a gelatin scaffold from 3D-printed porous titanium to repair and regenerate bones, and Cheng et al. [24] studies 3D-printed prosthesis for the repair and reconstruction of bone defects.

One way to investigate strain, load and stress distribution in a pin is by applying strain gauge technology. The basis and working principle of strain gauges is the strain/resistance relationship of electrical conductors, discovered by Wheatstone and Thomson; the bridge circuit was invented and first mentioned in a publication by Charles Wheatstone in 1843 [25], and the technique was further developed by Hook [26] and Ruge [27].

A cylindrical load pin will normally have two grooves going 360° around its circumference, one close to each support, with the groove depth depending on the maximum load expected, and the strain gauges are placed either on the inside wall of a pin center bore [28,29] or on some pockets on the outside wall [30]. The purpose of the grooves, or deformation zones, is to ensure enough strain concentration to guarantee the accuracy and repeatability of the measured results, which define their quality.

This study investigates a new technique for the temporary repair of a support bore wherein a standard cylindrical pin shaft has originally been applied, by comparing various possible options at a point in time at which severe wear and ovality have occurred in a joint support. The comparison is performed by the application of 3D scanning and printing techniques, and strain gauge measurements in the pin under external loading and different pin positions. The proposed procedure is much more time- and cost-efficient than the traditional means of repairing worn and damaged joints, wherein the machine and equipment are typically taken out of operation until the repairs are finished; when applying this procedure, the downtime due to the repair is minimized.

2. Experimental Methods and Materials

In this study, the quality of the functionality of the repaired joint was analyzed by comparing measured strains at the pin–joint connection in the following test cases (clearances listed in Table 1):

- Test 1—a standard cylindrical pin with wear evenly distributed at each end;
- Test 2—a cylindrical pin with additional severe wear and ovality at one end;
- Test 3—an expanding pin with evenly distributed wear at each end;
- Test 4—an expanding pin with additionally severe wear and ovality at one end;
- Test 5—an expanding pin with repaired support at the damaged end.

Table 1. Pin type, bore diameter and clearance for tests 1–5.

Test no.:	PIN Type and Size [mm]	Bore Diameter [mm]	Installed Diameter Clearance [mm]
1	Cylindrical pin: Ø88	Ø88.9 (L+R) *	0.9 (L+R)
2		Ø88.9, 0 to +5, (L) Ø88.9 (R)	0.9 to 5.9 (L) 0.9 (R)
3	Expanding pin: Ø88	Ø88.9 (L+R)	0 (L+R)
4		Ø88.9, 0 to +5, (L) Ø88.9 (R)	0 to 5 (L) 0 (R)
5		Ø85 (L) Ø88.9 (R)	0 (L+R)

* L: Left-hand end; R: Right-hand end.

The strains were measured using strain gauges, placed at the pin weakening grooves sections, close to the contact areas between pins and supports. The pin grooves were 6 mm wide, with a 3 mm radius, and 7.5 mm deep, which gave a minimum cross-sectional diameter of 73 mm.

Test 1 and 2 were performed on a cylindrical pin with a nominal diameter of Ø88 mm, while tests 3–5 were performed on a bondura® expanding pin. The samples in both cases had lengths of 150 mm. In these tests the strain gauges were placed on prepared spots close to the pins’ outer radii, as illustrated in Figures 2 and 3.

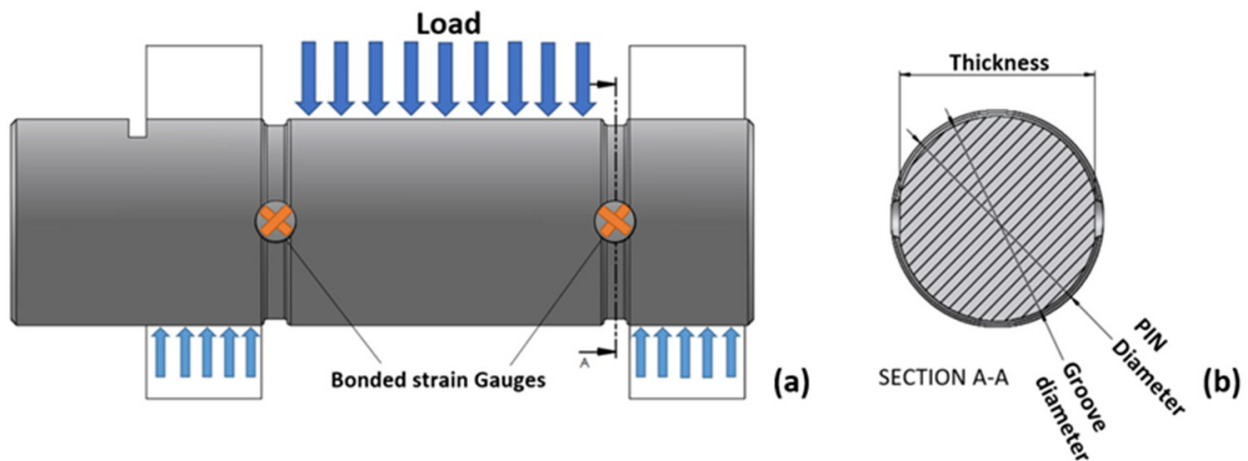


Figure 2. (a) Strain gauges on loaded cylindrical pin, and (b) cross-sectional area at grooves.

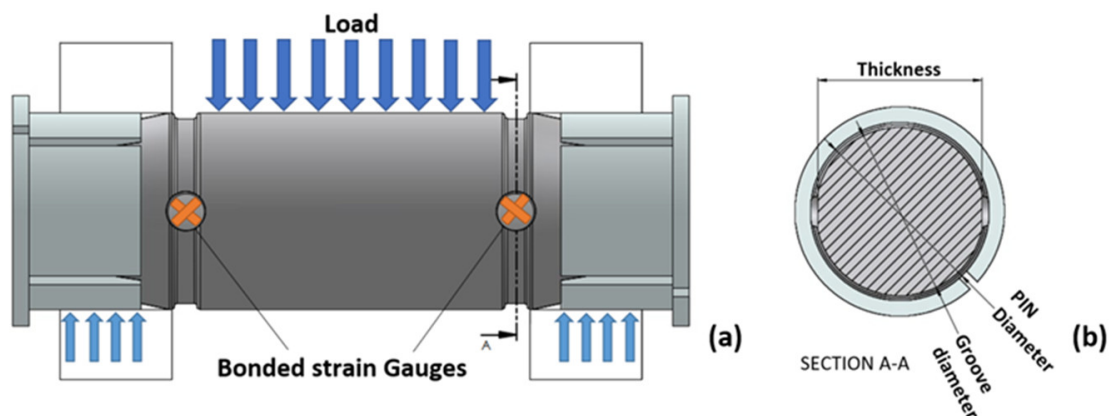


Figure 3. (a) Strain gauges on loaded expanding pin, and (b) cross-sectional area at grooves.

The load tests were performed in a jig with an Enerpac CLP 100-ton capacity hydraulic cylinder, an RTN 470-ton capacity load cell, and the CatmanEasy version 5.3.3.7 software. The pin–bore clearance was simulated by grinding a part of the inner diameter bore surface (L) to simulate wear and ovality of the used equipment for tests 2 and 4.

For each of the tests (tests 1–5) the pins were loaded from 0 to 500 kN in steps of 100 kN, and readings were taken after each loading. The pins were loaded three times at each step. All tests were first loaded at the 0° position with all four strain gauges placed in a plan in parallel with the external load direction, and then rotated to a 15° position, loaded again, and the results were recorded to see the effect of the rotation on the measured values. Both pins had a minimum safety factor of five in relation to the maximum external load, for design purposes.

2.1. 3D Scanning of Damaged Support Bore Surface

The damaged and oval bore surface in the case of test 4 was scanned with a 3D handheld scanner of model HandySCAN 700™ (AMETEK, Berwyn, PA, USA) [31], as illustrated in Figure 4a, and the 3D model was transferred to a CAD program (Autodesk Inventor®) [32] for processing purposes to design a new bushing (Figure 4b). The design model was thereafter converted into an STL file format for further processing by a 3D printer machine, and subsequently the bushing was printed out in four parts for easy installation. The outer surface of the printed bushing was designed to fit the worn inner surface of the left support, as described in Table 1, and the inner diameter of the bushing was $\text{Ø}85$ mm without ovality, as indicated in test 5, to fit the expanding pin sleeve.

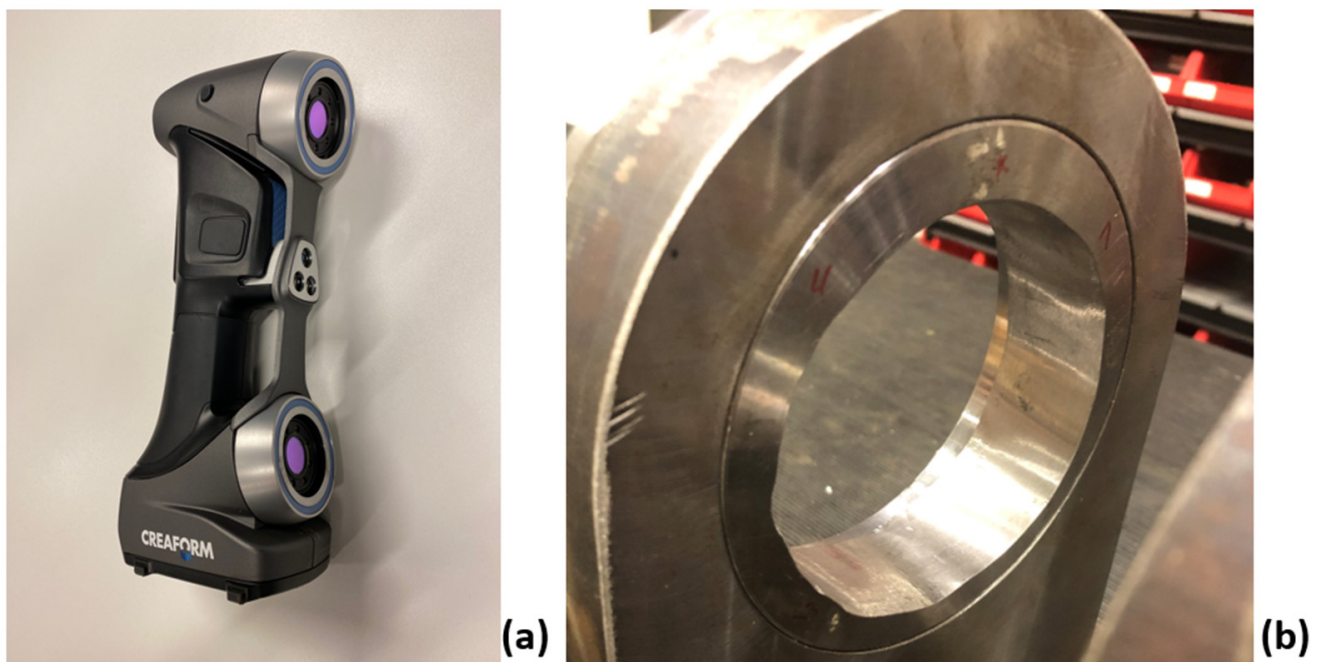


Figure 4. (a) Handheld 3D scanner, and (b) worn support.

2.2. 3D Printing and Fitting of Bushing to Damaged Support Bore

The 3D printer produced one bushing, fitted to the bore (L) surface with a circular $\text{Ø}85$ mm pin hole in the middle, for use in test 5, as illustrated in Figure 5. The ovalities at the support were generated by mechanically removing the material, and the two different bores (L and R) had different shapes and levels of wear and ovality. The bushing was produced in four separate parts with a 2 mm wide cut-through at the top/bottom and at the sides, for adjustment purposes during installation. The pin and bushing materials [33] are shown in Table 2. After 3D printing, but before use, the bushing went through a washing and sintering process to clean the parts of all support materials, and to transform the bushing from a

lightly bounded metal powder into a more solid metal part—alloy Inconel 625 in this case. The bushing was printed using a 3D printer machine of type Markforged METAL X (Markforged, Birmingham, UK) with machine ID c7d0db1e-12c2-4ee3-9ad0-601a62d2af3f, while the washing was performed in a Markforged Wash-1 machine with serial number 000166, and the sintering process in a Markforged Sinter-1 machine (Markforged, Birmingham, UK) with machine ID cd9c8c98-bc1a-45c6-8357-a7bcb75ecb6 [34].

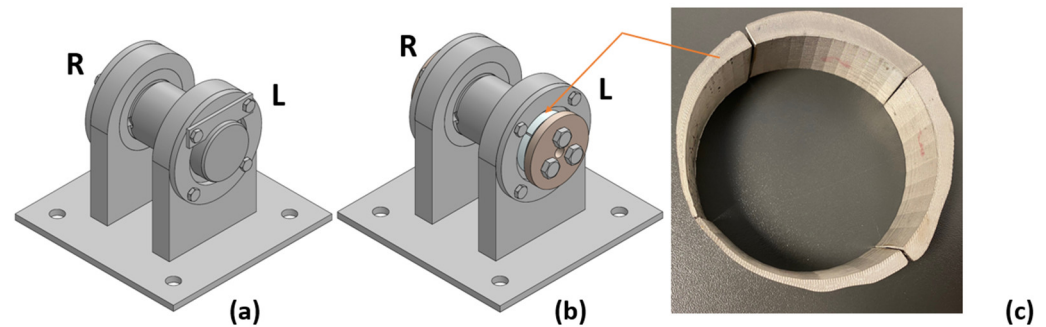


Figure 5. Test equipment, with (a) the cylindrical pin, (b) expanding pin, and (c) 3D-printed boss on the left (L) support of the expanding pin.

Table 2. Material quality for tests 1–5.

Part:	Material Quality
Load-bearing pins	EN 1.4418
Supports	S355
Bushing (3D printed)	Inconel 625

2.3. Strain Gauge Measurements

Figure 5a,b show the test equipment used for a cylindrical pin and for an expanding pin, respectively, while Figure 5c illustrates the 3D-printed boss used in the left-hand support of the expanding pin. The test setup is illustrated in Figure 6. To measure strain values, a total of four strain gauges per pin, named FCA-1-11-1LJB, were installed. The strain gauges were of type 90° (fish bone shape), half-bridge, with a capacity to measure shear and torsion, and they were installed at $\pm 45^\circ$ to the pin's central axis. These strain gauges were meant for the measurement of strains in mild steels, while the pins were made of high-strength stainless steel. Under controlled test conditions at a room temperature change of far less than $\pm 10^\circ\text{C}$, it was considered that this would not affect the results negatively. The glue was of type CN, single component room-temperature-curing (Cyanoacrylate). The strain gauge measurement system was equipped with an amplifier of the type QuantumX MX1615B, and data were processed with the CATMAN software (Version 5.5.3, Darmstadt, Germany).

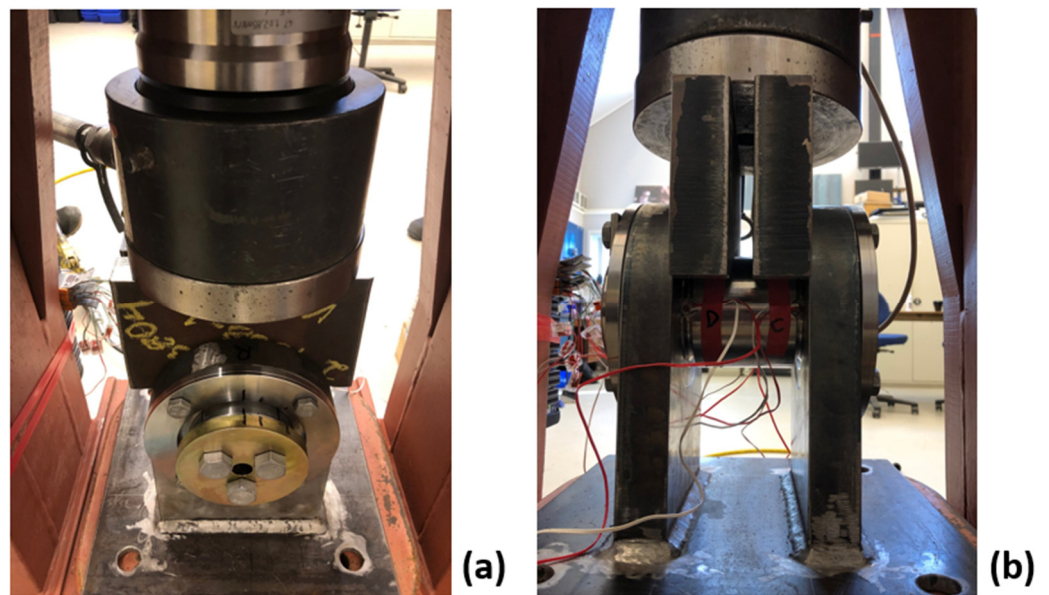


Figure 6. Test setup with (a) expanding pin, and (b) standard cylindrical pin.

3. Results and Analysis

The support bores in the cases of tests 1, 3 and 5 were identical on each side with Ø88.9 mm-diameter circular holes, and representative of a normal operational situation. On the other hand, Tests 2 and 4 showed increased wear on the left (L) supports compared to the right (R) support, which was prepared to simulate an unwanted, but typical, situation for a standard pin. For the expanding pin, however, the situation described in test 4 would not occur under normal circumstances during normal operation, but could be the result of an unwanted situation wherein the expanding pin has been installed in a severely worn joint.

The measured strain values, ϵ_{45° , were compared with the calculated average strain values, ϵ_{ca} , obtained from Equation (1), and the calculated maximum strain, ϵ_{cm} , from Equation (2), for each test. For circular cross-sections, the maximum shear stress, τ_{cm} , is assumed to be $\frac{4}{3}$ of the average value, τ_{ca} [35], as illustrated in Figure 7. The average shear stress can be expressed as the force (N) acting on the cross-section divided by the cross-sectional area (mm^2).

$$\epsilon_{ca} = \frac{F}{2 \times A \times G} \tag{1}$$

$$\epsilon_{cm} = \frac{4 \times \epsilon_{ca}}{3} \tag{2}$$

where F (N) = external load, A (mm^2) = cross-sectional area and G (MPa) = shear modulus.

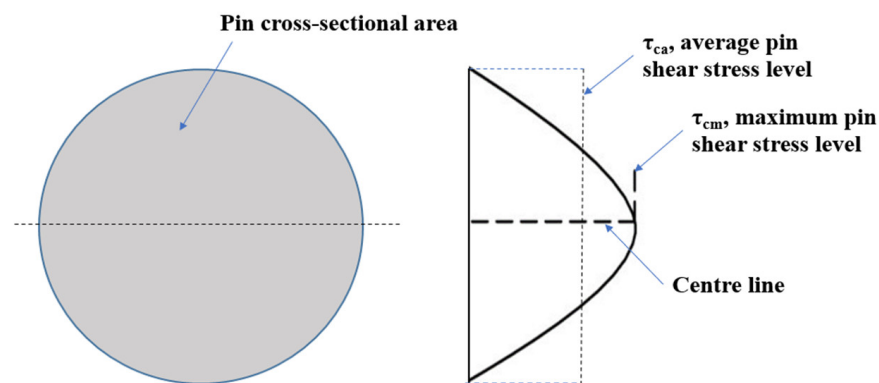


Figure 7. Shear stress distribution of the cylindrical pin section.

The cross-sectional shear stress area was adjusted (increased) to compensate for the strain gauges that were placed slightly offset to the ideal smallest cross-sectional area represented by the center line, as illustrated in Figure 8, for calculation purposes. The standard pin for tests 1 and 2 had a calculated average cross-sectional area below the strain gauges of 4.956 mm^2 , and an expanding pin area of 4.589 mm^2 , while the minimum cross-sectional area at the center of the groove was 4.162 mm^2 for both pins when considering the strain gauge pocket areas. The loads in the calculations and tests were applied in steps of 100 kN, from 100 to 500 kN, and the shear modulus of the pin steel was 78 GPa. A comparison between the measured and calculated strains at maximum load is shown in Tables 3 and 4.

The strains, ε_{45° , were measured at the real cross-section (at the offset) of the right-hand end and left-hand end for 0° and 15° pin rotation positions, and the values are shown in Tables 3 and 4. The calculated strain values for average, ε_{ca} , and maximum, ε_{cm} , strain at the real cross-section are also given in the same tables. The calculated strain values for the minimum cross-sectional area, at the center line in Figure 8, are $\varepsilon_{ca} = 378 \text{ } \mu\text{m}/\text{m}$ and $\varepsilon_{cm} = 504 \text{ } \mu\text{m}/\text{m}$ for 0° pin rotation, while the values for 15° pin rotation are $\varepsilon_{ca} = 365 \text{ } \mu\text{m}/\text{m}$ and $\varepsilon_{cm} = 487 \text{ } \mu\text{m}/\text{m}$, for both pins at both pin ends in tests 1, 3 and 5.

The applied types of strain gauges compensated for and eliminated the effects of the elongation or compression of the pin, due to, for example, changes of temperature, but a reduction in measured values was expected when the pin rotated. A pin rotation of 8° will normally result in approximately a 1% reduction in measured strain value, and 15° rotation results in approximately 3.4% reduction, according to the following formula: $\% \text{reduction} = (1 - \cos(\alpha)) \times 100\%$, where α represents the rotation angle.

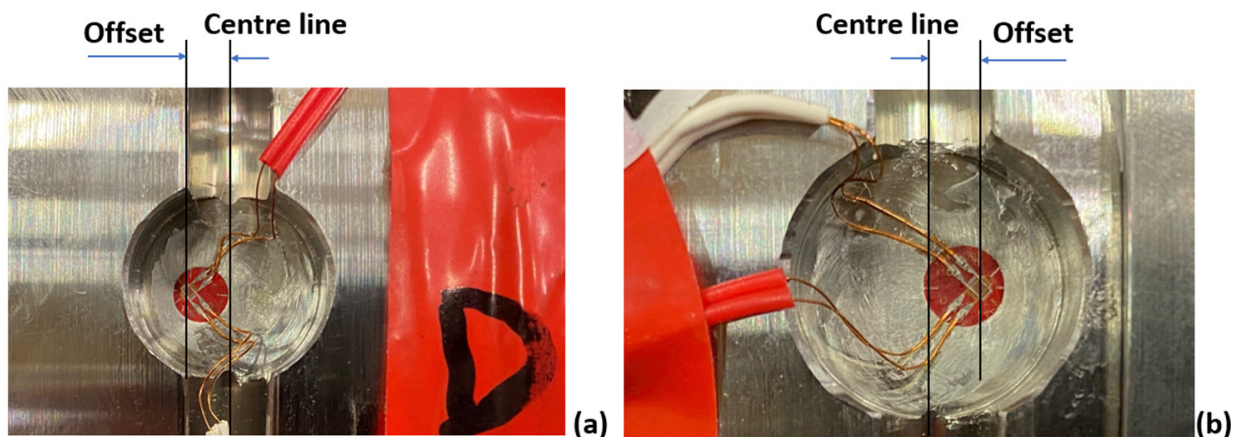


Figure 8. Examples of strain gauge offsets from pocket center line for (a) the cylindrical pin and (b) the expanding pin.

Table 3. Measured and calculated strain values at real cross-sections for 0° pin rotation and 500 kN external load.

Test No.	Pin End	Measured Strain Values, ϵ_{45° ($\mu\text{m/m}$)	Calculated Values:		
			For Average Shear Strains, ϵ_{ca} ($\mu\text{m/m}$)	For Max. Shear Strains, ϵ_{cm} ($\mu\text{m/m}$)	Max. to Measured Average Strain (%)
1	R	315	333	444	+26
	L	359	303	404	
2	R	355	>333	>444	
	L	320	<303	<404	
3	R	457	326	435	−3
	L	483	360	480	
4	R	581	>326	>435	
	L	115	<360	<480	
5	R	444	326	435	+8
	L	408	360	480	

Table 4. Measured and calculated strain values at real cross-sections for 15° pin rotation and 500 kN external load.

Test No.	Pin End	Measured Strain Values, ϵ_{45° ($\mu\text{m/m}$)	Calculated Values:		
			For Average Shear Strains, ϵ_{ca} ($\mu\text{m/m}$)	For Max. Shear Strains, ϵ_{cm} ($\mu\text{m/m}$)	Max. to Measured Average Strain (%)
1	R	330	322	429	+21
	L	346	293	391	
2	R	360	>322	>429	
	L	326	<293	<391	
3	R	430	315	420	−4
	L	493	348	464	
4	R	560	>315	>420	
	L	144	<348	<464	
5	R	434	315	420	+8
	L	384	348	464	

4. Discussion of Results

Severe joint wear and other damages can be expensive to repair, especially if the repairs must be performed outside of planned service and maintenance periods, and in addition they cannot always be performed on-site due to different restrictions or a lack of necessary tools. A long or complicated repair procedure or process can also shut down or reduce the production over a period, which can be the costliest consequence of the repair operation. Thus, the proposed repair procedure in this article aims to reduce the operational downtime in relation to the repair of the joint outside the planned service and maintenance stops, and prepare the joint to operate as normal until the next planned repair period. The repair procedure could also be applied as part of a planned repair, depending on the different companies' maintenance and operational requirements, statutory law, regulations and standards, when it comes to mechanical joints and their corresponding machines and equipment.

As part of this study, the measurement of the specific reduction in repair time and downtime by applying the proposed repair procedure compared to the alternative methods and procedures for repairing damaged pin joints has not been done. The values proposed for reduced repair time, and reduced downtime, are thus based on knowledge and experiences derived from different industries, in addition to studies from the literature. The

real repair time, costs and operational downtime due to such repairs depend highly on the type of industry, the types of machines, the type of break-down or damage, and in addition, the type of service and maintenance regime the operators of the machines are following. Several attempts have been made to develop different models to predict costs in relation to unwanted operational stops and unplanned downtime.

For instance, Edwards et al. [36] developed a three-staged model to predict hourly downtime costs of tracked hydraulic excavators that operated in the UK mining industry, where the first stage predicted the excavator cycles, the second predicted cost per hour, and the third gave an indication of the break-down cost based on the two previous predictions. Vorster and De La Garza [37] presented a model that was divided into four categories, which could quantify the consequential costs of downtime and the lack of availability of the machines. These were (i) the associated resources impact (ARI), which refers to costs that occur when a failure in one machine requires resources that are occupied elsewhere, or a negative impact on the productivity of one or several other machines, (ii) lack of readiness (LOR) penalty costs, if such exist, (iii) service-level impact (SLI) costs that represent more costly operations for machines working within the same work-group as the one that failed, and (iv) the alternative method impact (AMI), where a standard machine or vehicle may be forced to do the task instead of the specialized one that failed. Tignibidin et al. [38] developed algorithms for machine learning, with the aim of lowering operating costs by predicting unscheduled downtime, with a focus on oil and gas drilling and production facilities, where failure during drilling operations is important, but also mining activities. Both Scheu et al. [38] and Seyr et al. [39] have studied maintenance and repairs in relation to offshore wind farms, where operation and maintenance are significantly more demanding than in operations onshore, and production losses due to downtime are often much more significant than the costs of spare parts and repair actions. Weather conditions and especially the wave heights are factors that limit the accessibility of the wind farm.

The repaired joint (test 5) in this study has not been load-tested dynamically over time, but exposed to external static loads, from 100 kN to 500 kN, in both 0° and 15° rotational positions. The measured pin strains close to each pin-support joint, with repaired support bores, were compared to corresponding measurements from the four other tests:

- Test 1—a standard cylindrical pin with identically and distributed support clearance at each end;
- Test 2—a standard cylindrical pin with additional heavy wear and ovality at one of the ends (L);
- Test 3—an expanding pin with zero operational clearance at both ends;
- Test 4—an expanding pin with zero operational clearance at one end (R) and additional heavy wear and ovality at the other (L).

In addition, as part of the study, an investigation was performed on the easiness to (i) perform a 3D scan of the damaged bore surface, (ii) to make a 3D model of the required insert, (iii) to 3D-print the insert, and finally, (iv) to install it in the damaged joint and make the joint fit for further use. The 3D-printed insert was made in four parts for easy fit, as illustrated in Figure 5c. To make the insert one complete part with one single cut could reduce the risk of the loosening of one small part at the operation site, but in this test case, in a protected situation, it was produced in four parts to ease installation.

The 3D scanning process was relatively easy to perform when the bore surface was accessed from both sides of the support. The surface was cleaned and dried, and point markers were placed on the surface. In addition, the surface was sprayed to derive a matte white layer for the scanning tool to register the topography of the bore surface as accurately as possible. The 3D scanning process can obviously be more challenging under operational conditions, with humidity, salt, lubrication, and complicated access, compared to a clean and stable university laboratory. A digital 3D model of the insert was designed to fit well to the joint in question, and the final 3D model was inserted into the 3D printing machine for additive manufacturing. The CAD processing and the additive manufacturing can easily be performed at or close to any site where the damaged joint is operating, or at any

other site where such 3D tools are available, and the final product can be shipped to its destination. The complete process of scanning, modeling, and printing out the insert can be done on-site, if the required tools and knowledge are available.

The measured strain results from tests 1–5 are shown in Figures 9–13, for the 0° position, and we also show the percentage change in the strain when the pin was turned 15°, which should cause approximately a 3.4% reduction in measured strain values. An inaccuracy level of approximately ±1% is normally accepted for normal cylindrical load pins, which represents an 8° pin rotation. The errors can also result from the quality or type of strain gauges, the glue, the location of strain gauges, the test equipment and set-up, in addition to possible shifts of the pin position during loading. If applying an incorrect type of glue, the gauge wire might not be able to reflect the real dimension change of the main material. Wear and ovality at the support bore surface will often occur over time, due to heavy and repeating loads, vibrations, corrosion, etc., which again results in inaccuracy in the measurements of a standard cylindrical load pin. An expanding load pin can reduce or eliminate the inaccuracy due to unwanted movements in the pin during operation, due to its capability to wedge and lock the supports. In this investigation, the bore and pin production tolerances before any wear were H7/h7.

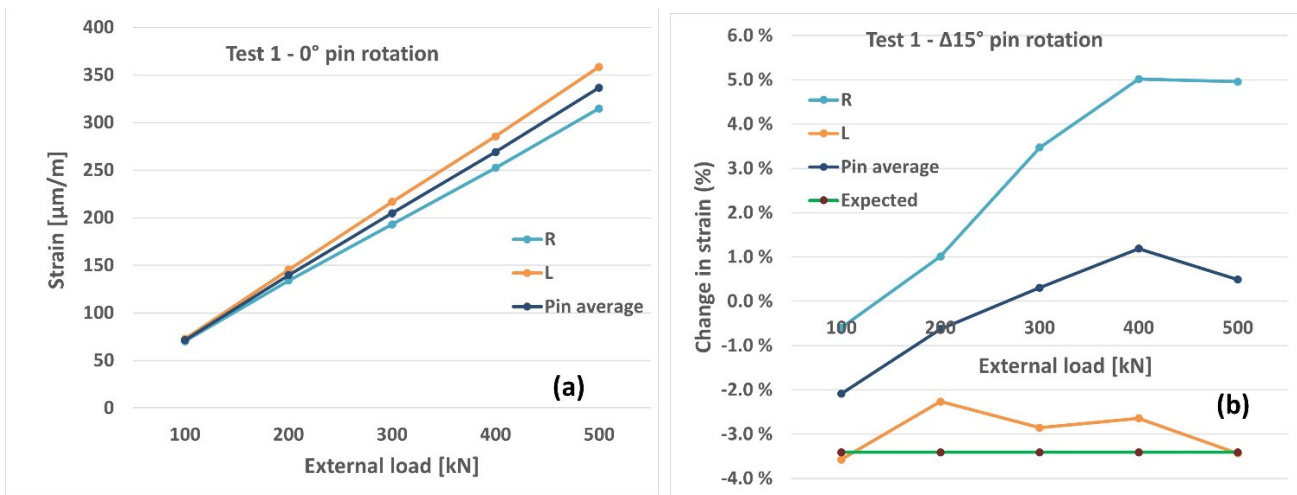


Figure 9. Test 1, (a) strains at 0° position, (b) percentage change of strains from 0° to 15° position.

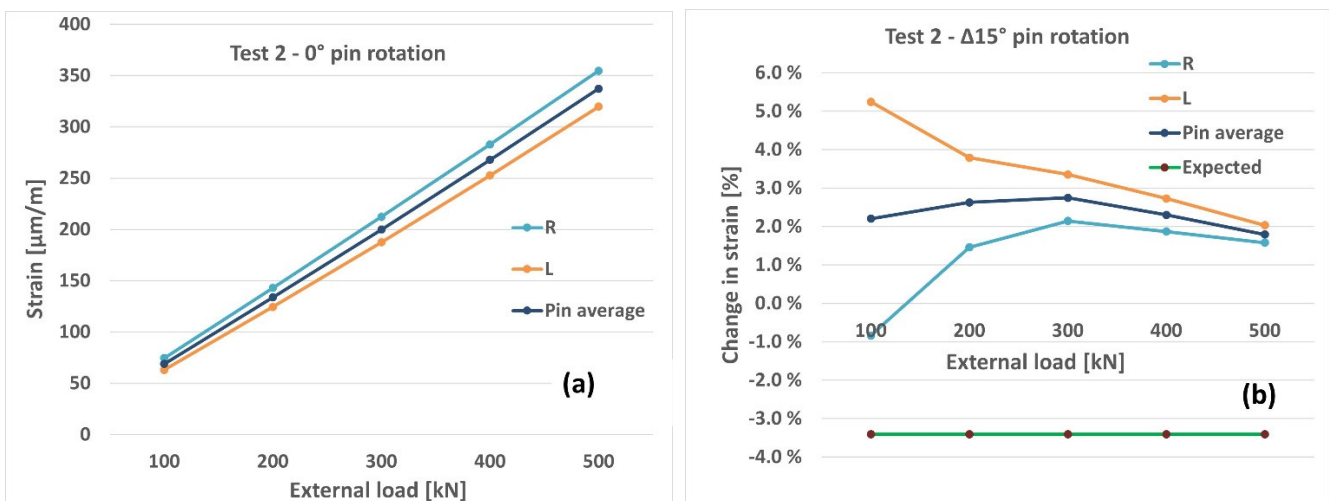


Figure 10. Test 2, (a) strains at 0° position, (b) percentage change of strains from 0° to 15° position.

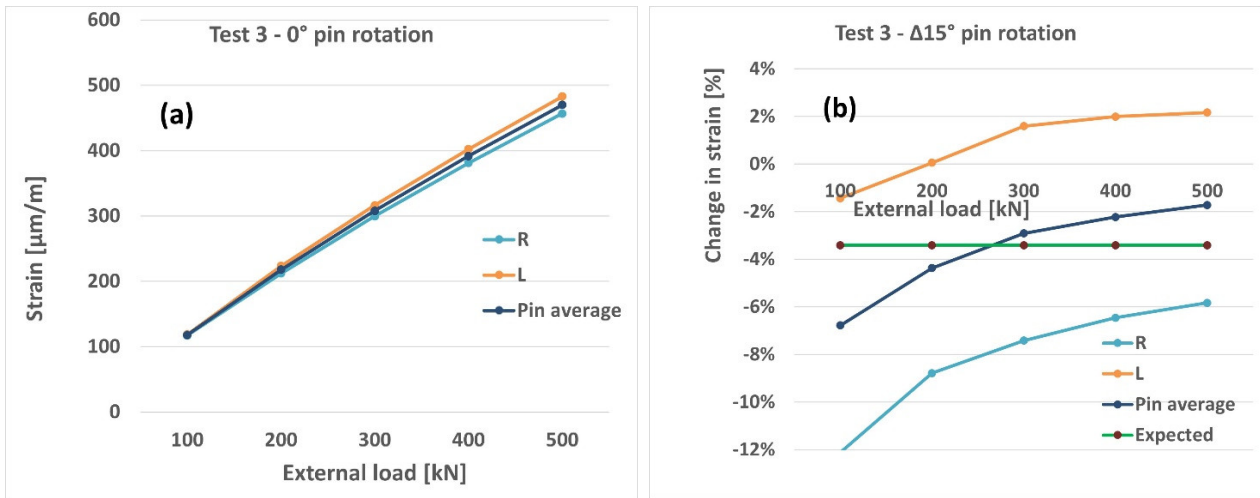


Figure 11. Test 3, (a) strains at 0° position, (b) percentage change of strains from 0° to 15° position.

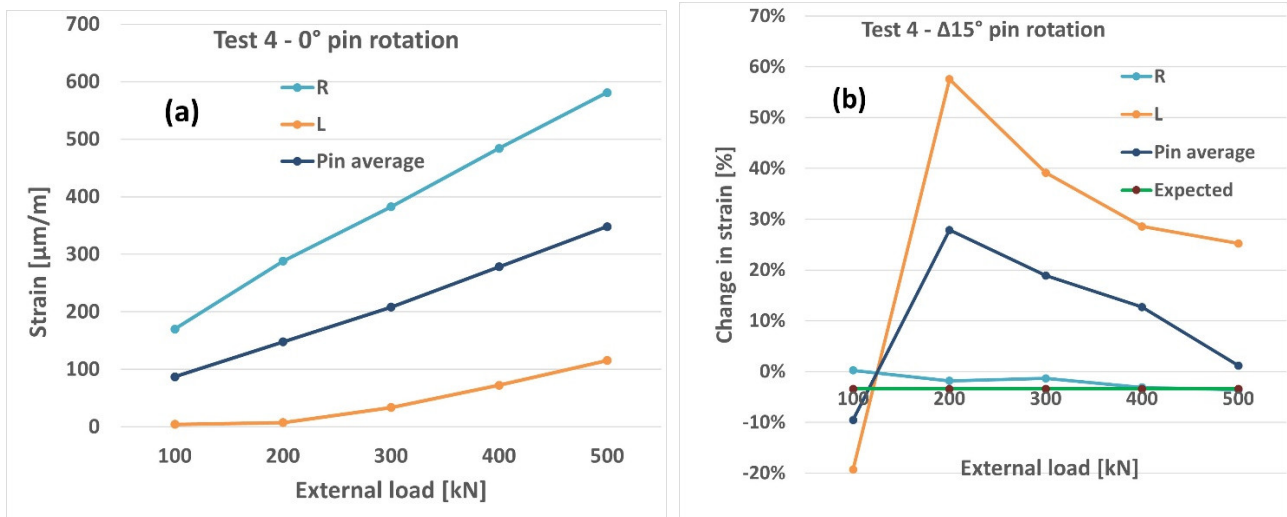


Figure 12. Test 4, (a) strains at 0° position, (b) percentage change of strains from 0° to 15° position.

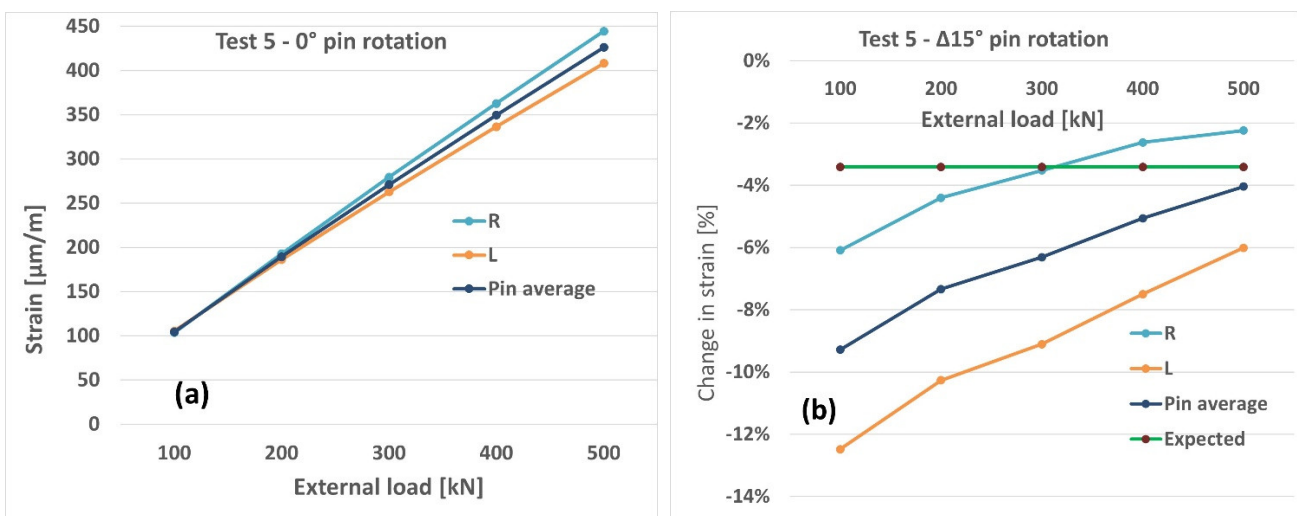


Figure 13. Test 5, (a) strains at 0° position, (b) percentage change of strains from 0° to 15° position.

Test 1 reflects a 0.9 mm diameter difference between pin and bore. This could represent both a wide installation clearance, which involves an even and identical wear on the two supports, and a normal joint situation. The results in Figure 9a illustrate the measured strains at the right and left pin ends for 0° pin rotation position, and Figure 9b shows the percentage changes in strain values after the pin has turned 15°. At 0° position the maximum strain of 359 [–] is seen on the right-hand side, which is 14% more than the left-hand side. For the 15° position the strain difference between the two pin ends decreased to 5%. The average pin strain value at 500 kN load increased 0.5%, instead of the expected decrease of 3.4% due to pin rotation from 0° to 15°. This gives a difference between measured pin average and expected strain values of +3.9%.

Test 2 (Figure 10) shows a situation with heavy wear and ovality (0–5 mm) in the left-hand support, and less but more evenly distributed (0.9 mm) in test 1 on the other. Such a wear and ovality pattern might force the pin to lock to the support at the right-hand side, and maybe only slightly touch the support on the left-hand side, and thereby bend and possibly turn when loaded, which resulted in the measured values illustrated in Figure 10a. We measured a strain value of 355 [–] at the right-hand side, at 0° position, which is 11% higher than on the left-hand side. Thus, the most loaded pin end shifted from left to right compared to the results from test 1. At the 15° position the measured difference was 10%. The pin average strain value at 500 kN load increased by +1.8%, instead of the expected decrease of 3.4%, as the pin turned from 0° to 15°, which gave a difference of +5.2%—see Figure 10b. Situations with heavy wear and ovality of the supports are common and result normally in higher inaccuracy of measurements, as indicated by the measured results of this study.

Similar to test 1, test 3 had evenly distributed wear at each end, but in this case an expanding pin was tested instead of a standard cylindrical pin. The expanding pin eliminated the existing diameter clearances of 0.9 mm, down to zero, and locked the pin to both the support bores and prevented any unwanted movements of the pin. The pin average strain value at 500 kN load decreased to –1.7%, which is close to the expected 3.4%, as the pin turned from 0° to 15°, and gave a difference of only +1.7%, as indicated in Figure 11b. The load distribution between the pin ends varied by 6% and 15% in the 0° and 15° pin positions, respectively, both with the highest strain values at the left-hand side.

Test 4 was identical to test 2 in terms of exposure to severe wear and ovality (0–5 mm) at one end, i.e., the left-hand support, but with an expanding pin instead of a cylindrical type of pin. The effect of the expanding pin compensated for all the clearance at the pin's right-hand side, but not all the excessive wear and ovality at the left-hand side. Thus, the pin was fixed at the right-hand side and hung partly loose at the left-hand side. When the pin was loaded with the maximum load, the right-hand side took most of the shear force, approximately five times more than the left-hand side, as illustrated in Figure 12. The pin average strain value at 500 kN load increased by +1.2%, instead of a decrease to –3.4% as would be expected, as the pin turned from 0° to 15°, which gave a difference of +4.6%—see Figure 12b. A major difference in strains between the two ends was measured here, as expected, as one end (R) was fixed to its support and the other (L) hung partly loose.

The assembly in test 5 compensated for the excessive wear and ovality by introducing a 3D-printed insert to fit the damaged bore, but with a new, circular and smaller bore diameter (Ø85 mm) that was made to fit the expanding pin. The average strain value at 500 kN load decreased to –4.0%, which is close to the expected decrease of 3.4%, as the pin turned from 0° to 15°, which gave a difference of only –0.6%—see Figure 13b. The load distribution between the pin ends varied by 9% and 13% for the 0° and 15° pin positions, respectively.

In general, the pin average strain level was lower for the cylindrical pin in test 1 than for the expanding pin in test 3, although the strain gauges compensated for the unplanned temperature changes during testing and any additional axial tensions or compressions in the pin, and since they were placed at the pins' neutral axis there should not have been any bending effects on the strain values either. The average strain at 500 kN load is in the range 457–483 $\mu\text{m}/\text{m}$ at 0° position for test 3, compared to around 315–359 $\mu\text{m}/\text{m}$ for test 1 at same pin position. A possible reason could be the inaccuracy or differences

regarding where the strain gauges were placed, as illustrated in Figure 8. The average pin cross-sectional area under the strain gauges was smaller for the expanding pin (4589 mm²) in tests 3–5, compared to the cylindrical pin (4956 mm²) in tests 1 and 2. In addition, the lengths of the axial bolt holes at the expanding pin ends reached up to where the strain gauges were installed, and could have affected the strain measurements by reducing the total cross-section area, and consequently increase the measured strain values. The measured strain values decreased with the inverse square of the diameter increase, as the cross-sectional area increased with the square value.

The measured strain values at the 0° pin position and 500 kN external load scenario have been compared with the calculated average and maximum strain values, as indicated in Tables 3 and 4, and they are in good compliance. The calculated maximum strain values for the whole pin are in the range of −3% to +26% of the measured values for test 1, 3 and 5. For the 15° pin position, the corresponding values were in the range of −4% to +21%, with smaller differences for the expanding pins in tests 3 and 5.

When a joint support bore with a cylindrical pin is damaged, a decision on what to do must be taken, including:

- No stop of production: continue with the damaged support (type test 2) until the next service stop. In this case, a severely damaged support could lead to pin breakage, a damaged machine, and put people in danger;
- Long stop of production: stop production to perform the necessary repair and continue with a new standard cylindrical pin (type Test 1). If severe wears and ovality have occurred, they will occur again after repair, under the same operational conditions;
- Long stop of production: stop production, perform the necessary repair and continue with a new expanding pin (type test 3). The expanding pin will prevent the wear process from repeating;
- Short stop of production: make a short stop of production and change from cylindrical to expanding pin (type Test 4), if the wear is not severe, but if the wear is severe the expanding pin will not wedge lock sufficiently at the damaged area;
- Short stops of production: make a short stop of production to 3D scan the damaged surfaces, and later, another short stop to introduce the temporary repair insert and continue with a new expanding pin (type Test 5), if the wear is severe. The joint and the machine will continue to operate until the next planned service stop, or longer.

A cylindrical pin will often damage the support bore and create increased play over time. If the same pin, or a new cylindrical pin, is installed into the same joint after the repair of the support (as for Test 1), the same problem with increasing play could easily repeat. Karlsen and Lemu [1] used the Hertz formula for contact pressure to calculate the contact width, and the maximum and average contact pressure, for a cylindrical pin with (a) h7 tolerance, and (b) play on the bore diameter, and for an expanding pin, as a function of an increasing external load. The calculations show a rapid increase in contact pressure when the play between a cylindrical pin and the bore increases, while for an expanding pin, the play stays constant at zero. The contact stresses for the expanding pin change linearly with the changing external load because the contact width is constant, but at zero external load this pin will still have a certain contact stress due to the wedge pressure from the expanding end-sleeve. For the cylindrical pin, the contact width increases with an increasing external load, which results in a less steep increase in the total contact stress compared to an expanding pin, but only as long as there is no wear at the supports. Even a small wear rate increases the clearance between the cylindrical pin and the bore, and as a result the contact area decreases, and the contact pressure increases, leading to even more increase in the wear rate (as indicated in test 2). As a result, the contact stresses increase to a level much higher than for an expanding pin assembly, with additional stick–slip situations.

5. Conclusions

When a cylindrical pin joint is damaged by wear and ovality, a decision must be taken as to whether to continue without taking any action, or acting and performing some repair

procedures. Five different options were investigated by loading the pin statically and measuring the pin strain close to each support, in two different pin positions, 0° and 15° . The measured and calculated strain values at those pin positions for tests 1, 3 and 5 were compared when loaded externally from 100 kN to 500 kN, in steps of 100 kN, and these tests were those with equal operational clearances between the pin and support at each end of 0.9 mm, 0 mm and 0 mm, respectively.

The standard cylindrical pin in test 1 showed +26% and +21% difference between the calculated maximum and measured pin strain, for the 0° and 15° pin positions, respectively, while for the expanding pin in test 3 the numbers were -3% and -4% , and for test 5 they were +8% and +8%. There seems to be good correlation between the calculated maximum strain values and the measured ones, especially for the expanding pin tests 3 and 5.

The differences in measured strain between each pin end, or the gap, were the highest for test 4 (damaged support), as expected since, that pin was fixed at one end and hung loose in the other. The smallest differences were noted for the three tests with no ovality at supports—tests 1, 3 and 5, with $\pm 6\%$, $\pm 3\%$ and $\pm 4\%$, respectively, of the average pin strain values. It can also be seen that the reduction in strain value when turning the pin from the 0° to the 15° position was close to the calculated 3.4%, especially for tests 3 and 5. For test 5 the result was only 0.6% away from the expected value, compared to 1.7% for test 3, and 3.9% and 5.2% for tests 1 and 2, respectively.

Based on the tests and analyses performed in this investigation, it can be concluded that the repair procedure of a damaged support bore, including the installation of a 3D-printed bushing, can be a viable solution. This is relatively easy to perform, and the 3D-printed insert seems to fit very well with both the damaged bore and the expanding pin. In addition, based on the results of this investigation, the tests of the pin with the repair insert (test 5) do not show any negative or weak results compared to the other tests, but rather the results are stronger. The procedure requires one short stop in operation for the 3D scanning of the damaged surface, and another short stop at a later stage to install the 3D-printed repair insert and a new expanding pin system. The machine can be operated during the production of the repair insert and pin system. The alternative is typically a longer stop in operation, which includes the time of removing the old pin, repairing the worn area, and installing the new pin, during which downtime due to the repair of wear damage can be extensive.

Author Contributions: Conceptualization, Ø.K.; methodology, Ø.K. and I.B.; software, Ø.K. and I.B.; validation, Ø.K. and H.G.L.; formal analysis, Ø.K.; investigation, Ø.K. and I.B.; resources, Ø.K. and H.G.L.; data curation, Ø.K.; writing—original draft preparation, Ø.K.; writing—review and editing, Ø.K. and H.G.L.; visualization, H.G.L.; supervision, H.G.L.; project administration, Ø.K.; funding acquisition, Ø.K. All authors have read and agreed to the published version of the manuscript.

Funding: The research was conducted as part of an Industrial PhD study funded by the Norwegian Research Council and Bondura Technology AS, Grant nr. 283821. This financial support is highly appreciated.

Institutional Review Board Statement: Not applicable.

Informed Consent Statement: Not applicable.

Data Availability Statement: Not applicable.

Conflicts of Interest: The authors declare no conflict of interest.

References

1. Karlsen, Ø.; Lemu, H.G. Questionnaire-based survey of experiences with the use of expanding PIN systems in mechanical joints. *Results Eng.* **2021**, *9*, 100212. [[CrossRef](#)]
2. Karlsen, Ø.; Lemu, H.G. Fretting fatigue and wear of mechanical joints: Literature study. *IOP Conf. Ser. Mater. Sci. Eng.* **2019**, *700*, 012015. [[CrossRef](#)]
3. Karlsen, Ø.; Lemu, H.G. On Modelling Techniques for Mechanical Joints: Literature Study. In *International Workshop of Advanced Manufacturing and Automation, Proceedings of the Advanced Manufacturing and Automation IX, IWAMA 2019, Plymouth, UK, 21–22*

- November 2019; Wang, Y., Martinsen, K., Yu, T., Wang, K., Eds.; Lecture Notes in Electrical Engineering; Springer: Singapore, 2020. [CrossRef]
4. Berkani, I.; Karlsen, Ø.; Lemu, H.G. Experimental and numerical study of Bondura® 6.6 PIN joints. *IOP Conf. Ser. Mater. Sci. Eng.* **2017**, *276*, 012028. [CrossRef]
 5. Chikmath, L.; Dattaguru, B. Prognostic analysis of fastener joints in straight attachment lugs. *Int. J. Struct. Integr.* **2017**, *8*, 404–422. [CrossRef]
 6. Bondura. Bondura Technology. Available online: <https://www.bondura.no> (accessed on 23 March 2022).
 7. Karlsen, Ø.; Lemu, H.G. Safety related study of Expanding Pin systems application in lifting and drilling equipment within Construction, Offshore, and Marine sectors. *IOP Conf. Ser. Mater. Sci. Eng.* **2021**, *1201*, 012026. [CrossRef]
 8. Soković, M.; Kopač, J. RE (reverse engineering) as necessary phase by rapid product development. *J. Mater. Process. Technol.* **2006**, *175*, 398–403. [CrossRef]
 9. Yao, A. Applications of 3D scanning and reverse engineering techniques for quality control of quick response products. *Int. J. Adv. Manuf. Technol.* **2005**, *26*, 1284–1288. [CrossRef]
 10. Helle, R.H.; Lemu, H.G. A case study on use of 3D scanning for reverse engineering and quality control. *Mater. Today Proc.* **2021**, *45*, 5255–5262. [CrossRef]
 11. Javid, M.; Haleem, A.; Singh, R.P.; Suman, R. Industrial perspectives of 3D scanning: Features, roles and it's analytical applications. *Sens. Int.* **2021**, *2*, 100114. [CrossRef]
 12. Gebisa, A.W. Design Procedures and Mechanical Behaviour Characterization of Additive Manufactured Components. Ph.D. Thesis, UiS No. 464. University of Stavanger, Stavanger, Norway, 2019.
 13. ASTM F2792-12; Standard Terminology for Additive Manufacturing Technologies. ASTM International: West Conshohocken, PA, USA, 2012.
 14. ASTM F2792-12A; ASTM International, Standard Terminology for Additive Manufacturing Technologies. ASTM International: West Conshohocken, PA, USA, 2012.
 15. Kim, H.; Cha, M.; Kim, B.C.; Lee, I.; Mun, D. Maintenance Framework for Repairing Partially Damaged Parts Using 3D Printing. *Int. J. Precis. Eng. Manuf.* **2019**, *20*, 1451–1464. [CrossRef]
 16. Wits, W.W.; García, J.R.R.; Becker, J.M.J. How Additive Manufacturing Enables more Sustainable End-user Maintenance, Repair and Overhaul (MRO) Strategies. In Proceedings of the 13th Global Conference on Sustainable Manufacturing, Ho Chi Minh City, Vietnam, 16–18 September 2015.
 17. Buchanan, C.; Gardner, L. Metal 3D printing in construction: A review of methods, research, applications, opportunities and challenges. *Eng. Struct.* **2019**, *180*, 332–348. [CrossRef]
 18. Ueda, E.K.; Barari, A.; Sato, A.K.; Tsuzuki, M.S. Detection of Defected Zone Using 3D Scanning Data to Repair Worn Turbine Blades. *IFAC-PapersOnLine* **2020**, *53*, 10531–10535. [CrossRef]
 19. Mortazavian, E.; Wang, Z.; Teng, H. Thermal-Mechanical study of 3D printing technology for rail repair. In Proceedings of the ASME International Mechanical Engineering Congress and Exposition, Pittsburgh, PA, USA, 9–15 November 2018; American Society of Mechanical Engineers: New York, NY, USA, 2019; Volume 52019, p. V002T02A052.
 20. Wan, M.L.; Liu, S.F.; Huang, D.; Qu, Y.; Hu, Y.; Su, Q.S.; Zheng, W.X.; Dong, X.M.; Zhang, H.W.; Wei, Y.; et al. Biocompatible heterogeneous bone incorporated with polymeric biocomposites for human bone repair by 3D printing technology. *J. Appl. Polym. Sci.* **2021**, *138*, 50114. [CrossRef]
 21. Zhao, L.; Pei, X.; Jiang, L.; Hu, C.; Sun, J.; Xing, F.; Zhou, C.; Fan, Y.; Zhang, X. Bionic design and 3D printing of porous titanium alloy scaffolds for bone tissue repair. *Compos. Part B Eng.* **2019**, *162*, 154–161. [CrossRef]
 22. Maroulakos, M.; Kamperos, G.; Tayebi, L.; Halazonetis, D.; Ren, Y. Applications of 3D printing on craniofacial bone repair: A systematic review. *J. Dent.* **2019**, *80*, 1–14. [CrossRef]
 23. Zhu, W.; Zhao, Y.; Ma, Q.; Wang, Y.; Wu, Z.; Weng, X. 3D-printed porous titanium changed femoral head repair growth patterns: Osteogenesis and vascularisation in porous titanium. *J. Mater. Sci. Mater. Med.* **2017**, *28*, 62. [CrossRef]
 24. Cheng, J.; Gao, Y.; Long, Z.; Pei, G.; Li, Z.; Meng, G. Repair of distal fibular and lateral malleolus defects with individualized 3D-printed titanium alloy prosthesis: The first case report from China. *Int. J. Surg. Case Rep.* **2022**, *94*, 107057. [CrossRef]
 25. Wheatstone, C. An account of several new instruments and processes for determining the constants of a voltaic circuit. *Philos. Trans. R. Soc. Lond. Ser. A* **1843**, *4*, 469–471.
 26. Hooke, R. *De Potentia Restitutiva*; John Martyn Printer: London, UK, 1678.
 27. Hoffmann, K. *An Introduction to Measurements Using Strain Gages*; Hottinger Baldwin Messtechnik GmbH: Darmstadt, Germany, 1989.
 28. Nässelqvist, M.; Gustavsson, R.; Aidanpää, J.-O. Bearing Load Measurement in a Hydropower Unit Using Strain Gauges Installed Inside Pivot Pin. *Exp. Mech.* **2012**, *52*, 361–369. [CrossRef]
 29. Straininstall. Available online: <http://www.straininstall.com> (accessed on 1 September 2021).
 30. Sensy. Available online: www.sensy.com (accessed on 15 September 2021).
 31. Creaform. Creaform3d. 2002. Available online: <https://www.creaform3d.com/> (accessed on 11 February 2021).
 32. Autodesk. Available online: <https://www.autodesk.com/> (accessed on 11 February 2021).
 33. Sverdrup Steel. Available online: <https://www.sverdrupsteel.com> (accessed on 13 September 2021).
 34. Markforged. Available online: <https://markforged.com/> (accessed on 11 February 2021).
 35. Budynas, R.G.; Nisbett, J.K. *Shigley's Mechanical Engineering Design*, 9th ed.; McGraw-Hill: New York, NY, USA, 2011.

36. Edwards, D.J.; Holt, G.D.; Harris, F.C. Predicting downtime costs of tracked hydraulic excavators operating in the UK opencast mining industry. *Constr. Manag. Econ.* **2002**, *20*, 581–591. [[CrossRef](#)]
37. Vorster, M.C.; De La Garza, J.M. Consequential Equipment Costs Associated with Lack of Availability and Downtime. *J. Constr. Eng. Manag.* **1990**, *116*, 656–669. [[CrossRef](#)]
38. Scheu, M.; Matha, D.; Hofmann, M.; Muskulus, M. Maintenance Strategies for Large Offshore Wind Farms. *Energy Procedia* **2012**, *24*, 281–288. [[CrossRef](#)]
39. Seyr, H.; Muskulus, M. Value of information of repair times for offshore wind farm maintenance planning. *J. Phys. Conf. Ser.* **2016**, *753*, 092009. [[CrossRef](#)]

Appended Paper IV

Safety related study of Expanding Pin Systems Application in Lifting and Drilling Equipment within Construction, Offshore, and Marine sectors

KARLSEN, Ø.; LEMU, H. G.

IOP Conference Series: Materials Science and Engineering. IOP Publishing, 2021. p. 012026.

[doi:10.1088/1757-899X/1201/1/012026](https://doi.org/10.1088/1757-899X/1201/1/012026)

PAPER • OPEN ACCESS

Safety related study of Expanding Pin systems application in lifting and drilling equipment within Construction, Offshore, and Marine sectors

To cite this article: Ø Karlsen and H G Lemu 2021 *IOP Conf. Ser.: Mater. Sci. Eng.* **1201** 012026

View the [article online](#) for updates and enhancements.

You may also like

- [Critical current density and flux pinning in \$\text{BaFe}_{1-x}\text{Pt}_x\text{As}_2\$ and La doped \$\text{Ba}_{2-x}\text{La}_x\text{Fe}_{1-x}\text{Pt}_x\text{As}_2\$ polycrystals](#)
Y Öner and C Boyraz
- [Vision-based adaptive stereo measurement of pins on multi-type electrical connectors](#)
Delong Zhao, Feifei Kong and Fuzhou Du
- [Dependence of the IBEX Ribbon Geometry on Pitch-Angle Scattering outside the Heliopause](#)
E. J. Zirnstein, M. A. Dayeh and J. Heerikhuisen

ECS Toyota Young Investigator Fellowship



For young professionals and scholars pursuing research in batteries, fuel cells and hydrogen, and future sustainable technologies.

At least one \$50,000 fellowship is available annually.
More than \$1.4 million awarded since 2015!



Application deadline: January 31, 2023

Learn more. Apply today!

Safety related study of Expanding Pin systems application in lifting and drilling equipment within Construction, Offshore, and Marine sectors

Ø Karlsen^{1,2,*} and H G Lemu²

¹ Bondura Technology AS, Bryne, Norway

² Department of Mechanical and Structural Engineering and Materials Science, University of Stavanger, Stavanger, Norway

*Corresponding author: oyvind.karlsen@uis.no

Abstract. A questionnaire-based survey has been performed among original equipment manufacturers (OEMs), sub-suppliers, engineering companies, end-users, service & maintenance, and “others”, as part of an investigation to clarify their relationship to expanding pin system, compared to standard, cylindrical pins. In addition, a short literature study on onshore cranes is conducted. The survey is based on 9 questions about safety for personnel and machine, breakage, and wear of pins and supports, and installation and retrieval easiness of pins. The analysis of the responses indicates that safety for personnel and machines/equipment is regarded mainly as either “Important” or “Crucial and decisive”, and that the expanding pin solution is regarded as “better” or “equal” compared to the standard, cylindrical pin, both for “safety level”, “risk for breakage of pin & support”, “tear & wear on pin & support” and “installation and retrieval time”.

Keywords: Expanding pins, heavy equipment, tear and wear, breakage, lifetime, downtime, safety

1. Introduction

Almost any kind of heavy equipment in almost any type of industry has shear pins in the joints to make movements possible between the different parts. These joints are typically called Rotary Joints where the Revolute Joints ideally provide 1 Degree of Freedom (DOF) and the Spherical Joints provide up to 3 DOF. A cylindrical pin in a joint will normally have some installation clearance, which remains and increases during operation due to wear and compression of the support bore surface. The increased clearance in combination with axial loading, planned or unplanned, rotational, and normal radial loading from its operation, can result in a multiaxial stress distribution at the pin and bore surface [1,2]. This is especially the case when the support or lug material is of higher strength steel, which is a common way of reducing the equipment total weight and increase the lifting or loading capacities. Such multiaxial stress patterns from the combination of normal stresses and tangential stresses can result in fretting crack initiation and propagation, with a rupture of the support as a possible result, with increased risk of damage and fatalities. This phenomenon is well known and documented and called fretting fatigue failure and could reduce the component lifetime considerably under the right conditions [3,4]. Talmi et al. [1] concluded that the fretting fatigue mechanism is the dominating failure mechanism in a pin



joint subjected to cyclic loading conditions, by comparing their extended finite element (XFEM) results with observed results from the literature.

Lifting and hoisting equipment such as cranes are often subject to strict rules and certifications due to the nature of the operations they are performing, and the risks involved. The dynamic loading could increase the stress level up to two times, or more [5], depending on the operational loads and internal joint clearance, and a twenty-fold increase in accelerations of pin movements. Lagerev and Lagerev [5,6] have investigated ways to increase the life of hinge lugs by eliminating backlash by use of elastic damping, and other techniques are to implement antifriction bushes, polymer coatings or different hardening methods on the adjacent contact surfaces [7]. Another technique to control rapid movements and reduce the dynamic reaction forces in the joints is the heave compensation approach [8-11], typically for offshore, maritime, floating wind cranes, and sub-sea operations. A floating structure such as a ship can have six degrees of movement; a) heave, b) sway, c) surge, d) roll, e) pitch, and f) yaw, which all can affect negatively lifting and loading operations. Without a compensation system, such uncoordinated relative movements can generate high dynamic and shock loads into the equipment and specially into the pinned joints, who can suffer friction wear, corrosion wear, fretting wear, and deformations which again can result in increased play in the joint, see Figure 1 (a), or even breakage of the pin.

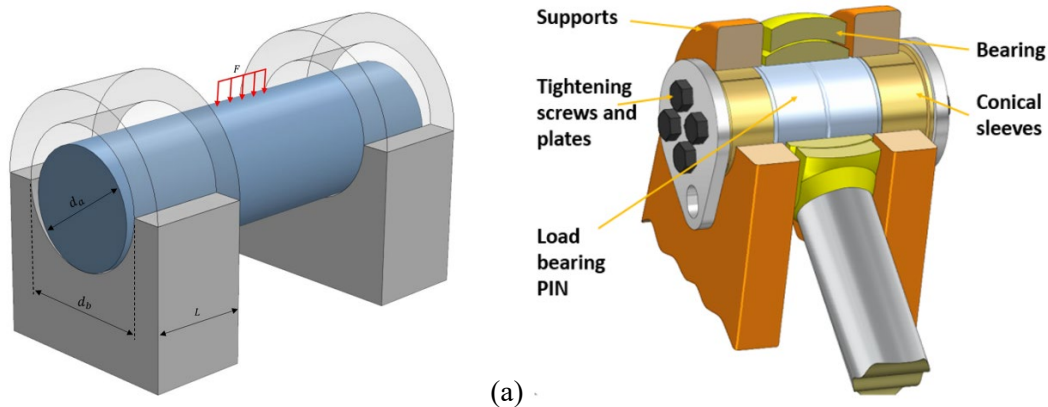


Figure 1. An illustration of pin in support – (a) standard cylindrical pin, and (b) expanding pin

The purpose of this study is to analyse the importance of use of expanding pins, Figure 1 (b), related to safety for personnel, equipment, and environment, on cranes, drilling equipment, and other heavy machinery. The study is based on analysis of previous publications, investigations, and reports, in addition to a questionnaire-based survey [14], and communication with some companies operating in the Norwegian and global energy area.

2. Background and applications of expanding pin systems

2.1. Background

Any heavy lifting equipment within any industry involving standard cylindrical shear pins will be exposed to a relative movement between pin and support with the wear issues it brings, due to the diameter difference between the pin and the support bore, typically for installation purposes. The expanding pin system [12,13] has got the ability to expand towards the support bore surfaces and lock the pin with a radial wedge pressure, and by that eliminate the wear issues at the pin – bore contact surfaces. Normally the wear problems occur at the support bores surfaces which normally have a lower steel quality grad, see Table 1, but the pin which has a higher strength and harder surface can suffer breakage if the shock loads are increased over maximum design value.

An expanding pin will lock the pin 360° to the support during the complete operation, independent of external load size and direction and thereby prevent the wear-risk experienced in the standard cylindrical pins. The steel qualities of the bearing element of an expanding pin will be customized, but

normally of same quality as the cylindrical pin, as shown in Table 1 [14]. The risk to be exposed to wear for the expanding pin solution and for a cylindrical one is different, and both are shown in Figure 2.

Table 1. Physical properties of typical pin and support materials for heavy machinery

Steel grade:	Typically use:	Yield, $R_{p0.2}$ min. [MPa]	Tensile, R_m min. [MPa]	Size range [mm]
S355 (EN 10025-3)	Supports	355	470	40 - 80
S420 (EN10027-2)	Supports	370	520 - 680	63 - 80
42CrMo4+QH (EN10083-3)	Pin	650	900	$\leq \text{Ø}100$
34CrNiMo6+QH (EN10083-3)	Pin	800	1000	$\leq \text{Ø}100$
30CrNiMo8+QH (EN10083-2)	Pin	900	1100	$\leq \text{Ø}100$
S17-4 PH D1150 / 1.4542	Pin	725	930	-
S165M / 1.4418	Pin	700	900-1100	-

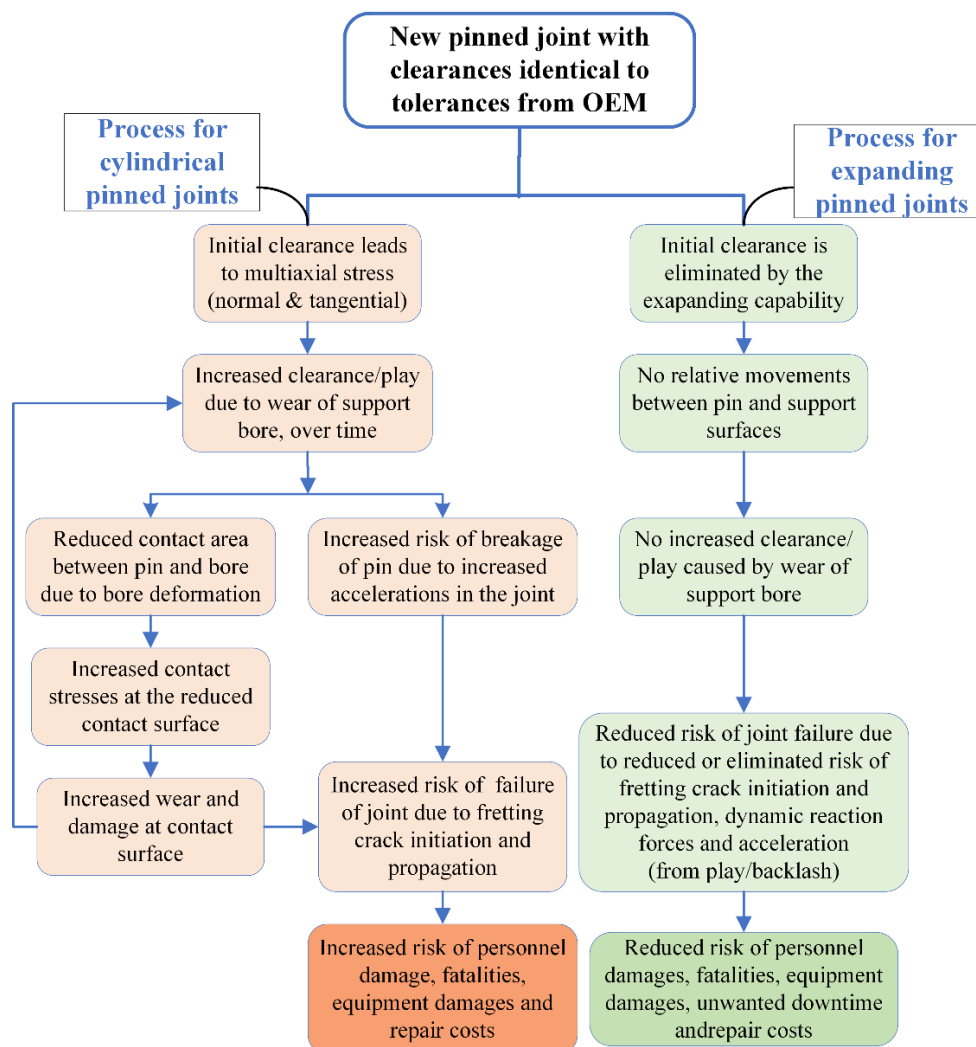


Figure 2. Load - failure processes for cylindrical pinned joints and expanding pinned joints (arrows indicate the outcome)

Typical support materials can be S355 construction steel or S420 quality, which is a high strength weldable structure with fine grain steel quality. For some specific grades, it can reach high impact properties at temperatures as low as -50°C . The pin is often exposed to high, oscillating, dynamic or

even shock loads, and it serves as an important and critical connection element between different parts of the machine. The pin material is therefore normally of a higher strength steel grade than the supports, often of quality 42CrMo4+QH, 34CrNiMo6+QH, 30CrNiMo8+QH, 17-4 PH, or S165M / 1.4418, whose physical properties are given in Table 1 [14].

A standard pin will have a contact surface and pressure with the support bore up to a maximum width of 180° with changing direction depending on the external load size and direction, which results in a stick-slip situation moving around, also depending on external load size and direction. Any initial damage or deformation of the support bore will increase and accelerate the damage of the joint, see Figure 2.

2.2. Applications of expanding pin systems

The expanding pin system can be applied in any joint where a standard cylindrical pin can be used but is normally considered in positions where there is problem or potential issue that cannot be resolved by the traditional solution. Such issues can be vibrations, shock loads, challenges with wear and fretting, requirements for quick and safe installation and retrieval of pins, and low life-costs and high production rate. The expanding pin is widely applied in drilling equipment both offshore and onshore, offshore cranes and maritime cranes, maritime hatches, winches, and rudder systems, within paper and steel mills, construction vehicles and mining equipment, and even in the space industry. The pin system is relatively well known within the Norwegian OEMs (Original Equipment Manufacturer) of maritime and offshore cranes, and drilling equipment, and considered as the safest, quickest, and most economical solution [14].

3. Research methodology

A questionnaire-based survey was sent to 256 potential responders during the first weeks and months of the COVID-19 pandemic in 2020, and 58 responded. A study based on that survey was published in 2021 [14], and this investigation is partly based on some of the responses from the original survey. The responders in the original survey were from 10 different countries with companies from Norway as the main group (67%). In addition, there are companies from Sweden, Canada, Scotland, Greece, Brazil, Finland, The Netherlands, USA, and Germany. The different responders operate in various markets as, (a) Offshore Oil&Gas, (b) Maritime, (c) Subsea, (d) Dredging, (e) Mining onshore & offshore, (f) Construction & earth moving, (g) Specialized machines and equipment, (h) Steel and paper industry, and (i) Other. In this study, only the following segments are included: (a), (b), (c), (d) and (f), and some of the companies have activities in more than only one of the segments. The survey was directed to persons and positions with responsibility related to pin solutions, or related machines and equipment.

In addition, a short literature study on safety and accidents with construction cranes was performed to better understand the importance of pins in such events. The third part of the research is based on a short questionnaire answered by three national and international energy companies established in the Stavanger region, Norway.

4. Literature study and survey

As part of this study, a short literature study on accidents with onshore construction cranes, mainly tower cranes, was performed, together with a look into the Norwegian and foreign Petroleum and Offshore & Maritime sectors.

4.1. Onshore construction cranes

Three Hammerhead Tower cranes of same model collapsed [15] the same day, within hours of each other, in Miami and Fort Lauderdale on September 10th, 2017, during the Hurricane Irma. More specifically, the common failure of the three cranes was the detachment of the crane jibs from their turntables due to turbulent wind loads. The bottom of the tubular framed tower top was attached with pins at four locations at the top of the turntable. The long pendants consist of several shorter pieces, connected with pins. The bottom chords of the jib were pinned to the turntable, and the counter jib was

connected to the turntable also with pins. During the heavy winds the jib came off the pinned connection, and two pins failed when the cotter pins loosened, for all three cranes.

Peraza and Travis [16] investigated the rapidly changing regulations and presented a review of crane accident statistics at a local (New York) and national (USA) level. In the period from 1992 to 2006, there were an average of 42 construction worker fatalities per year, which had increased to 54 in 2008. Seven crane related accidents were analysed with the 540 feet high “Big blue” crane with rated lifting capacity of 500 tons as the biggest one. These accidents resulted in some legislation changes in regulation of tower crane operations, and it was imposed additional requirements for testing of specific critical crane components, as joints, pins, and bolts. This shows the importance of pins and bolts as critical elements in cranes, where increased clearances between pin and support generates increased dynamic reaction forces and highly increased accelerations. Such increased dynamic forces could surpass the bolts design loads and initiate fretting wear issues at the bore surface.

The Department of Occupational Safety and Health in Malaysia sent out a Safety Alert [17] in 2017 regarding a tower crane accident, due to failure of counter jib platform connection pin, see Figure 3. The safety alert indicates the breakage of the two cylindrical pins as the main reason for the accident, without further explanations.



Figure 3. Tower crane accident – (a) crane after accident, and (b) broken pins

The UK Government through Health and Safety Executive (HSE) aims to reduce work-related death, injury, and ill health, and requested Health and Safety Laboratory (HSL) to prepare a report [18] about tower crane incidents around the world between 1989 and 2009, and if possible, specify the reason for each incident and the crane involved. The background for requiring the report was five major crane accidents in the UK between 2000 and 2009, where subsequent investigation revealed that the collapses were due to different causes. The report contains information about 85 incidents and is categorized with percentage distribution of incidents as follows: Erection/dismantling/extending of the crane (34%), Extreme weather (18%), Foundation issues (2%), Mechanical or structural issues (5%), Misuse (7%), Electrical/control system issues (1%), Unknown cause (33%).

It is worth to notice that 85% of the incidents are within 3 of the 7 categories, erection / dismantling / extending, mechanical / structural and unknown cause, where the latter has 33% of all the incidents, which means that it was impossible with the given information to define the exact reason for the accident. In general, it was also discovered that the reason for the failures or the incidents often are described as the immediate consequences more than a possible original or root cause. Descriptions as “the crane fell to the ground”, “the top had parted from the mast section”, “during dismantle the crane collapsed”, “the structure gave away”, “strong wind blew the jib over the A-frame”, “counterweight collapsed first, followed by the main jib”, and “it was believed that...”, “reports suggest that...” are much used, but not completely accurate explanations.

The expression “a normal accident” seems to exist within the industry and originates from Charles Perrow [19] where the expression represents a “sociological explanation for accidents in complex technological systems” [20]. Certain accidents were called *normal accidents* or *system accidents* because they seemed to be inevitable in highly complex systems due to a multiple number of trivial and

“unimportant” initial failures which interact with each other in unpredictable ways, to finally cause major or severe accidents. It has been noted that some investigations or reports on crane incidents use the explanation of “normal accident” instead of giving a more specific reason.

4.2. The Norwegian and foreign Petroleum and Offshore & Maritime sectors

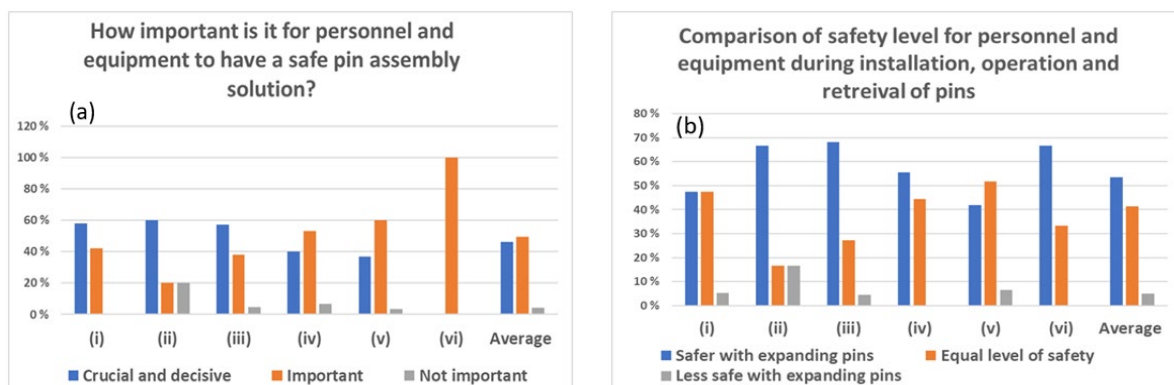
The Offshore and Maritime sectors have a wide range of equipment applying or having a potential for applying expanding pin solutions [14], among them; offshore and maritime cranes with and without motion compensator systems, A-frames both at foot/leg connection and at hydraulic cylinders, power driven winches, anchor systems, hatches, rudder systems, Dollies, travelling blocks, pipe handler cranes, and excavators. Such equipment is normally subjected to comply with certain standards and certifications to be allowed to be in use. These standards and certifications can typically be NORSOK based [21], with the following treating lifting activities; R-002 (Lifting Equipment), R-003 (Safe use of lifting equipment), and R-005 (Safe use of lifting and transport equipment in *onshore* petroleum plants), and a variety of other standards within Drilling, Mechanical work, etc., in addition to third party certification and classification bodies as Lloyd’s Register, different TÜV bodies, DnV, ABS and others.

The Petroleum Safety Authority (PSA) is an independent government regulator with responsibility for safety, emergency preparedness and the working environment in the Norwegian petroleum industry, and its regulations can be found at the Standards Norway web page [21].

Non-compliance with the required and statutory laws, regulations and standards could have serious consequences, such as (a) stop in production and / or operations based on own decision or by direct order from PSA, (b) problems with the license to operate, (c) police or PSA investigations resulting in fines from authorities and (d) loss of reputation in the market, according to various energy companies operating in the Stavanger region (Norway). The personnel health, safety and life are extremely important and there will normally not be accepted any situations which can affect that negatively.

4.3. Questionnaire-based survey regarding pin solutions for lifting and drilling equipment.

Safety, and safe and secure operations and equipment, often focus on quality of procedures, training, tools, and equipment, but should also focus more on how to prevent damages in pinned joints and ease installation and retrieval jobs. This survey reveals how the involved companies value safety for personnel and equipment in general, how safe the expanding pin solution is compared to the standard cylindrical pin, and their capabilities when it comes to tear, wear, breakage and easiness of installation and retrieval, see Figure 4. The types of involved companies are OEM (i), supplier to OEM (ii), engineering (iii), end-user (iv), service & maintenance (v), or others (vi).



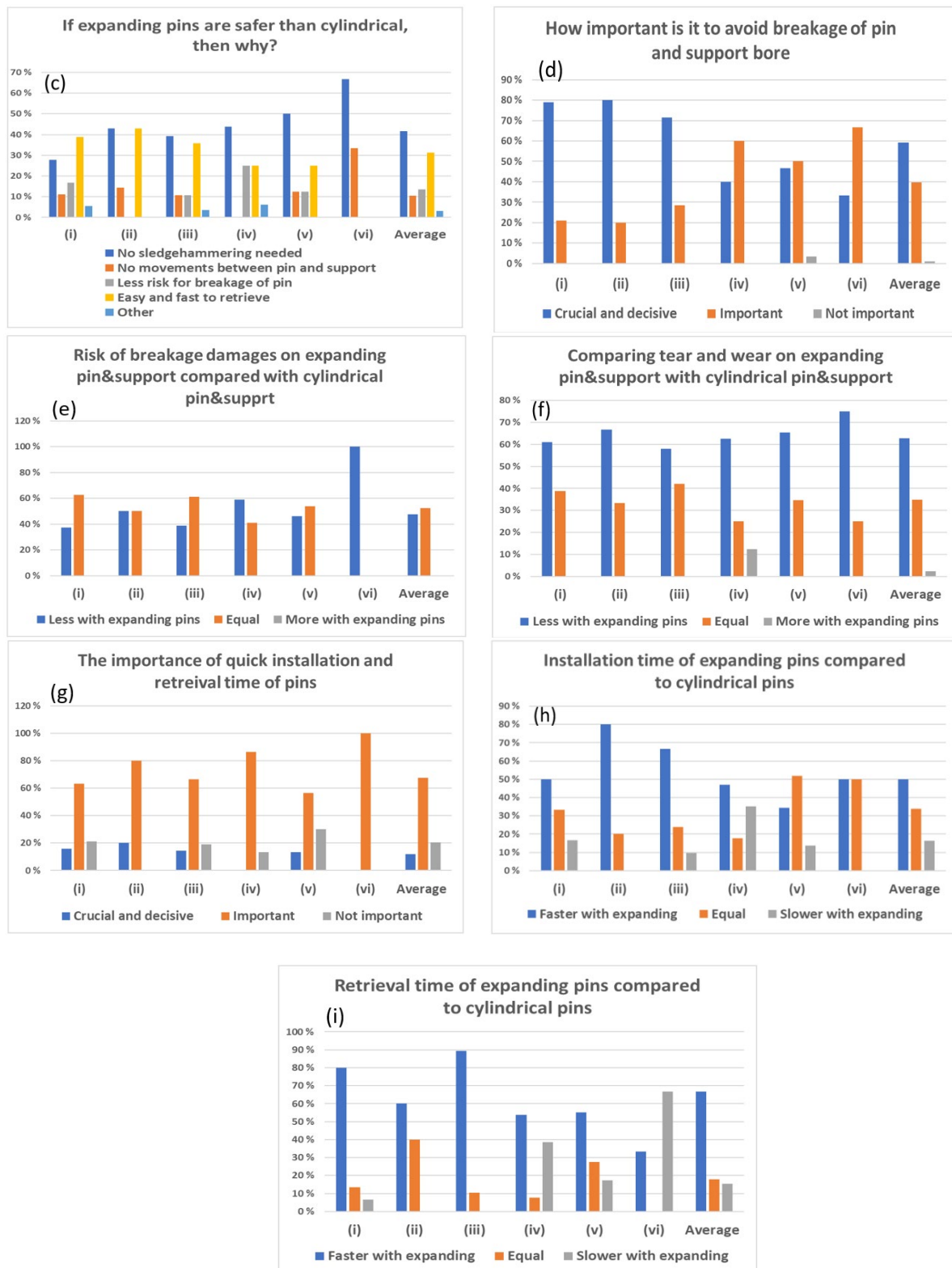


Figure 4. Statistics from questionnaire-based survey – (a) the importance of safe pin solution, (b) comparison of safety levels, (c) why safer with expanding pin, (d) the importance of avoid breakage, (e) risk of breakage, (f) comparing tear and wear with different pins, (g) the importance of quick pin installation and retrieval, (h) installation time, and (i) retrieval time

5. Analysis, discussions of results and outlooks

Analysis of previous crane incidents, specially within onshore construction tower cranes, indicate that pins and bolts play an important role within the machinery, to keep each part in its position, but the pin – support interaction itself is seldomly focused on. Although pins and bolts are relatively small units they are of extreme importance when it comes to criticality in relation to safe and sound operations, both for mechanical equipment and for people working in the proximity. A standard cylindrical pin will over time damage the joint supports by deforming and making the support bore bigger and oval, which can result in unstable and less controllable operations, less accuracy in lifting operations, unwanted high accelerations and shock reactions in the joints and increased risks for both the equipment and personnel. The relative movements between pin and support and slip-stick contact over time increases the risk of failure due to fretting crack initiation and propagation.

When an incident happens, it seems to be explained with *strong winds, the jib or counterweight collapsed, the structure gave away*, or even simply as *normal accidents*. Undoubtedly this happens, but the explanation of *normal accident* seems to be used as a substitute of a more in-depth investigation. It seems like it never is performed analysis of the negative consequences the play between pin and support in a joint can have on such tower crane accidents, or how the incident could have developed if the play had been eliminated by an expanding pin system. The effect of an important reduction of accelerations and dynamic reaction forces in the crane joints should be of interest to analyse both before and after these accidents.

The questionnaire-based survey gives some interesting relationships between the participants view on safety, and the different pin solutions, divided into which area they belong, being OEM (i), supplier to OEM (ii), engineering (iii), end-user (iv), service & maintenance (v), or others (vi). It is a 96% score as *Crucial and decisive*, and *Important*, see Fig. 4 (a), on the question of “How important is it for personnel and equipment to have a safe pin assembly solution”, where OEM/Production (i/ii) and Engineering (iii) score highest on *Crucial and decisive*. This shows how the stakeholders value the importance of safety when it comes to pinned joints.

On the question of *safety level*, Figure 4 (b), the responders evaluate the safety level, as they define and experience it, for personnel and equipment, during installation, operation, and retrieval of pins, for the two different pin solutions in question. Figure 4 (c) shows the results from a following-up question for those who responded that the expanding pins are safer. Four specific alternatives plus one open (Other) are given, and the results show 97% of the responders chose the given alternatives, and only 3% gave an alternative reason. The responders’ main concerns regarding safety is related to personnel and equipment, and their economic appraisals and concerns are reported in a study by Karlsen and Lemu [14].

As demonstrated in Fig. 4 (b), 54% aimed at the expanding solution as the safest, and only 4% stating this pin as less safe. The stakeholder (ii), (iii), (iv) and (vi) clearly indicate this with a 65% average score on *Safer with expanding pins*. The reasons for *why* the expanding pin is considered safer Fig. 4 (c), there are two main reasons given, (1) *No sledgehammering needed*, and (2) *Easy and fast to retrieve*. These are the main reasons for all the defined stakeholders, (i) – (v). Retrieval of pins which are stuck in the support bore, due to cold-welding, corrosion, or deformation can be a high-cost and high-risk operation, with use of high-pressure hydraulic tools, flame-cutting equipment, welding and line-boring. Pin solutions which can prevent such high-risk operations are highly evaluated by the stakeholders.

For all the participants, the *importance of avoiding breakage* is naturally highly valued, with OEM (i), supplier to OEM (ii) and engineering (iii) scoring 79%, 80% and 71% on *Crucial and decisive*, with the others almost equally divided between *Crucial and decisive*, and *Important*, see Fig. 4 (d).

When it comes to the *risk of having pin/support breakage*, Fig. 4 (e) and/or *wear issues*, Fig. 4 (f), there is no one (0%) indicating that expanding pins are more exposed to breakage, than the std pin. It is relatively equally divided between *Less with expanding pins* and *Equal*, with 48% and 52% as total values, respectively. Analysing the tear and wear comparison between expanding pins and cylindrical ones, it shows that within each of the stakeholder segments (i) – (vi) in Figure 4 (f), it exists a clear

opinion and experience that there is less wear issues with expanding pins compared to standard pins, with 63% and 35%, respectively. Only 2% see more wear issues with expanding pin solutions.

The stakeholders have a clear opinion on the *importance of quick* installation and retrieval of pins, Fig. 4 (g), with 80% indicating that as *Crucial and decisive*, and *Important*. Service, Repair and Maintenance (v) have the highest score on *Not important* with 30%.

When comparing *installation and retrieval time* for expanding and cylindrical pins, Fig. 4 (h) and (i), respectively, most of the stakeholder segments (Figure 4 (h) (i) – (iv)) responds that the expanding pins are the fastest to install, and the total average states 50% for expanding pins as fastest, 34% as equal, and 16% stating standard pins as fastest. For the retrieval time the stakeholder segments (i) – (v), Figure 4 (i), responds that the expanding pin is the fastest to retrieve, and the corresponding numbers for the total average are 67%, 18% and 15%, respectively.

OEM/Production (i/ii) and Engineering (iii) score lowest on the statement *Slower (retrieval) with expanding pins* with 7%, 0% and 0%, respectively.

Although the survey got feed-back from 58 responders it is limited to those who have some practical knowledge or experience with expanding pin solutions, but very little information from scientific investigations and studies around expanding pin solutions. It would increase the knowledge if more scientific work in combination with real case studies were performed.

6. Conclusion

Expanding pin solutions seems to be recognized as a safer pin solution compared to standard cylindrical pins, specially within the Offshore and Maritime segments, where the safety is valued highly by all the stakeholders. The stakeholders in this survey are both OEM, suppliers to OEM, Engineering companies, End-users, and Service companies. The fact that there is, in general, no need for sledgehammering to get the pin in or out of the joint, given its capability to expand after installation and contract before retrieval, makes the solution score high on safety compared to the cylindrical solution. The expanding pin can be installed and retrieved easily without hammering, flame-cutting, welding and line-boring, which is recognized by the stakeholders as important regarding safety for both personnel and equipment. In addition, the stakeholders also recognize that the wear problem is considerably less with expanding pins, as also for breakage of pins and supports.

Onshore crane manufactures of tower cranes and mobile cranes seems to be less aware of the expanding pin solutions, and maybe also less aware of the problem with cylindrical pins that could have been resolved by use of expanding pins. Several reports have indicated a high level of accidents with such construction cranes.

Author Contributions: Ø. Karlsen: Conceptualization, Methodology, investigation, Writing—original draft; H.G. Lemu: Supervision, Visualization, Resources, Writing – Reviewing and Editing, Project Administration, Validation. All authors have read and agreed on the final version of the manuscript.

Funding: This research is conducted under the Industrial PhD funding provided by the Research Council of Norway and the company Bondura Technologies AS, Grant nr. 283821.

Acknowledgements: The authors gratefully acknowledge the financial support provided by the Research Council of Norway and Bondura Technologies AS. The authors would like to thank the companies and individuals who provided feedback on the conducted survey.

Conflicts of Interest: The authors declare no conflict of interest.

References

- [1] Talemi R H, Zhang J, Hertelé S and De Waele W 2018 Finite Element Analysis of Fretting Fatigue Fracture in Lug Joints Made of High Strength Steel, *Proc. of 12th Int Fatigue Cong - MATEC Web of Conferences – Fatigue 2018*. **165**.
- [2] Karlsen Ø and Lemu H G 2019 Fretting fatigue and wear of mechanical joints: Literature study: IN: 2nd COTech & OGTech (Stavanger: 27-29 November 2019), IOP Conference Series: *Mater Sci Eng* **700**.
- [3] Talemi R H 2014 Numerical Modelling Techniques for Fretting Fatigue Crack Initiation and Propagation (PhD Thesis), (*Ghent University, Faculty of Engineering and Architecture, Belgium, 2014*).
- [4] Talemi R H, Zahedi A and De Baets P 2014 Fretting fatigue failure mechanism of automotive shock absorber valve, *Int. J. Fatigue* **73**, 58-65.
- [5] Lagerev A V, Lagerev I A 2020 Dynamic processes of loader cranes manipulators with excessive backlashes and elastic damping in their hinges, *Period. Polytech. Mech. Eng.* **64**(1), 7-14.
- [6] Lagerev A V, Lagerev I A 2018 Increasing operating life of hinge lugs in manipulators of mobile transportation and production machines, (IOP Conf. Ser.: Earth Environ. Sci). **194**.
- [7] Krasnyy V, Maksarov V and Olt J 2016 Increase of wear and fretting resistance of mining machinery parts with regular roughness patterns, *Proc. of the 27th DAAM International Symposium on Intelligent Manufacturing and Automation*, Vienna, 151-156.
- [8] Zhang C, Qian Y, Dui H, Wang S and Shi J 2019 Component failure recognition and maintenance optimization for offshore heave compensation systems based on importance measures, *J Loss Prev Process Ind.* **63**, 103996.
- [9] Ren Z, Skjetne R, Verma S A, Jiang Z, Gao Z and Halse K H 2021 Active heave compensation of floating wind turbine installation using a catamaran construction vessel, *Mar Struct.* **75**, 102868
- [10] Quan W, Liu Y, Zhang Z, Li X and Liu C 2016 Scale model test of a semi-active heave compensation system for deep-sea tethered ROVs, *Ocean Eng.* **126**, 353-363.
- [11] Neupert J, Mahl T, Haessig B, Sawodny O and Schneider K 2008 A Heave Compensation Approach for Offshore Cranes, *American Control Conference*, (Seattle, 2008).
- [12] Bondura Technology AS, <https://www.bondura.no> [Accessed 16 August 2021].
- [13] Berkani I, Karlsen Ø and Lemu H G 2017 Experimental and numerical study of Bondura® 6.6 PIN joints. In: 1st COTech Conf. (Stavanger: Nov 30 – Dec, 2017), IOP Conference Series: *Mater Sci Eng.* **276**,.
- [14] Karlsen Ø and Lemu H G 2021 Questionnaire-based survey of experiences with the use of expanding PIN systems in mechanical joints, *Results Eng.* **9**, 100212
- [15] Ayub M and Lu A 2018 Investigation of the Failures of Three Hammerhead Cranes on September 10, 2017, in Miami and Fort Lauderdale in the Wake of Hurricane Irma, U.S. Dept. of Labor, Occupational Safety and Health Administration, Directorate of Construction, Washington
- [16] Peraza D B and Travis J A 2009 Crane Safety - an Industry in Flux, 5th *Forensic Eng. Cong 2009*
- [17] Department of Occupational Safety Health, Ministry of Human Resources, Malaysia 2017, Safety Alert, <https://www.dosh.gov.my/index.php/safety-alert-v/safety-alert-2017?limit=10> [Accessed 31 July 2021]
- [18] Richard I 2010 Tower crane incidents worldwide - RR820 Research Report, Health and Safety Executive, (UK, Buxton, Derbyshire, UK) <https://www.hse.gov.uk/research/rrhtm/rr820.htm> [Accessed 03 October 2021]
- [19] Perrow C 1999 *Normal accidents : living with high-risk technologies*, (New Jersey: Princeton University Press)
- [20] Swuste P 2013 A "normal accident" with a tower crane? An accident analysis conducted by the Dutch Safety Board, *Saf. Sci.*, **57**, 276-282.
- [21] Standards Norway "NORSOK Standards," <https://www.standard.no/en/sectors/energi-og-klima/petroleum/norsok-standards/#.YQ18G0gzZPY> [Accessed 03 August 2021].

Appended Paper V

Study of Bondura® Expanding PIN System-Combined Axial and Radial Locking System

AKHTAR, M. M.; KARLSEN, Ø.; LEMU, H. G.

Strojniski Vestnik/Journal of Mechanical Engineering, 2021, vol. 67, no 12. p. 625-634.

© The Authors, CC-BY 4.0 Int.

<https://doi.org/10.5545/sv-jme.2021.7306>

Study of Bondura® Expanding PIN System – Combined Axial and Radial Locking System

Muhammad Maaz Akhtar¹ – Øyvind Karlsen^{1,2} – Hirpa G. Lemu^{1,*}

¹ University of Stavanger, Norway

² Bondura Technology AS, Norway

Bolted connections are widely used in parallel plates and flanged joints to axially lock using the preload generated by the tightening torque and to constrain radial movements of the flanges by the surface friction between mating surfaces. The surface friction depends on the micro-asperities of mating surfaces; under the influence of vibrations and other external radial loads, these asperities tend to deform over time, resulting in the failure of the connection. The Bondura expanding pin system presented in this article is an innovative axial and radial locking system, in which the failure of bolted connections due to radial movements is eliminated by relying on the mechanical strength of the pin system along with the surface friction. The present study describes an experimental design to verify the maximum possible preload on the axial-radial pin at different levels of applied torque. The article also provides a realistic comparison of the pin system with standard bolts in terms of handling axial and radial loads. With some alterations in the axial-radial pin system's design, the joint's capability to resist failure improved appreciably compared with the original design and standard bolts with higher preload. As a result, the estimated capability improvement of the joint against the connection failure due to the external radial load by the axial-radial pin is observed to be more than 200 % compared to standard bolts. Considering the pros and cons of both fasteners, i.e., axial-radial pin and standard bolts, a practical solution can be chosen in which both fasteners are used in a connection, and an optimized situation can be developed based on the working conditions.

Keywords: axial locking, expanding pin system, bolt preload, contact asperities, flanged connection, radial locking, shear resistance, shrink fit

Highlights

- The expanding pin technology that provides an innovative axial-radial locking system is described.
- The advantages of the innovative combined radial and axial locking system to eliminate the radial movement of bolted connections in flanges and pipes are studied.
- Experimental tests are conducted to verify the maximum possible preload that the axial-radial pin can generate at different applied torques.
- The shear capacity of a parallel plate joint using the axial-radial pin is compared with the capability of standard bolts of the same size.

0 INTRODUCTION

The flange connection is one of the most widely used pipe joints [1]; it involves bolts with nuts under pre-tension or preload. The preload in the bolts is generated by torquing the nuts that force the two flanges towards each other or by hydraulic tensioning of the shank and careful tightening of the nuts and realizing the hydraulic tensioning. This prevents axial movement of the flanges relative to each other, whereas the radial movements are prevented by the contact pressure between the mating flange surfaces under this preload [2] and [3].

Studies [4] show a direct relationship between the strength of the flanged joints and the level of the tightness. The drawback of this conventional practice comes from restricting the radial movements only on the shear resistance of the mating surfaces of flanges. The existence of minor radial movements can lead to total failure of the connection [5]. Further, in

pressurized big diameter pipe systems, leakage could occur because there always exist small vibrations in flange connections caused by the exposure to heavy loads and external vibrations caused by the flow of fluid [6]. These vibrations and radial movements reduce the surface friction between the bolt heads, nuts, and flanges by deforming the surfaces' micro-asperities and, eventually, it could cause a reduction in the preload, which could lead to failure of the connection [7]. In the presence of cyclic loading, bolted joints are one of the most exposed parts [8], and the fatigue performance of the joint is mostly governed by existing guidelines or standards, such as Eurocode recommendations [9], that are mostly conservative.

In flange-bolted joints, the thread friction and surface friction at the bearing surface of washers or nuts are influenced by the surface roughness, lubrication conditions, and the number of tightening and loosening events that influence the effectiveness of

*Corr. Author's Address: University of Stavanger, N-4036, Stavanger, Norway, Hirpa.g.lemu@uis.no

the joints to transfer the shear resistance. Furthermore, such connections require precise torquing to provide the necessary preload [10]. The tolerance that is kept between the diameter of the bolt and the bolt hole diameter of the flange for easy installation allows radial movements to occur. Theoretically, such a problem can be avoided by eliminating the tolerance by implementing an interference fit solution, such as press-fit or shrink-fit solutions [11] and [12].

Press-fitted solutions in bolted flange connections are challenging because obtaining a perfect match of all adjacent flange bores is quite difficult and often impossible, considering the combination of their sizes and positions. In addition to the installation difficulties, it would be challenging to retrieve the bolts without damaging the flange structure. In addition, applying press or shrink interference fit may be impossible to increase the contact pressure between the two main flanges due to the high friction contact pressure between the pins and flange bores. Tightening of the nut will possibly not overcome, or only partly overcome, the resistance due to contact pressure between the pin and the flange bore. In contrast, a shrink-fit solution could ease the installation compared to the press-fit, but it would suffer the same issues when it comes to tightening and retrieval [13].

Following this introduction section, this article is divided into five main sections. Section 1 describes the combined axial-radial locking system and the objectives of researching this invention. Then the

materials and methods used in the study are presented in Section 2, followed by the experimental setup in Section 3. The results of the experimental work are discussed in Section 4, and finally, the conclusions drawn from the investigation are presented in Section 5.

1 SYSTEM DESCRIPTION AND OBJECTIVES

To address the above-discussed problems with flanged joints, Bondura Technology AS has designed a technical solution for this rather complex problem with its “Expanding PIN System – Combined axial-radial locking system”, for which the company has received a Norwegian patent (number 344799). This pin system, which is currently in the design phase, has full potential to prevent connection failure due to the radial movements. This is because this pin system is designed to include the mechanical strength of the pin instead of just depending on the surface friction between mating surfaces of flanges.

For the application of the axial radial pin system, the connecting flanges or plates must be adopted accordingly by increasing the pin bore diameter partly through the flange, as shown in Fig. 1. The increased bore diameters are at the opposite flange faces compared to the mating flange faces. The axial radial pin system is symmetrical as illustrated by the three dimensional (3D) view in Fig. 1, which means the central pin is the centre of the pin system, and the

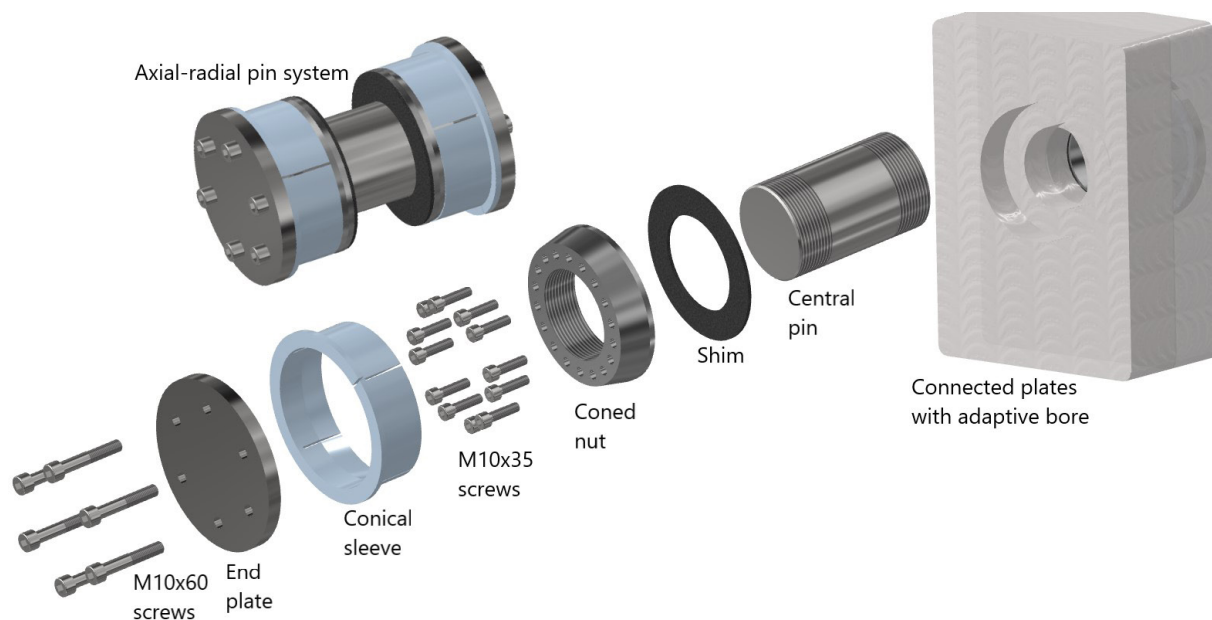


Fig. 1. Axial-radial pin system with exploded view and adaptive connecting plates

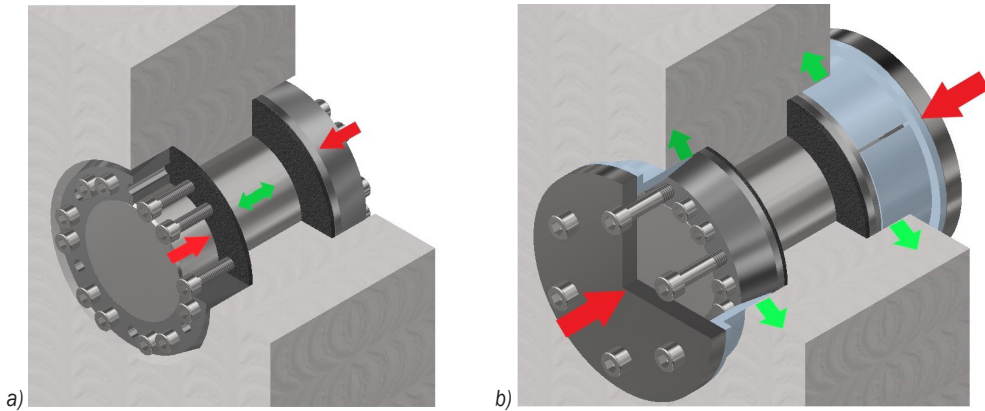


Fig. 2. Function of screws; a) M10×35, and b) M10×60

same six components are employed on both sides, as shown by the exploded view from one side.

In assembling, the central pin, which has threads on both ends, goes through the bolt holes of the flanges, and shims are inserted on both sides and placed at the bottom of the increased pin bore. The two coned nuts are then screwed by hand on each side of the central pin until both coned nuts touch shims.

The M10×35 screws are torqued through the coned nuts and create a pushing force on the flange surfaces, as shown by the red arrows in Fig. 2a. In reaction to the pushing force, the central pin, which is screwed by coned nuts on both sides, is tensioned to its final preload, indicated by green arrows in Fig. 2a.

After preloading the pin, the conical sleeves are installed on both sides of the central pin, which function as wedges to eliminate the radial tolerance between the pin system and the flange bore. End plates are used to transfer the force from the tightening of M10×60 screws into the coned nut to the conical sleeves, as illustrated in Fig. 2b.

Fig. 3 illustrates the difference between the design approaches to eliminate the failure of a flange connection by both fastener systems, standard and axial-radial pin systems. For the standard bolt and nut system, the restriction of both the axial and radial movements depends on the bolt's preload. If the preload is not sufficient or reduced over its functional period, the result would be loss of contact pressure, which could lead to the connection's failure.

For the axial-radial pin system, the restriction of the radial movements between the flanges does not entirely depend on the preload in the central pin. The expanded conical sleeve between the pin and flanges transfers the radial load to the central pin; for a failure to occur due to radial movements, the external radial

load must have sufficient magnitude to surpass the shear yield strength of the central pin.

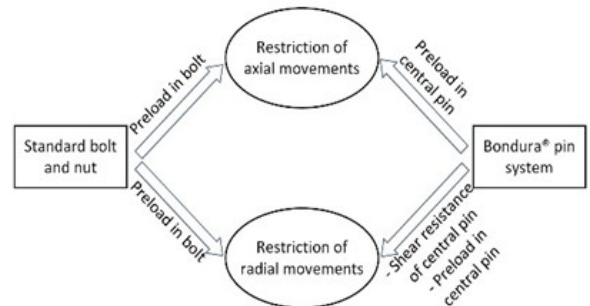


Fig. 3. Design approaches for axial-radial pin system and standard bolt in terms of restricting axial and radial movements

The work reported in this article is conducted as a collaboration project between Bondura Technology AS and the University of Stavanger as a part of a master's thesis [14]. As the axial-radial pin system with combined axial and radial locking system is in the testing and verification phase, theoretical, numerical, and experimental analyses are required to finalize and optimize the product. To optimize the product, two main objectives are identified: (1) investigate maximizing the preload in the axial-radial pin system as a function of numbers and sizes of tightening screws and factors that are limiting the maximum preload, and (2) to make a comparative study of axial-radial pin system with the standard conventional bolt system in terms of maximum preload and locking capability against radial and rotational movements.

Therefore, a study on both Ø50 mm and Ø80 mm axial-radial pin systems was conducted. In this regard, the maximum possible preloads for different torque levels were first estimated by using bolted connection theories [2] and [11]. An experimental setup was

designed for both pin systems to verify the calculated results. For the comparative study, two standard bolts, M50 and M80, were selected, and a comparison was made in terms of maximum possible preload and the ability to avoid failure emanating from radial movements. The experimental study is limited to the two sizes of axial-radial pin systems, i.e., Ø50 mm and Ø80 mm, which are provided by the company [15].

2 METHODS AND MATERIALS

Preload in bolted connection is possible by applying torque; to achieve the desired preload, it is important to understand the relationship between torquing level and resulting preload. The common method to define the relationship between maximum applied torque (T) and resulting preload (F_i) is given by the relation,

$$F_i = \frac{T}{Kd}, \quad (1)$$

where K is an experimental factor that is set equal to 0.18 for lubricated surfaces (on bearing surface and on threads) and d is thread diameter of the bolt/screw [2]. To verify the calculated preloads by an axial-radial pin system for different levels of applied torque according to the above equation, an experiment was designed in which different levels of torque are applied on both axial-radial pin systems. The purpose of the experiment was to observe the normal stress in the central pin. Therefore, instead of using a complete flange, a test jig was used, as shown in Fig. 4, which was bolted on the test bench.



Fig. 4. Experiment setup and manual application of torque on axial-radial pin system in the test jig

In this experiment, average normal stress along the central pin's longitudinal axis was measured using

two strain gauges of type KLY41 from HBM company [16], which were connected in parallel at an angle of approx. 180° on the pin. The reference temperature for this strain gauge is 23 °C, and the operating range for static analysis was from -70 °C to +200 °C. The strain gauge selected for this experiment has a grid length 3 mm and 200 Ω of grid resistance with a gauge factor of 2. The method employed in this experiment for the application of strain gauges is called the active dummy method [17]. It is a widely implemented method for compensating thermally induced strains. In this experiment, four strain gauges were used on a single pin, two of such strain gauges were applied on the central pin, and the other two were applied as dummy strain gauges on a member, which is made of the same material as of the central pin.

The used data acquisition system (DAQ) module is from HMB company and consists of a measurement electronics gadget known as Spider8 and software called Catman® professional [16]. For the application of controlled load, the torque in this experiment was applied by hand using a torque wrench from USAG company [18], as shown in Fig. 4. This torque wrench works on the turn-of-the-nut method and has an application range of 40 Nm to 200 Nm, which is sufficient for the present experiment because the maximum calculated torque that the M10 screw can sustain is approx. 147 Nm.

In terms of material, the end plate and conical sleeve are made of S355J2 with a minimum ultimate tensile strength of 450 MPa and a minimum yielding strength of 295 MPa, whereas the central pin, shim, and coned nut are made of 34CrNiMo6 material with a minimum ultimate tensile strength of 900 MPa and a minimum yielding strength of 700 MPa.

Furthermore, two sizes of ISO 4762 tightening screws were used in the pin system, (1) M10×35 screws with the property class of 12.9 with further hardening to property class 16.9 and (2) M10×60 screws with the property class of 12.9. Table 1 presents the tested material properties of the components.

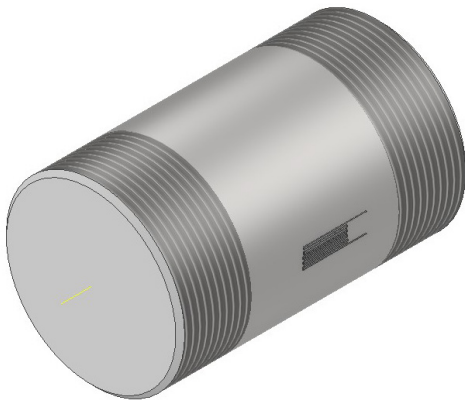
3 EXPERIMENTAL SETUP

The test jig was bolted to the test bench with the M8 bolt and nut. Both M10×35 and M10×60 screws were lubricated prior to the testing. The central pin, which has two strain gauges bounded on it with the difference of approximately 180°, see Fig. 5, was inserted in the test jig, and then one of the shims was inserted on each side of the pin. Coned nuts were screwed on both sides of the pin, which were also lubricated for easy installation. By using the recommended

Table 1. Tested material properties of the components of both axial-radial pin systems

Component	Ø50 mm pin system		Ø80 mm pin system	
	Tensile strength [MPa]	Yield strength [MPa]	Tensile strength [MPa]	Yield strength [MPa]
Central pin	1083	978	1081	980
Shim	1858	1438	1858	1438
Conned nut	1494	1352	1494	1352
Conical sleeve	540	391	500	379
End plate	547	403	505	379
M10×35	1625	–	1625	–
M10×60	1293	–	1312	–

cross-pattern from ASME PCC-1-2010 [19], M10x35 screws were screwed on both sides consecutively with a torque wrench starting from 40 Nm, as it is the minimum limit of the torque wrench. Then, the torque is increased stepwise by 20 Nm until the first screw breaks. Real-time strain values were measured with the help of the DAQ.

**Fig. 5.** Locations of the strain gauges on the central pin**Table 2.** Measured strains in the central pin for different levels of applied torque

Torque levels [Nm]	Measured strain [$\mu\text{m/m}$]	
	Ø50 pin system	Ø80 pin system
0	0	0
40	368	222
60	609	312
80	873	416
100	1104	585
120	1366	676
140	1538	790

These measured strains are shown in Table 2 for both Ø50 mm and Ø80 mm pins for the given range of the applied torque levels. After setting the applied

torque to 160 Nm on the torque wrench, the screws broke for both pin systems.

4 DISCUSSION OF RESULTS

For the sake of comparison with experimental results, preload per screw was calculated at different torque levels, which is shown in Table 3. The Ø50 mm pin system contains 7 screws at each pin end, and there are 12 screws in the Ø80 mm pin system. Therefore, multiplication of the number of screws with the “preload per screw” results in the maximum possible preload of pin system, shown in Table 3 for both pin systems.

To validate the theoretical calculations by experimental results, the average normal stress in the central pin is calculated at different levels of torque by using the equation:

$$\sigma = \frac{F_t}{A_t}, \quad (2)$$

where A_t is the tensile stress area of the central pin and can be estimated by using [20],

$$A_t = \frac{\pi}{4} \times [d - 0.93815 \times p]^2, \quad (3)$$

where $p = 3$ mm is the pitch and d is the diameter of the central pin. Values of theoretical average normal stresses for both pin systems are shown in Table 3.

Measured strain values from Table 2 are utilized to calculate the average normal stresses by using Young’s modulus of $E = 210$ GPa for the central pin and the relationship between stress and strain. These relations are shown in Table 4 for different levels of the applied torque, along with percentage differences from the theoretical values. A positive difference means the measured value is higher than the theoretical value and vice versa for The negative difference. The average deviation of the experimental values from the theoretical values for Ø50 mm pin

Table 3. Theoretical values of preload per screw, max. preload, and normal stress for both axial-radial pin systems

Torque level [Nm]	Preload per screw [kN]	Ø50 mm pin		Ø80 mm pin	
		Max. Preload [kN]	Normal stress [MPa]	Max. Preload [kN]	Normal stress [MPa]
0	0	0	0	0	0
40	22.7	159.1	91.0	272.7	58.3
60	34.1	238.6	136.4	409.0	87.4
80	45.4	318.1	181.9	545.3	116.6
100	56.8	397.6	227.4	681.7	145.7
120	68.2	477.2	272.9	818.0	174.8
140	79.5	556.7	318.4	954.3	204.0
149.2	84.8	593.4	339.3	1017.3	217.4

Table 4. Calculated values of average normal stress from measured strains, and difference with theoretical stress

Torque level [N]	Ø50 mm pin		Ø80 mm pin	
	Normal stress from measured strain [MPa]	Difference from theoretical stress [%]	Normal stress from measured strain [MPa]	Difference with theoretical stress [%]
0	0	0	0	0
40	77.4	-14.9	46.5	-20.2
60	127.9	-6.3	65.4	-25.2
80	183.4	+0.8	87.4	-25.0
100	231.8	+1.9	122.8	-15.7
120	286.9	+5.1	142.0	-18.8
140	322.9	+1.4	165.8	-18.7

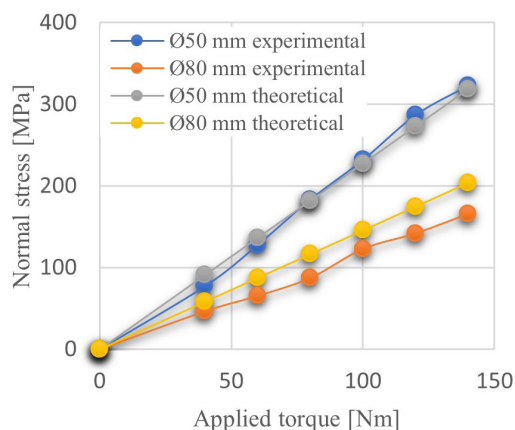
system is -2.0% with A standard deviation of 7.4 and for the Ø80 mm pin system is about -20.6% with a standard deviation of 3.8.

As illustrated in Fig. 6, there is a relatively good correlation between the theoretical values, given in Table 3, and the calculated values based on the strain measurements, Table 4, for both pin systems. However, the Ø80 mm pin reaches clearly a lower maximum pre-tension compared to that of the Ø50 mm pin. The reason is that when the pin diameter increases the number of tightening screws increases approximately linearly, but the cross-section area increases as a square of the pin diameter. The current design of both pin systems can be further optimized to yield higher preloads, which will be investigated later in this section.

For the Ø50 mm pin system, the values of measured strains are used only from strain gauge 1, due to an error incumbent while soldering the wires for strain gauge 2. Possible reasons for the deviation of the experimental values is the fact that, while applying torque, a fixture was used with torque wrench which might have absorbed some part of the torque.

As shown in Table 5, the calculated maximum preloads for the tested axial-radial pin systems are lower than the theoretical preloads for the standard bolts. Therefore, optimization is done regarding the

numbers and sizes of tightening screws of the axial-radial pin.

**Fig. 6.** Theoretical and experimental normal stresses vs applied torque for both pin systems**Table 5.** Maximum possible preload for both standard bolts and tested axial-radial pin systems

Fastener size [mm]	Standard bolt [kN]	Tested pin [kN]	Diff. [%]
50	1067.6	593.4	-44.4
80	2741.1	1017.3	-62.9

The preload in the axial-radial pin systems is contributed by the torque applied to the M10×35

screw; to increase the applied torque, the combination of screw size and number must be optimized. The experiment showed by increasing the torque on the M10 screws results in the breakage of the screw.

The number of M10×60 screws is limited to 4, and the clearance between the two bolt heads is fixed to 1.5 mm. Based on these conditions, a relationship is derived to estimate the maximum number (X) of M10×35 screws in axial-radial pin system as:

$$X = \frac{\pi d_B}{d_H + 1.5} - 4, \quad (4)$$

where d_B is the bolt circle diameter of coned nut and d_H is the bolt head diameter. This relation is used to estimate the number of different sizes of screws for both Ø50 mm and Ø80 mm axial-radial pin systems, as shown in Table 6. There is a geometrical restriction on the number of screws as the bolt head diameter should be less than the difference between the minimum outer diameter and inner diameter of the coned nut.

Considering the described geometrical restriction, the possible screw sizes for the Ø50 mm and Ø80 mm pin systems are M12 and M14, respectively. It was also found important to investigate the possibility of using smaller size screws than M10, when M8 screws were used. Using thread diameters of M8, M10, M12, and M14 according to ISO 4762 and minimum tensile strength of 1600 MPa and the relationship presented in Section 2 as Eq. (1), maximum torque and “preload per screw” was estimated; then the maximum preloads for both pin systems were calculated. All the calculated values are presented in Table 6.

Table 7 compares the preloads for improved axial-radial pin systems as a percentage difference between the standard bolt and the tested axial-radial pin system. The percentage difference is reduced significantly for both axial-radial pin systems as previously (Table 5).

As shown in Fig. 7a, the radial load is being applied on the connected flanges, leading to the relative radial movements, and this connection

Table 6. Theoretical max. possible preload for both axial-radial pin systems for different screw sizes and numbers

Size	Thread diameter [mm]	Max. torque [Nm]	Preload per screw [kN]	Ø50 mm pin system		Ø80 mm pin system	
				Max. number of screws [-]	Preload [kN]	Max. number of screws [-]	Preload [kN]
M8	7.78	74.0	52.8	11	581.0	18	950.8
M10	9.78	146.9	83.5	9	751.2	14	1168.6
M12	11.73	253.5	120.1	7	840.5	12	1440.9
M14	13.73	406.6	164.5	–	–	10	1645.1

Table 7. Comparison of preload for improved axial-radial pin system with standard bolts and tested pin system

Fastner size [mm]	Preload [kN]			Difference [%]	
	Standard bolt	Tested axial-radial pin	Improved axial-radial pin	Improved axial-radial pin vs std. bolts	Improved axial-radial pin vs tested pin
50	1067.6	593.4	840.5	–21.3	29.4
80	2741.1	1017.3	1645.1	–40.0	38.2

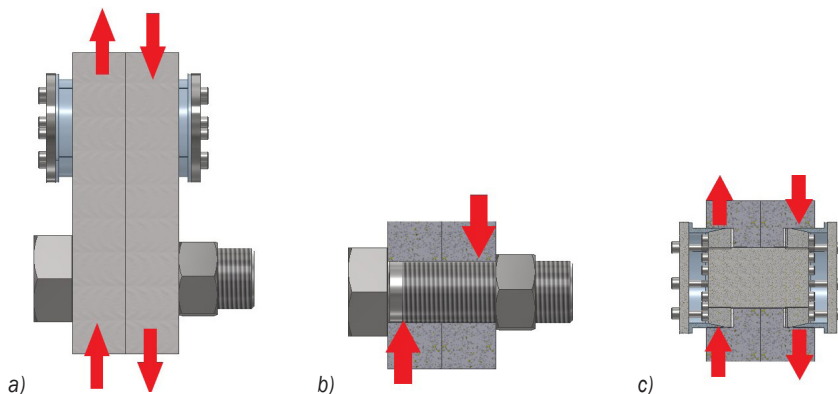


Fig. 7. Application of loads; a) Radial load on the connected flanges, b) radial load on a standard bolt, c) radial load on the conical sleeve of axial-radial pin system

contains both axial-radial pin system and standard bolt and nut. There is a surface resistance between mating surfaces of flanges, and it is acting in the opposite direction of the external radial load. This surface resistance is controlled by the permissible shear load or shear capacity and, according to Boris et al. [2], this shear capacity depends on the initial preload (F_i) and the coefficient of the friction (μ) between the mating surfaces of the flanges. This shear capacity is expressed as:

$$Q_p = \frac{F_i \mu}{k}, \quad (5)$$

where k is the factor of safety.

When the external radial load exceeds this shear capacity of a standard bolt, the external radial load starts to act freely on the bolt as shear load, as depicted in Fig. 7b. In contrast, the conical sleeves in the novel pin system are employed to make the connection as rigid as possible and to have a relative movement between connecting flanges. The external radial load applied on the conical sleeve, as shown in Fig. 7c, should be large enough to surpass the minimum shear strength of the central pin. This allows the inclusion of as another factor in the equation of shear capacity, which becomes:

$$Q_p = \frac{F_i \mu + \tau_y A_t}{k}, \quad (6)$$

where τ_y is the yield limit for shear strength of the central pin.

Eq. (5) is used to calculate the shear capacity of both standard bolts; the results are presented in Table 8, where the factor of safety is equal to 1. The values in this table do not account for the contribution of shear strength of bolt in the shear capacity of the connection.

Table 8. Theoretical shear capacity of both M50 and M80 standard bolts

Standard bolts	Maximum possible preload [kN]	Shear capacity [kN]
M50	1067.6	320.3
M80	2741.1	822.3

Table 9 presents the theoretical shear capacity of both axial-radial pins by using Eq. (6), along with the percentage increment of shear capacity in comparison to standard bolts. This increment illustrates the advantage of the axial-radial pin system over the standard bolt in terms of preventing the connection failure due to radial load. Here, the factor of safety is entirely dependent on the environmental condition of the flange joint, and it must be customized for each individual case, but for the sake of fair comparison, $k = 1$, $\mu = 0.3$, and $\tau_y = 450$ MPa.

Table 9. Theoretical shear capacity of both axial-radial pins and comparison of shear capacity increment

Pin size [mm]	Max. preload [kN]	Tensile area [mm ²]	Shear capacity [kN]	Shear capacity Inc. [%]
Ø50	840.5	1748.7	1043.0	225.7
Ø80	1645.1	4679.1	2599.1	216.1

Figs. 8 and 9 show comparative simulated situations between the axial radial pin system and standard bolt-nut connection, where two parallel plate connections are created by each fastener. In these simulations, an equal pressure load of 50 MPa as a radial load on each plate is applied in opposite directions, as shown in Figs. 8a and 9a, respectively. As expected, both fasteners have created the surface friction between plates, which are shown in Figs. 8b and 9b.

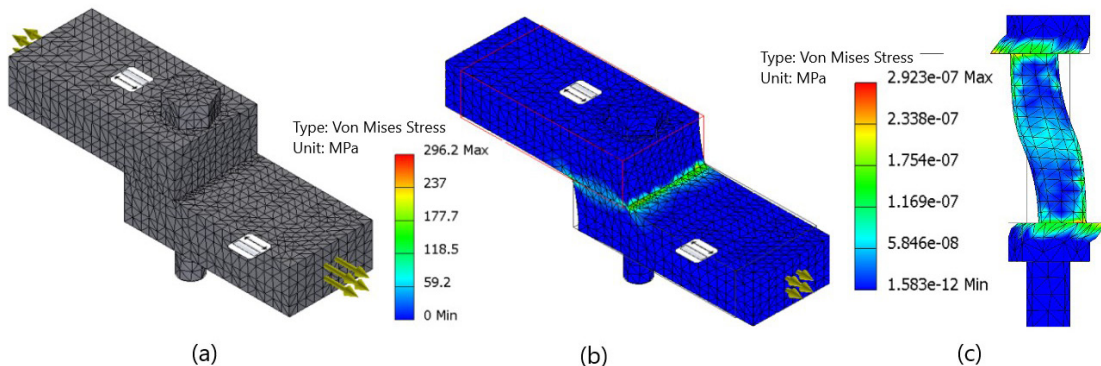


Fig. 8. a) Mesh view of the parallel plate connection by standard bolt and nut, b) surface friction between two plates, and c) isolated view of the bolt and nut

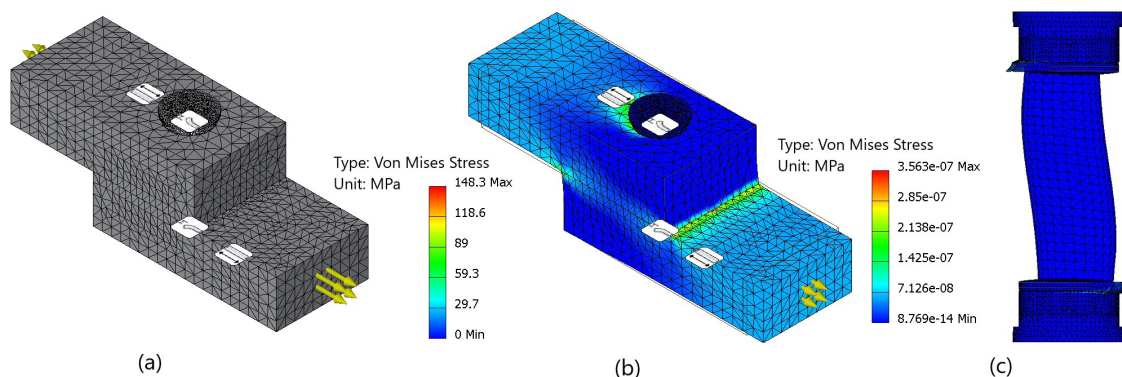


Fig. 9. a) Mesh view of the parallel plate connection by axial radial pin system, b) surface friction between two plates, and c) isolated view of the pin system

To understand the behaviour of both fasteners, they were isolated from the assembly and presented in Figs. 8c and 9c. In this case, the effect of the 50 MPa pressure is much disastrous for standard bolt-nut connection as there is major slipping in the high-stress areas (close to the bolt head and nut) as well as higher stress distribution in the centre of the shank, as compared to the axial-radial pin, where the relatively higher stress occurred in the conical sleeve, but the stress level in central pin is within elastic limit.

As shown in Table 10, the level of required torque to reach the maximum preload for each fastener is much higher for the standard bolt connection when compared to the axial-radial pin system connection. This is because torque is applied to several M12 and M14 screws in the axial-radial pin system, compared to high torque on a single M50 and M80 bolt for the standard bolts. Therefore, it is possible to apply torque by a simple torque wrench to the axial-radial pin system connection, whereas the standard bolt connection needs a high torque from a high-capacity torquing tool, typically hydraulic or electrical.

Table 10. Required torque for axial-radial pin systems and standard bolts to reach maximum possible preload

	Fastener	Required torque [Nm]
Axial-radial pin system	Ø50 mm /M12	253.5
	Ø80 mm /M14	406.6
Standard bolt	M50	9505.7
	M80	39106.8

Though the axial-radial pin system’s improved design can provide a higher preload than the tested design, it is still less than the preload per pin for the standard bolts. The axial-radial pins require more space per pin than the standard bolts, and fewer

pins will, therefore, fit on a defined flange system. To maximize the shear resistance for the complete flange system, it is, therefore, possible to apply a combination of standard bolts and axial-radial pins, for optimization purposes. The configuration can be decided by the design parameter responsible for radial movements.

5 CONCLUSION

With some deviation from the theoretical values, experiments confirm the maximum possible preload by both pin systems. In comparison with standard bolts of the same sizes, preload produced by an axial-radial pin system is lower than the standard bolt system, but with the presented changes in the initial design in this study, the difference in maximum preload is reduced significantly, 29 % in Ø50 mm pin system and 38 % in Ø80 mm pin system. The axial-radial pin has a locking mechanism based on the mechanical strength of the central pin. Theoretically, this locking system improves the capability of axial-radial pin connections by more than 200 % to avoid a failure due to radial loading as compared to the standard bolt connection. Along with that, the axial-radial pin requires significantly lower torque applied per screw as compared to standard bolts to obtain the maximum possible preload for a connection. Considering the advantages of the axial-radial pin in terms of capability to reduce or eliminate the failure due to radial loading and the ability of standard bolts to produce higher maximum possible preload, a practical solution is proposed, where a combination of both fasteners can be used to have a safe and secure flange connection. This expanding pin technology, particularly the axial-radial pin solution, is not well

known in the research community. With the results from this study, it is evident that the axial-radial pin solution is worth investigating further to obtain more knowledge about its potential, especially as a function of dimensions, material qualities and torque levels.

6 REFERENCES

- [1] Luan, Y., Guan, Z.-Q., Cheng, G.-D., Liu, S. (2012). A simplified nonlinear dynamic model for the analysis of pipe structures with bolted flange joints. *Journal of Sound and Vibration*, vol. 331, no. 2, p. 325-344, DOI:10.1016/j.jsv.2011.09.002.
- [2] Boris M.K., Barlam, D.M., Nystrom, F.E. (2008). *Machine Elements: Life and Design*. CRC Press, Taylor & Francis Group, Boca Raton.
- [3] Abid, M., Nash, D.H. (2003). Comparative study of the behaviour of conventional gasketed and compact non-gasketed flanged pipe joints under bolt up and operating conditions. *International Journal of Pressure Vessels and Pipes*, vol. 80, no. 12, p. 831-841, DOI:10.1016/j.ijpvp.2003.11.013.
- [4] Urse, G., Durbacá, I., Panait, I.C. (2018). Some research results on the tightness and strength of flange joints. *Journal of Engineering Sciences and Innovation*, vol. 3, no. 2, p. 107-130.
- [5] Takaki, T., Satou, K., Yamanaka, Y., Fukuoka, T. (2008). Effects of flange rotation on the sealing performance of pipe flange connections. *Proceedings of the ASME/JSME 2004 Pressure Vessels and Piping Conference*, DOI:10.1115/PVP2004-2630.
- [6] Ibrahim, R.A. (2010). Overview of mechanics of pipes conveying fluids-Part I: Fundamental studies. *Journal of Pressure Vessel and Technology*, vol. 132, no. 3, art. ID 034001, DOI:10.1115/1.4001271.
- [7] Bai, Y., Yang, M. (2016). The influence of superimposed ultrasonic vibration on surface asperities deformation. *Journal of Materials Processing Technology*, vol. 229, p. 367-374, DOI:10.1016/j.jmatprotec.2015.06.006.
- [8] Zhao, Y., Yang, C., Cai, L., Shi, W. Hong, Y. (2016). Stiffness and damping model of bolted joints with uneven surface contact pressure distribution. *Strojniški vestnik - Journal of Mechanical Engineering*, vol. 62, no. 11, p. 665-677, DOI:10.5545/sv-jme.2016.3410.
- [9] Eurocode 3 (2005). *Design of steel structures - Part 1-9: fatigue*. EN-2005.
- [10] Croccolo, D., De Agostinis, M., Vincenzi, N. (2011). Failure analysis of bolted joints: Effect of friction coefficients in torque-preloading relationship. *Engineering Failure Analysis*, vol. 18, no. 1, p. 364-373, DOI:10.1016/j.engfailanal.2010.09.015.
- [11] Chu, S.J., Jeong, T.K., Jung, E.H. (2016). Effect of radial interference on torque capacity of press- and shrink-fit gears. *International Journal of Automotive Technology*, vol. 17, p. 763-768, DOI:10.1007/s12239-016-0075-0.
- [12] Karlsen, Ø., Lemu, H.G. (2019). On modelling techniques for mechanical joints: Literature study. *International Workshop of Advanced Manufacturing and Automation*, vol. 634, p. 116-125, Springer, Singapore, DOI:10.1007/978-981-15-2341-0_15.
- [13] Chakherlou, T.N., Vogwell, J. (2004). A novel method of cold expansion which creates near-uniform compressive tangential residual stress around a fastener hole. *Fatigue & Fracture of Engineering Materials & Structures*, vol. 27, no. 5, p. 3423-351, DOI:10.1111/j.1460-2695.2004.00727.x.
- [14] Akhtar, M.M. (2020). *Expanding PIN System - Combined Radial and Axial Locking System*, MSc. Thesis, University of Stavanger, Stavanger.
- [15] Bondura AS, Bondura Technology. from <https://bondura.no/>, accessed on: 2021-06-30.
- [16] HBM. from: <https://www.hbm.com/en/>, accessed on: 2021-06-30.
- [17] Purwasih, N., Kasai, N., Okazaki, S., Kihira, H. (2018). Development of amplifier circuit by active-dummy method for atmospheric corrosion monitoring in steel based on strain measurement. *Metals*, vol. 8, no. 1, art. ID 5, DOI:10.3390/met8010005.
- [18] USAG company. Torque wrench with reversable ratchet. from: <https://www.usag.it/catalog/en/products/pdf/2309/Torquewrenches%20with%20reversibl%20ratchet.pdf>, accessed on 2021-06-30.
- [19] ASME (2010). *Guidelines for Pressure Boundary Bolted Flange Joint Assembly*. USA Patent ASME PCC-1-2010.
- [20] Norton, R.L. (2011). *Machine design: An integrated approach*, 4th Ed. Pearson Education Inc., New York.

Appended Paper VI

Experimental and Numerical Studies of Stress Distribution in an Expanding Pin Joint System

SALAHSHOUR, S.; KARLSEN, Ø.; LEMU, H. G.

Applied Mechanics, 2021, vol. 3, no 1, p. 46-63.

<https://doi.org/10.3390/applmech3010003>



Article

Experimental and Numerical Studies of Stress Distribution in an Expanding Pin Joint System

Soheil Salahshour *, Øyvind Karlsen and Hirpa Gelgele Lemu

Department of Mechanical and Structural Engineering and Materials Science, University of Stavanger, N-4036 Stavanger, Norway; oyvind.karlsen@uis.no (Ø.K.); hirpa.g.lemu@uis.no (H.G.L.)

* Correspondence: salahshoor.soheil@gmail.com

Abstract: Pin joints are widely used mechanisms in different industrial machineries such as aircrafts, cranes, ships, and offshore drilling equipment providing a joint with possibility of relative rotation about one single axis. The rigidity of the joint and its service lifetime depend on the clamping force in the contact region that is provided by the applied torque. However, due to the tolerance needed for insertion of a pin in the equipment support bore, the pin is prone to relative displacement inside the bore. The amplitude of this relative displacement usually increases as time passes and since the material of the support often has lower quality grade than the pin, it leads to creation of slack in the equipment and malfunctioning of the machine. An Expanding Pin System (EPS) can be a solution to this problem where the split sleeve expands to remove the gap while the joint is torqued. Therefore, slack in the joint system disappears and 360° contact area could be achieved, providing a better stress distribution and preventing the stress localization. Determining the EPS preload and the resulting contact pressure and stresses in the joint parts are important to avoid damaging to the contact surfaces of the joints and making the dismantling of the EPS difficult. Therefore, finding the amount of the required torque is a compromise between preventing slack in the EPS and prohibiting damage to the joint parts. Stress analysis in this study is performed based on the industrially recommended torque for the EPS type under study. This article reports the study conducted on the stress distribution and the magnitude of stresses exerted to the equipment support when EPS is installed on the machine. To achieve this purpose and to investigate the stress distribution in the joint, both experimental and finite element (FE) methods were used. The experimental results show how much of the applied energy to the EPS in the form of torque is spent to expand the split sleeve and test boss and also to overcome friction. The finite element analysis provides magnitude and distribution of stresses in the EPS components.

Keywords: expanding pin system joint; stress distribution; finite element analysis; split sleeve; friction effect



Citation: Salahshour, S.; Karlsen, Ø.; Lemu, H.G. Experimental and Numerical Studies of Stress Distribution in an Expanding Pin Joint System. *Appl. Mech.* **2022**, *3*, 46–63. <https://doi.org/10.3390/applmech3010003>

Received: 20 November 2021

Accepted: 25 December 2021

Published: 30 December 2021

Publisher's Note: MDPI stays neutral with regard to jurisdictional claims in published maps and institutional affiliations.



Copyright: © 2021 by the authors. Licensee MDPI, Basel, Switzerland. This article is an open access article distributed under the terms and conditions of the Creative Commons Attribution (CC BY) license (<https://creativecommons.org/licenses/by/4.0/>).

1. Introduction

A pin joint is a type of connection between two objects that provides relative rotation about a single axis. All translations as well as rotations about other axes are prevented and it is considered a single degree of freedom (DoF) system. In kinematics, a pin joint is formally called a revolute joint and when analyzing motion in two dimensions, it may also be referred to as a pivot point or a hinge. A pin joint has many applications in oil and gas, lifting, offshore, shipping and other heavy machineries in many industries. A pin joint is always susceptible to wear and tear due to slip between metal surfaces in contact, regardless of greasing time intervals. When support bores become worn, it requires restoring the holes to their original diameters and tolerances and the pivot joint has direct impact on the functioning of the machine. When the machine supports wear out, the machine will not perform properly and necessitates repair to avoid any further failures. The support bores for cylindrical pins are usually a little bit larger than the pin diameter to let the pin enter, but at the same time the diameter difference creates slack.

The expanding pin system (EPS) shown in Figure 1 is a pivot pin assembly with a high potential for replacement of old cylindrical type of pivots. EPS is a perfect solution for slack problem in pin-support connections. In the EPS, normally both ends of the pin are tapered and a pair of expansion sleeves are fitted at both ends of the pin followed by end plates or load transfer elements. As the tightening screws or bolts are tightened, the expansion sleeves are forced over the tapered ends of the pin creating a wedge force and contact pressure between the pin and the support holes, which locks the EPS into the pivot. This system eliminates the wearing process on the contact surfaces between the pin, sleeve and support bore. The expanding pin system can be installed and retrieved easily without using forces such as by sledgehammering, hence wear and crack initiation are hindered. Additionally, it provides greater safety [1].

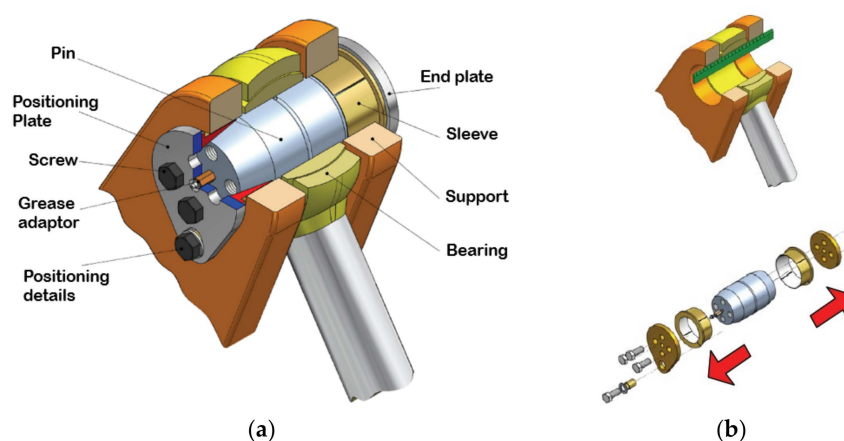


Figure 1. Illustration with section view of EPS. (a) EPS installed in a joint (b) Exploded view.

One of the main advantages of EPS is providing larger contact areas between pin and machine supports, which means reduction of stress localization induced to the supports of the machines and elimination of relative movements between contact surfaces. When torque is applied to the EPS that is locked inside the support bore, the contact area will be 360° while this does not occur for standard cylindrical pins. Upon applying external loads on this locked EPS joint, the alternating pressure area becomes 180° in radial pulling or pushing sequences [1], and 360° in axial directions and also when unloaded.

Investigation and analysis of stress inside the support of the pin started from works of Timoshenko and Goodier [2], where solution for the stress concentration at a hole in an infinite plate loaded by a pin were obtained. Several analytical and experimental studies were also carried out by other researchers on both isotropic and orthotropic materials [3–5]. For instance, Yavari et al. [6] investigated stress around a hole in Timoshenko plate numerically considering connection design aspects such as plate geometry, clearance and friction. Though the subject of stress analysis of an expanding pin assembly has not attracted so much attention, studies on interference and shrink fitted joints are reported in the literature, which are related topics. For instance, Bozkaya and Müftü [7] investigated the mechanics of the taper interference fit analytically. They compared the analytical results with FE analysis results. It was observed that for the central 90% of the contact length, the results of the two methods are in good agreement, but they have significant differences at the beginning and the end of the contact length due to the ability of FE to find local stresses. Dongliang et al. [8] studied a conical expansion sleeve joint numerically and analyzed the magnitude of contact stresses in the joint conical surface. Yu and Yang [9] studied the torque capacity and contact stress for a new shrink disc both numerically and experimentally, which is applicable in wind turbines. Their analysis predicted the effectiveness of mechanical transmission and gave stress-strain curves to characterize the material behavior. Siemiatkowski et al. [10] investigated shrink-fitting of the marine diesel crankshaft and measured the stresses inside the crank using non-destructive method via ultrasonic measuring device. Croccolo et al. [11] provided an experimental methodology to

determine the friction coefficient in bolted joints in order to relate the tightening torque to the preload force more precisely. Nigrelli and Pasta [12] applied 3D FE method to simulate cold expansion of a split-sleeve to determine residual stress field around an expanded hole. Their simulation highlights the effect of the split-sleeve and the plate thickness on the residual stress field. Ismonov et al. [13] performed similar 3D FE analysis to that of Nigrelli and Pasta's study [12] to predict the resulting residual stress field taking into account the effects of geometrical and material nonlinearities.

In earlier research at University of Stavanger, which is partly used as source for this study, Berkani et al. [14] conducted experimental and numerical study of the stress level in the supports. The experimental work was performed using a test boss that acted as the host support. By installing strain gauges (SGs) on four different points on the circumference of the test boss, they managed to read the strains created during tightening of screws of the assembly. Their experiment includes two EPS assemblies with 88.9 mm and 120 mm diameters. For numerical analysis, ANSYS software was used to analyze stress distributions and magnitude in steps defined for inserting preload on screws and they considered the model of test boss both with free (like their experimental test) and fixed boundary conditions. The FE results of a fixed test boss showed a more even stress distribution.

Since the sleeve is embedded between the pin and the support holes, its radial expansion was restricted leading to dissipation of part of tightening energy. A similar study was performed by Andrzejuk et al. [15] where a conical sleeve with pivot joint under axial loading was studied. In their study, they evaluated energy dissipation between cooperating surfaces of a friction pair theoretically and experimentally, and additionally they included structural friction, elastic, and frictional effects by considering the Lamé's problem.

Based on the previous studies, it could be concluded that there is a need for more study and investigation on stress distributions in the equipment supports and interaction between different parts of the EPS assembly. Therefore, in this study, which is based on master thesis research conducted by the first author [16], a combination of experimental and numerical methods are used to investigate stress distribution in the joint components. The equipment support is replaced with a test boss for measuring the strains created in the equipment support while tightening the joint screws. Three different experiments are conducted to assess energy loss in the EPS, which often happens in the form of friction and the energy for expanding the sleeve. FE simulation of EPS is created in Abaqus/CAE software and its results are compared with the experimental results obtained for the test boss. Since the pin and the expansion sleeve both are embedded inside the support, acquiring strains using strain gauge is infeasible. However, the stresses and the contact pressure at the interaction surface of the pin-sleeve extracted from FE analysis are compared with theoretical formulas available in [15], even though these formulas are developed for a sleeve without any cuts. The EPS sleeve has four cuts where one of them is a complete cut-through. The comparison provides an insight into what extent these formulas are applicable for an EPS.

2. Analysis Methods

The study was conducted by using both experimental and numerical methods. In this section, the experimental and FE methods of analyzing the EPS joint are described.

2.1. Experimental Setup

To evaluate the stress distribution inside the equipment support bore of the machinery where EPS is used, a test boss was designed and manufactured for this experiment. The inner and outer diameters of the test boss are 89 mm and 129 mm, respectively. The pin has a diameter of 88.9 mm with both ends tapered. The external hoop strains of the test boss were recorded using strain gauges installed on the outer surface of the test boss. Application of torque to the tightening screws of the system was performed stepwise. HBM strain gauges of type LY4-1-5/120 were used in this experimental study.

The test was conducted at room temperature in the range of 21.7 °C to 23 °C. Even though the temperature difference is very low and may not have any significant effect

on the strain measurements, a compensation method was deployed to omit the effect of temperature variations. This method is known as dummy gauge. In this technique, a dummy gauge which is identical to the active one is installed on an unstrained sample of the same material as the test specimen [17]. The sample with the dummy gauge was placed in thermal contact with the test specimen, adjacent to the active gauge, as illustrated in Figure 2a. In this experiment, the dummy gauges were wired into a half-Wheatstone bridge [18] and placed close to the active gauges so that the temperature effects on the active and dummy gauges cancel each other.

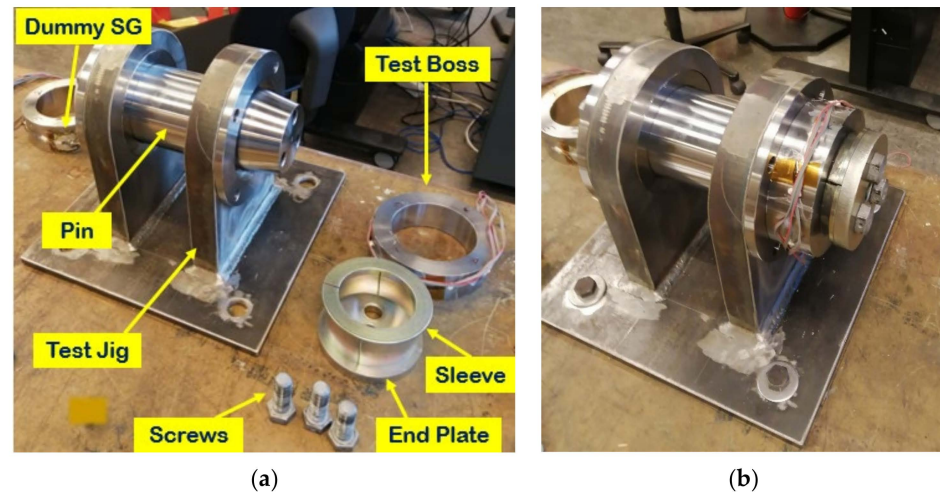


Figure 2. Experimental setup with active-dummy gauge technique. (a) Disassembled EPS joint components (b) Assembled EPS joint components.

In the test setup of this study, the half-Wheatstone bridge configuration was applied to 3 pairs of active-dummy gauges and all of them were plugged into the HBM's amplifier QuantumX.

Catman 4.5 software, which is a data acquisition software, was used for recording of strains generated during the tests. The software interprets the data received from QuantumX and allows visualization, analysis and storage of data during the strain measurement process. Parameters such as strain k-factor and bridge type are inputs and in addition, calibrating the gauges can be implemented. The strain output is given in (micrometer/meter) vs. time. The test procedure was implemented by rotating the test boss for 90° after each test. In this way, the strains were measured for each location with angular distance of 90° from each other according to standard polar coordinate.

To investigate the stress distribution of the EPS, three different test layouts were performed, namely (1) non-lubricated partly cut sleeve, (2) lubricated partly cut sleeve and (3) lubricated completely cut sleeve. The purpose of doing a test with lubricated partly cut sleeve in layout (2) was to evaluate the effect of friction, compared with the non-lubricated part, and to analyze how much of applied torque dissipates by friction. In addition, the point of interest for performing tests on lubricated completely cut sleeve in layout (3) was to analyze how much of the applied torque to the joint system is merely used to expand the sleeve elastically. In addition, in the case of test layouts (1) and (2), i.e., non-lubricated and lubricated partly cut sleeve, the effect of position of the complete cut-through is investigated by rotating the sleeve.

The test jig (shown in Figure 2) was used to resemble the equipment supports and the assembly of the pin system. The test boss was restricted to move axially during the process of applying torque which presents the real situation in practice, and this is an important purpose of conducting this experimentation.

The EPS with $\text{Ø}88.9$ pin system has three 8.8 quality M16 tightening screws and by tightening them, the locking mechanism of the system is triggered. The recommended torque for this pin system is 160 Nm. To provide a wider view of the joint performance,

torques in the range between 40 Nm and 200 Nm were applied to the system. The yield stress of the screw material is 640 MPa and applying 200 Nm torque, the highest in the range, induced 311 MPa tensile stress in the screws which is less than the yield strength of the screw material. This implies that the deformations in the screws are within the elastic region. To reduce the effect of friction force in the screws, lubricant was applied before installation. In many dry threaded fastener applications, up to 90% of the torque is consumed to overcome the bearing and the thread friction, while only 10% of the actual work is usefully transformed into tightening the screw [19]. The lubricant was applied using lubrication paste with the trade name of MOLYKOTE(R) P-74 PASTE.

2.2. Finite Element Analysis in Abaqus/CAE

To simulate a more realistic behavior of EPS joint applying FE analysis, using the true stress and true plastic strain relation is suggested [20]. The true stress (σ_{true}) and the true strain (ϵ_{true}) can be determined based on material test results using the following equations [20]:

$$\sigma_{true} = \sigma_{eng}(1 + \epsilon_{eng}) \tag{1}$$

$$\epsilon_{true} = \ln(1 + \epsilon_{eng}) \tag{2}$$

where σ_{eng} and ϵ_{eng} are engineering stress and strain measured in tensile tests. True stress is the applied load divided by the actual cross-sectional area of specimen where the area changes with time while engineering stress is the applied load divided by the original cross-sectional area of specimen.

According to data from material certificates for different parts of EPS, including yield strength (R_e), ultimate tensile strength (R_m) and final elongation ($A5$), the material modeling in Abaqus was performed. The data for strain corresponding to ultimate strength was not available, however, based on stress–strain diagram available for S355 steel in the literature [21], it was assumed that the respective strain for ultimate strength is equal to one third of the strain value corresponding to the $A5$ where the rapture for test material occurs. This assumption may contribute with some modelling error in the results. $A5$ is permanent elongation for proportional specimens with length L_0 equal to 5 times the diameter. In this way, a linear strain hardening has been introduced for different grades of S355 steel.

Material characteristics of different parts of EPS are listed in Table 1. In Abaqus, post-yielding behavior of the material can be defined in the plasticity section of material features. The plastic data define the true yield stress of the material as a function of the true plastic strain [20]. Table 2 shows, for instance, the conversion from engineering to true material properties data for sleeve. The plastic true strain is obtained by subtracting the elastic strain from the value of the total true strain as it is expressed in the following equation:

$$\epsilon_{pl.true} = \epsilon_{true} - \epsilon_{elastic} = \epsilon_{true} - \frac{\sigma}{E} \tag{3}$$

Table 1. Material characteristics of EPS parts.

Part	Yield Strength R_e [MPa]	Ultimate Strength R_m [MPa]	Elongation, $A5$ [%]
End Plate	404	547	25.6
Pin	962	1074	16.8
Sleeve	404	547	25.6
Test Boss	420	583	21.2

Table 2. Sleeve stress and strain conversions.

	Eng. Stress σ_{eng} [MPa]	Eng. Strain ϵ_{eng} [–]	True Stress σ_{true} [MPa]	True Strain ϵ_{true} [–]	True Plastic Strain $\epsilon_{pl.true}$ [–]
Yield stress point, R_e	404	0.0019	404.77	0.0019	0
Ultimate stress point, R_m	547	0.0853	593.66	0.0819	0.0800

At small values of strain, the differences between the engineering and true strains are negligible, but the differences become significant at larger strain values. Thus, providing the proper stress–strain data to Abaqus is important especially for simulations with high strain values.

The parts are modelled as a 3D homogeneous solid, and assembly of the parts implemented according to the manner conducted in experimental set-up. The cylindrical parts have been set in place by defining coaxial and a face-to-face constraint.

A simplification was applied to the EPS joint to make the model simpler and to decrease the simulation time. This was obtained by omitting the tightening screws of the end plate and therefore equivalent axial load is defined instead of screw preload. In this way, the number of contact surfaces were decreased, and complexity of the analysis was reduced since the main focus of this FE analysis is evaluation of stresses in the contact surfaces of pin-sleeve-test boss.

The contact between EPS components was modelled based on Coulomb friction. Coulomb model characterizes the frictional behavior between two surfaces using a friction coefficient, μ , and actually contacting surfaces will not slip until the shear stress equals the amount of $\mu \times p$ where p is the contact pressure between the two surfaces. The friction coefficient was considered equal to 0.2, similar to the value considered in theoretical calculations.

The quality of the mesh element determines the accuracy of the solution in a FE simulation [22]. The element selected to mesh EPS parts is C3D8R, a continuous three-dimensional, eight-node linear brick, reduced integration, and hourglass controlled element. Due to the reduced integration, the locking phenomena that is a problem with some element types such as the C3D8 element did not appear [23]. A uniform mesh with 4 mm in size was applied to all joint components. The meshed model is shown in Figure 3a.

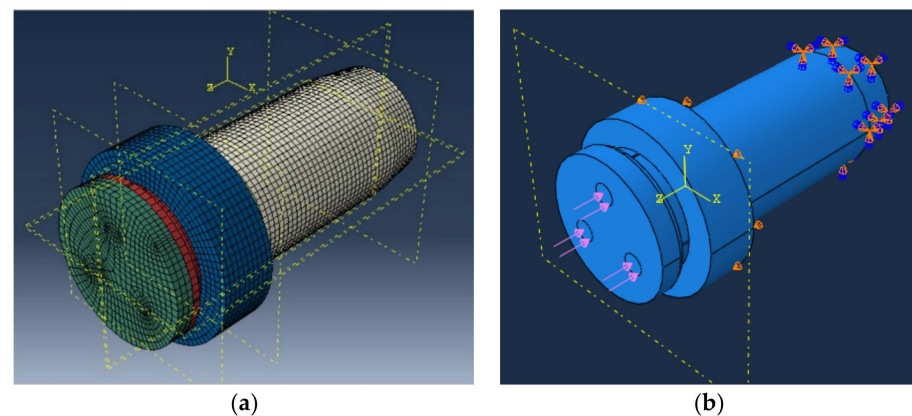


Figure 3. EPS model in Abaqus/CAE. (a) Mesh model (b) Boundary conditions.

Boundary conditions applied to FE model of EPS include clamping of the taper end of the right side of the pin and moreover preventing axial movement of the test boss. The loading of the system is modelled by inserting axial pressure to three circular partitions on the face of the end plate which resembles the axial preload of the EPS created by fastening torque (Figure 3b).

Abaqus dynamic/implicit solver was selected to conduct the simulation analysis and the quasi-static state was activated since the nature of this simulation is not completely static and during applying load to the joint system, the momentum effects cannot be ignored.

3. Results

In this section, the test results for the three different test layouts are provided separately. The test results provide stresses experienced by the test boss.

3.1. Non-Lubricated Partly Cut Sleeve

Coefficient of friction depends upon the surface roughness, especially with the dry friction. The conical sleeve, pin and test boss used in this experiment have similar surface roughness of 3.2 μm . The friction coefficient for non-lubricated condition is assumed equal to 0.2 while for lubricated condition, it is ideally assumed null. The first test layout for the experimental study is the non-lubricated sleeve with three partial cut and one complete cut which resembles the real case application of the EPS. The cleanliness of the contact surfaces of all joints components is very important on locking mechanism of the assembly, because the existence of oil, grease or any other substance can have negative effect on the functioning of the mechanism and hence the measurements may lead to fault data acquisition.

As mentioned before, the strain measurements are undertaken on three points along the outer surface of the test boss. Since the test boss is a thick cylindrical shell with thickness to radius ratio greater than 0.05, the radial and hoop stresses in inner and outer surfaces can be determined using thick-walled cylinder formulas [24]. The inner and outer radii of the test boss are “ a ” and “ b ”, respectively and the general radial and hoop stresses are as follows [25].

$$\sigma_r = \left(1 - \frac{a^2}{r^2}\right)C_1 + \frac{C_2}{r^2}, \quad \sigma_\theta = \left(1 + \frac{a^2}{r^2}\right)C_1 - \frac{C_2}{r^2} \quad (4)$$

The constants C_1 and C_2 can be determined based on the boundary conditions. The test boss was subjected to a radial stress of $\sigma_r = -p$ (the radial pressure) at its inner surface, $r = a$, and since there is no external pressure acting on its outer surface i.e., radial stress $\sigma_r = 0$ at $r = b$ which simplifies Equation (4) to the following form.

$$\sigma_r = \frac{pa^2}{b^2 - a^2} \left(1 - \frac{b^2}{r^2}\right), \quad \sigma_\theta = \frac{pa^2}{b^2 - a^2} \left(1 + \frac{b^2}{r^2}\right) \quad (5)$$

The test boss does not have any movement in axial (z) direction. The outer surface of the test boss experiences no force, but its inner surface is exposed to friction force created by outer surface of the split sleeve. Overall equilibrium of forces in the axial direction requires the following condition:

$$\int_a^b \sigma_z 2\pi r dr = \mu N \quad (6)$$

In Equation (6), N is the radial force created by expansion of the sleeve and it can be calculated by considering internal pressure multiplied by the internal surface area of the test boss as

$$N = \sigma_{r,int} A = \sigma_{r,int} (2\pi a L) \quad (7)$$

where $\sigma_{r,int}$ is the internal radial stress and L is the length of the test boss. Therefore, the axial stress on the inner surface of the test boss is obtained as

$$\sigma_{z,int} = \frac{2aL\mu}{b^2 - a^2} \sigma_{r,int} \quad (8)$$

By measuring the hoop strain on the outer surface of the test boss and using Equation (9), stress components including radial, hoop and axial stresses can be easily determined.

$$\epsilon_r = \frac{1}{E} [\sigma_r - \nu(\sigma_\theta + \sigma_z)], \quad \epsilon_\theta = \frac{1}{E} [\sigma_\theta - \nu(\sigma_r + \sigma_z)], \quad \epsilon_z = \frac{1}{E} [\sigma_z - \nu(\sigma_r + \sigma_\theta)] = \text{constant} \quad (9)$$

where E and ν denote the modulus of elasticity and Poisson’s ratio of the test boss, respectively.

The strain measurements for one of the tests are provided in Figure 4a as an example. The positions of the strain gauges are changed with respect to sleeve cut-through by rotating the test boss 90° after each test. The start position of strain gauges and the four sleeve cuts are demonstrated in Figure 4b, and the strain gauges are all placed adjacent to the sleeve cuts.

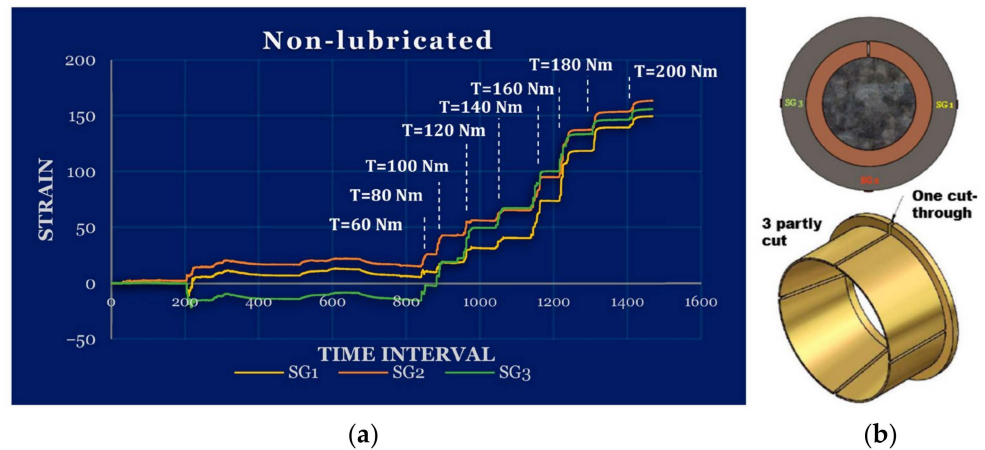


Figure 4. Non-lubricated partly cut sleeve with cut-through at top and strain gauges at 0, π and $3\pi/2$. (a) Recorded strains, (b) pin-sleeve-test boss.

Based on the measured strains for the non-lubricated layout and obtaining the average values, the internal and external radial and hoop stresses were calculated using Equations (5) and (9). Images (a–c) in Figure 5 show the position of the strain gauges and calculated stress values at those spots. Image (d) in the same figure shows the average stresses. It is worth mentioning that external radial stress in the test boss is zero. The stress distribution inside the test boss is not uniform, and these stresses are considered as contact pressure [26]. One of the main reasons for this uneven stress distribution is the friction. The compressive force among the contact surfaces of the conical sleeve, boss and pin creates friction force which prevents the relative slippage. In addition, the regions of the test boss at the complete cut-through experience higher stress level than the partly cuts, and the partly cuts give lower stress level than the areas between the cuts. Hence, another reason for non-uniform stress distribution is due to the cuts where the sleeve expands more in these regions and as a result varying stress levels are induced into the test boss.

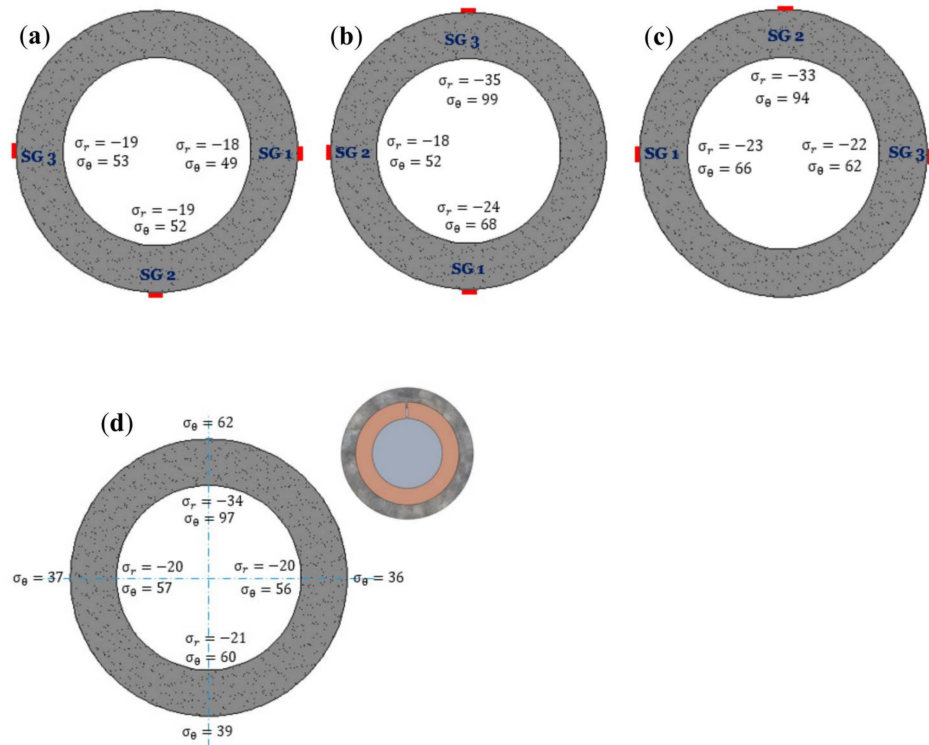


Figure 5. Non-lubricated sleeve with sleeve complete cut-through at $\pi/2$ (stresses in MPa). (a) Test 1 (b) Test 2 (c) Test 3 (d) Average value of the three tests.

3.2. Lubricated Partly Cut Sleeve

For evaluation of the effect of friction between contact surfaces of sleeve-pin-test boss, lubrication was applied to the sleeve. In this test layout, both the inner and the outer surfaces of the conical sleeve were lubricated. The purpose of these tests is to investigate how much of the applied torque dissipates in the form of hysteresis deformation along contact surfaces of the sleeve.

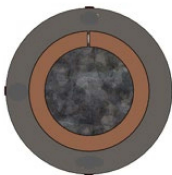
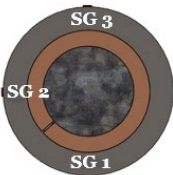
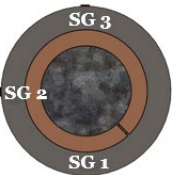
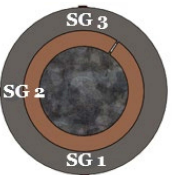
In practice, it is recommended to use a rubber or plastic hammer and tap all around the end plate after applying a definite amount of torque and then resume tightening. The purpose of this task is to release accumulated stresses due to existence of the static friction and to provide a better stress distribution. This step had to be skipped while tightening the screws in non-lubricated test layout, because this could affect the connectivity and accuracy of the strain gauges and lead to their damage. However, this task was implemented for lubricated test layout since lubrication decreases the level of static friction and by gently tapping on the end plate, unwanted accumulated stresses are relieved.

In this test layout, again the position of the cut-through is at $\pi/2$. The strain graphs show that the amount of stress inside the test boss has increased significantly, compared to non-lubricated condition. The stress distribution in lubricated condition is not uniform and it is, to some extent, similar to non-lubricated condition. By comparing the change of stresses with non-lubricated condition, it is concluded that generally the stresses distribute more uniformly as friction decreases. This fact is observed in another research related to loading of a cylinder, for instance in the article of Al-Chalabi, et al. [27].

Elastic hysteresis is defined as the difference between the strain energy required to generate a definite stress in a material, and the material's elastic energy at that stress [28]. This energy is dissipated through internal friction or heat inside material during loading and unloading. Basically, hard metals do not show elastic hysteresis under a moderate loading [29], but the magnitude of stresses inside the test boss in lubricated test series is noticeable and makes this phenomenon to happen.

In order to better evaluate the effect of the sleeve cut-through, a series of tests have been carried out by placing it at different locations. In these series of the tests, the test boss is fixed and just the sleeve is rotated. The sleeve cut-through was placed at three different positions, $\pi/4$, $5\pi/4$ and $7\pi/4$, respectively, shown in Table 3, while keeping the test boss strain gauges at $\pi/2$, π and $3\pi/2$. This gives a relative angular distance of $\pi/4$ between each strain gauge and its closest sleeve cut.

Table 3. Hoop stress [MPa] based on location of cut-through inside the test boss.

		Position of Complete Cut-Trough			
		$\pi/2$	$5\pi/4$	$7\pi/4$	$\pi/4$
Test Layout	Strain Gauge Nr. (Locations)				
	Unlubricated	No SG (0)	56	-	-
	SG 3 ($\pi/2$)	97	107	102	100
	SG 2 (π)	57	85	104	79
	SG 1 ($3\pi/2$)	60	88	76	93
Lubricated	No SG (0)	150	-	-	-
	SG 3 ($\pi/2$)	210	236	212	237
	SG 2 (π)	188	216	209	220
	SG 1 ($3\pi/2$)	165	203	181	230

The hoop stress values measured on the boss at the four cuts are compared to the corresponding values measured at location with $\pm\pi/4$ angular distance, for both dry and lubricated sleeves. For the unlubricated case, the measurements on the boss at the cuts, which are provided in Figure 6, show a higher value, 97 MPa, for the complete cut at $\pi/2$ compared to the opposite partly cut $3\pi/2$ and neighbor cuts at π and 2π , with values equal to 60 MPa, 57 MPa and 56 MPa, respectively. This gives 68% higher stress at the complete cut, compared to the average of the three partly cuts. For the lubricated case, the corresponding measured values are 210 MPa, 165 MPa, 188 MPa and 150 MPa, respectively, which gives 25% higher stress level for the complete cut, compared with the average value of the other three.

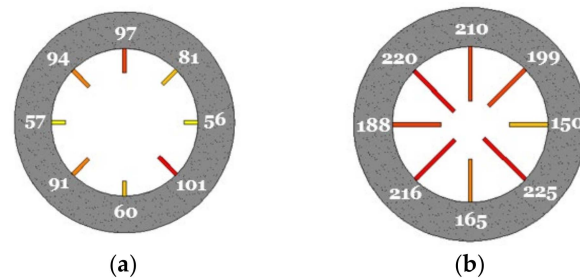


Figure 6. Hoop stresses (MPa) along inner surface of test boss. (a) Non-lubricated (b) Lubricated.

Measurements taken at positions $\pm\Delta\pi/4$ are compared to the cut positions, and these measurements indicate changes in the stress level compared to the measurements at the cuts. The stress level close ($\pm\Delta\pi/4$) to the complete cut at $\pi/2$ shows reductions from 97 MPa to 94 MPa, and 81 MPa, respectively. The corresponding values for the opposite partly cut at $3\pi/2$ show an increase from 60 MPa to 101 MPa, and 91 MPa, respectively. All values for both non-lubricated and lubricated partly cut cases are shown in Figure 6, which resembles a kind of stress distribution in the test boss.

In this test layout, the regions around the location of the sleeve cut-through experience higher stresses than other regions, which is similar to non-lubricated condition. By comparing the strains and stresses of the lubricated condition with the non-lubricated, it is found out that both radial and hoop stresses at positions of $0, \pi/4, \pi/2, 3\pi/4, \pi, 5\pi/4, 3\pi/2$ and $7\pi/4$ are increased with ratios of 2.68, 2.46, 2.16, 2.34, 3.30, 2.37, 2.75 and 2.23 times, respectively. The average of stresses in the lubricated condition is 2.54 times greater compared with the non-lubricated condition.

3.3. Lubricated Completely Cut Sleeve

Another test layout investigated in this experiment was lubricated completely cut sleeve. In clamping mechanism of the EPS, a part of the applied torque is used to deform the sleeve in elastic range. In the EPS, the sleeve slits make the expansion easier, but still a part of the applied torque is used to deform the sleeve. Thus, by cutting the sleeve into four separate parts, the dissipation of energy related to elastic deformation of sleeve would be omitted. The aim of these tests is to evaluate how much of torque is spent for the elastic deformation of sleeve. The sleeve is cut into four identical parts. The results of these series of tests are exhibited in Figure 7. The strains and stresses are increased significantly in comparison with previous non-lubricated and lubricated sleeve test layouts, and it is obvious that the stress distribution is to a great extent uniform along the whole inner surface of the test boss. It is concluded that radial and hoop stresses in the inner surface of the test boss at positions of $0, \pi/4, \pi/2, 3\pi/4, \pi, 5\pi/4, 3\pi/2$ and $7\pi/4$ are increased with ratios of 4.64, 3.23, 2.70, 2.78, 4.68, 2.88, 4.37 and 2.59 times, respectively, compared with the non-lubricated partly cut condition. The average ratio is 3.48.

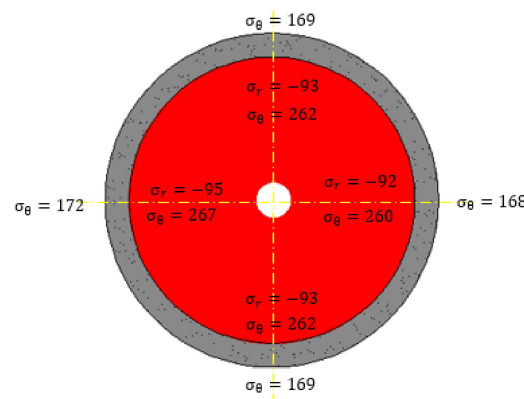


Figure 7. Distribution of hoop and radial stress for lubricated completely cut sleeve.

By making a comparison between unlubricated partly cut sleeve and lubricated completely cut sleeve test results, it is revealed that 71.3% of the total applied energy is dissipated which is actually used to deform the sleeve in elastic region of material and to overcome the friction force, i.e., elastic hysteresis. The rest of the applied energy to the EPS which is 28.7% is spent to expand the test boss elastically.

On the other hand, by comparing the test results of the unlubricated partly cut sleeve with the lubricated cut sleeve, it is found out that 60.6% of the dissipated energy is dedicated to overcoming the friction, i.e., around 43.2% of the total applied energy to the EPS is spent in the form of friction. The share of elastic expansion of the sleeve from dissipated energy is 39.4% which means a share of 28.1% of the total applied energy to the EPS, and this amount of energy remains in the clamped system in the form of residual contact pressure and disappears when the system is unlocked.

Surface roughness of the joint components is an important parameter, and it must receive special attention. The conical sleeve, pin and test boss used in this experiment have similar surface roughness of 3.2 μmRa according to ISO 2768 standard.

The characteristic of hoop stress inside the test boss is tensile while radial and axial stresses are compressive. For further analysis of the test boss stress distribution through different test layouts and to find out whether it has experienced yielding or not, maximum shear stress (MSS) theory based on Tresca stress and distortion energy (DE) theory based on von Mises stress are evaluated [30]. The respective maximum Tresca and von Mises stresses are calculated for each condition based on the highest values of stresses registered during measurements. Based on the obtained results, the maximum stress has occurred on the inner surface of the test boss. For a general state of stress with principal stresses ordered as $\sigma_1 > \sigma_2 > \sigma_3$, the maximum shear stress is $\tau_{max} = (\sigma_1 - \sigma_3)/2$. Thus, the MSS is violated, or yielding happens when the following condition dominates

$$\tau_{max} = \frac{\sigma_1 - \sigma_3}{2} \geq \frac{R_e}{2} \tag{10}$$

Equation (10) gives the maximum shear stress and compares it with yield stress to evaluate the failure condition of the materials. Based on the stress state in the test boss which is $\sigma_{\theta,int} > \sigma_{z,int} > \sigma_{r,int}$, then the MSS is determined by:

$$\tau_{max} = \frac{\sigma_{\theta,int} - \sigma_{r,int}}{2} \tag{11}$$

where $2\tau_{max}$ corresponds to the Tresca stress criteria. The von Mises criteria, which is derived from strain energy of the elements of a part, takes the following form for a three-dimensional stress state:

$$\sigma_{von\ Mises} = \left[\frac{(\sigma_1 - \sigma_2)^2 + (\sigma_2 - \sigma_3)^2 + (\sigma_3 - \sigma_1)^2}{2} \right]^{1/2} \tag{12}$$

Therefore, the von Mises stress for the test boss is calculated similar to the above equation as follows:

$$\sigma_{von\ Mises} = \left[\frac{(\sigma_{\theta,int} - \sigma_{z,int})^2 + (\sigma_{z,int} - \sigma_{r,int})^2 + (\sigma_{r,int} - \sigma_{\theta,int})^2}{2} \right]^{1/2} \quad (13)$$

It is worth mentioning that $\sigma_{z,int}$ which is given in Equation (4) can be calculated based on the geometry of the test boss for inner diameter $a = 44.5$ mm and outer diameter $b = 64.5$ mm and also assuming a friction coefficient of $\mu = 0.2$, which yields $\sigma_{z,int} = 0.31\sigma_{r,int}$. Tresca and von Mises values are given in Table 4. It can be seen from the combined stresses that in lubricated partly cut sleeve, the Tresca and von Mises stresses have increased with a factor of 2.22 and 2.23, respectively, compared to the non-lubricated partly cut sleeve. For the lubricated completely cut sleeve the corresponding values are 2.64 and 2.58, respectively.

Table 4. Evaluation of failure (yield criteria) based on measured stresses.

Test Layout	Tresca Stress [MPa]	von Mises Stress [MPa]	Yield Strength of Test Boss [MPa]
Non-lubricated Partly Cut Sleeve	137	126	420
Lubricated Partly Cut Sleeve	304	281	420
Lubricated Completely Cut Sleeve	362	325	420

According to the calculated values for non-lubricated sleeve which resembles the application of the EPS in practice, both Tresca and von Mises stresses are much lower than the failure limits, but for lubricated completely cut sleeve, von Mises and Tresca stresses reach 77% and 86% of the material yield strength. Tresca criteria is a more conservative than von Mises criteria.

4. Comparison of the Results and Discussion

The FE results obtained from Abaqus simulation will be compared with experimental results of the test boss measured from non-lubricated partly cut sleeve test layout. Since there is no experimental result for the pin and the expansion sleeve, the FE results of these parts will be compared with results of the theoretical formulas of Andrzejuk et al. [15]. Here, the comparison is performed separately for each EPS part including sleeve, pin and test boss.

4.1. Partly Cut Sleeve

The sleeve plays an important role in any EPS joint, because its expansion leads to creation of the clamping force. The level of von Mises stress (shown in Figure 8a) obtained from FE method is in the elastic region in different parts of the sleeve. The maximum von Mises value is 338 MPa which occurred in the collar edge near the contact surface of end plate and sleeve. The characteristic of this stress is tension which is related to expansion of the sleeve. As it was expected, the back side of the sleeve collar has experienced a low level of stress since it does not have any contact with other parts and the stress of this region is resulted from Poisson's effect. Tresca stress distribution is similar to von Mises stress distribution, and it points out the maximum stress at the same region as von Mises criteria with magnitude of 384 MPa, which is around 14% higher than maximum von Mises stress.

Figure 8a shows that three regions in the sleeve experience higher stresses. One of these regions is at the complete cut-through. The other two regions are the regions between the cuts. One of the reasons for this matter is related to freedom of sleeve to deform at cuts and slip along the pin circumference which results in accumulation of stress in surrounding regions.

The corresponding radial stress for the sleeve in FE simulation is S11 (the first stress component, σ_1) when it is in horizontal plane, because other planes will add stress components that require further calculation to find the radial stress. This is valid as if the effects of shear stresses are ignored. Therefore, a path is defined in the horizontal plane across the tapered length of the sleeve equal to the contact length. This path is shown in Figure 8b. S11 in xz-plane gives the radial stress in the test boss at 0 and π , while S22 in yz-plane gives the

radial stress at $\pi/2$ and $3\pi/2$. It is along one of the sleeve slits (it could also be defined on the other side due to symmetry). The radial stress is obtained from S11 value in xz-plane on the defined path, shown in Figure 9a. It is compared with the result of Andrzejuk et al. [15]. Figure 9b shows the contact length between the sleeve and pin which is approximately 35 mm.

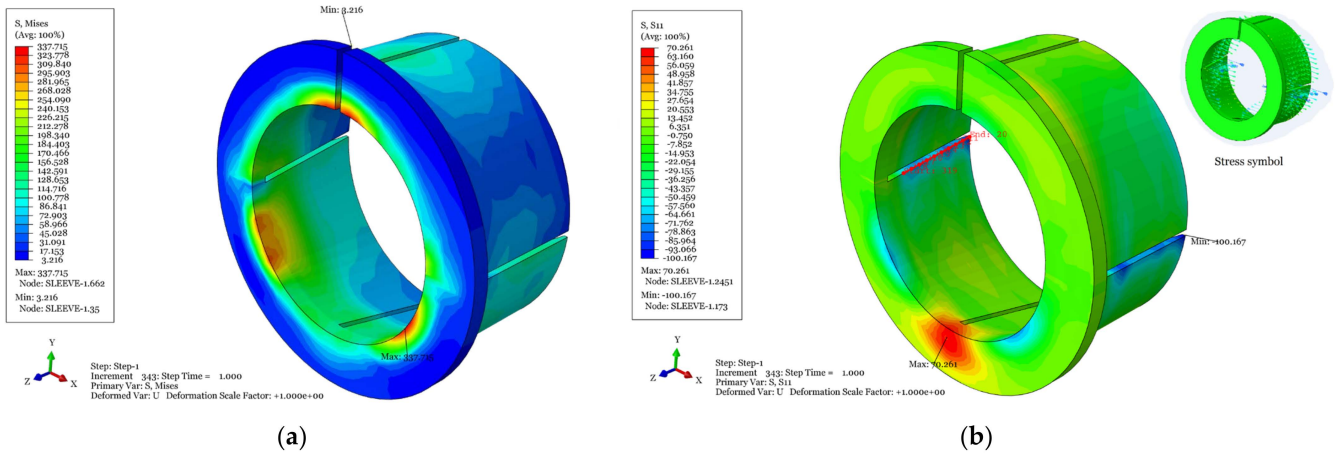


Figure 8. Stresses in sleeve resulted from 200 Nm torque. (a) von Mises stress distribution in sleeve (b) S11 (x-dir) stress distribution in sleeve.

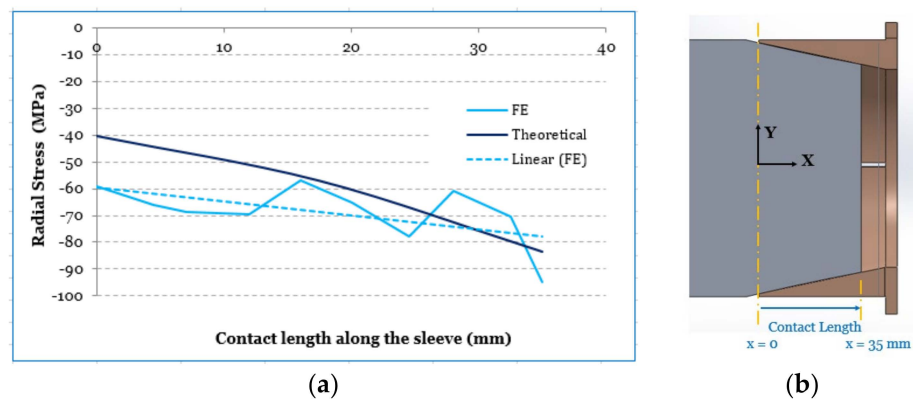


Figure 9. Sleeve radial stress along contact length. (a) Comparison of sleeve radial stress; (b) illustration of contact length.

Figure 9a shows that both theoretical and FE results predict an increase in the magnitude of radial stress as it moves from the edge of the sleeve towards its collar which is equivalent to a move from approximately beginning of pin taper towards its end. However, FE curve has some dramatic jumps which could be related to inaccuracy of FE calculations on the integration points due to mesh size. The dash line in the figure is a linear trend line for FE curve which highlights the stress increase at the end of the pin. Furthermore, it could be expressed that the prediction of formula in Andrzejuk et al. [15] for maximum radial stress is in good agreement with FE results even though it is for a sleeve without any cuts or slits.

4.2. Pin

Similar to the case indicated for sleeve, S11 stress in Abaqus which is the stress component in x-direction resembles pin radial stress at xz-plane. Distribution of S11 and a path parallel to the one used for presenting radial stress for sleeve are shown in Figure 10. Variations of radial stress along the corresponding path for both the theoretical method of Andrzejuk et al. [15] and the FE results are shown in Figure 11a. It is observed that FE and theoretical results are in good agreement with each other. In different regions along the contact length discrepancies exist between the two curves. FE method calculates the stress

values for each element and since the sleeve has four slits which one of them is a complete cut, the induced pressure of sleeve to pin is not symmetric and it is actually non-uniform. Therefore, existence of non-uniformity in radial stress of the pin is not strange. FE method shows this matter and local differences are visible in the FE curve. Both FE and theoretical methods show increase in the magnitude of radial stress along the contact length.

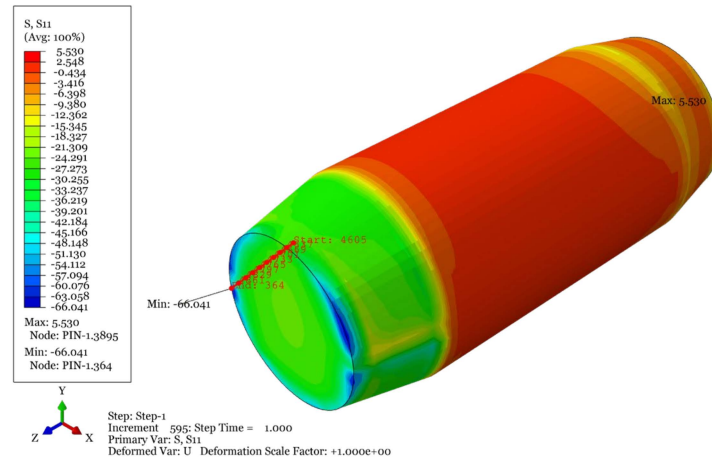


Figure 10. S11 stress distribution in pin resulted from 200 Nm torque.

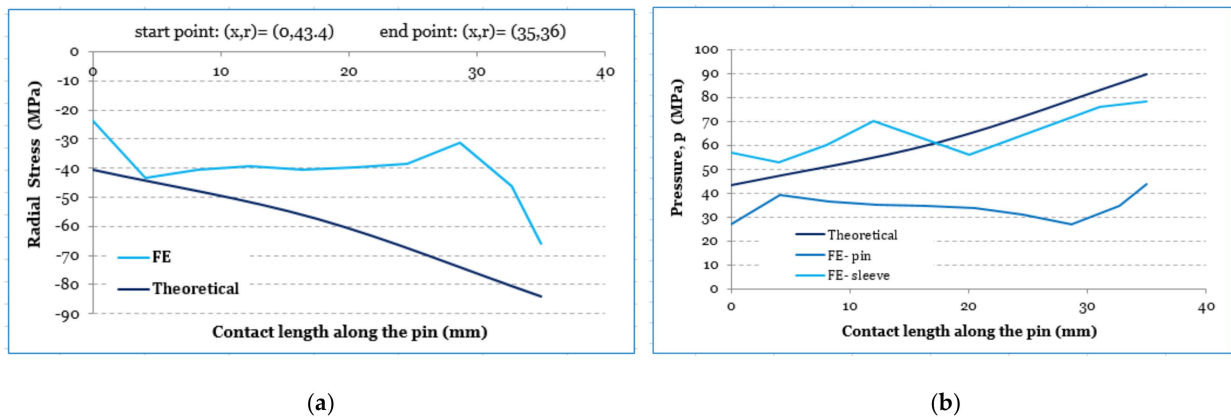


Figure 11. Stresses in pin along contact length. (a) Comparison of pin radial stress (b) Comparison of contact pressure.

FE results show that the maximum von Mises and Tresca stresses happen at the same point that the maximum stress component in x -direction, S11, has occurred and their values are 57.62 MPa and 66.31 MPa, respectively.

Another parameter of interest to investigate is the contact pressure between pin and sleeve. This pressure in the EPS is transferred to the equipment support. The contact pressure increases from sleeve edge towards its collar. The contact pressure obtained from FE analysis is given in the same graph for both sleeve and pin in Figure 11b. The contact pressure of the sleeve obtained from FE is in good agreement with the graph of theoretical formula from Andrzejuk et al. [15] even though it is not completely uniform and has some dramatic peaks and troughs. It was expected that FE results for both the sleeve and the pin would have the same value, but they are different due to modelling features. Based on the comparison between the theoretical and FE results, it can be concluded that formulas in Andrzejuk et al. [15] are appropriate for prediction of contact pressure of the sleeve-pin as an initial estimation.

4.3. Test Boss

FE results of the test boss are compared with experimental results. The *von Mises* stress distribution for the test boss produced in post-processing of Abaqus is shown in Figure 12. The magnitude of the maximum *von Mises* stress in the test boss predicted by FE method is 108 MPa. This result is close to the experimental value of 126 MPa, which is presented in Table 4. However, there is a difference between positions of the maximum *von Mises* in the test boss predicted by FEM. Abaqus gives the position of the maximum *von Mises* stress at angular position of 155° , while based on the experimental measurements, the maximum *von Mises* has been found to occur at $\pi/2$, $5\pi/4$ and $7\pi/4$ radian. The FE predicted point was not at a position where strain gauges were located during experiments. Therefore, it could be concluded that further experimental research is required to investigate this matter.

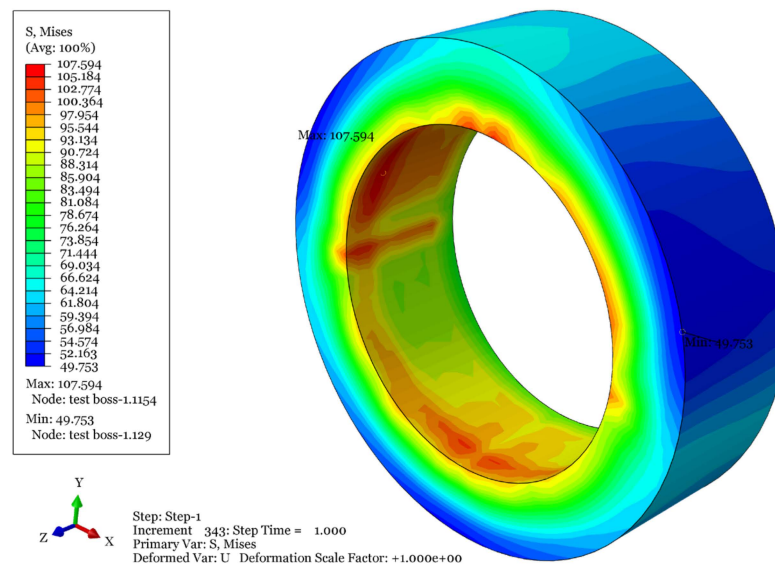


Figure 12. The *von Mises* stress distribution in the test boss resulted from 200 Nm torque.

In addition, Tresca stress was used as another criterion to compare the stress level for the test boss. The location of the maximum Tresca stress from the FE method is at the same location for the *von Mises* stress, and its magnitude is 120 MPa, which compared with experimental value of 137 MPa (Table 4) could be considered as a close result.

Different stress components in Abaqus for each joint part provide hoop, radial and axial stresses on different planes. In order to extract hoop stress for the test boss, two different cuts were applied. S11 in yz-plane gives the hoop stress in the test boss at $\pi/2$ and $3\pi/2$ positions, while S22 in xz-plane gives the hoop stress at 0 and π locations.

Abaqus calculates S11 and S22 in each node and it shows a non-uniform stress distribution along the cross sections on the xz- and yz-planes with higher values on inner surface of the test boss. To make a comparison with experimental results, only the maximum value on each cross section is considered. The comparison of FE and experimental hoop stress on inner and outer surfaces of the test boss is given in Table 5.

Table 5. Comparison of hoop stress in the test boss on both inner and outer surfaces.

Angular Position [rad]	Inner Surface			Outer Surface		
	Experimental [MPa]	FE [MPa]	Error [%]	Experimental [MPa]	FE [MPa]	Error [%]
0	55.93	85.9	53.58	36.12	51.59	42.83
$\pi/2$	96.82	75.77	-21.74	62.37	50.97	-18.28
π	57	84.85	48.86	36.75	49.44	34.53
$3\pi/2$	60.19	83.82	39.26	38.83	48	23.62

From the comparative results from Table 5, it is observed that accuracy of the FEM to predict the hoop stress has some considerable deviations from experimental values. FEM predictions for the hoop stress on outer surface of the test boss are better than those on the inner surface, but still the errors are significant.

Radial stress is another subject of comparison, whose values from FE analysis are compared with corresponding values from experimental measurements given in Table 6. Compared to the hoop stress, FEM predictions for radial stress are closer to the experimental measurements. Moreover, FEM predicts the position of maximum radial stress correctly, which is at top of the test boss at angular position of $\pi/2$ rad where the complete cut through is located, similar to the test results.

Table 6. Comparison of radial stress in the test boss.

Angular Position [rad]	Experimental [MPa]	Inner Surface	
		FE [MPa]	Error [%]
0	−19.86	−19.07	4.14
$\pi/2$	−34.37	−27.91	23.15
π	−20.24	−18.65	8.53
$3\pi/2$	−21.37	−15.84	34.91

The axial stress from experimental method can be calculated using Equation (8). Based on the assumption of the friction coefficient $\mu = 0.2$, the maximum and minimum experimental axial stresses are −6.16 MPa and −10.65 MPa, respectively. The FEM prediction gives the axial stress of the test boss ranging between −22.67 MPa and +5.5 MPa indicating that both the compressive and tensile stresses occur in the test boss, as shown in Figure 13. Occurrence of tensile stress in some parts of the test boss is due to compressive frictional force in inner side of the test boss which pulls the surrounding materials. This can be considered as one of the advantages of FEM that can capture material behavior locally and it is not restricted to provide only an overall response as the theoretical method does. Most parts of the test boss experience an axial stress in the range from −4 MPa to −13 MPa, which is close to the range observed from the experimental results.

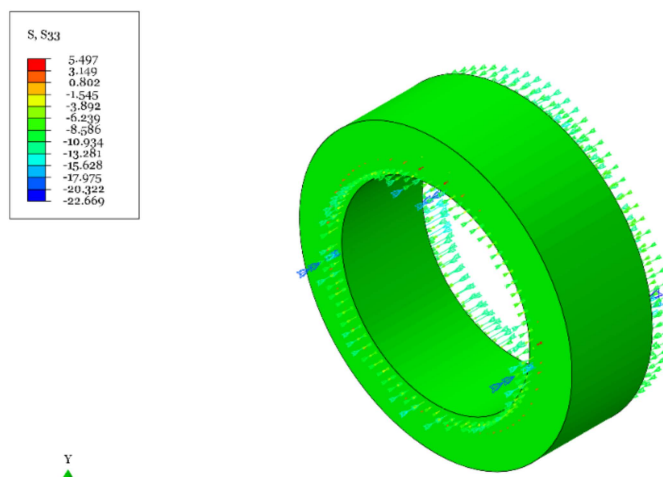


Figure 13. Test boss axial stress resulted from 200 Nm torque.

5. Conclusions

In this study, an expanding pin system is analyzed in detail and the stress distribution in the joint system after tightening the fastening screws is clarified. The experimental part of this study, which was performed for three different test layouts namely non-lubricated partly cut sleeve, lubricated partly cut sleeve and lubricated completely cut sleeve, has provided detailed information about stress distribution and its magnitude in the test boss that simulates the equipment support. The experimental results indicate that stress

concentrations take place in regions near sleeve cut-through and in regions next to it (with 180° angular distance from sleeve cut-through).

Other findings of the experimental study obtained from non-lubricated partly cut sleeve and lubricated completely cut sleeve are related to dissipation of energy applied to the EPS via torquing. Approximately 71% of the applied energy dissipates to overcome the friction and to expand the sleeve while only 29% of the torque is used to expand the test boss. Comparison of the test results of the non-lubricated partly cut sleeve with lubricated partly cut sleeve showed that about 61% of the loss of energy is due to friction and the rest, which is 39%, is due to elastic expansion of the sleeve. Therefore, it is concluded that around 43% of the total applied energy to the EPS is lost due to friction in different joint components (including pin, sleeve and test boss) and 28% is spent to deform the sleeve elastically. The values are valid as long as we assume that friction coefficient in lubricated condition is zero which is an ideal assumption. The elastic deformation, i.e., expansion of the partly cut sleeve results in creation of the clamping force in the EPS. On the other hand, the friction which always behaves as a resisting force has positive effect on producing a better clamping effect since its absence leads to a slack joint which will result in malfunction of the joint system when it is exposed to sudden loads or vibrations.

The FEA results for the sleeve, including radial stress and contact pressure, are very close to the calculated values using formulas of reference [15]. Therefore, it is concluded that those formulas can be used to estimate pin-sleeve contact pressure and radial stress, even though they are derived for a sleeve without any slits. However, the FEA results for pin are not in agreement with the corresponding theoretical formulas. One of the reasons maybe related to mesh size, which can affect results of the FEA considerably and moreover due to discreteness of the contact.

The FEA results for test boss are in good agreement with experimental results. Particularly, the FEA results for von Mises, Tresca and radial stresses are in very good agreement with experimental results and the minor deviations can be attributed to the assumptions and simplifications considered during FE modelling.

Author Contributions: Conceptualization, Ø.K. and H.G.L.; methodology, S.S. and Ø.K.; experimentation, S.S.; software, S.S.; validation, S.S. and Ø.K.; analysis, S.S., Ø.K. and H.G.L.; writing-original draft preparation, S.S.; writing-review and editing, H.G.L. and Ø.K.; supervision, H.G.L. All authors have read and agreed to the published version of the manuscript.

Funding: This research received no external funding.

Institutional Review Board Statement: Not applicable.

Informed Consent Statement: Not applicable.

Data Availability Statement: Not applicable.

Conflicts of Interest: The authors declare no conflict of interest.

References

1. Karlsen, Ø.; Lemu, H.G. Questionnaire-based survey of experiences with the use of expanding PIN systems in mechanical joints. *J. Results Eng.* **2021**, *9*, 100212. [[CrossRef](#)]
2. Timoshenko, S.; Goodier, J. *Theory of Elasticity*; McGraw-Hill: New York, NY, USA, 1951.
3. Eriksson, I. On the bearing strength of bolted graphite/epoxy laminates. *J. Compos. Mater.* **1990**, *24*, 1246–1269. [[CrossRef](#)]
4. Wang, H.S.; Hung, C.L.; Chang, F.K. Bearing failure of bolted composite joints. Part I: Experimental characterization. *J. Compos. Mater.* **1996**, *30*, 1284–1313. [[CrossRef](#)]
5. Hung, C.L.; Chang, F.K. Bearing failure of bolted composite joints. Part II: Model and verification. *J. Compos. Mater.* **1996**, *30*, 1359–1400. [[CrossRef](#)]
6. Yavari, V.; Rajabi, I.; Daneshvar, F.; Kadivar, M.H. On the stress distribution around the hole in mechanically fastened joints. *Mech. Res. Commun.* **2009**, *36*, 373–380. [[CrossRef](#)]
7. Bozkaya, D.; Müftü, S. Mechanics of the tapered interference fit in dental implants. *J. Biomech.* **2003**, *36*, 1649–1658. [[CrossRef](#)]
8. Dongliang, Z.; Binwu, W.; Fei, L. The contact stress analysis about the conical expansion sleeve connection. In Proceedings of the Fifth International Conference on Measuring Technology and Mechatronics Automation, Hong Kong, China, 16–17 January 2013. [[CrossRef](#)]

9. Yu, K.; Yang, X. Torque capacity and contact stress analysis of conical interference fit shrink disc of wind turbine. *Multidiscip. Modeling Mater. Struct.* **2018**, *14*, 189–199. [[CrossRef](#)]
10. Siemiatkowski, Z.; Rucki, M.; Kudlacek, J. Internal Stresses Analysis in the Shrink-Fitted Joints of the Assembled Crankshafts. In *Advances in Manufacturing. Lecture Notes in Mechanical Engineering*; Hamrol, A., Ciszak, O., Legutko, S., Jurczyk, M., Eds.; Springer: Berlin/Heidelberg, Germany, 2018. [[CrossRef](#)]
11. Croccolo, D.; Agostinis, M.D.; Vincenzi, N. Failure analysis of bolted joints: Effect of friction coefficients in torque–preloading relationship. *Eng. Fail. Anal.* **2011**, *18*, 364–373. [[CrossRef](#)]
12. Nigrelli, V.; Pasta, S. Finite-element simulation of residual stress induced by split-sleeve cold-expansion process of holes. *J. Mater. Processing Technol.* **2008**, *205*, 290–296. [[CrossRef](#)]
13. Ismonov, S.; Daniewicz, S.R.; Newman, J.C.; Hill, M.R.; Urban, M.R. Three dimensional finite element analysis of a split-sleeve cold expansion process. *J. Eng. Mater. Technol.* **2009**, *131*, 31007. [[CrossRef](#)]
14. Berkani, I.; Karlsen, Ø.; Lemu, H.G. Experimental and numerical study of Bondura®6.6 PIN joints. *IOP Conf. Ser. Mater. Sci. Eng.* **2017**, *276*, 012028. [[CrossRef](#)]
15. Andrzejuk, A.; Skup, Z.; Zalewski, R. Analysis of a conical sleeve with pivot joint loading of axial force. *J. Theor. Appl. Mech.* **2014**, *52*, 345–358.
16. Langeroodi, S.S. Experimental Study and Optimization of Expanding Pin Technology for Heavy Duty Machine Joint Application. Master’s Thesis, University of Stavanger, Stavanger, Norway, 2021. Available online: <https://hdl.handle.net/11250/2786185> (accessed on 29 September 2021).
17. Hannah, R.L.; Reed, S.E. *Strain Gage Users’ Handbook*; Chapman & Hall: London, UK, 1992.
18. Hoffmann, K. *Applying the Wheatstone Bridge Circuit*; HBM: Darmstadt, Germany, 1974.
19. Zou, Q.; Sun, T.S.; Nassar, S.A.; Barber, G.C.; Gumul, A.K. Effect of lubrication on friction and torque-tension relationship in threaded fasteners. In Proceedings of the International Joint Tribology Conference, San Antonio, TX, USA, 23–25 October 2006; pp. 591–602. [[CrossRef](#)]
20. Abaqus 2016 User Manual. *Getting Started with Abaqus/CAE, Dassault Systems*. 2016. Available online: http://130.149.89.49:2080/v2016/pdf_books/GET_STARTED.pdf (accessed on 29 September 2021).
21. Forni, D.; Chiaia, B.; Cadoni, E. Strain rate behaviour in tension of S355 steel: Base for progressive collapse analysis. *Eng. Struct.* **2016**, *119*, 164–173. [[CrossRef](#)]
22. Lee, N.S.; Bathe, K.J. Effects of element distortions on the performance of isoparametric elements. *Int. J. Numer. Methods Eng.* **1993**, *36*, 3553–3576. [[CrossRef](#)]
23. MITEducation, Eight-Node Brick Element with Reduced Integration (Blog). Available online: https://web.mit.edu/calculix_v2.7/CalculiX/ccx_2.7/doc/ccx/node27.html#int1 (accessed on 15 April 2021).
24. Ventsel, E.; Krauthammer, T. *Thin Plates and Shells: Theory, Analysis, Applications*; Routledge: New York, NY, USA, 2001.
25. Boresi, A.P.; Schmidt, R.J.; Sidebottom, O.M. *Advanced Mechanics of Materials*, 6th ed.; Wiley: New York, NY, USA, 1985.
26. Hong, Y.; Wang, X.; Wang, Y.; Zhang, Z. Study on reducing the risk of stress corrosion cracking of austenitic stainless steel hydraulically expanded joints. *J. Eng. Fail. Anal.* **2020**, *113*, 104560. [[CrossRef](#)]
27. Al-Chalabi, M.; Huang, C. Stress distribution within circular cylinders in compression. *Int. J. Rock Mech. Min. Sci. Geomech. Abstr.* **1974**, *11*, 45–56. [[CrossRef](#)]
28. INSTRON. Elastic Hysteresis. Available online: <https://www.instron.us/en-us/our-company/library/glossary/e/elastic-hysteresis#> (accessed on 12 March 2021).
29. Hopkinson, B.; Williams, T.G. The Elastic Hysteresis of Steel. *Proc. R. Soc. Lond. Ser. A Contain. Pap. A Math. Phys. Character* **1912**, *87*, 502–511. [[CrossRef](#)]
30. Budynas, R.G.; Nisbett, J.K.; Tangchaichit, K. *Shigley’s Mechanical Engineering Design*, 8th ed.; McGraw Hill: New York, NY, USA, 2005.

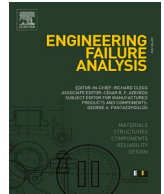
Appended Paper VII

Comparative Study on Loosening of Anti-loosening Bolt and Standard Bolt System

KARLSEN, Ø.; LEMU, H. G.

Engineering Failure Analysis, 2022, vol. 140, 106590

<https://doi.org/10.1016/j.engfailanal.2022.106590>



Comparative study on loosening of anti-loosening bolt and standard bolt system

Øyvind Karlsen^{a,b,*}, Hirpa G. Lemu^a

^a Faculty of Science and Technology, University of Stavanger, Norway

^b Bondura Technology AS, Norway

ARTICLE INFO

Keywords:

Self-loosening
Bolt-loosening
Pre-loaded bolt
Anti-loosening
Fasteners
Vibration

ABSTRACT

In general, bolted connections are exposed to vibrations or repeated over-loads that could lead to self-loosening due to loss of preload. Pre-tensioned bolts in ring flanges are critical parts in Offshore Floating Wind Power Systems, and normally a certain percentage of the installed bolt connections are checked and re-tightened every year. This re-tightening is often done at a high cost and a short weather window due to strong winds and high waves. In this paper, three bolt dimensions (M20, M30 and M42) of the anti-loosening bolt system have been tested. The M30 and M42 bolt systems were preloaded and exposed to transverse oscillating loading, and the loss of preload as a function of load amplitude and number of cycles were measured and compared to standard bolts of HV type, exposed identically. The tested novel bolt system has shown superior capacities to withstand self-loosening, compared to standard bolts.

1. Introduction

Hundreds of billions of fasteners are produced around the world every year [1], and in almost any mechanical connection, there will be solutions for how to transmit power from one part to the other, in the most efficient way, and the transmitted power will often be of mechanical type. There exists a wide range of technical solutions for how to transmit such power, and for mechanical systems, several methods can be mentioned including: riveted and interference fitted pins, pre-tensioned, open-hole bolts and expanding pin solutions [2-4] as standard choices, depending on type of exposure, loads, sizes, and preferences. In general, increasing transmitted power in a mechanical system will result in increased exposure of the mechanical connections to higher loads, with increased probability for damages or malfunctions as a result, especially at the contacting surfaces.

Relative movements between connected parts, typically because of vibrations or over-loads, can result in fretting related problems, like fretting wear, corrosion, and fatigue [3]. Many studies have been performed regarding fretting, and how to prevent the fretting related problems in joints [5-11]. The most important factor in relation to reliability and functionality of bolted joints is the clamping force, where both friction and torque are important factors [12].

Vibrations in mechanical systems can result in loss of clamp forces in preloaded bolts, whose effect depends on vibration type and level, preload level, contact surface and size, reduction and loss of asperities, thread type and size, thread pitch, lubrication of threads, etc. Loss of clamp force in bolts in a bolted connection can easily result in failure and damages of both the bolts, the connection, and the mechanical system itself. After fatigue, self-loosening of bolts is one of the most common causes of failure in bolted connections.

* Corresponding author at: Faculty of Science and Technology, University of Stavanger, Norway.
E-mail address: oyvind.karlsen@uis.no (Ø. Karlsen).

Grabon et al. [12] indicated that surveys from the USA show that up to 23% of all car service problems were related to loosening fasteners, and even for new cars around 12% had this problem.

Standard preloaded bolts, with bolt head, shank and one or two nuts, are often applied when connecting huge flanges like the ring flange connections in wind turbine towers, illustrated in Fig. 1, and in many different constructions, heavy machineries, flange connections of tubes, etc. Such standard preload bolt solutions have a relatively low cost and are normally easy to install. Generally, there are two methods of generating the required pretension in bolts: (1) by torquing the nut directly by hand torquing tool or torquing tools with external energy source, or (2) by hydraulic tensioning of the shank [13,14] followed by a light torquing of the nut, pressure release and disconnection of the hydraulic tool thereafter. In the first case, an additional second nut can be applied and torqued. In both cases, with direct torquing or hydraulic tensioning, the nuts are exposed to vibrations and possible fatigue and fretting problems over time, which again can lead to self-loosening. The two nuts in such a situation would normally be working at the same identical bolt threads, with same shape, size and pitch and surface conditions. This means that the two nuts could loosen their grip together, and turn together, without the second nut having any specific locking effect. If the two nuts are identical, the locking nut would not have any specific locking effect or locking capabilities that the main nut doesn't have, and in addition it can be argued that the locking nut is weakening the locking effect of the main nut by reducing the contact pressure at the main nut threads.

Standard bolts and nuts are often made in strength class 8.8, 10.9 or 12.9 with typically zinc plated, hot dipped galvanized (HDG) surface protection, but also coatings with zinc and aluminium flakes like Geomet500®, Dacromet®, or Delta® are in use. All surface treatments will have a certain amount or level (height) of asperities that must be taken into consideration when analysing self-loosening behaviour of the bolt-nut system, in addition to relaxing and creep effects due to structural changes in the material, over time.

Re-tightening of standard bolts at critical positions, for instance, for floating Offshore Wind Power systems has become a high-cost activity that the system owners and operators both want and need to minimize. For safety reasons, all critical pre-tensioned bolt positions are normally checked yearly by re-tightening 10% of the bolts. These activities require a great number of resources, but at a limited time window due to operational limitations as weather and wave conditions, as investigated by Gintautas and Sørensen [15].

The first author of this paper has designed a new anti-loosening bolt solution where all three parts; bolt, main nut and locking nut, are designed to work together to reduce any self-loosening effects of the bolt assembly, and by that reduce or prevent the need for re-tightening pretensioned bolts in critical positions. Such a reduced need for re-tightening bolts would have a great cost-impact, especially at Offshore Wind Power sites, where the cost for re-checking and re-tightening is substantial.

Today's Offshore Wind Power systems require bolts up to M72 size on the ring flanges, and bolt sizes for future systems will reach M100 or bigger, typically of 10.9 or 12.9 quality class, typically with HDG surface protection. It is a known "problem" that the bolts must be checked or re-tightened after a few weeks or months due to plastic deformation of asperities and creep of the metal, where both effects could lead to turning of the nut and loss of tightening force consequently. Vibrations and oscillating loads in both axial and transverse directions will often lead to self-loosening of the bolted systems, and therefore a yearly re-tightening schedule of a certain amount of the bolts, typically 10%, is normally introduced. Vibrations tend to deform and reduce the height of asperities at the contact surfaces, and a high pre-load could lead to material yield at the first engaged threads. Both lead to reduced clamp force and increased risk of nut turning, which generate further clamp force loss and possibly total failure of the bolted system.

The anti-loosening bolt system, Vibralock® [16], illustrated in Fig. 2, contains a bolt with a bolt head, a shank, and threaded parts with two different diameters, and hence with different thread pitches. Two nuts, a main nut, and a locking nut, are used on the same

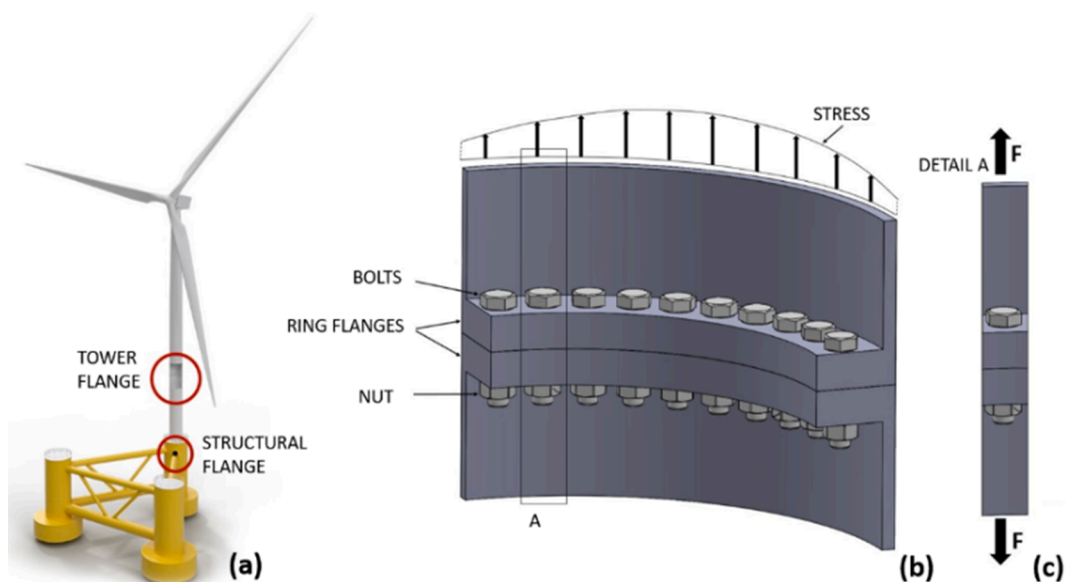


Fig. 1. Wind turbine tower, (a) floating system, (b) flange details, and (c) force directions.

bolt where the bigger diameter is for the main nut and the smaller diameter is for the locking nut. The two nuts will therefore have different thread pitches, with fine pitches on the smaller diameter, and the contact surface between the nuts has a conical contact area. These two nuts can never loosen and turn together, given the differences in pitches, where due to larger pitch the main nut (inner nut) would move faster axially in loosening direction than the locking nut, and therefore increase the contact pressure on the conical contact surface between them. This prevents the locking nut from turning. Due to the conical contact area between the two nuts, the locking nut will not be exposed to transversal loads and displacements relative to the main nut.

The aim of this study is to investigate how the anti-loosening bolt concept reacts and resists on external axial and transverse loads including loads due to vibrations. To conduct the study, two different experiments and one Finite Element Analysis (FEA) were conducted, all on different bolt sizes. The two experiments are designated as Test 1 and Test 2, where:

- Test1: M20 bolts were used, but without the bolt head, to make it possible to install and test two bolt systems at the same time. The aim of the test is to investigate whether the nuts were exposed to self-loosening during the *axial* dynamic loading, and if there were dimensional and surface changes at the contact surfaces, like the threads and nut cones.
- Test 2: M30 and M42 bolt systems were exposed to *traversal* dynamic loads and any loss of clamp load were measured. The FE analysis was performed to analyse the structural integrity of the experimental test, but on bigger pin diameter, M72.

2. Literature study

Many investigations have been conducted to get more knowledge about self-loosening of bolted joints, often based on studies by Junker [17] regarding criteria for self-loosening of fasteners under vibrations. Zhu et al. [18] proposed torque-preload formulas to estimate anti-loosening and control preload in threaded fasteners, and Zhang et al. [19] studied the roles of thread wear on self-loosening behaviour. Some of the studies have focused specifically on axial excitation on bolted joints [20-22], and others on transverse vibrations [1,19,23], but also torsional and prying loads are important, which all can lead to vibration-induced bolt loosening.

In general, it is commonly accepted practice that up to 85–90% of the input-torque in threaded fasteners is converted into heat when overcoming the two main friction torque components, and down to 10–15% contributes to increased preload in the bolt [12,18], if not sufficient or correct lubrication is applied. The two components that the friction torques need to overcome are: (1) between the bolt head/nut or bearing surface and (2) between male and female threads. Croccolo et al. [24] provided an experimental methodology to determine the friction coefficient in bolted joints, and Zhu et al. [18] proposed torque-preload formulas to estimate anti-loosening performance, and control preload.

In general, as Liu et al. [21] indicates, there are two basic loosening mechanism: (1) fastener elongation beyond its elastic limit at the threads, and (2) microslip on the thread and bearing surfaces. Vibration will increase the risk of wear on the threads and then also increase the loosening of the bolted joint, with risk of losing completely the clamp load. By experimental and numerical studies of bolted joints subjected to axial excitation, they found that the clamp force decreases rapidly at a *first stage* because of the cyclic plastic deformation, and at a *second stage* a slower decrease due to fretting wear [20,23,25-27]. The same conclusion was made by Zhang et al. [19].

At the first stage of self-loosening, there is no relative rotation between the bolt and the nut, but there could be a local cyclic plasticity near the engaged thread roots, typically the three first threads. Earlier studies by Guan et al. [28] and others show that the first engaged thread is the most loaded, and will therefore be the most damaged, with about 30% of the total load on the first threads, which results in a stress redistribution in the bolt, and consequently a gradual loss of clamping force. The second stage is characterized by relative rotation of the nut to the bolt. It has been found that, by increasing the pre-load, decreasing the load amplitude of the axial excitation, and lubricating with MoS2, the damages on threads will be smaller and the anti-loosening effect will increase [20,21]. Furthermore, finer threads or threads with smaller pitches are more resistant to loosening than coarse threads or larger pitches [18]. At higher tightening torques, which create higher preload/clamp load, the slippage at contact areas will be reduced and the sticking effect increase and thereby increasing the anti-loosening effect. It is a near linear relationship between the preload and the self-loosening

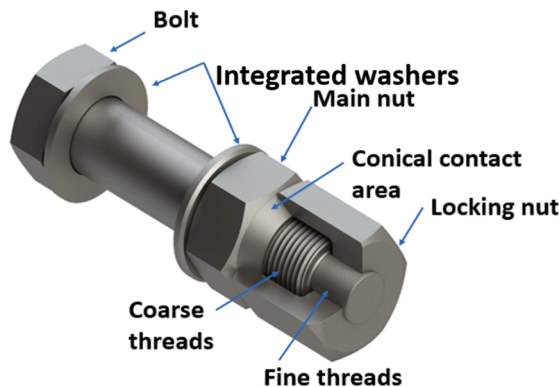


Fig. 2. Vibralock® anti-loosening bolt-nut system.

resistance, according to an experimental study performed by Jiang et al. [23]. The plastic deformation of asperities is large under high excitations amplitude, which results in reduction and possibly complete loss of clamp force over time. There exists an endurance limit for the self-loosening curve, much like the one for steel and other metals, and larger preload results in a larger endurance limit, but a large preload can also result in an increased risk of fatigue failure [23], especially in combination with high excitation amplitudes.

Fretting wear is a type of wear damage typically induced by a short amplitude sliding motion between two loaded surfaces [3] and can reduce the fatigue life substantially and is therefore one of the main reasons for failure. This microscopic dynamic process involves deformed structures, cracks and oxidation processes which include oxide debris between contact surfaces, heat generation and possible cold welding of contact surfaces. Fretting can be understood as three interrelated problems: (1) Fretting wear, (2) fretting corrosion and (3) fretting fatigue, where fretting wear is typically a wear damage due to a fretting problem, and important for prediction of fretting fatigue.

In the study reported by Karamiş and Selçuk [29], it was concluded that improvement of the surface roughness is vital in the joint reliability. The friction at the contacting surfaces depends not only on the contact area, but also strongly on the surface quality and level of asperities. The real contact area can be described as the sum of the contact areas for each asperity, which in total is much smaller than the apparent or nominal contact area. As a result of relative movements between the contacting surfaces due to typically axial or transverse excitation, the asperities will be plastically deformed, and the real contact area will increase. Such a deformation of asperities results therefore in loss of clamp load in the bolted connection, and possibly self-loosening of the bolts.

It has been found that a given set of system parameters that change in preload can result in changing from loosening to tightening of the nut [22,30]. Such behaviour involves nonlinear dynamic interaction of both friction and vibration, frequency, and amplitude of vibration, contact stiffness, pre-load, and mass of the clamped components. By taking all these factors into consideration, it could be possible to tune the input factors to exhibit loosening, tightening or no twist at all, of the nut.

Several studies have concluded that transverse loading of a bolted joint is the most severe when it comes to self-loosening [17,26]. Pai and Hess [31,32] were the first to propose and concluded that a complete slip is not an absolute condition for self-loosening of bolts, and that a localized slip can be sufficient. They concluded that there are four possible processes for loosening.

- (1) localized slip both at threads and head at the same time,
- (2) localized head slip in combination with complete thread slip,
- (3) localized thread slips in combination with complete head slip, and
- (4) complete slip both on thread and head at the same time.

The complete slip can be a result of an accumulation of localized slips in the form of elastic deformation over time. The analysis also indicated that the loosening processes are mainly independent of the frequency but depend highly on the applied load amplitude.

Already in 1973, Junker [17] had showed the relationships between the relative displacement between clamped parts, the transverse load, and the axial preload for a bolt, using a new kind of machine (at that time), now called the “Junker machine” [26].

For a bolt or nut to rotate, it must overcome the resisting friction torques at the bolt head and threads. Zadoks and Yu [1] showed that for transverse excitation, the relative motion between bolt head and flange is the most important when it comes to self-loosening because of a larger friction radius than on the threads. Housari and Nassar [26] studied the effect of thread and bearing friction coefficients on the transverse vibration-induced loosening of threaded fasteners, and both the torque and the thread friction force magnitude are affected. They showed the relationship between thread friction coefficient and loosening rate, for various bearing friction coefficients, and the relationship between bearing friction coefficient and loosening rate, for various thread friction coefficients.

Loss of preload in flanged bolted connections is a major concern in most industries, as in the relatively new industry of Offshore Wind, and several factors are involved in the process. Braithwaite et al. [33] performed a sensitivity analysis of friction and creep deformations on preload loss in bolted connections for Offshore Wind turbine systems. They concluded that the higher the friction coefficient between the contacting surfaces are the lower the preload into the bolt is. In addition, preload relaxation can come from

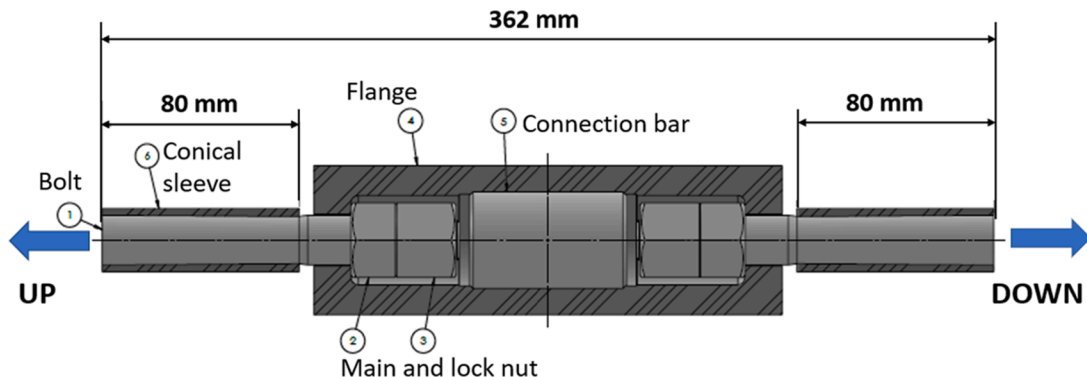


Fig. 3. Test setup for the anti-loosening M20 bolt system.

material creep, but normally not at low temperatures if the pretension stress stays below 75% of the material yield limit.

It can be concluded, based on the literature study, that many investigations have been performed on self-loosening of bolts, over many years. This is because self-loosening of bolts represents a major problem in many industries and is heavily related to high costs and safety issues. Transverse loads in oscillation represent the type of external exposure that generate most self-loosening issues in preloaded bolt system, where elongation beyond the elastic limit of the threads and microslip on the thread and bearing surfaces are the two basic loosening mechanisms.

3. Experimental methods and materials

3.1. Experimental setup for test 1

Fig. 3 shows the test setup of the anti-loosening bolt system with M20 bolts, where the bolt system is installed vertically in the fatigue machine. The bolt heads are removed for this test to ease the clamping connection with the fatigue machine, and the test setup allows two different anti-loosening bolt systems to be tested simultaneously, with axial loading and oscillation. Three bolt system setups were considered:

- 1) Bolt system A: lubricated, exposed to 498×10^3 cycles
- 2) Bolt system B: unlubricated, exposed to 498×10^3 cycles
- 3) Bolt system C: lubricated, exposed to 668×10^3 cycles

Each bolt system, A, B and C, was loaded with 100 kN axial tension, and oscillating (amplitude) load of ± 15 kN, which gives a utilization level of approximately 60% to material yield, at 10 Hz frequency and without washers. The bolts are made of material quality 10.9, and the locking nut was torqued with 200 Nm against the main nut. The axial force from the test machine was intended to simulate the preload from torquing the main nut, or hydraulic tension of the bolt. All threads on bolts A and C were lubricated with Molykote P74. The threads in contact between bolt and nuts, and the nuts coned contact surface were inspected with Stereo (binocular) microscope (Olympus SZX16) and scanning electron microscope (SEM) (Zeiss Supra 35 VP) to discover any surface damages due to the imposed vibrations. In addition, the bolt thread pitches and nuts were measured with a coordinate measuring machine (CMM)(Zeiss Contura) both before and after loading. This was done to investigate any dimensional changes, and it was checked whether any of the nuts had turned loose, by comparing photos before and after loading. The fatigue test was conducted using MTS 809 Axial/Torsional Test System, Model 319.25.

3.2. Experimental setup for test 2

To conduct this experiment, the following test and measuring equipment were used whose specifications are also provided:

- Fatigue test machine: MTS 809 Axial / Torsional Test System, Model 319.25.
- Displacement measurement unit: LVDT – linear variable differential transformer.
- Clamp force loss measuring unit: Instrumentation / 2 strain gauges at each bolt

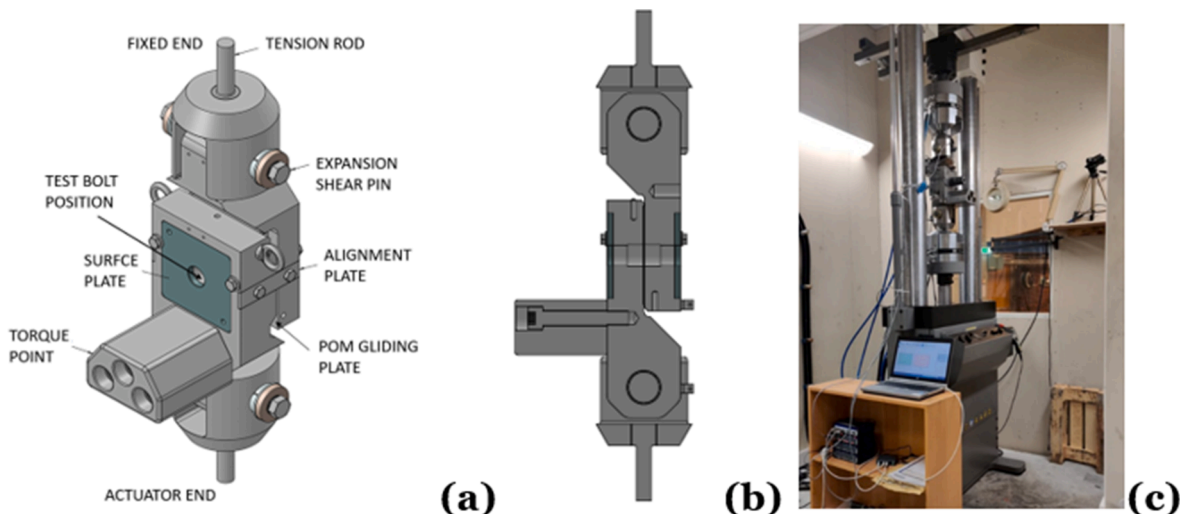


Fig. 4. (a) Test jig schematics, (b) cross-section view, and (c) jig installed in hydraulic test rig.

The test setup and test jig are shown in Fig. 4 and implemented in a 260 kN dynamic standard test rig (MTS Series 809), which achieves the load, amplitude and frequency needed for the applied Junker test. The load jig was designed for this scenario specifically with two main structure plates where one is moving by connection to the hydraulic test machine cylinder and the other is stationary. The jig is connected to the hydraulic test machine by a tension rod and pivot pin connection on the top and bottom. A Polyoxymethylene (POM) gliding plate was located between the two structure plates to reduce friction and provide a smooth and even movement of the jig. Replaceable surface steel plates were used under the bolt head and the nut to ensure the same surface conditions for each test. Alignment plates were used for the installation of bolts to centre the test samples. Molykote® G-Rapid Plus was used as thread and assembly paste to maintain a consistent friction coefficient between threads and surfaces for the duration of the test.

The calculations of the preloads, effective cross-section area and required torque for the tests of the two bolt dimensions are given by the German guidelines of the VDI 2230:2014 [34], which is the standard reference for calculating highly stressed bolted joints with one cylindrical bolt. The calculated pre-tension for a M30 and M42 bolts of grade 10.9 was 353 kN and 706 kN, respectively, which represent 70% of the material yield strength and achieved by using (a) a tensioning tool, and (b) a torque tool. The displacement amplitudes to be achieved for the M30 and M42 tests are ± 1.0 mm and 1.5 mm, respectively, and was defined by DNV (Germanischer Lloyd) based on earlier similar tests. The M30 bolt has 3.5 mm pitch on the main nut and 1.5 mm on the locking nut, and for the M42 bolt the pitch values are 4.5 mm and 2.0 mm, respectively. The design requirements for the bolt systems are shown in Table 1.

The actuator forces and displacements are logged by the MTS test machine control unit and computer, the data from the strain gauges and displacement transducers are logged by a HBM QuantumX data acquisition device via Catman AP. The test frequency of amplitude is 1 Hz with data logging of 100 Hz.

Tension and torque tools were used to achieve the preload specified to test both methods. Some test runs of the reference bolts were found necessary in the start to determine the correct amplitude to be used for the testing, where the reference HV bolts were calculated to loose more than 90% of their preload in the range of 200–400 cycles, and afterwards the test was repeated 3 times with the determined amplitude. The VIBRALOCK® assemblies were tested for verification of the system with a minimum of 3000 cycles for each test samples, with the same loads and displacement amplitudes as for the reference bolts. The reference bolts were both of type HV, produced according to NS-EN 14399-4 [35] of material quality 10.9. The following parameters were logged; amplitude, clamp load at start, clamp load at end, number of cycles, while the loss of preload over the duration of the test was calculated. All loads were given in kN and the loss of preload was in addition given in percentage values.

3.3. Finite element analysis

The finite element analysis was performed prior to experimental Test 2, and the ANSYS 19 R2 program was used with 3D elements. Both linear and non-linear models (with quadratic element order for the 3D elements and linear element order for axisymmetric model) were checked to verify the structural integrity of the bolt system. The friction coefficient between threads was set to 0.12, while the friction between the two nuts was set to 0.35. The conical contact between the nuts is 30° to the bolt axis and includes a fabrication tolerance of 0.5°.

Two different analyses were done, whose finite element model is shown in Fig. 5(a). The first analysis was conducted using linear material model, with non-linear geometry (large deformation theory) and contacts. First stage of this analysis was done by pre-tensioning the bolt shank up to 2 180 kN, and the second stage was done by tightening the locking nut up to pre-tension of 930 kN. The second type analysis was the same as the previous analysis, but with non-linear material model. The analysis was conducted with the following conditions regarding geometry and material, boundary, contact and mesh.

Boundary conditions: Identical boundary conditions were used for both analyses. The locking nut was torqued until required pre-tension was achieved. As illustrated in Fig. 5, the washers were set as fixed outside the jig bore. The bolt head and the nut end centers were locked against rotation and displacement in the YZ plane, which were placed perpendicular to the bolt axis.

Geometry and material: The analysis was performed on a bolt system with coarse threads M72 × 6 and fine threads M48 × 3 (Fig. 6 (a)). The clamp length between the washers is 157 mm. For the linear elastic model, Young’s modulus of 210 GPa, and Poisson’s constant of 0.3 were used, while bilinear isotropic hardening was assumed for the non-linear material model.

Contact conditions: Normal Lagrange formulation was employed on all frictional surfaces for the linear analysis, as it allows no contact surface penetration. In addition to previous friction coefficients, the coefficients between washers and nuts/bolt are set to 0.2.

Table 1
Design requirements for the anti-loosening bolt systems.

General requirements for the bolt system		NO-EN 14399-4:2015 & DAST-Richtlinie 021
Threads on bolt	Tolerance	6 g
	Standards	ISO 261 & ISO 965-2
Threads on main and lock nut	Tolerance	HDG – 6AZ*
	Standard	ISO 261 & ISO 965-5, ISO 261 & ISO 965-1
Mechanical properties for bolt and nuts	Property class	10.9
	Standard	ISO 898-1/-2
General tolerances on bolt and nuts	Product grade	C / B
	Standard	EN ISO 4759-1
Finish - coating	Standard	EN ISO 10684 & DSV-GAV guideline for the manufacturing of hot-dip galvanized screws.

* Internal threads of the nuts are first coated (HDG) and then the threads are cut.

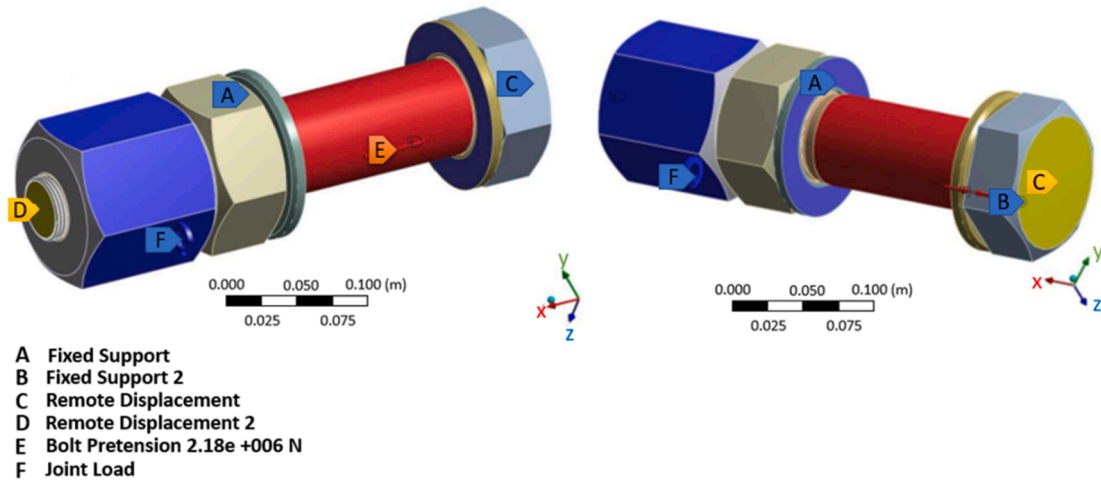


Fig. 5. Boundary conditions.

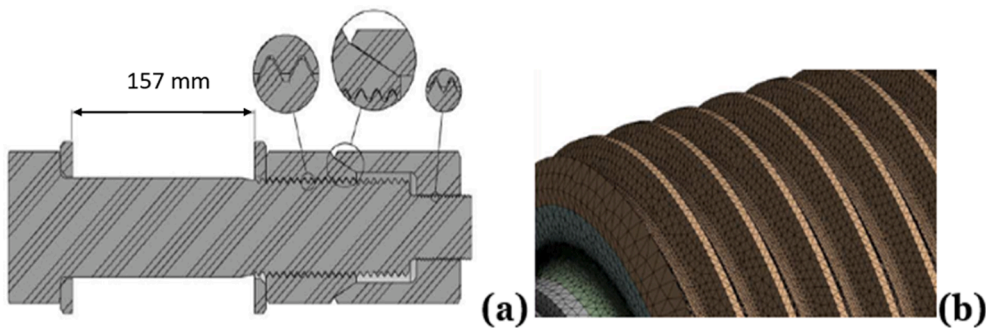


Fig. 6. (a) Bolt assembly, and (b) Meshed model of bolt.

For the non-linear analysis, the conditions were the same, but with the exception that the Augmented Lagrange formulation was used instead of the normal. This is acceptable if the penetration is insignificant.

Mesh: Linear and full integration elements were used for the linear analysis (Fig. 6 (b)), and the meshed model has a total number of 1 157 297 nodes and 5 792 650 elements. For the non-linear analysis the number of nodes and elements reduced to 532 513 and 2 460 415, respectively. The models were meshed using the default element sizes of 0.0022 mm and 0.001 mm for the linear and quadratic element models respectively.

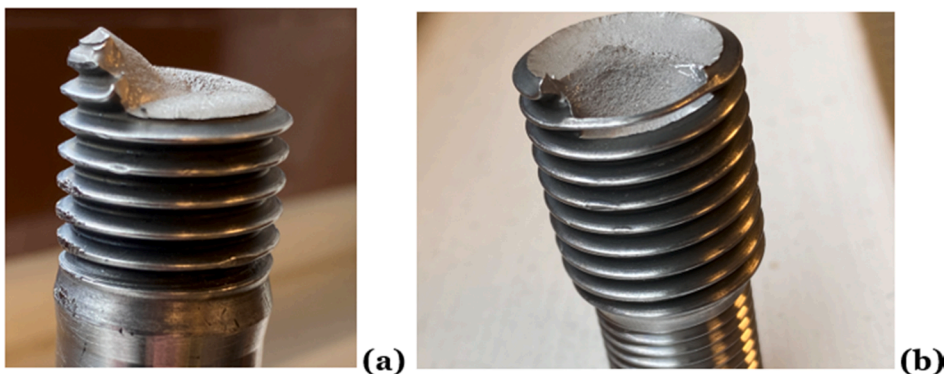


Fig. 7. Breakage of bolt B, (a) threads outside the main nut, and (b) threads within the main nut.

4. Discussion of results

4.1. Results of test 1

The study results reported in this paper indicate that the new bolt locking concept shows a superior locking, or anti-loosening capacity compared to the standard HV bolt-nut system. The HV bolt system had a preload loss of 86–92% within 200–400 transverse load cycles, while the novel locking bolt system had a loss of only 3–9% within 3000 cycles. Both systems were preloaded to 70% of yield with the same forced displacement amplitude in transverse direction. The preload loss in the tested anti-loosening bolt system did not occur due to turning of the nuts, which indicates that the registered preload drop is mainly due to an immediate reduction of asperities, and probably not due to any material creep effects since the pretension stress in the bolt is maximum 70% of material yield, and the temperature is low, 20–25 °C.

Test 1 was conducted on M20 bolt size with minor shank size M16 subjected to an axial oscillational excitation and the test contained 3 bolt systems, designated as bolt A, bolt B and bolt C. Bolt B was not lubricated nor the most loaded, and the break initiated at the first engaged thread into the main nut towards the flange. Fig. 7 show the broken bolt images and Figs. 8 and 9 show the SEM images of this bolt. The images indicate that first threads are taking the highest loads. Although it is not possible to conclude with certainty, this may be due to lack of thread lubrication, which damaged the surface and initiated the breakage. The locking nut and the main nut did not have relative rotation during the testing, for neither of the test bolts.

4.2. Results of test 2

This test was conducted on M30 bolt size with minor shank size M16, and M42 with minor M24, both with transverse oscillation excitation. The test procedure was developed by DNV GL Oil&Gas in accordance with Junker vibration test method. The bolts were tested at alternating transverse loading to determine their resistance against loss of preload and consequently loosening.

All the HV bolts, tensioned and torqued, showed an immediate and almost linear loss of preload from the start of each test, until the nut came completely loose. The Vibralock® bolts showed generally an immediate minor loss of preload, and thereafter practically no further loss until the end of the test.

The tests of the M30 and M42 bolt locking systems showed a superior resistance to self-loosening compared to the HV reference bolts of same sizes, see Figs. 10 and 11. The HV reference bolts lost 86–92% of their preload before 400 cycles, while the bolt locking systems had a loss of 3–9% before 3000 cycles, for the same tests. The test requirements were specified by DNV, for a possible approval of concept at a later stage, and therefore assumed to correctly represent the comparison technique between the two concepts, the locking bolt and standard HV bolt concepts.

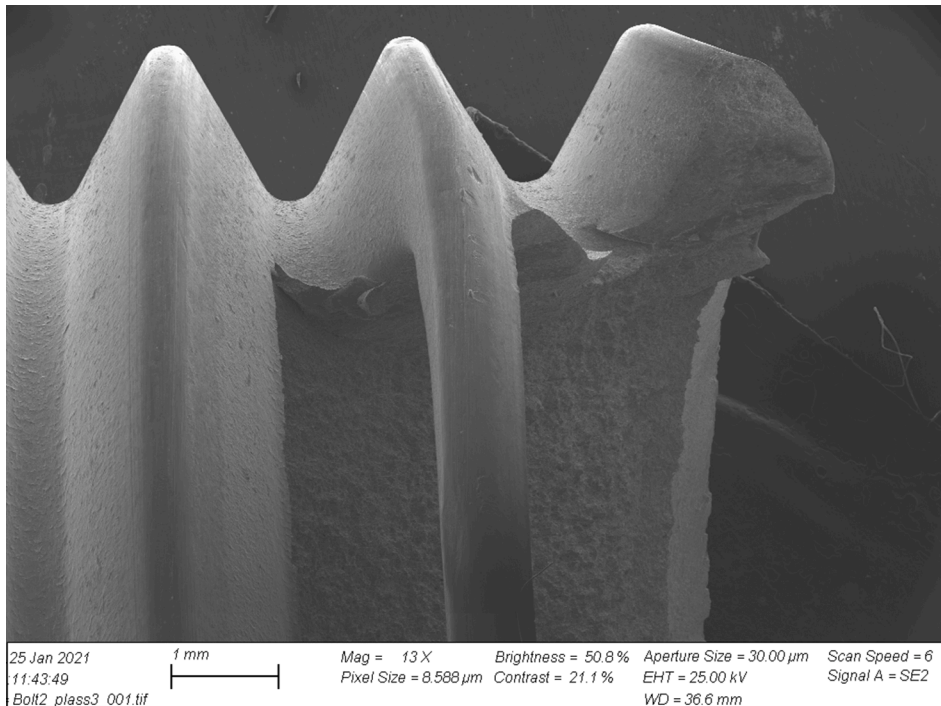


Fig. 8. SEM image of broken bolt B at first engaged threads, with Mag = 13X.

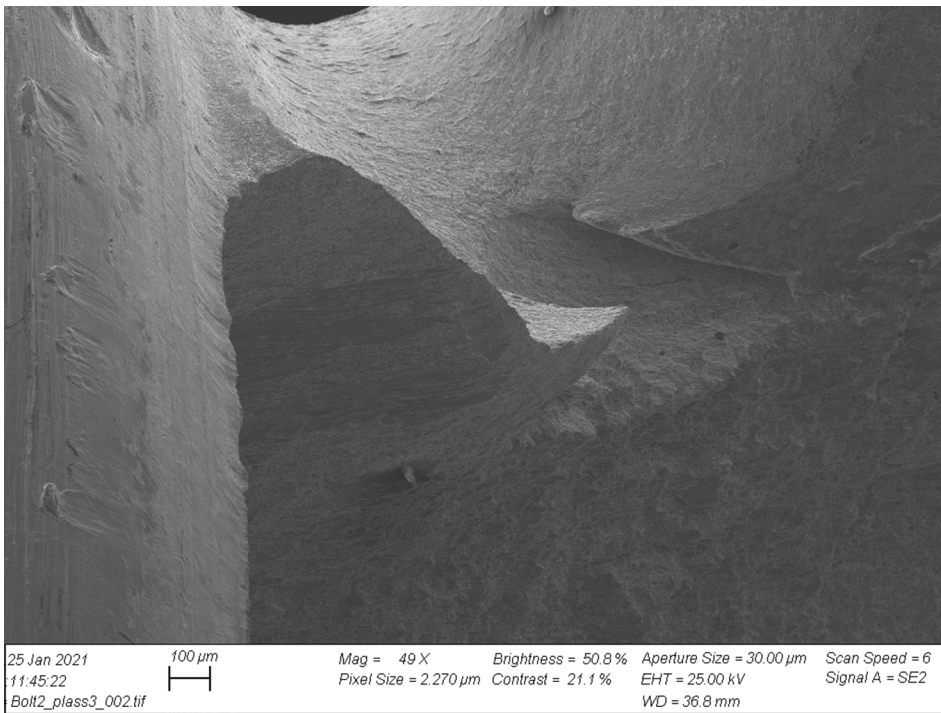


Fig. 9. SEM image of broken bolt B at first engaged threads, with Mag = 49X.

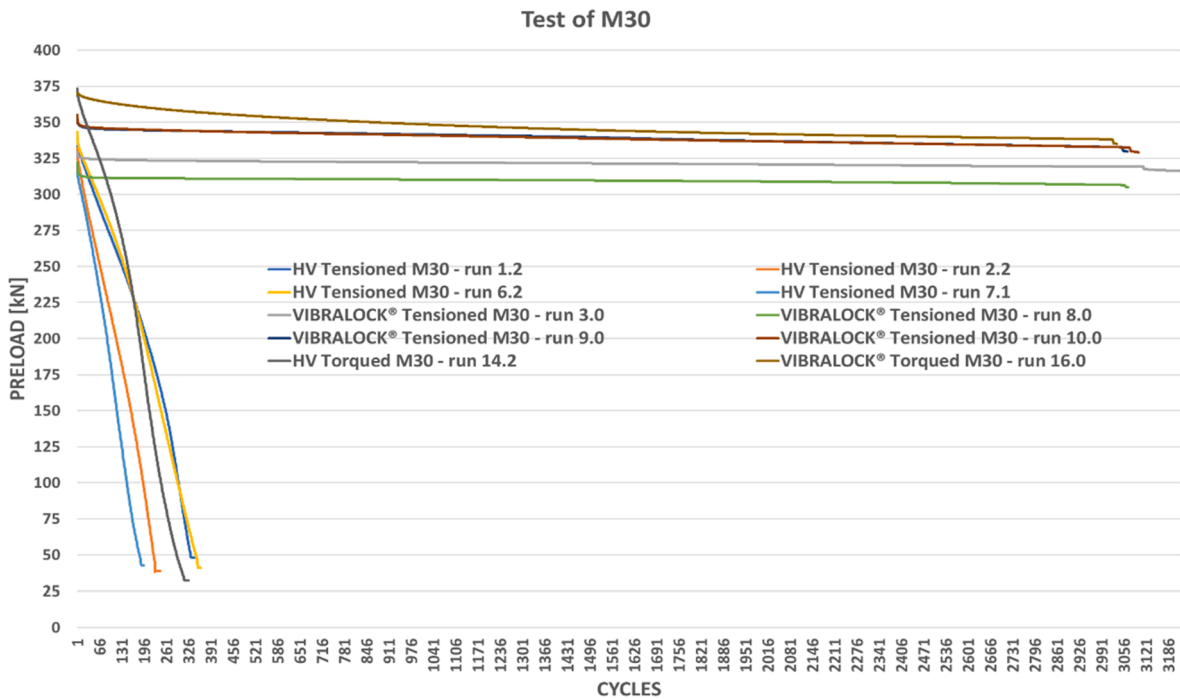


Fig. 10. Loss of preload VIBRALOCK® versus HV bolts for bolt size M30.

4.3. FE results

The FE analysis was performed by an external company on a M72 bolt, which is bigger than the bolts tested physically, i.e., M20, M30 and M42. The linear FE analysis was performed mainly to investigate the structural integrity of the threads in the bolt and nut

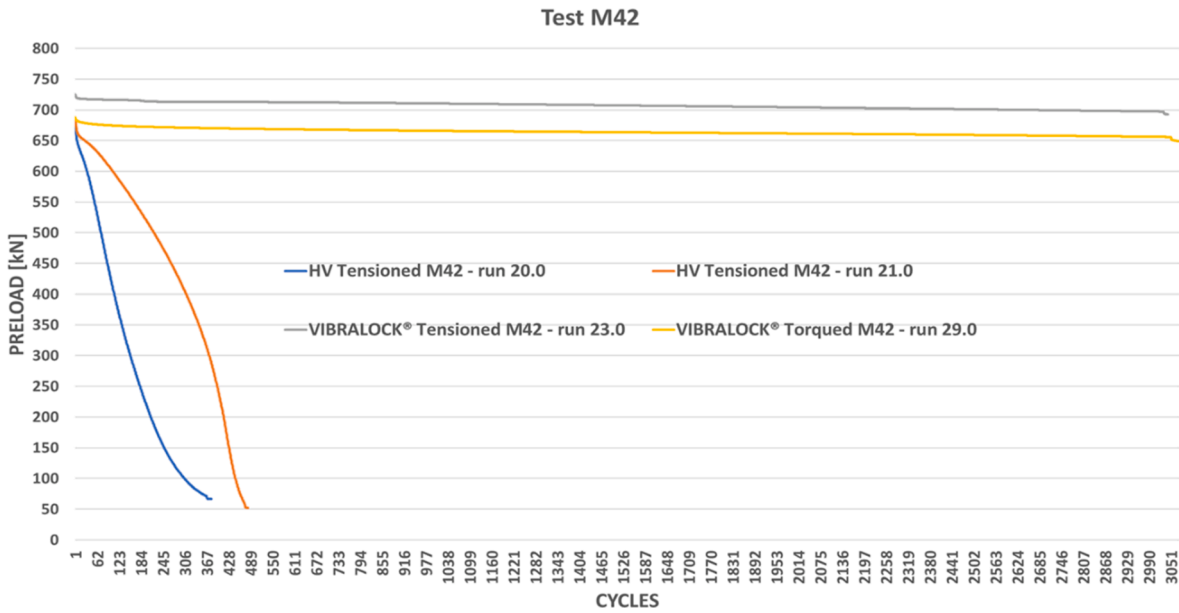


Fig. 11. Loss of preload Vibralock® versus HV bolts for bolt size M42.

system. The analysis was done based on the predefined clamp loads in both bolt diameters, whose values are 2 180 kN in the main shank and 930 kN in the minor shank. The torque value result from ANSYS to reach the locking nut preload of 930 kN is 29 967 Nm, which is almost identical to the value obtained by manual calculation using the formula in Eq. (1) [34], which gave calculated preload value of 29 440 Nm. In the non-linear analysis, the corresponding preloads required to reach the locking nut preload of 930 kN were 32 105 kN from the FE analysis and 32 890 kN as calculated from Eq. (1).

$$T = \frac{F_p}{2} \left[\frac{(\mu_n \times d_n)}{\sin 30^\circ} + 1.155 \times \mu_t \times d_t + \frac{p}{\pi} \right] \tag{1}$$

Where the symbol definitions and values are as given in Table 2 and the Sin 30° value is due to the conical shape of the nut contact surfaces.

Figs. 12 and 13 show the von Mises distribution of the FEA results from the linear analysis and non-linear analysis, respectively. In the linear analysis, a fabrication tolerance of 0.5° was introduced between the nut angles where the contact point between the nuts where at the lower conical area with an average contact diameter of 80 mm. In the non-linear analysis the conical fabrication tolerance was set to 0°, which resulted in a wider contact area between the nuts and increased contact diameter, up to 90.6 mm.

When comparing the two models, it can be seen that the stress pattern is almost identical, as illustrated in Fig. 11(a) and 12(a). The linear analysis resulted in the maximum stress level of 820 MPa at the main nut contact area against the locking nut, and at the first engaged coarse bolt threads, in addition to the first engaged fine bolt threads. In the non-linear analysis, the over-all stress level is approximately the same as for the linear analysis, also at the most stressed areas, where the stress level is in the range of 788 – 900 MPa. A very small portion of the main nut to locking nut contact area shows an increased stress level of 900–1350 MPa.

Though the simulation was done on a bigger bolt size, the plots in Fig. 12 (c) and 13 (c) coincide well with the fracture condition of bolt B in Test 1, which occurred at or close to the first engaged thread against the main nut (Figs. 7 - 9) and reflects the description from literature [36]. In general, the combination of physical tests and FEA, and the combination of 4 different bolt dimensions is meant to give a wider proof of concept of the bolt locking system.

Bolted connections are widely used in many different applications and machines, and it is commonly known that the initial bolt preload will be reduced over time, due to vibrations. Xu et al. [37] performed dynamic analysis and loosening evaluation of bolted connections in machine tools, exposed to vibrations. They introduced a new experimental design method called The quadratic rotary

Table 2
Symbol definitions and values used in Eq. (1).

Parameter and symbol	Linear analysis	Non-linear analysis
Required bolt pretension, F_p [kN]	930	930
Friction coefficient at nut bearing surface, μ_n	0,35	0,35
Effective contact diameter of nut face, d_n [mm]	80	90,6
Friction coefficient at threads, μ_t	0,12	0,12
Effective mean contact diameter of threads, d_t [mm]	45,925	45,925
Pitch, p [mm]	3	3

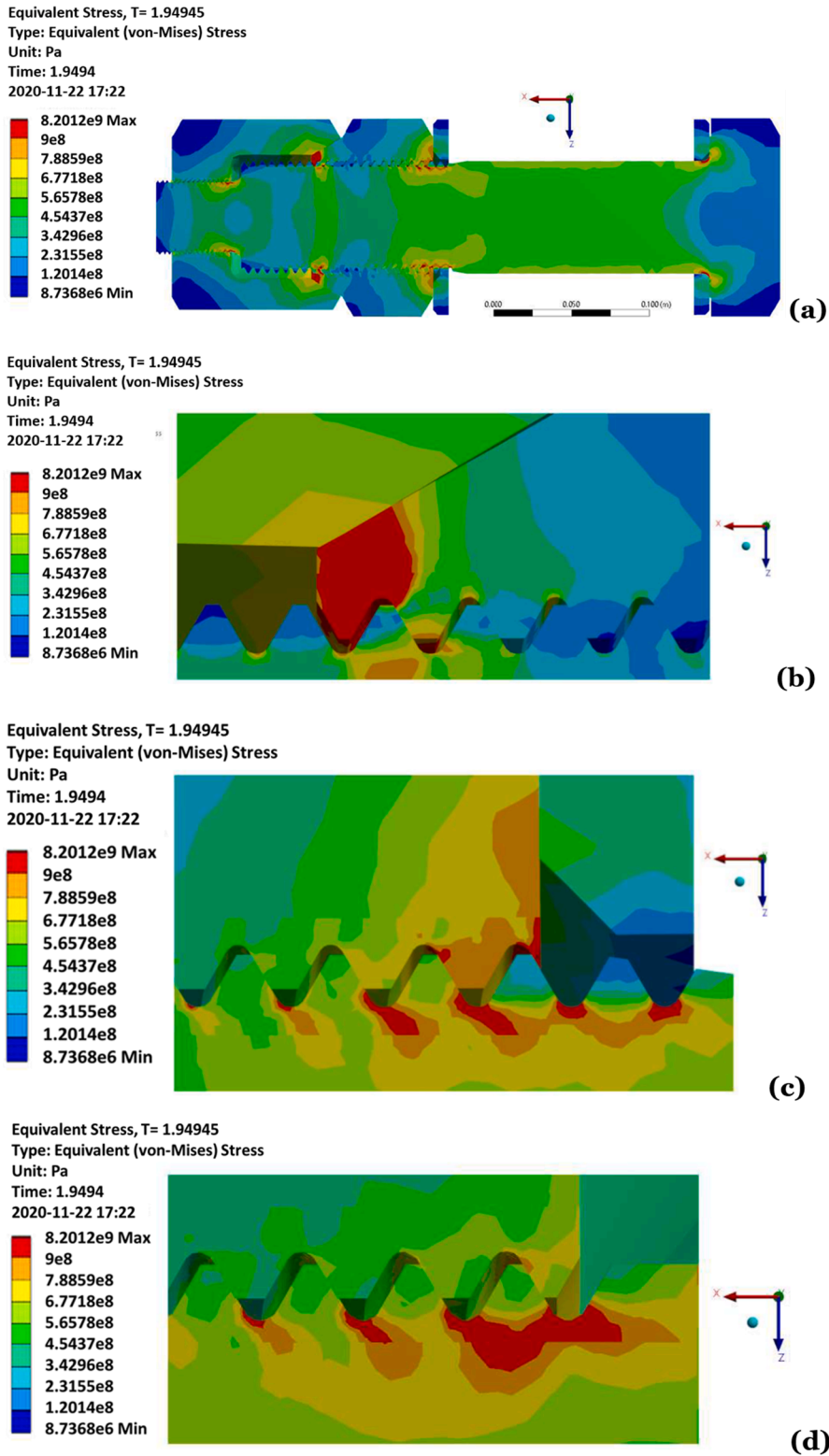


Fig. 12. von Mises stresses from the linear FE analysis, (a) overall view, (b) conical contact area, (c) coarse threads, and (d) fine threads.

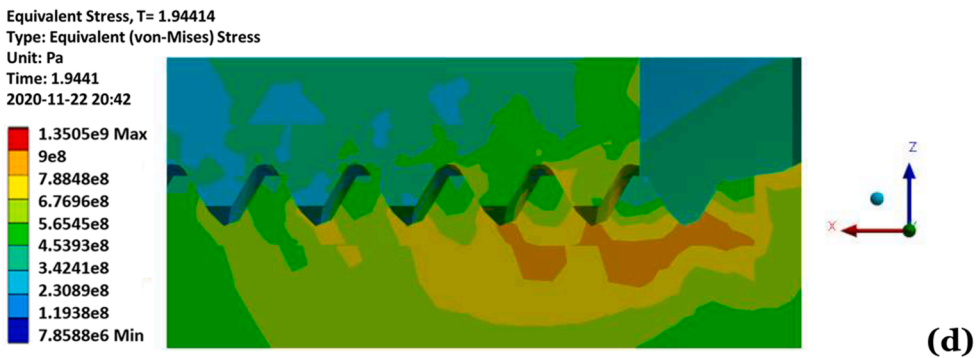
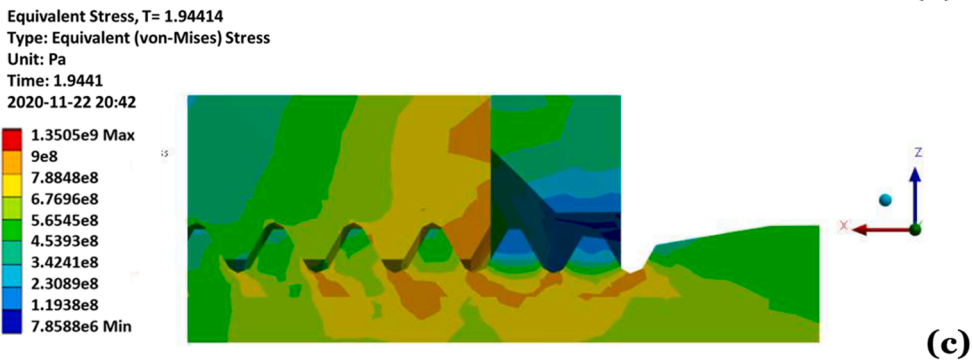
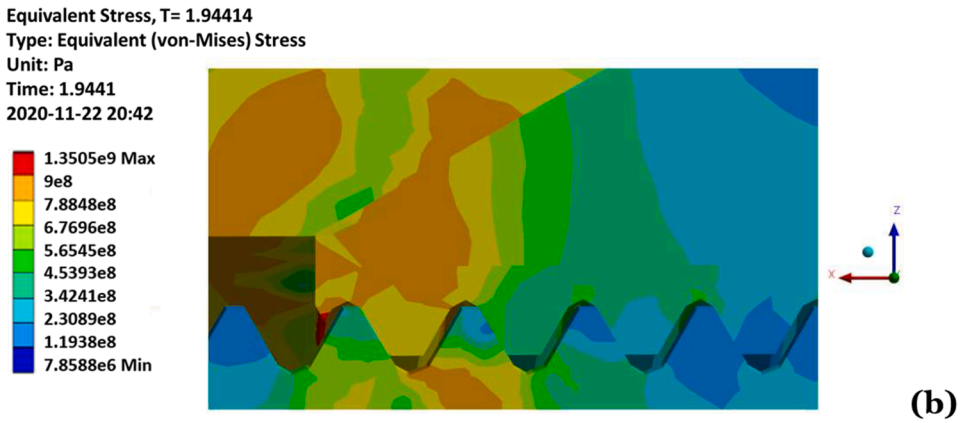
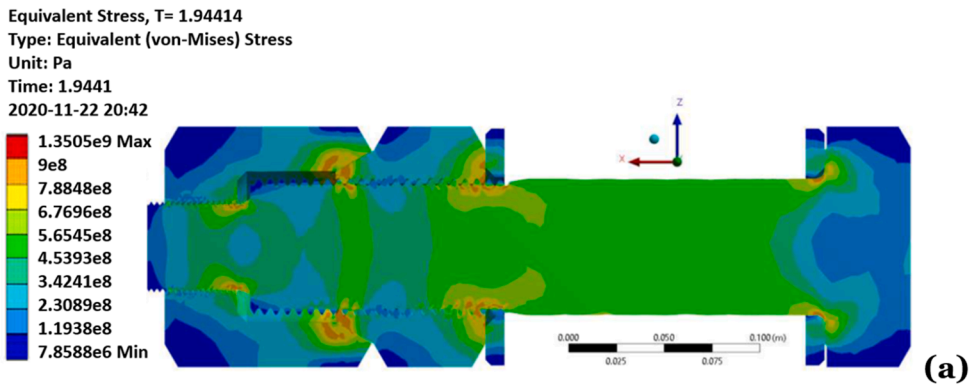


Fig. 13. von Mises stresses from the non-linear FE analysis, (a) overall view, (b) conical contact area, (c) coarse threads, and (d) fine threads.

unitized design, from where the principal factors affecting the preload loss can be obtained, such as preload, working load (cyclic), frequency, temperature, bolt form and diameter, and surface state, such as coefficient of friction. Based on the obtained results, the authors concluded that the preload attenuation rate decreases with increased preload but increases with increasing cyclic load and increased frequency. Vilela et al. [38] presented a numerical simulation by finite element method (of ANSYS software) of a model with one bolt only connecting two and three plates. Bolts subjected to tension, shear, and a combination of the two were modeled with two, three and two plated, respectively. The unitary model includes all necessary and required considerations such as contact between all friction surfaces involved, bolt preload, parallel and perpendicular forces compared to plate contact surfaces, including slip and prying effects. The authors concluded, based on all the analyses developed, that the methodology used in the unitary model is capable of simulate with great accuracy the behavior of a single bolt subjected to tension, shear, and a combination of the two.

5. Conclusions

The new bolt locking system can be used in any joint, location or mechanical system where self-loosening is real or potential problem, or where the consequences of loose bolts are high. This could be in wind power systems (offshore and onshore), huge valve connections, tube connections exposed to high pressure and/or chemical fluids, bridges, or other constructions, and many more.

Based on the test and simulation results, the following main conclusions can be made regarding the new bolt locking system:

- The bolt system is superior to standard bolt-nut systems when it comes to anti-loosening resistance
- It experiences a minimum of preload loss over time.
- No turning of nut relative to bolt takes place.
- It is easy to preload and disarm, if required.

Declaration of Competing Interest

The authors declare that they have no known competing financial interests or personal relationships that could have appeared to influence the work reported in this paper.

Acknowledgements

The authors are grateful for all help and service given by Mr. Andreas Sigvardsson at Stavanger Engineering AS for the support provided in running the Finite Element Analysis for this project, Teo Teknikk AS and Torq/Lite Europe AS for providing their services within strain gauges and torque & tensioning, and DNV for designing the test procedures.

Funding

The research is conducted as part of Industrial PhD study funded by the Norwegian Research Council and Bondura Technology AS, Grant nr. 283821. This financial support is highly acknowledged.

References

- [1] R.I. Zadoks, X. Yu, An investigation of the self-loosening behaviour of bolts under transverse vibration, *J. Sound Vib.* 208 (2) (1997) 189–209, <https://doi.org/10.1006/jsvi.1997.1173>.
- [2] I. Berkani, Ø. Karlsen, H.G. Lemu, Experimental and numerical study of Bondura® 6.6 PIN joints, *IOP Conf. Ser.: Mater. Sci. Eng.* 276 (2017) 012028, <https://doi.org/10.1088/1757-899X/276/1/012028>.
- [3] Ø. Karlsen, H.G. Lemu, Fretting fatigue and wear of mechanical joints: Literature study, *IOP Conf. Ser.: Mater. Sci. Eng.* 700 (1) (2019) 012015, <https://doi.org/10.1088/1757-899X/700/1/012015>.
- [4] Ø. Karlsen, H.G. Lemu, On modelling techniques for mechanical joints: Literature study. *Int. Workshop of Advanced Manufacturing and Automation (IWAMA 2019)*. Springer, Singapore, 634 (2020) 116–125. https://doi.org/10.1007/978-981-15-2341-0_15.
- [5] I.R. McColl, J. Ding, S.B. Leen, Finite element simulation and experimental validation of fretting wear, *Wear*. 256 (11–12) (2004) 1114–1127, <https://doi.org/10.1016/j.wear.2003.07.001>.
- [6] V. Sabelkin, S. Mall, Investigation into relative slip during fretting fatigue under partial slip contact condition, *Fatigue Fract. Eng. Mater. Struct.* 28 (9) (2005) 809–824, <https://doi.org/10.1111/j.1460-2695.2005.00918.x>.
- [7] J.J. Madge, S.B. Leen, P.H. Shipway, The critical role of fretting wear in the analysis of fretting fatigue, *Wear* 263 (1–6) (2007) 542–551, <https://doi.org/10.1016/j.wear.2006.11.021>.
- [8] A.T. Kasarekar, F. Sadeghi, S. Tsergounis, Fretting fatigue of rough surfaces, *Wear* 264 (7–8) (2008) 719–730, <https://doi.org/10.1016/j.wear.2007.06.016>.
- [9] C. Song, M.X. Shen, X.F. Lin, D.W. Liu, M.H. Zhu, An investigation on rotatory bending fretting fatigue damage of railway axles, *Fatigue Fract. Eng. Mater. Struct.* 37 (1) (2014) 72–84, <https://doi.org/10.1111/ffe.12085>.
- [10] M. Luke, M. Burdack, S. Moroz, I. Varfolomeev, Experimental and numerical study on crack initiation under fretting fatigue loading, *Int. J. Fatigue* 86 (2016) 24–33, <https://doi.org/10.1016/j.ijfatigue.2015.09.022>.
- [11] X. Mi, Z.B. Cai, X.M. Xiong, H. Qian, L.C. Tang, Y.C. Xie, J.F. Peng, M.-H. Zhu, M.-H. Zhu, Investigation on fretting wear behavior of 690 alloy in water under various temperatures, *Tribol. Int.* 100 (2016) 400–409, <https://doi.org/10.1016/j.triboint.2016.05.012>.
- [12] W.A. Grabon, M. Osetek, T.G. Mathia, Friction of threaded fasteners, *Tribol. Int.* 118 (2018) 408–420, <https://doi.org/10.1016/j.triboint.2017.10.014>.
- [13] Enerpac, <https://www.enerpac.com>, [Online; accessed 15-March-2022].
- [14] Torq/Lite Europe, <https://www.torqlite.eu>, [Online; accessed 15-March-2022].
- [15] T. Gintautas, J.D. Sørensen, Improved methodology of weather window prediction for offshore operations based on probabilities of operation failure, *J. Mar. Sci. Eng.* 5 (2) (2017) 20, <https://doi.org/10.3390/jmse5020020>.
- [16] Bondura Technology AS, <https://www.bondura.no/>, [Online; accessed 15-March-2022].

- [17] G.H. Junker, Criteria for self-loosening of fasteners under vibration, *Aircr. Eng. Aerosp. Technol.* 45 (1) (1973) 12–17, <https://doi.org/10.1108/eb03498>.
- [18] L. Zhu, J. Hong, X. Jiang, On controlling preload and estimating anti-loosening performance in threaded fasteners based on accurate contact modelling, *Tribol. Int.* 95 (2016) 181–191, <https://doi.org/10.1016/j.triboint.2015.11.006>.
- [19] M. Zhang, L. Lu, W. Wang, D. Zeng, The roles of thread wear on self-loosening behavior of bolted joints under transverse cyclic loading, *Wear* 394 (2018) 30–39, <https://doi.org/10.1016/j.wear.2017.10.006>.
- [20] S. Basava, D.P. Hess, Bolted joint clamping force variation due to axial vibration, *J. Sound Vib.* 210 (2) (1998) 255–265, <https://doi.org/10.1006/jsvi.1997.1330>.
- [21] J. Liu, H. Ouyang, J. Peng, C. Zhang, P. Zhou, L. Ma, M. Zhu, Experimental and numerical studies of bolted joints subjected to axial excitation, *Wear* 346 (2016) 66–77, <https://doi.org/10.1016/j.wear.2015.10.012>.
- [22] J. Liu, H. Ouyang, Z. Peng, Z. Cai, X. Liu, M. Zhu, Study on self-loosening of bolted joints excited by dynamic axial load, *Tribol. Int.* 115 (2017) 432–451, <https://doi.org/10.1016/j.triboint.2017.05.037>.
- [23] Y. Jiang, M. Zhang, T.-W. Park, C.-H. Lee, An experimental study of self-loosening of bolted joints, *J. Mech. Des.* 126 (5) (2004) 925–931, <https://doi.org/10.1115/1.1767814>.
- [24] D. Crococo, M. de Agostinis, N. Vincenzi, Failure analysis of bolted joints: Effect of friction coefficients in torque–preloading relationship, *Eng. Fail. Anal.* 18 (1) (2011) 364–373, <https://doi.org/10.1016/j.engfailanal.2010.09.015>.
- [25] S.A. Nassar, P.H. Matin, Clamp load loss due to fastener elongation beyond its elastic limit, *J. Press. Vessel Technol.* 128 (3) (2006) 379–387, <https://doi.org/10.1115/1.2217971>.
- [26] B.A. Housari, S.A. Nassar, Effect of thread and bearing friction coefficients on the vibration-induced loosening of threaded fasteners, *J. Vib. Acoust.* 129 (4) (2007) 484–494, <https://doi.org/10.1115/1.2748473>.
- [27] A.M. Zaki, S.A. Nassar X, Yang, Effect of thread and bearing friction coefficients on the self-loosening of preloaded countersunk-head bolts under periodic transverse excitation. *J. Tribol.* 132(3) (2010) 031601. <https://doi.org/10.1115/1.4001621>.
- [28] Z. Guan, J. Mu, F. Su, T. Bian, Y. Huang, Z. Li, Pull-through mechanical behavior of composite fastener threads, *Appl. Compos. Mater.* 22 (3) (2015) 251–267, <https://doi.org/10.1007/s10443-014-9404-5>.
- [29] M.B. Karamiş, B. Selçuk, Analysis of the friction behaviour of bolted joints, *Wear* 166 (1) (1993) 73–83, [https://doi.org/10.1016/0043-1648\(93\)90281-P](https://doi.org/10.1016/0043-1648(93)90281-P).
- [30] D.P. Hess, S.V. Sudhirkashyap, Dynamic loosening and tightening of a single-bolt assembly, *J. Vib. Acoust.* 119 (3) (1997) 311–316, <https://doi.org/10.1115/1.2889725>.
- [31] N.G. Pai, D.P. Hess, Experimental study of loosening of threaded fasteners due to dynamic shear loads, *J. Sound Vib.* 253 (3) (2002) 585–602, <https://doi.org/10.1006/jsvi.2001.4006>.
- [32] N.G. Pai, D.P. Hess, Three-dimensional finite element analysis of threaded fastener loosening due to dynamic shear load, *Eng. Fail. Anal.* 9 (4) (2002) 383–402, [https://doi.org/10.1016/S1350-6307\(01\)00024-3](https://doi.org/10.1016/S1350-6307(01)00024-3).
- [33] J. Braithwaite, I.G. Goenaga, B. Tafazzolimoghaddam, A. Mehmanparast, Sensitivity analysis of friction and creep deformation effects on preload relaxation in offshore wind turbine bolted connections, *Appl. Ocean Res.* 101 (2020) 102225, <https://doi.org/10.1016/j.apor.2020.102225>.
- [34] VDI 2230:2014, Systematic calculation of highly stressed bolted joints – Joints with one cylindrical bolt, Available at: <https://www.vdi.de/en/home/vdi-standards>.
- [35] NS-EN 14399-4:2015, High-strength structural bolting assemblies for preloading-Part 4: System HV - Hexagon bolt and nut assemblies, Available at:<https://www.standard.no/en/webshop/productcatalog/productpresentation/?ProductID=747126>, [Online; accessed 15-March-2022].
- [36] W. Wang, K.M. Marshek, Determination of the load distribution in a threaded connector having dissimilar materials and varying thread stiffness, *J. Eng. Ind.* 117 (1) (1995) 1–8, <https://doi.org/10.1115/1.2803273>.
- [37] W. Xu, Q. Cheng, C. Yang, Y. Li, Dynamic analysis and looseness evaluation of bolted connection under vibration of machine tools, *Int. J. Adv. Manuf. Technol.* (2021) 1–10, <https://doi.org/10.1007/s00170-021-07615-0>.
- [38] P.M.L. Vilela, H. Carvalho, L.F. Grilo, P.A. Montenegro, R.B. Calçada, Unitary model for the analysis of bolted connections using the finite element method, *Eng. Fail. Anal.* 104 (2019) 308–320, <https://doi.org/10.1016/j.engfailanal.2019.06.001>.

Appended Paper VIII

Fretting Fatigue and Wear of Mechanical Joints: Literature Study

KARLSEN, Ø.; LEMU, H. G.

IOP Conference Series: Materials Science and Engineering. IOP Publishing, 2019. p. 012015.

[doi:10.1088/1757-899X/700/1/012015](https://doi.org/10.1088/1757-899X/700/1/012015)

PAPER • OPEN ACCESS

Fretting fatigue and wear of mechanical joints: Literature study

To cite this article: Ø Karlsen and H G Lemu 2019 *IOP Conf. Ser.: Mater. Sci. Eng.* **700** 012015

View the [article online](#) for updates and enhancements.

You may also like

- [Fretting fatigue behaviour of Ni-free high-nitrogen stainless steel in a simulated body fluid](#)
Norio Maruyama, Sachiko Hiromoto, Eiji Akiyama et al.
- [Study on Fatigue Life of Aluminum Alloy Considering Fretting](#)
Maosheng Yang, Hongqiang Zhao, Yunxiang Wang et al.
- [Microscopic Study of 5083-H321 Aluminium Alloy Under Fretting Fatigue Condition](#)
S Eslamian, B B Sahari, Aidy Ali et al.

ECS Toyota Young Investigator Fellowship



For young professionals and scholars pursuing research in batteries, fuel cells and hydrogen, and future sustainable technologies.

At least one \$50,000 fellowship is available annually.
More than \$1.4 million awarded since 2015!



Application deadline: January 31, 2023

Learn more. Apply today!

Fretting fatigue and wear of mechanical joints: Literature study

Ø Karlsen* and H G Lemu

Department of Mechanical and Structural Engineering and Materials Science,
University of Stavanger, Stavanger, Norway

*Corresponding author: oyvind.karlsen@uis.no

Abstract. Most mechanical connections are in one way or another exposed to some form of tear, wear, corrosion and fatigue, and likely to fail over time. If the contacting surfaces in a connection are exposed to tangential loading due to vibrations, small amplitude displacements called fretting can be induced at the surface, and might result in crack nucleation and possible propagation. The review and analysis reported herein are based on review of a wide range of studies reported in the literature during the last 25 years, which look into earlier studies around fretting fatigue in interference fit connections. In addition, a new method on how to obtain an interference fit is being mentioned as a possible way of increasing the joints fretting fatigue life. Previous investigations show clearly positive effects of finding and operating with the correct combinations of interference fit levels, palliative treatments and material choices to increase the fretting fatigue life.

1. Introduction

In most mechanical systems, there are needs for power transmission and connection techniques using various shapes and dimensions, and the most familiar transmission systems might be of electrical or mechanical type. Among those, spline, dovetail, riveted, interference fitted, pre-stressed and open-hole pin/bolt connections are the typical mechanical joint types [1].

In general, with an increasing transmitted power, the mechanical connections are exposed to increasing loads and stresses at contact areas, and the probability for damages at the contact areas is therefore increasing. Already early in the Nineteenth century, when the railway still had a very important role and position, it was known that repetitive loads caused failure in the axles and connected components. At the time, the number of axles in England was around 200 000, and in the middle of the 19th century, hundreds of people lost their lives in accidents all over Europe due to axle failures [2].

Many studies have been conducted during the last decades to analyse and increase the understanding and perception of the mechanisms that work in the contact areas and surfaces of different mechanical connections, like train wheels and axles (wheel seats, gear seats, brake disk seat) [3, 4]. The press-fitted parts on a railway vehicle are extremely important and critical because of the easily initiation of cracks in those areas and spots [2, 5, 6].

This literature study aims to look deeper into previous studies and investigations on the mechanisms of damages that occur in interference fitted connections of mechanical systems with relative movements between the connected parts. A special focus will be on fretting fatigue, what the causes are, and what can be done to prevent or to avoid factors that reduce the life of the component and the system. In addition, this review aims to have a critical approach to the previous studies and identify research issues



and ways to approach problematics around these connection types. The review will focus on a few specific mechanical systems, but still mainly on interference fit challenges that could occur in mechanical systems with interference fitted couplings.

2. Mechanical connection techniques

There are a variety of different mechanical connections in use, depending on the type of industry, type of machine, equipment or joint, type and level of loads, materials involved, etc. Different connection types transfer forces and loads between different parts in the connection in different ways, and with an increasing power, the stress level increases, with damage and reduced fatigue life as a possible result. The damages in a contact surface can range from minimal surface or topographic changes to severe crack initiation, which again can lead to crack propagation if exposed to cyclic and/or dynamic forces. Such dynamic forces can originate from the type of operation and type of connection the system is designed for, or from external sources not within the original operational scope, like vibrations. It is well known that crack initiation at a contact surface, with crack propagation due to dynamic loading results easily in fretting fatigue and reduced fatigue life [3, 4, 7-10].

2.1. Interference fit connection

Interference fit, also known as press fit or friction fit, is a fastening method where two parts, typically circular cross section shape, are pushed together (one into the other) and kept in place due to the pressure between them. Typically, the inner part will have a nominal outer diameter slightly greater than the nominal inner diameter of the outer part, and when pushed or forced together the contact friction forces keep the parts from moving relative to each other (nominally). The level of interference depends on the negative difference in nominal diameters.

Figure 1 shows a principle sketch for an interference fit. The interference fit causes the bore to expand and induces the tensile tangential (tangent to the bore surface) stresses, i.e. Hoop pre-stresses at the bore edge. This increases the mean stress level but this pre-stress considerably reduces the magnitude of the local cyclic stress, meaning the alternating stress, which has a much more fatigue life reducing effect [11]. An advantage of this kind of connection is the superior level of possible torque transmission between two assembled parts, but the pressure distribution is the source responsible for fatigue failure.

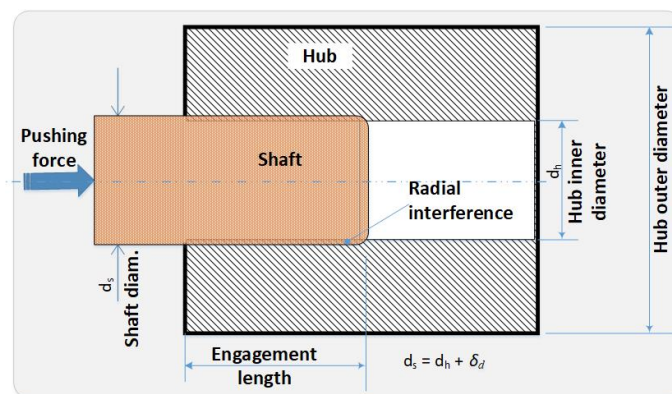


Figure 1. Principle sketch of an interference fit

The classical analytical pressure in the connection, under the assumption of solid shaft, hollow hub, axis symmetry and plane stress, is given by [12]:

$$p_f = \frac{E\delta_d}{2D_f} \left(1 - \left(\frac{D_f}{D_h} \right)^2 \right) \quad (1)$$

where p_f is interference pressure (MPa); E is the elasticity modulus (MPa); δ_d is the interference fit level (mm); D_f is nominal shaft diameter and hub inner diameter (mm) and D_h hub outer diameter (mm).

There are other equations, known as Lamé's equations (elasticity theory) for thick-wall cylinder, commonly used to calculate stresses and deformations at interference fit connections [13-16]. Although the shapes typically used in Lamé's analysis could differ from the real shape of interference fit machine components, and they give approximate results, they are often used due to their practical applicability.

Lamé's equations are based on certain assumptions, among others:

- The thickness of the cylinder wall is constant.
- Thick-wall cylinder.
- Material of the cylinder is homogeneous and isotropic.
- The two mating parts (hub and cylinder) have the same axial length.
- Plane sections of the cylinder perpendicular to the longitudinal axis remain plane under the pressure.

The Lamé's equations indicate that Hoop stress and radial stress in an interference fit joint, and in addition axial stress in a closed cylinder, are subjected to a defined outer and inner pressure.

2.2. Shrink fitted connection

Shrink fit is an interference fit technique where typically the inner part is being cooled down (shrinks), or the inner surface of the outer part is being heated up, to make the fit possible. After assembly, the temperature-affected part will adjust its size back to original size, and there will be an interference fitted connection. The dimension-change of the temperature affected part will decide the final interference fit level, and contact pressure. Induction heating is a typical technique for heating and liquid nitrogen is often used for cooling.

The basic formula for calculating the required temperature (T) for the expansion of the metal is:

$$T = \frac{d}{c \cdot \alpha} \quad (2)$$

where d is the required radial expansion (of the radius), c is the nominal hub inner radius and α is the coefficient of thermal expansion.

2.3. Open hole pin/bolt connection

A typically open-hole connection is a cylindrical pin in a joint with an operation tolerance equal to the installation tolerance, which means that the pin is "loose" within the bore and having the possibility to move relative to the bore during operation, as moveable joints in cranes or heavy machinery.

For instance, Bondura PIN technology (Figure 2 [17]) utilizes such open hole pin connection or expanding pin that is a form of an interference fit technique, where it is possible to expand and shrink the pin, mechanically, without need for any heating, cooling or axial force to push the pin into the bore, neither before nor during or after the expanding process. The pin has tapered ends, and end-sleeves with a conical inner surface that fits to the tapered pin. The sleeves are pushed into the pin by torquing the tightening end screws or nut and the sleeves climb the tapered pin ends, lock the pin to the bore as a wedge, and prevent any relative movement between the pin and the supports. The interference fit level depends on the torquing level of the tightening screws, and/or nut. By reversing the process, the complete expanding pin assembly can easily be removed, and the technique works well on all pin/hole sizes.

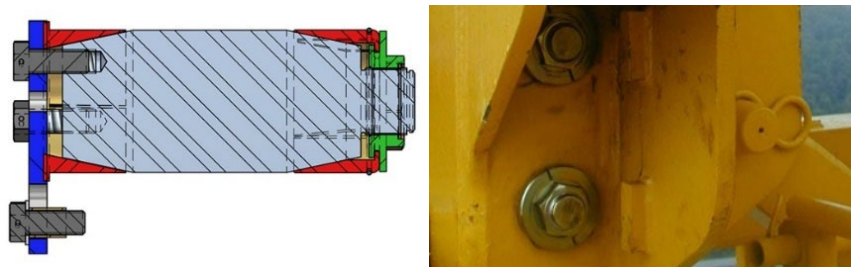


Figure 2. Bondura PIN technology (a) Expanding pin solution (b) Expanding pin in a joint

3. Fretting fatigue in different types of connections

3.1. Fatigue - general

The American Society for Testing and Materials (ASMT) defines the concept fatigue as [18]: “The process of progressive localized permanent structural change occurring in a material subjected to conditions that produce fluctuating stresses and strains at some point or points and that may culminate in cracks or complete fracture after a sufficient number of fluctuations”.

It is well known and experienced during many years that many mechanical joints subjected to cyclical loads will develop fatigue cracks at the hole or bore where the bolt or pin is inserted. Many studies have been performed in the last decades to investigate problems with fatigue in mechanical connections [1, 3, 4, 7-9, 11, 13, 19, 20].

The process of fatigue involves three main stages:

1. An initial fatigue damage, which leads to a crack nucleation and possibly crack initiation.
2. Cyclic growth of a crack (propagation) until the remaining cross-section becomes too weak to withstand the loading.
3. A sudden fracture of the remaining cross section.

Among the various types of fatigue failure, the typical ones include: mechanical fatigue, creep fatigue, thermo-mechanical fatigue, corrosion fatigue, and fretting fatigue. Most of these fatigue forms and related failures are caused by cyclic loads combined with frictional sliding, or micro movements.

3.2. Fretting - general

Fretting as indicated by ASTM [21] is: “A small-amplitude oscillatory motion, usually tangential, between the solid surfaces in contact” and: “The process of crack formation at a fretting damage site, progressive crack growth, possibly culminating in complete fracture, occurring in a material subjected to concomitantly fretting and fluctuating stresses and strains”.

Another term related with fretting wear arises as a result of a combination of fretting and corrosion. This is a form of fretting wear in which different types of corrosion play a significant role and could reduce fretting fatigue life substantially [22-25]. The risk of fretting arises when two or more material surfaces are repeatedly moved against each other under load. Such loads can be cyclic loads from the normal operation, or maybe unwanted vibrations. The fretting process from first mechanical wear to a breakdown, Figure 3 (adapted from [26]), can be explained as: The loss of material due to fretting may not be so significant, but it might be enough to degrade the structural strength and to reduce the fatigue life. If the combination of amplitude and normal force is “right” the debris from the wear process could be trapped between the contact surfaces, and play an important role in the further wear process, and the topographies of the wear scars become complicated [24].

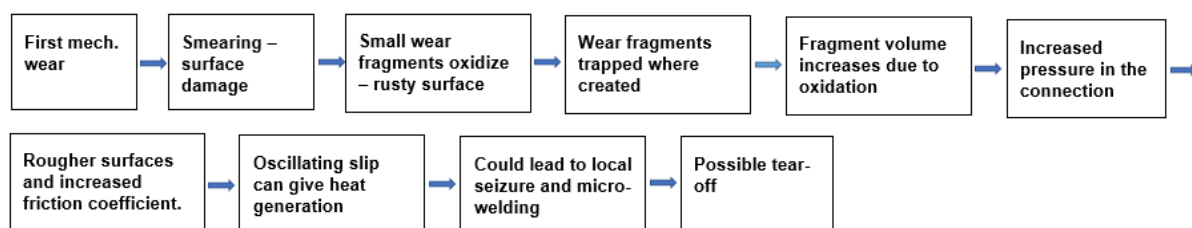


Figure 3. The fretting process

Fretting wear is one of the main reasons for failure of key components and can reduce the fatigue life up to 20 – 50% [27]. It is a type of wear damage induced by a short amplitude sliding motion between two loaded surfaces [24, 28]. It is a microscopic dynamic process involving deformed structures, cracks, oxidation process and subsequent behaviour of oxide debris between contact surfaces [29-32].

In general, fretting can be treated as three interrelated problems: (1) Fretting wear, (2) fretting corrosion and (3) fretting fatigue. Fretting wear is typically wear damage due to a fretting problem, whose prediction is a critical aspect for prediction of fretting fatigue [33-38]. Fretting corrosion, on the

other hand, is a chemical reaction problem in combination with a fretting problem [22, 23, 28, 39-44], while fretting fatigue can occur when both fretting and fatigue conditions are working at the same time. Investigations have shown that by increasing the normal force, the fretting regime transforms from typically gross slip towards partial slip [24, 45, 46]. The main parameters affecting fretting wear normally include: Normal load, slip amplitude, cyclic frequency, surface roughness, material properties and contact geometry.

3.3. Contact surface zones and geometrical shapes

Different bodies in a joint will have different geometric shapes, and therefore often different contact surface shapes, and they could act differently under loading. Figure 4 [1] shows examples for different contact geometries. The contact zone will vary with loading, and the contact status can be defined as sticking, slip/sliding and opening area, as shown in Figure 5 [27]. The stick zone is the area with no relative movement between the two surfaces, and therefore wear will not occur. In the slip-zone, there will be relative movement between the surfaces, and fatigue and abrasive wear will occur. The fretting corrosion behaviour depends strongly on the fretting regime, being a microscopic dynamic process involving deformed structures, cracks, oxidation process and subsequent behaviour of oxide debris between contact surfaces [28-32].

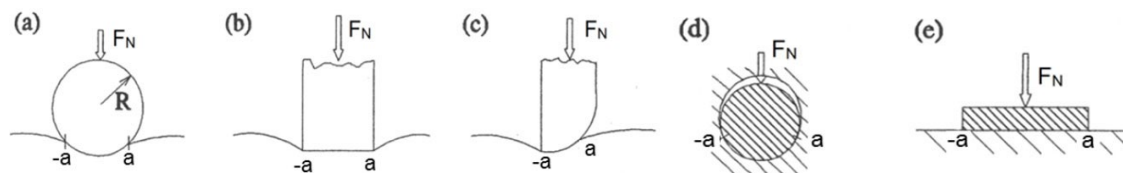


Figure 4. Different contact geometries

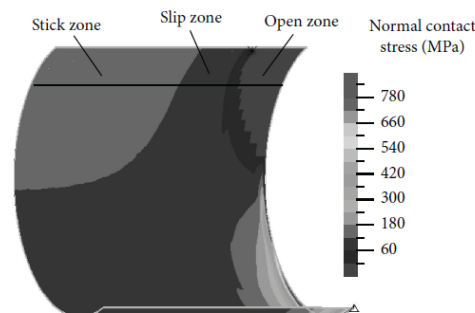


Figure 5. Stick, slip and open zone

3.4. Fretting fatigue in railway interference fit connections, and aircraft fuselage connections

Fretting problems such as fretting wear, fretting corrosion and fretting fatigue have been studied for many years, with the latest studies adding new knowledge to previous knowledge. Fretting fatigue, which is a typical and frequently appearing type of fatigue, results from infinitesimal relative surface motion between two contact materials when cyclic loads are applied. In pressurized water reactors [23, 24] for instance, fretting fatigue is a common corrosion fatigue degradation phenomenon between the steam generator tubes and anti-vibration bars/tubes supports [22, 47, 48].

A number of studies have been performed to investigate more about the different fretting and fatigue problems that occur in different industries and mechanical systems. Some of the studies were aimed to find possible solutions to decrease the negative effects of fretting, and increase the parts' and the systems' fatigue life, among them, the following can be mentioned as examples: Railway axles with interference fit connections, aircraft structure and fuselage with riveted or pinned connections, steam generators in nuclear energy production environment, threaded tube connections, and high power excavator tracks.

3.4.1. Railway axles with interference fit connections

From a safety point of view, the axle with its connections is the most important component in railway vehicles. The axle, gear seats and wheel seats are joined by interference / press fit, and they are critical parts, due to the long-time exposure to crack initiation because of fretting fatigue [2, 5, 6]. Figure 6 [3] shows a typical interference fitted railway wheel axle with wheel hub and seat. Many actions have been taken and a number of investigations have been reported with an objective of reducing the problems related to fretting fatigue and improve the fretting fatigue life [5, 6, 49]. Examples can be; optimizing the contact pressure/interference level, surface treatments, stress relief grooves, strength, and more. For rotary bending axles the wear mechanism of fretting damage is typically combinations of abrasive wear, oxidative wear and delamination [50].

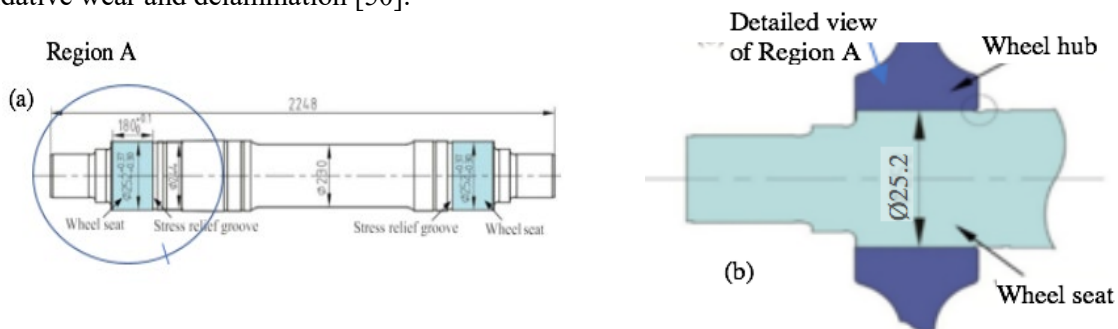


Figure 6. Railway axle (a) with hub and seat (b)

(a) *Optimizing the contact pressure / interference level:* Studies conducted to investigate the fretting fatigue life consequences of changing interference fit level, or contact pressure between the two contact surfaces shown that the transmission from high wear regime to low wear regime occurs when the contact pressure drops below a critical mean pressure of approx. 150 MPa (Figure 7 (a) [51]). As it is observed in the figure, the evolution of the wear kinetics as a function of the mean pressure identifies a critical pressure between mild and severe wear regimes.

These results are based on the fretting rig test (Figure 7 (b)) by imposing displacement independent of the normal force. As a result, one can read that with an imposed displacement combined with an increased normal pressure (> 150 MPa), the contact area will suffer severe wear. In many cases, and maybe in an interference fitted railway axle with hub and seat, it can be expected that there exists no relation between the normal force (interference fit level) and the actual displacement (relative movements between the hub and the axle). It could be expected that an increased normal force level would decrease the displacement, and therefore possibly decrease of the wear, or at least change the wear pattern.

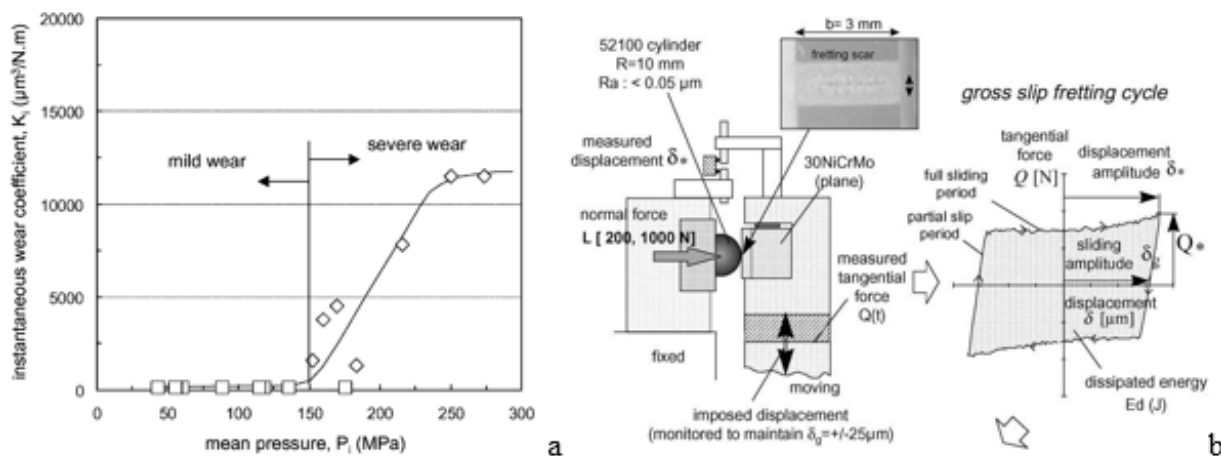


Figure 7. (a) Evolution of the wear kinetics as a function of the mean pressure, and (b) schematic of the fretting rig test set-up.

(b) *Surface treatment and fretting fatigue palliatives*: One way to avoid fretting fatigue and its negative consequences is to avoid fretting fatigue contacts; though not always possible. There exist palliative mechanisms for fretting fatigue that could reduce the problem, including [1];

- reduction of friction (expected reduction of the tangential contact force) [52]
- introduction of residual compressive stresses (reduction of fretting wear) [7, 11, 53, 54]
- increasing surface hardness (by different peening processes) [55-61]
- altering surface chemistry and modifying the micro-topography [55]

(c) *Stress relief grooves and fillets*: For many years, it has been investigated on how to achieve important improvements of fatigue life [2, 3, 5, 62-64]. One way is to optimize the place, size and form of the stress relief grooves and fillets, to maximize their effect and increase the fatigue strength and life [62, 63]. The European Norm EN13104 [65] states the requirements for calculations for powered axles.

The other method is use of finite elements methods such as the one conducted by Zeng, et al. [3] who used the method for prediction of fretting fatigue crack initiation in a full-scale railway axle, powered railway axles used in China, taking into consideration the stress redistribution and surface change due to fretting wear. Thereafter, the influence of stress relief groove on the fretting wear and fatigue was investigated.

3.4.2. Aircraft structure and fuselage with riveted or pinned connections

The normal method how to connect skin plates, or fuselage, for an aircraft construction is by rivets, as shown in Figure 8 [1]. Fatigue of the pressurized fuselages of transport aircraft is a significant problem all designers of aircraft have to take into consideration for assuring a sufficient lifetime and safety. Such joints in a fuselage require holes that could easily weakens the strength, increase the risk of fatigue, and reduce lifetime. Due to the cyclic nature of the service loading of the joints in aircraft structures, fatigue failures are most common failure types. Both pins, bolts, and rivets are commonly used in these structures, often with an interference interface, or an open-hole connection, often cold expansion treated.

Cold expansion: Cold expansion does not include a cooling, or any other temperature dependent processes, so “cold” is referring to the absence of “introduction of heat” into the process, which is the normal way when forming metal. Cold expansion is a cold forming of the bore wall to make the material more resistant, before introducing a pin or bolt for operationally purposes [7, 11, 53, 54].

Interference fit: At the junction of the main load-bearing components in the aircraft, such as wing beams, fuselage strengthening frames, and other important structural connected parts, interference fit bolted joints are widely used to improve the structural fatigue performance. Connections like press-fit, shrink-fit and mechanical radial expansion can be seen as variations within the definition of interference fit.

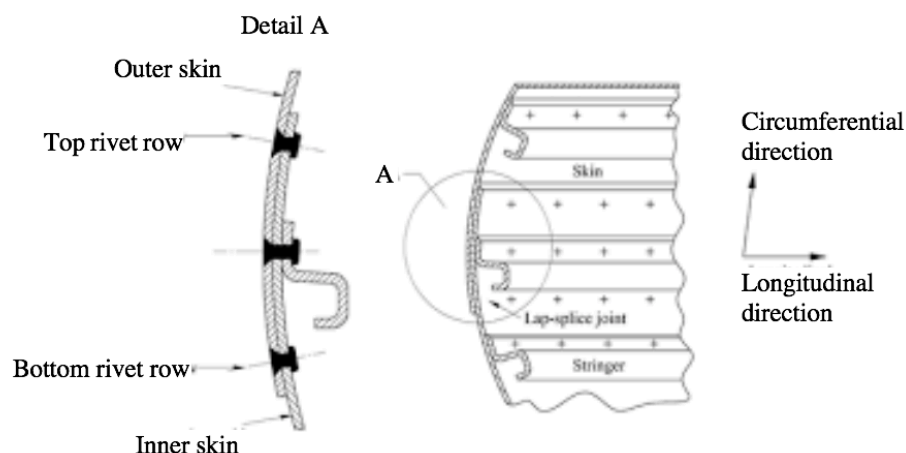


Figure 8. Riveted lap joints in a pressurized aircraft fuselage

Iyer, et al [66] concluded in their study that an interference fit of 2% tended to inhibit fretting fatigue. In a related work Iyer et al. [67] studied the influence of interference and clamping on fretting fatigue in single rivet-row lap joints, and the study was concerned with the determination of the three-dimensional contact stress and displacement fields in the panels of realistic riveted lap joints.

Moreover, Chakherlou, et al. [9] investigated both experimentally and numerically the effect of interference fit on holed plate with interference fit levels of 1%, 1.5%, 2% and 4%. The results showed that by increasing the interference fit level from 1% to 1.5% and further to 2%, the fatigue life also increased, but by increasing the level further up to 4%, it did not give any more increase in fatigue life.

To improve fatigue life of holed plates made of aluminum, in double shear lap joints, Chakherlou, et al. [11] conducted experimental and numerical studies of cold expansion (CE) and interference fit (IF) techniques. Both the cold expansion and the interference fit test levels were set to 1.5% and 4.7%. With increasing IF level, the amplitude of the alternating stress reduces, but the mean stress increases. At CE and IF level of 1.5%, the interference fit connection gives a longer fatigue life, and at 4.7% level the differences between cold expansion and interference fit are small.

Bi, et al. [68] have also performed experiments and FE analysis and concluded, in their case, that the maximum hoop tensile stress was at its minimum at an interference fit size of 1.5%. The interference fit size of 1.5% was therefore defined as the optimal value in aircraft interference assembly. Mirzajanzadeh, et al. [20] also conducted similar studies by considering different friction factors for different interference levels.

4. Discussions and outlooks

Fretting problems and challenges are well known and still be a continuous issue in many industries, although numerous investigations have been conducted for many years. Within the railway industry, especially when it comes to the axle/hub connections, many actions have been taken, and a number of investigations are conducted in order to reduce the problems related to fretting fatigue and improving the fretting fatigue life [5, 6, 49]. It has been focused on optimizing the contact pressure / interference level, palliatives, stress relief grooves and more, with the aim to prevent fretting related problems, and consequently prolong the fatigue life of the components and equipment. In general, the newer investigations are building their results on results from earlier investigations combined with new and often better techniques, test equipment and improved FE tools and methods, in addition to improved materials and palliatives / surface protection techniques.

When it comes to interference / press fit, and other treatments like cold expansion, it seems that all try to use similar techniques. An interference fit is made by forcing an axle axially into a hub, where the nominal axle diameter is slightly greater than the nominal hub diameter. The difference in nominal diameters defines the interference fit level. An alternative is to cool down the axle before inserting into the hub, and let it expand back towards nominal diameter, and create the interference fit level required.

The mechanical radial expansion, or expanding PIN technology [17] mentioned earlier, i.e. by companies like Bondura Technology and Expander, is not mentioned in any of the investigations found in this literature study. The mechanical radial expansion creates the interference fit slightly different from both the “normal” press fit and shrink fit techniques, and it is possible to control and adjust the fit level over time. The cold shrink energy issue is not present, neither the press force for reaching the fit level, nor the effects of temperature differences and friction between the connecting surfaces of the joint. This indicates future possibilities for improving press-fitted connection solutions of powered axles, typically like the axle/hub connection in a railway wheel. Further research and investigations will be necessary to clarify how efficient an expanding PIN solution can be, compared to existing solutions, like the traditional press-fit and shrink-fit.

Fatigue, in different forms, has caused many very serious accidents for many years, also within the aircraft and offshore oil & gas industries. A world-wide survey of aircraft accidents covering both fixed-wing aircraft and helicopters for the period 1934 – 1979, having metal fatigue as a related cause, showed 306 fatal accidents with 1803 fatalities [69]. Two-thirds of the accidents involved fixed-wing aircraft, with wing failure as the most common cause followed by engine failure. For the helicopter accidents, a

third were due to failure in the main-rotor system, and a quarter due to tail-rotor failure. Some of the most serious accidents at the Norwegian shelf would be the Alexander L. Kielland hotel platform fatal accident in March 1980, with 123 lost lives [70]. A hydrophone was fillet welded to a tube, and due to low mechanical strength combined with poor welding and high residual stresses, the fillet weld partially cracked, which again resulted in a fatigue fracture of the tube.

The Eurocopter AS332 Super Puma helicopter accident in the North-Sea in 1997, also called the Norne accident, had 13 fatalities. The official report [71] from 2001 stated that the initial and direct reason for the accident was due to fatigue in the spline-sleeve of the right gear box. The Eurocopter EC225 Super Puma helicopter had a fatal accident with 16 lives lost, close to Turøy (Norway) in 2016, when coming in from the North-Sea. The AIBN (Norwegian Accident Investigation Board) released their final report [72] in 2018 stating that the accident was a result of a fatigue fracture in a second stage planet gear in the main rotor gearbox which initiated from a surface micro-pit in the upper outer race of the bearing, propagating subsurface while producing a limited quantity of particles from spalling, before turning towards the gear teeth and fracturing the rim of the gear without being detected.

In general terms, the influence of fretting fatigue can be reduced or eliminated by means of the methods mentioned previously in this study; optimizing contact pressure, correct use of palliatives, correct use of stress relief grooves, improved test techniques, methods and numeric analysis tools and methods, and maybe also by investigating the use of expanding pin technology. The previously mentioned accidents [70-72] prove that the influence or consequence of fatigue can be fatal, and often a result of a highly complex chain of reactions. The investigation of the Turøy accident [72] has shown that the combination of material properties, surface treatment, design, operational loading environment and debris gave rise to a failure mode which was not previously anticipated or assessed. The investigators at the Norne accident [71] could not determine the exact cause why the fatigue fracture occurred, but it was discovered serious problems with the hard-metal coating of the spline-sleeve, with over-sized carbide grains and out-of-standard thickness variations of the coating, in combination with some undefined scratches on the coating surface from before the accident, which all together could be (partly) the reason for breakage. The Alexander L. Kielland platform accident investigation [70] revealed quality problems with material, weld, heat treatment and design. All these accidents could probably have been avoided, or had reduced consequences, with improved quality control of design and construction (platform), and of parts and materials (Norne and Turøy) and a higher general knowledge among the engineers and designers about the consequences of combinations of various individual fatigue-risk mechanisms (platform, Norne, Turøy).

5. Conclusion

Fretting problems and challenges are sources for concerns not only in most mechanical industries, but also in other industries that experience vibrations and micro movements relatively between adjacent material surfaces. In addition to continued investigations, it is imperative to improve material qualities, palliative methods, test techniques and the way of how to connect the parts of the joint. It is imperative to understand how combinations of mechanisms can result in fatigue problems, although each and one of them may not result in such problems. In practical life, minimizing the possible damage effects of a fatigue problem could be as important as avoiding having the fatigue problem itself. New methods, as the mechanical radial expansion technique have been in the marked for many years, but are possibly not well enough known among the researches. The mechanical radial expansion technique should be applied more in future investigations regarding how to reduce fretting fatigue and other related issues, in interference fitted joints. Its advantages when it comes to installation, retrieval, elimination of the need for heat/cold, and possibility to quickly adjust the interference fit level, makes this solution worth investigate further.

References

- [1] De Pauw J 2016 *Experimental research on the influence of palliatives in fretting fatigue*, Ghent University, Faculty of Engineering and Architecture, Ghent, Belgium.
- [2] Hirakawa K and Kubota M 2001 *Proc. Instit. Mech. Eng.*, Part F, **215**(2) 73-82.
- [3] Zeng D, Zhang Y, Lu L, Lang Z and Zhu S 2019, *Int. J. Fatigue*, **118** 225-236.
- [4] Luke M, Burdack M, Moroz S and Varfolomeev I 2016 *Int. J. Fatigue*, **86** 24-33.
- [5] Hirakawa K, Toyama K and Kubota M 1998 *Int. J. Fatigue*, **20**(2) 135-144.
- [6] Makino T, Kato T and Hirakawa K 2011 *Eng. Fract. Mech.*, **78**(5) 810-825.
- [7] Sun Y, Hu W, Shen F, Meng Q and Xu Y 2016 *Int. J. Mech. Sci.*, **107** 188-200.
- [8] Croccolo D, De Agostinis M, Ceschini L, Morri A and Marconi A 2013 *Fatigue Fract. Eng. Mater. Struct.*, **36**(7) 689-698.
- [9] Chakherlou T N, Mirzajanzadeh M, Abazadeh B and Saeedi K 2010 *Eur. J. Mech., A/Solids*, **29**(4) 675-682.
- [10] Liu J, Liu D, Liu Y and Tang C 2005 *J. Mech. Strength*, **27**(4) 504-509.
- [11] Chakherlou T N, Taghizadeh H and Aghdam A B 2013 *Aerosp. Sci. Technol.*, **29**(1) 351-362.
- [12] Pedersen N L 2016 *Struct. Multidiscip. Optim.*, **54**(2) 349-359.
- [13] Alfredsson B 2009 *Int. J. Fatigue*, **31**(10) 1559-1570.
- [14] Gutkin R and Alfredsson B 2008 *Eng. Fail. Anal.*, **15**(5) 582-596.
- [15] Truman C E and Booker J D 2007 *Eng. Fail. Anal.*, **14**(4) 557-572.
- [16] Özel A, Temiz S, Aydin M D and Şen S 2005 *Mater. Des.*, **26**(4) 281-289.
- [17] Bondura, "Bondura," [Online]. Available: www.bondura.no. [Accessed 28th January 2019].
- [18] ASTM, Standard Terminology Relating to Fatigue and Fracture Testing, 2013.
- [19] Oku Y, Sugino M, Ando Y, Takazaki D and Kubota M 2017 *Tribol. Int.* **108** 111-120.
- [20] Mirzajanzadeh M, Chakherlou T N and Vogwell J 2011 *Eng. Fract. Mech.*, **78**(6) 1233-1246.
- [21] ASTM, E2789: Standard guide for fretting fatigue testing, 2015.
- [22] Liao J, Wu X, Tan J, Qian H and Xie Y 2018 *Corros. Sci.*, **133**, 423-431.
- [23] Zinkle S J and Was G S 2013 *Acta Materialia*, **61**(3) 735-758.
- [24] Chung I and Lee M 2011 *Nuclear Eng. Des.*, **241**(10) 4103-4110.
- [25] Abbas F and Majzoubi G H 2018 *Theor. Appl. Fract. Mech.*, **93** 144-154.
- [26] Klebanov B M 2008 *Machine Elements Life and Design*, 2008.
- [27] Han C and Zhang J 2014 *Sci. World J.*, **2014**.
- [28] Li J, Yang B, Lu Y, Wang Z and Shoji T 2017 *Mater. Charact.*, **131** 224-233.
- [29] Xin L, Wang Z, Li J, Lu Y and Shoji T 2016 *Mater. Charact.*, **115** 32-38.
- [30] Lee Y H and Kim I S 2002 *Wear*, **253**(3 to 4) 438-447.
- [31] Lee Y, Kim H K, Kim H D, Park C Y and Kim I S 2003 *Wear*, **255**(7 to 12) 1198-1208.
- [32] Diomidis N and Mischler S 2011 *Tribol. Int.*, **44**(11) 1452-1460.
- [33] Madge J J, Leen S B and Shipway P H 2007 *Wear*, **263**(1 to 6 SPEC. ISS.) 542-551.
- [34] Jin O and Mall S 2004 *Wear*, **256**(7 to 8) 671-684.
- [35] McColl I R, Ding J and Leen S B 2004 *Wear*, **256**(11 to 12) 1114-1127.
- [36] Nakazawa K, Maruyama N and Hanawa T 2003 *Tribol. Int.*, **36**(2) 79-85.
- [37] Hattori T and Watanabe T 2006 *Tribol. Int.*, **39**(10) 1100-1105.
- [38] Sabelkin V and Mall S 2005 *Fatigue Fract. Eng. Mater. and Struct.*, **28**(9) 809-824.
- [39] Wang Z H, Lu Y H, Li J and Shoji T 2016 *Tribol. Int.*, **95** 162-169.
- [40] Lgried M, Liskiewicz T and Neville A 2012 *Wear*, **282 - 283**, 52-58.
- [41] Kwok C T, Cheng F T and Man H C 2000 *Mater. Sci. Eng., A* **290** (1 to 2) 145-154.
- [42] Mi X, Cai Z B, Xiong X M, Peng J F and Zhu M-H 2016 *Tribol. Int.*, **100** 400-409.
- [43] Xin L, Yang B, Li J, Lu Y and Shoji T 2017 *Corros. Sci.*, **123** 116-128.
- [44] Zhong X, Han E-H and Wu X 2013 *Corros. Sci.*, **66** 369-379.
- [45] Zhang X and Liu D 2009 *Acta Metall. Sinica*, **22**(2) 131-137.
- [46] Xin L, Yang B B, Wang Z H, Lu Y H and Shoji T 2016 *Wear*, **368 - 369** 210-218.
- [47] Young B A, Gao X, Srivatsan T S and King P J 2007 *Mater. Des.*, **28**(2) 373-379.

- [48] Hong S M and Kim I S 2005 *Wear*, **259**(1- 6) 356-360.
- [49] Yamamoto M and Ishiduka H 2017 *Int. J. Fatigue*, **97** 48-55.
- [50] Song C, Shen M X, Lin X F, Liu D W and Zhu M H 2014 *Fatigue Fract. Eng. Mater. Struct.*, **37**(1) 72-84.
- [51] Fouvry S 2001 *Wear*, **250 - 251** (PART 2) 1320-1331.
- [52] Zhou Z R and Vincent L, 1999 *Wear*, **225 - 229** (PART II) 962-967.
- [53] Chakherlou T N and Vogwell J 2003 *Eng. Fail. Anal.*, **10**(1) 13-24.
- [54] Chakherlou T N and Vogwell J 2004 *Fatigue Fract. Eng. Mater. Struct.*, **27**(5) 343-351.
- [55] Kasarekar A T, Sadeghi F and Tseregounis S 2008 *Wear*, **264**(7 - 8) 719-730.
- [56] Menezes M R, Godoy C, Buono V T, Schvartzman M M and Wilson J C 2017 *Surf. and Coat. Technol.*, **309** 651-662.
- [57] Donzella G, Gerosa R, Pertogalli C, Silva G and Beretta M 2011 *Procedia Eng.*, **10** 3399-3404.
- [58] Cseh D, Mertinger V and Lukács J 2013 *Mater. Sci. Forum*, **752**, 95-104.
- [59] Mordyuk B N and Prokopenko G I 2007 *J. Sound Vib.*, **308**(3 - 5) 855-866.
- [60] Kumar S A, Raman S G S, Narayanan T S S and Gnanamoorthy R 2012 *Surf. Coat. Technol.*, **206**(21) 4425-4432.
- [61] Montross C S, Wei T, Ye L, Clark G and Mai Y-W 2002 *Int. J Fatigue*, **24**(10) 1021-1036.
- [62] Kubota M, Kataoka S and Kondo Y 2009 *Int. J. Fatigue*, **31**(3) 439-446.
- [63] Kataoka S, Sakae C, Kubota M and Kondo Y 2007 *Key Eng. Mater.*, **353 - 358** (PART 2) 856-859.
- [64] Cervello S 2016 *Int. J. Fatigue*, **86** 2-12.
- [65] European Norm 2009, *EN 13104 Railway applications. Wheelsets and bogies. Powered axles. Design method.*
- [66] Iyer K, Hahn G T, Bastias P C and Rubin C A 1995 *Wear*, **181 - 183** (PART 2) 524-530.
- [67] Iyer K, Rubin C A and Hahn G T 2001 *J. Tribol.*, **123**(4) 686-698.
- [68] Bi Y, Jiang J and Ke Y 2015 *Adv. Mech. Eng.*, **7**(6) 1-12.
- [69] Campbell G S 1981 *Int. J. Fatigue*, **3**(4) 181-185.
- [70] Almar-Naess A, Haagensen P J, Lian B, Moan T and Simonsen T, 1984 *J. Energy Res. Technol.*, **106**(1) 24-30.
- [71] Havarikommissjonen for Sivil Luftfart, 2001, RAP.:47/2001.
- [72] AIBN, 2018, Report SL 2018/04.

Appended Paper IX

On Modelling Techniques for Mechanical Joints: Literature Study

KARLSEN, Ø.; LEMU, H. G.

International Workshop of Advanced Manufacturing and Automation. Springer, Singapore, 2019. p. 116-125.

https://doi.org/10.1007/978-981-15-2341-0_15

This paper is not available in Brage due to copyright restrictions.

Part II: Appended Papers

Appendix A

Questionnaire applied in [Paper I](#) and [IV](#), including the introduction part, and all questions and alternative responses, with options to make comments or give other answers.

Appendices



The Industrial PhD project is funded by The Research Council of Norway and executed in cooperation with the University of Stavanger, Norway, and named "Effect and consequence analysis regarding expanding PIN-technology in various types of heavy machinery".

Introduction

This is a survey to be conducted as part of an Industrial PhD at University of Stavanger. The Industrial PhD project is a cooperation project between the Research Council of Norway, the University of Stavanger, the PhD candidate and the company Bondura Technology AS. The project aims to investigate and evaluate the reasons for the use of expanding pin solutions, and the effects and consequences on the equipment where the expanding pin solutions are installed and in operation.

The expanding pin solution works in such a way that the pin expands radially when torqued and locks the pin system 360° to the equipment supports by a wedge force, and prevents any relative movement between the contacting surfaces, and as a result prevents tear, wear and ovality from developing.

The aim of this survey is to gather enough relevant information about use of expanding pin solutions and to conclude what the effects and consequences are for the equipment and pins where these solutions are operating, and then also for the owners or operators of the equipment. The survey is made for both original equipment manufacturers (OEMs) and engineering companies who are specifying the use of expanding pins, users and service companies of equipment with expanding pins, and others who are in position to take decisions regarding the use of such technology.

Although the candidate of this PhD project is related to the company Bondura Technology, who is doing design, engineering, production and sale of expanding pins, this survey is not specifically related to the bondura® PIN systems. The survey is based on the use of expanding pin technology in general, produced by any company independent of being specialist in the technology or being end-users with their own design for their own specific use.

There will not be any questions about who is the owner, supplier or producer of the pin technology, nor where the pin technology you are using is coming from, geographically, if the pin design does not belong to your company.

The final report will be completely anonymous, so the names of companies and persons responding to this survey will not be included in the report, only the analysis and conclusions of the received material.

The final report will be presented as an investigation report and scientific paper(s) may be published, and finally be a part of the Industrial PhD dissertation. After the paper has been published all who have responded the survey will receive a copy, if interested.

Place and date: Stavanger, 13/April -2020

.....
Øyvind Karlsen
PhD Candidate, Faculty of Science and Technology
University of Stavanger, Norway
CTO at Bondura Technology AS

Appendices



The Industrial PhD project is funded by The Research Council of Norway and executed in cooperation with the University of Stavanger, Norway, and named "Effect and consequence analysis regarding expanding PIN-technology in various types of heavy machinery".


Questionnaire

Please fill in your company's information:

Company name:

Company location:

Type of products:

Please respond to the questions to your best knowledge with one or more , and return to ovind.karlsen@uis.no

1. Size of your company:

- 1 – 20 employees
- 20 – 100 employees
- Over 100 employees

2. Company profile:

- Production – OEM (Original Equipment Manufacturer)
- Production – supplier to OEM
- Engineering – design and calculation
- End-user – buying from OEM
- Service/repair/maintenance
- Other profile

3. For how long have your company applied, specified or worked with expanding pin technology?

- 0 – 1 year
- 1 – 10 years
- More than 10 years
- Other

Appendices

4. In which markets and type of equipment and machineries are or have your company applied, specified or worked with expanding pin technology?

- a) Offshore – Oil&Gas
- Drilling and pipe handling eqp.
 - Offshore cranes
 - Other eqp.

- b) Maritime – ships:
- Maritime cranes
 - Winches
 - A-frames
 - Hatches and doors
 - Other eqp.

- c) Subsea – ROV and structures:
- Movable joints on ROV
 - Fixed joints on frame
 - Other eqp.

- d) Dredging – sea, lakes and rivers:
- Cranes
 - Winches
 - A-frames
 - Hatches and doors
 - Other eqp.

- e) Mining – onshore and offshore:
- Drilling eqp.
 - Bolting eqp.
 - Earth moving eqp.
 - Crushing eqp.
 - Feeding, conveying and vibration eqp.
 - Other eqp.

- f) Construction and earth moving – onshore:
- Tower cranes
 - Vehicles
 - Other eqp.

- g) Specialized machines and eqp.:
- Harbour cranes
 - Sea, flood and dike doors and barriers
 - Other eqp.

Appendices

- h) Steel and Paper industry:
 - Handling, lifting, cutting eqp.
 - Other eqp.
- i) Another type of industry:
 - Another eqp.

- 5. Are the expanding pins you are using your own design, or from others?
 - Company's own design for own products
 - From external supplier
 - Other solution

- 6. Effects and consequences of applying expanding pin solutions:
 - a) What is the reason for your company to choose or work with expanding pin technology?
 - It is a strong wish or requirement from our clients
 - It is based on our own previous experience
 - It is new for us and we want to test it
 - The pins come with the equipment when we receive it
 - Other reasons:
 -

 - b) How do you compare installation time for expanding pins with standard cylindrical pins?
 - Faster – less time with expanding pins
 - Equal – same time
 - Slower – more time with expanding pins
 - Comments:
 -

 - c) How do you compare retrieval time for expanding pins with standard cylindrical pins?
 - Faster – less time with expanding pins
 - Equal – same time
 - Slower – more time with expanding pins
 - Comments:
 -

Appendices

- d) How important is for your company and your clients to have pins which are quick to install and retrieve when required?
- Crucial and decisive
 - Important
 - Less, or not important at all
 - Comments:
-
- e) How do you compare tear and wear damages on supports and pins for expanding pins with standard cylindrical pins?
- Less tear and wear issues with expanding pins
 - Equal level
 - More tear and wear issues with expanding pins
 - Comments:
-
- f) How do you compare breakage damages on supports and pins for expanding pins with standard cylindrical pins?
- Less breakage issues with expanding pins
 - Equal level
 - More breakage issues with expanding pins
 - Comments:
-
- g) How important is for your company and your clients to avoid breakage issues of pins and supports?
- Crucial and decisive
 - Important
 - Less, or not important at all
 - Comments:
-

Appendices

- h) Have your company ever used an expanding pin solution that locks not only to the supports, but also to the bearings?
- Yes, we have
 - No, we have not
 - Comments:
 -
- i) If your company is using or has used expanding pin solutions that locks to the bearings, what was the effects and results of that?
- Longer lifetime of bearings
 - More efficient machine or equipment
 - Shorter lifetime of bearings
 - No specific effect at all
 - Comments:
 -
- j) If your company has never used expanding pin solutions that locks to the bearings, what is the reason for that?
- We don't know such a solution
 - We have no need for such a solution
 - Comments:
 -
- k) How do you compare safety for personnel and equipment during installation, operation and retrieval, for expanding pins with standard cylindrical pins?
- Safer with expanding pins
 - Equal safety level
 - Less safe with expanding pins
 - Comments:
 -
- l) If you marked expanding pins as safer than standard cylindrical pins in the previous question, why?
- No need for sledgehammering to get the expanding pin into the joint

Appendices

- No relative movements between expanding pin and supports during service / operation
- Less chance for breakage of pin during service / operation
- Easy and fast to retrieve when required
- Comments:

.....

m) How important is for your company and your clients to have a pin assembly solution that is safe for personnel and equipment?

- Crucial and decisive
- Important
- Less, or not important at all
- Comments:.....

.....

n) Which other effects and consequences do you see for the equipment and machines in relation with repair, service and operation, when using expanding pin solutions instead of standard cylindrical pins?

- Reduced unwanted downtime on production with expanding pins
- Reduced number and length of planned downtime for service
- Less or no wear damage on expanding pins and supports
- Reduced corrosion on expanding pins
- Longer lifetime of equipment and machines, with expanding pins
- We don't see any specific advantages with expanding pins
- Comments:.....

.....

o) What are the economic effects and consequences for your company and/or your clients when using expanding pin technology, instead of standard cylindrical pins?

- Crucial and decisive
- Important
- Less, or not important at all
- Comments:.....

.....

Appendices

Thank you so much for your time and effort!

Please return the questionnaire to: oyvind.karlsen@uis.no

.....
Company name / product area

.....
Your name and signature

.....
Place/date

Appendix B

Standard declaration of authorship, from UiS